The role of monocytes in ANCA associated vasculitis

Eóin O'Brien, B.A. (mod)

A thesis submitted to the University of Dublin for the degree of Doctor of Philosophy

School of Medicine,

Trinity Translational Medicine Institute,

Trinity College Dublin

Declaration

I declare that this thesis has not been submitted as an exercise for a degree at this or any other university and it is entirely my own work.

I agree to deposit this thesis in the University's open access institutional repository or allow the library to do so on my behalf, subject to Irish Copyright Legislation and Trinity College Library conditions of use and acknowledgement.

_____

Eóin O'Brien

Acknowledgement

Firstly, I must thank my supervisors, Dr. Fionnuala Hickey and Prof. Mark Little for your constant support and guidance throughout my PhD research. This, along with the occasional kick to get me back on track, has helped me more than words can describe. I am sure that the lessons which they have thought me will be extremely helpful going forward in my career and life.

I have to give huge thanks to everyone in the Renal Inflammation group, both past a present, for their friendship, assistance in the lab and patience when sitting through yet another presentation about metabolism. In particular I would like to thank Vinny; for always saying yes to lending a hand and giving me someone to talk about sports with, Alice; for her unending ANCA and mouse knowledge (and patience during my first i.v. injections!) and Michelle; for providing welcome tennis and snooker distractions on the long Seahorse days. Without their initial help I don't know where this project would have gone. I would also like to thank Dearbhaile and Barbara for their help in the lab and contrasting sense of enthusiasm (but enthusiasm none the less!)

To everyone in the Trinity Translational Medicine Institute, particularly everyone in the Doherty lab who sat through biochemistry that had long since been forgotten, I must say a big thank you. Your encouragement and advice on all aspects of science has been of great help. The chats and hillwalks have been interesting to say the least. Also, thanks to Eamon for all of his help with flow and cell sorting, and for his mix of pessimism and optimism to get through the day.

I of course have to thank my family; Mam, Dad, Stephen, and Shauna for your unending support over the last 4 years. In particular, my Mam for offering to type everything whether you understood it or not! I also have to thank my Nana who gave me constant support, was always willing to listen and I know would be proud of me now.

Last, but by no means least, I have to give a massive thank you to Aimee. I still don't know how you put up with having a perpetual student as a boyfriend and listening to me go on about "The Flow" and Seahorse repeatedly. I could have done none of this without your help and support. Thanks for everything.

Abstract

ANCA associated vasculitis (AAV) encompasses several autoimmune conditions characterised by destruction of small vessels, inflammation of the respiratory tract, and glomerulonephritis. Most patients harbour autoantibodies directed against myeloperoxidase (MPO) or proteinase 3 (PR3). These antigens are found mainly in the lysosomes of neutrophils and monocytes and can be externalised when these cells are activated. Clinical and experimental data suggest that pathogenesis is driven by ANCA-mediated activation of neutrophils and monocytes. The function of monocytes in disease has been relatively understudied. Here, I investigated the role of monocytes in AAV.

I first determined the relative proportion of monocyte subsets in patients, and found an increase in the proportion of intermediate monocytes in patients versus control individuals. I found that this subset preferentially expressed MPO and PR3 on their surface, and that the expression of PR3 is not associated with CD177 as it is in neutrophils. I also found that monocytes respond differently to antibodies directed against MPO and PR3, with anti-MPO but not anti-PR3 leading to increased IL-1β, IL-6 and IL-8 production. In concordance with the observed higher surface expression of MPO on intermediate monocytes, this subset produces the highest quantity of IL-1β in response to anti-MPO stimulation suggesting a potential role in ANCA vasculitis.

Changes in cellular metabolism, particularly a switch to glycolysis, have recently been linked to activation of immune cells and to production of IL-1β. Therefore, I next investigated the metabolic profile of monocytes in response to ANCA stimulation. In contrast to their cytokine production, I found a similar increase in glucose uptake from both anti-MPO and anti-PR3 stimulated monocytes. This increase corresponded to an increase in glycolysis, as measured by Seahorse extracellular flux analysis, immediately following antibody treatment. Interestingly, only the anti-MPO treated cells increased oxidative phosphorylation 4hr post stimulation and these cells were also the only producers of IL-1β. These data suggest a potential differential activation of monocytes treated with ANCA compared to other inflammatory cell types.

The final aspect of this work was attempting to induce disease in a humanised mouse model, and to study the effects of monocytes on disease pathogenesis in this *in vivo* setting. I was unable to effectively induce disease in this model. However, I have shown for the first time that distinct monocyte subsets are present in these mice. The presence of these subsets provides a future model for the study of these cells in an *in vivo* setting and may benefit research into other diseases along with AAV.

Taken together, these data strongly support a role for monocytes in the pathogenesis of AAV and implicate changes in their cellular metabolism as a mechanism of activation. These metabolic pathways may therefore be potential targets for therapeutic intervention.

Table of Contents

List of Figures

List of Tables

Abbreviations

Abbreviation	Explanation
°C	Degrees Celsius
2-DG	2-Deoxyglucose
2-NBDG	2-(N-(7-nitrobenz-2-oxa-1,3-diazol-4-yl)amino)-2-deoxyglucose
AAV	ANCA associated vasculitis
ACPA	Anti-cytoplasmic antibody
ANCA	Anti-neutrophil cytoplasmic antibody
APC	Antigen presenting cell
ATP	Adenosine triphosphate
BMDM	Bone marrow derived macrophage
B_{reg}	Regulatory B cell
BSA	Bovine serum albumin
BVAS	Birmingham vasculitis activity score
CHCC	Chapel Hill Consortium Criteria
CLASS	Classical monocyte
COX-2	Cyclooxygenase-2
CRP	C-reactive protein
CTRL	Control antibody
DC	Disease control
DCA	Dichloroacetate
DCs	Dendritic cells
DHR123	Dihydrorhodamine123
DMEM	Dulbecco's modified eagle's medium
DMSO	Dimethyl sulfoxide
EAV	Experimental autoimmune vasculitis
EBV	Epstein-Barr virus
ECAR	Extracellular acidification rate
EDTA	Ethylenediaminetetraacetic acid
EGPA	Eosinophilic granulomatosis with polyangiitis

ELISA	Enzyme linked immunosorbent assay
ETC	Electron transport chain
FACS	Fluorescence associated cell sorting
FAO	Fatty acid oxidation
FCCP	Carbonyl cyanide-p-trifluoromethoxyphenylhydrazone
FCS	Foetal calf serum
FMO	Fluorescence minus one
GBM	Glomerular basement membrane
G-CSF	Granulocyte colony stimulating factor
GFR	Glomerular filtration rate
GN	Glomerulonephritis
GPA	Granulomatosis with polyangiitis
GRAN	Granulocytes
GVHD	Graft versus host disease
HBSS	Hanks buffered salt solution
HC	Healthy control
HGF	Haematopoietic growth factor
HIV	Human immunodeficiency virus
HK-1	Hexokinase-1
HLA	Human leukocyte antigen
HPP-CFC	Higher proliferative potential, capable of forming colonies
HRP	Horse radish peroxidase
HSC	Haematopoietic stem cell
hu-mSCF	Human membrane stem cell factor
i.p.	Intra-peritoneal
i.v.	Intra-venous
IgG	Immunoglobulin G
IL	Interleukin
INT	Intermediate monocyte
Irg-1	Immune responsive gene-1

ISO	Isotype
LAMP-2	Lysosomal membrane protein-2
LDL	Low density lipoprotein
LPS	Lipopolysaccharide
mAb	Monoclonal antibody
MACS	Magnetic associated cell sorting
MB	Mannose binding
MCP	Monocyte chemoattractant protein
MFI	Median fluorescence intensity
MHC	Major histocompatibility complex
MMP	Matrix metalloproteinase
MONO	Monocytes
MPA	Microscopic polyangiitis
MPO	Myeloperoxidase
mTOR	Mechanistic target of rapamycin
NB-1	Neutrophil binding protein 1
NC	Non-classical monocytes
NK	Natural killer
NOD	Non-obese diabetic
NSG	NOD SCID IL-2rγ$^{-/-}$
OCR	Oxygen consumption rate
OLIGO	Oligomycin
OSM	Oncostatin M
OX PHOS	Oxidative phosphorylation
PAN	Polyarteritis nodosa
PAS	Periodic-acid Schiff
PBMC	Peripheral blood mononuclear cells
PBS	Phosphate buffered saline
PDH	Pyruvate dehydrogenase
PDHK	Pyruvate dehydrogenase kinase

PET	18-F-Fluorodeoxyglucose Positron Emission Tomography with Computed Tomography
PFA	Paraformaldehyde
PI	Propidium Iodide
PLP	Phosphate-lysine-periodate
PR3	Proteinase-3
RAG	Recombinase activating gene
RET	Reverse electron transport
RKD	Rare kidney disease
ROS	Reactive oxygen species
RPMI	Roswell parks memorial institute
s.c.	Sub cutaneous
SCG	Spontaneous crescentic glomerulonephritis
SCID	Severe combined immunodeficiency
SDH	Succinate dehydrogenase
SGM3	Stem cell factor, GM-CSF and IL-3 mice
SLE	Systemic Lupus Erythematosus
SPF	Specific pathogen free
SVV	Small vessel vasculitis
T_H	T helper cell
TMB	3, 3', 5, 5' – tetramethylbenzindine
TNF	Tumour necrosis factor
T_{reg}	Regulatory T cell
WKY	Wistar Kyoto
Δψm	Mitochondrial membrane potential

Publications and presentations arising from this work

Publications:

- EC O'Brien, WH Abdulahad, A Rutgers, MG Huitema, VP O'Reilly, AM Coughlan, M Harrington, P Heeringa, MA Little, FB Hickey
  Intermediate monocytes in ANCA vasculitis: increased surface expression of ANCA autoantigens and IL-1β secretion in response to anti-MPO antibodies.
  Sci Rep, 2015; 5: 11888.

- AM Coughlan, C Harmon, S Whelan, EC O'Brien, VP O'Reilly, P Crotty, P Kelly, M Ryan, FB Hickey, C O'Farrelly, and MA Little
  Myeloid Engraftment in Humanized Mice: Impact of Granulocyte Colony Stimulating Factor Treatment and Transgenic Mouse Strain
  Stem Cells Dev. 2016 Apr 1;25(7):530-41

- EC O'Brien, C White, S Mohamed, B Brinkmann, MA Little, FB Hickey
  The effect of ANCA stimulation on monocyte metabolism
  Manuscript in preparation

Presentations:

- EC O'Brien, VP O'Reilly, AM Coughlan, M Harrington, P Heeringa, MA Little, FB Hickey
  Monocyte subsets and their role in ANCA vasculitis
  Oral presentation, Irish Nephrology society, 2014

- EC O'Brien, WH Abdulahad, A Rutgers, MG Huitema, VP O'Reilly, AM Coughlan, M Harrington, P Heeringa, MA Little, FB Hickey
  The role of monocyte subsets in ANCA-associated vasculitis
  Poster presentation chosen for short oral presentation, Irish Society of Immunology, 2014

- EC O'Brien, C White, S Mohamed, B Brinkmann, MA Little, FB Hickey
  ANCA stimulation of monocytes leads to an immediate change in their cellular metabolism
  Oral presentation, Irish Nephrology Society, 2017
- EC O'Brien, WH Abdulahad, A Rutgers, MG Huitema, VP O'Reilly, AM Coughlan, M Harrington, P Heeringa, MA Little, FB Hickey
  The role of monocyte subsets in ANCA-associated vasculitis
  Poster presentation, American Society of Nephrology, 2014

- AM Coughlan, C Harmon, S Whelan, EC O'Brien, VP O'Reilly, P Crotty, P Kelly, M Ryan, FB Hickey, C O'Farrelly, and MA Little
  Myeloid Engraftment in Humanized Mice: Impact of Granulocyte Colony Stimulating Factor Treatment and Transgenic Mouse Strain
  Poster presentation, American Society of Nephrology, 2015

- EC O'Brien, B Brinkmann, MA Little, FB Hickey
  ANCA stimulation increases oxidative phosphorylation in monocytes
  Poster presentation, Irish Nephrology Society, 2016

- EC O'Brien, C White, S Mohamed, B Brinkmann, MA Little, FB Hickey
  The effect of ANCA stimulation on monocyte metabolism
  Poster presentation, American Society of Nephrology, 2017

Chapter 1: Introduction

1.1 Anti-neutrophil cytoplasmic antibody associated vasculitis

1.1.1 AAV

Anti-neutrophil cytoplasmic antibody (ANCA) associated vasculitis (AAV) is a term which encompasses several complex autoimmune conditions affecting the microvasculature. AAV is distinguished from other small vessel vasculitis (SVV) by the lack of immune complex deposition (Jennette et al., 2013). It presents mainly as a pauci immune necrotising vasculitis which affects multiple organs and tissues, with the kidneys and lungs being particularly vulnerable. AAV is the leading cause of rapidly progressive glomerulonephritis (GN) which is characterised be crescent formation in the glomeruli of patients leading to kidney necrosis. Currently, the Revised Chapel Hill Consensus Nomenclature is used to define different disease subsets within AAV (Jennette et al., 2013). These diseases are; microscopic polyangiitis (MPA), granulomatosis with polyangiitis (GPA) and eosinophilic granulomatosis with polyangiiitis (EGPA). AAV is a rare disease with an incidence of ~19/million in Europe (Watts et al., 2001). The prevalence of the different AAV subtypes has been shown to vary dramatically with patients from Japan and Southern Europe having predominantly MPA while Northern European countries have predominantly GPA (Hilhorst et al., 2015).

These conditions all share a number of similar clinical features, one of which is the presence in most patients of antibodies (ANCAs) directed against myeloperoxidase (MPO) and proteinase-3 (PR3). If left untreated these conditions have a 1 year mortality rate of 80% (Booth et al., 2003). Even with treatment, MPA and GPA patients have a 5 year mortality rate of ~25% (Phillip and Luqmani, 2008). Current therapies involve a two-fold strategy. Initial induction therapy is designed to induce remission and usually consists of high dose glucocorticoids, cyclophosphamide or rituximab for 12 weeks before switching to maintenance therapy of azathioprine, methotrexate or rituximab to prevent relapse (Yates et al., 2016).

1.1.2 Granulomatosis with polyangiitis

GPA, formerly Wegener's granulomatosis, is defined as "*Necrotizing granulomatous inflammation usually involving the upper and lower respiratory tract, and necrotizing vasculitis affecting predominantly small to medium vessels (e.g., capillaries, venules, arterioles, arteries and veins). Necrotizing glomerulonephritis is common*" (Jennette et al., 2013). GPA was first described as a form of polyarteritis nodosa (PAN) by Klinger in 1931 (Klinger, 1931). It was later characterised as a separate vasculitis by Wegener in 1939 (Wegener, 1939). The term GPA, which better encompasses the multiple vessels involved, was first used to describe the disease in 1954 by Godman and Churg and this has since become the accepted term (Godman and Churg, 1954). 70% of GPA patients will present with upper respiratory symptoms and >90% will develop these symptoms over the course of their disease (Hoffman et al., 1992).

GPA can be limited to the respiratory system or can be more systemic affecting the kidney and ocular vasculature. In cases where renal disease occurs it manifests as rapidly progressive glomerulonephritis and often requires dialysis (Specks and DeRemee, 1990). As the name suggests one of the key clinical characteristics of GPA is the presence of granulomatous inflammation.

1.1.3 Microscopic polyangiitis

Wainwright and Davson first described patients with segmental glomerulonephritis who also had features of PAN (Wainwright and Davson, 1950). This condition is now known as MPA. MPA shares many of the same clinical features of GPA and is defined as "*Necrotizing vasculitis, with few or no immune deposits, predominantly affecting small vessels (i.e., capillaries, venules, arterioles). Necrotizing arteritis involving small and medium arteries may be present. Necrotizing glomerulonephritis is very common. Pulmonary capillaritis often occurs. Granulomatous inflammation is absent*" (Jennette et al., 2013). The defining difference between GPA and MPA is therefore the presence of granulomatous inflammation in the former. Renal involvement is more common and severe in MPA patients than GPA patients with up to 50% of patients developing end-stage renal disease after 9 months (Borao-Cengotita-Bengoa et al., 2010).

1.1.4 Eosinophilic granulomatosis with polyangiitis

EGPA was first defined by Churg and Strauss in 1951 (Churg and Strauss, 1951). It is defined as "*Eosinophil-rich and necrotizing granulomatous inflammation often involving the respiratory tract, and necrotizing vasculitis predominantly affecting small to medium vessels, and associated with asthma and eosinophilia. ANCA is more frequent when glomerulonephritis is present*" (Jennette et al., 2013). The main distinguishing feature between EGPA and GPA or MPA is the presence of asthma and, as the definition suggests, eosinophilia. While eosinophils are thought to play an important role in disease their exact pathogenic effects have not yet been elucidated (Khoury et al., 2014).

1.2 What are ANCA?

1.2.1 Why ANCA matter

While the aetiology of AAV is still unknown it is considered to be an autoimmune disease due to the strong association with ANCA. ANCA were first described by *Davies et al* in 1982 as anti-cytoplasmic antibodies (ACPA) with unknown specificity which could stain the cytoplasm of neutrophils (Davies et al., 1982). The association of ACPA with GPA was then found in 1985 (van der Woude et al., 1985). These antibodies were found to be directed against two main constituents of neutrophil granules, PR3 and MPO. A specific immunofluorescent staining pattern was observed for each antibody with anti-PR3 antibodies having a cytoplasmic pattern (c-ANCA) and anti-MPO having a perinuclear staining pattern (p-ANCA). c-ANCA were found to be highly specific (>90%) for GPA while p-ANCA are more common in MPA and EGPA, although the latter is less specific (Hagen et al., 1998). ANCA have been linked to disease activity and were initially thought of as a useful biomarker for diagnosis (van der Woude et al., 1985). However, increasing evidence has shown that ANCA can be pathogenic and are likely to be driving disease (Jennette et al., 2011). Evidence of their pathogenic effect includes the fact that targeting B cells is an effective treatment for disease (Jones, 2014), as well as a number of animal models which use ANCA to induce disease (Coughlan et al., 2012a). This pathogenic effect can also be observed *in vitro* with ANCA having pro-inflammatory effects on both neutrophils and monocytes (Falk et al., 1990, Ralston et al., 1997).

1.2.2 MPO

MPO is a key peroxidase enzyme involved in the inflammatory response (Reber et al., 2017). It is a heme protein expressed mainly in the azurophilic granules of neutrophils (Kinkade et al., 1983). In response to immune stimuli MPO is released during degranulation. This release of MPO has direct anti-bacterial effects as well as increasing neutrophil vascular adhesion to allow for diapedesis (Klinke et al., 2011, Reber et al., 2017). Upon priming using TNF-α, MPO can become expressed on the surface of neutrophils (Falk et al., 1990). MPO expressed in this way is thought to act as an e-selectin ligand and therefore increases cellular adhesion (Silvescu and Sackstein, 2014). This extracellular expression also allows for antibodies directed against MPO to bind and activate the neutrophil to degranulate (Porges et al., 1994). MPO has no transmembrane domain and so is incapable of signalling alone. Activation of neutrophils by anti-MPO antibodies is therefore thought to be mediated by the association of MPO with other surface molecules such as CD11b and CD18 (**Figure 1.1**). This complex is generally referred to as Mac-1. The precise mechanisms behind neutrophil activation as a result of anti-MPO binding are not known, however, Mac-1 interacting with MPO is thought to play a key role in this process (Lau et al., 2005).

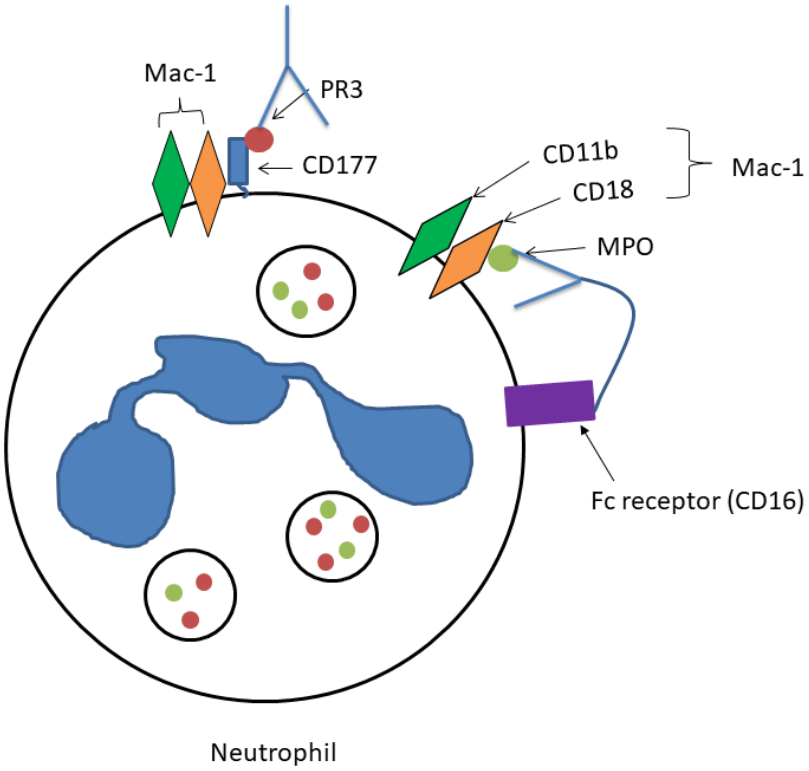

Figure 1.1 Neutrophil surface expression of MPO and PR3.
MPO interacts directly with Mac-1 and anti-MPO antibodies likely signal through this complex. PR3 is bound to CD177 which can interact with Mac-1 to transduce anti-PR3 antibody signals. Antibodies against MPO and PR3 are thought to also bind to Fc receptors both in *cis* and in *trans* to activate the neutrophil.

While MPO is most abundantly expressed in neutrophils it is also expressed in the lysosomes of monocytes (Ludemann et al., 1990). The cell surface expression of MPO in these cells has been shown to differ from that seen in neutrophils, with basal levels of cell-surface MPO expression without priming (Weidner et al., 2001). *In vitro* studies have shown that monocytes can be activated in a similar way to neutrophils by anti-MPO antibodies (Weidner et al., 2001). Signalling and molecular pathways associated with MPO surface expression on monocytes are not well defined and require further study. The importance of anti-MPO antibodies in the pathogenesis of AAV is illustrated by their use in several *in vivo* models of disease (Coughlan et al., 2012a).

1.2.3 **PR3**

PR3, like MPO, is also found in neutrophil azurophilic granules (Campanelli et al., 1990). It is one of a number of serine proteases whose main function is the breakdown of extracellular proteins during inflammation (Kao et al., 1988). There is also evidence for PR3 having direct microbicidal activity, with effects seen on both bacteria and fungi (Gabay et al., 1989). One of

the most interesting effects of PR3 is its interaction with cytokines and other compounds involved in the immune system, and thus it's potential to alter the immune response. In this regard, PR3 has been shown to cleave pro-interleukin (IL)-1β resulting in IL-1β release (Dinarello, 2011), inactivate IL-6 (Bank et al., 1999) and activate TGFβ (Csernok et al., 1996). These effects suggest a possible dual role for PR3 with both pro inflammatory and anti-inflammatory effects being observed. The anti-inflammatory role is also emphasised by the ability of PR3 to inhibit NADPH oxidase and thus inhibit the immune response (Tal et al., 1998). Interestingly, PR3 has also been shown to upregulate the important neutrophil chemokine IL-8, which may result in increased neutrophil trafficking to sites of PR3 release (Padrines et al., 1994).

Unlike MPO, PR3 has been shown to be expressed on unstimulated neutrophils in a bimodal pattern (Halbwachs-Mecarelli et al., 1995), with different phenotypes being observed between cells which express high levels of membrane PR3 ($mPR3^{high}$) vs those that are $mPR3^{low}$ (Schreiber et al., 2004). High levels of $mPR3^{high}$ cells have been associated with a risk of GPA, as well as rheumatoid arthritis (Rarok et al., 2002, Witko-Sarsat et al., 1999). As PR3 does not contain a transmembrane domain its surface expression, similar to MPO, involves its association with other proteins. This interaction is well described in neutrophils, with PR3 associating with the GPI-linked protein CD177 (also known as neutrophil binding protein (NB)-1) on the majority of cells (von Vietinghoff et al., 2007). This interaction has been demonstrated by co-localisation experiments and also by demonstration that the hydrophobic patch on PR3 can bind to CD177 (Bauer et al., 2007, Hajjar et al., 2008). It has also been shown that in order to be $mPR3^{high}$ a neutrophil must express both CD177 and PR3 (Jerke et al., 2011).

Due to the lack of a transmembrane signalling domain on both proteins, the mechanism though which the PR3:CD177 complex signals in response to anti-PR3 antibody binding is not fully understood. It is likely that this signalling occurs through interactions with other cell surface proteins, in fact, PR3:CD177 has been shown to be part of lipid rafts which also contain the Mac-1 complex as well as the FcγRIIIb (David et al., 2003, David et al., 2005) (**Figure 1.1**). Signalling by anti-PR3 is therefore likely to be similar to the signalling of anti-MPO antibodies with CD11b and CD18 providing the transmembrane component (Jerke et al., 2011). Interestingly, some neutrophils which express surface PR3 do not co-express CD177. In these cells the method by which PR3 is anchored to the surface is thought to be through insertion into the plasma membrane via interactions between amino acid residues (Hajjar et al., 2008). The method through which anti-PR3 binding signals in these cells is yet to be elucidated but it is likely that lipid raft formation, and subsequent clustering of signalling proteins, plays an important role.

Surface expression of PR3 on monocytes has been relatively understudied in the literature, however, anti-PR3 antibodies have been shown to activate these cells *in vitro* (Ralston et al., 1997). Unlike MPO the pathogenic effects of anti-PR3 antibodies have not been fully shown *in vivo*. This is largely due to the absence of a suitable mouse model in which to induce disease. Recently, humanised mice, which have a functional human immune system, have been used to overcome this lack of *a* suitable model. These models have shown promise in providing an *in vivo* system to study anti-PR3 ANCA and their use is discussed in more detail later. Despite the lack of *in vivo* models, the large amount of *in vitro* evidence indicates a prominent role for anti-PR3 antibodies in disease.

1.2.4 **Other ANCA targets**

While anti-MPO and anti-PR3 antibodies are the autoantibodies most frequently associated with AAV, autoantibodies directed against other antigens can also occur in AAV patients. These include antibodies directed against other antigens found in the granules of neutrophils such as lysosomal membrane protein (LAMP)-2, elastase, cathepsin G and lactoferrin. LAMP-2 antibodies were initially described by *Kain et al* and have actually been found to be more prevalent in patients (up to 93%) than the more commonly known ANCA (Kain et al., 1995, Kain et al., 2008). *Kain et al* have also shown *in vitro*, that neutrophils treated with monoclonal anti-LAMP-2 antibodies release MPO and cause vascular damage, indicating a potential role for these antibodies in disease (Kain et al., 2008). This group have also suggested that LAMP-2 antibodies may play a role in the initial break in tolerance in patients, and this break may be due to molecular mimicry between LAMP-2 and the bacterial protein FimH. Anti-elastase antibodies have been shown to elicit a c-ANCA pattern similar to anti-PR3 antibodies, while cathepsin G and lactoferrin display a p-ANCA pattern similar to anti-MPO. The clinical relevance of these antibodies remains unclear however they have all been found at varying frequencies in patients suggesting a possible role in disease (Nishiya et al., 1999, Talor et al., 2007). Due to their similar staining patterns, these antibodies may lead to discrepancies in anti-MPO and anti-PR3 detection assays and their potential role in disease requires further study.

1.3 Immunology of AAV

1.3.1 **Neutrophils**

Neutrophils are polymorphonuclear cells involved in the innate immune response. They are short lived cells which survive for 1-2 days in the circulation, and account for approximately 70% of circulating leukocytes. Neutrophils play an important role in the initial immune response to infection as they are usually among the first cells to encounter immune stimuli. This initial response is often important in activating the overall immune response with other cells being

recruited and activated at a later stage. Although they have beneficial effects in their role in fighting infection, neutrophils have also been shown to have negative effects in some conditions. These effects have resulted in several studies claiming that neutrophils can be both friend and foe to the host, depending on the conditions and stimulus met (Lowe et al., 2012, Drescher and Bai, 2013, Fridlender and Albelda, 2012).

In response to immune stimuli, such as bacterial infection, cancers, or environmental exposure, neutrophils can transmigrate to sites of inflammation (Craig et al., 2009, Liang and Ferrara, 2016, Jacobs et al., 2010). This process occurs through extravasation from the circulation in response to chemokines such as IL-8 and C5a (Zeilhofer and Schorr, 2000, Ehrengruber et al., 1994). The main effector functions of these cells are to directly phagocytose material, to produce microbicidal compounds capable of killing bacteria and to produce cytokines and chemokines which propagate the immune response (Amulic et al., 2012). As mentioned previously, the majority of research into the pathogenesis of AAV has focused on the role of the neutrophil in disease. The evidence for the importance of neutrophils in AAV is derived from both *in vitro* and *in vivo* studies. *In vitro*, ANCA have been shown to cause neutrophil degranulation and respiratory burst, along with increased inflammatory cytokine release resulting in damage to endothelial cell walls (Falk et al., 1990, Brooks et al., 1996, Savage et al., 1992). While activation of these cells requires ANCA binding to antigen and Mac-1 activation as discussed above, in order to be fully activated binding of the Fc portion has been shown to be required through the FcγIII receptor CD16. Interestingly, this binding is thought to occur through both interactions with neighbouring neutrophils as well as in *cis* interactions on single cells (Fig1.1) (Hewins and Savage, 2003). This CD16 binding emphasises the important role of this molecule in ANCA pathogenesis.

The particular importance of these cells has been demonstrated *in vivo*, where depletion of neutrophils abrogated disease in a passive transfer mouse model (Xiao et al., 2005). Clinically, neutrophils are found in biopsies of affected glomeruli in patients and the number of activated neutrophils found in this area correlates with disease severity (Brouwer et al., 1994). The current model of disease pathogenesis in AAV places neutrophils as the primary instigators of vascular damage. In this model neutrophils are primed through an external stimulus which leads to the expression of PR3 and MPO on the cell surface. This priming allows for the binding of ANCA leading to activation of the neutrophil in the form of degranulation which leads to vascular damage (**Figure 1.2**).

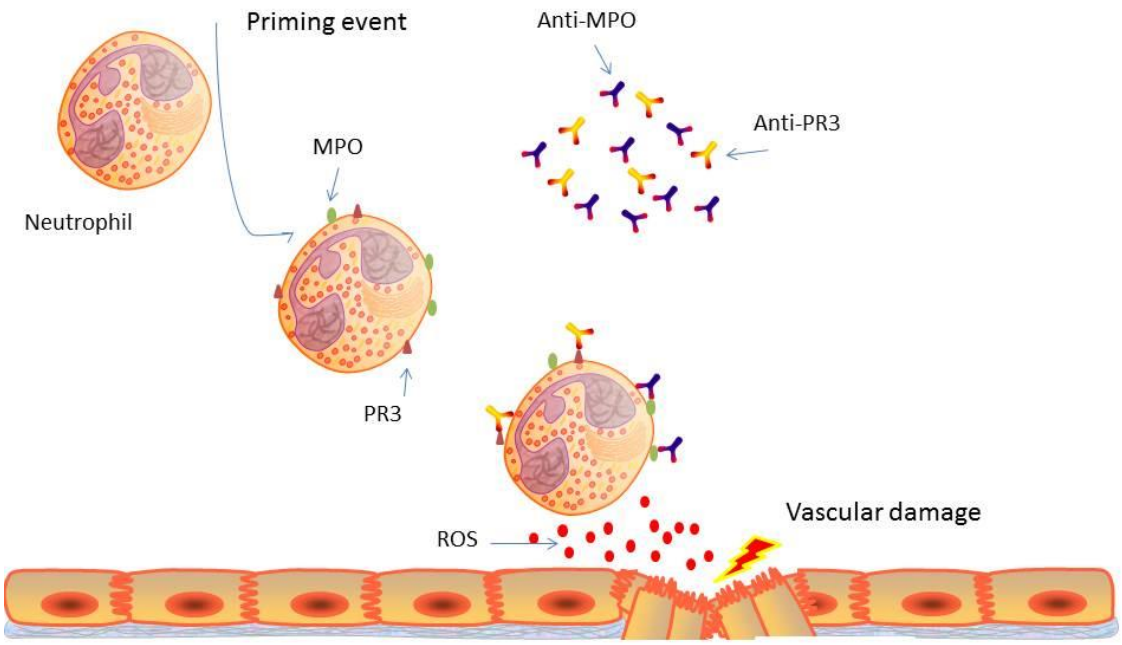

Figure 1.2 Current model of neutrophil driven damage
The current model of AAV postulates that neutrophils are primed by a stimulus such as infection. This priming leads to surface expression of MPO and PR3. This expression allows ANCA antibodies to bind and activate the cell resulting in vascular damage.

1.3.2 **Monocytes**

Monocytes are mononuclear cells of the myeloid lineage making up approximately 10% of human leukocytes in blood. Together with macrophages they are often referred to as mononuclear phagocytes (Ziegler-Heitbrock et al., 2010). These cells derive from bone marrow precursors and are found in the circulation for only a few days before either sequestration in the spleen or migrating to different tissues and developing into macrophages or dendritic cells (DCs) (Ziegler-Heitbrock, 2015). The main function of monocytes is in immune defence, as well as playing a role in homeostasis and tissue repair. Monocytes can mediate an immune response directly through phagocytosis as well as through release of cytokines and other inflammatory mediators such as reactive oxygen species (ROS) (Serbina et al., 2008). The transmigration of monocytes from the circulation and differentiation into monocyte-derived macrophages is also vital for an adequate immune response to infection (Shi and Pamer, 2011). These macrophages have an initial pro-inflammatory phenotype which can switch to a more anti-inflammatory and wound healing role in tissue remodelling post infection. The recruitment of monocytes from the vasculature to tissues is mediated by chemokines.

Monocyte chemoattractant protein (MCP) 1, 2, 3 and 4 are chemokines of the CCL family which are important in mediating transmigration of monocytes into tissues (Deshmane et al., 2009).

Initially monocytes were defined based on their appearance under light microscopy. These cells contained a unilobed nucleus which was kidney-shaped. With the development of flow cytometry, surface markers were found which could be used to define these cells. Several markers can be used to define monocytes with the most commonly used being the co-receptor for LPS, CD14. Defining monocytes in this way also allowed for the classification of subpopulations based on their expression levels of the FcγIII receptor CD16. These subpopulations were found to have differing roles in host defence. Initially these subsets were divided into CD16- and CD16+ populations (Ziegler-Heitbrock et al., 1991). These subpopulations were categorised as being inflammatory (CD14++ CD16-) and resident (CD14+CD16+) monocytes (Geissmann et al., 2003). The CD16+ population has since been further subdivided so that three current monocyte subsets are defined in the literature (Ziegler-Heitbrock and Hofer, 2013). These subsets are; classical (CD14++CD16-), intermediate (CD14++CD16+) and non-classical (CD14+CD16++) (**Figure 1.3)**. The relationship between these different subsets and whether they represent different cell types or simply transitional developmental stages is poorly understood, however, several key physiological differences have been found between the three groups. These subsets have been implicated as having a role in diseases such as rheumatoid arthritis (Rossol et al., 2012), sarcoidosis (Heron et al., 2008), severe asthma (Moniuszko et al., 2009) and atherosclerosis (Woollard and Geissmann, 2010)

1.3.2.1 Classical monocytes

Classical monocytes are the most abundant monocyte subset found in humans. These cells are highly responsive to TLR agonists and have been shown to produce high levels of IL-10, IL-6, IL-8 and MCP-1 in response to these stimuli (Cros et al., 2010). In addition to their cytokine producing functions, classical monocytes have also been shown to act as scavengers and to have strong phagocytic functions (Yang et al., 2014). These effector functions are supplemented by the production of ROS and anti-microbial enzymes such as myeloperoxidase in these cells upon activation (Wong et al., 2011). In spite of their strong phagocytosing ability these cells are thought to have poor antigen presenting capabilities (Liaskou et al., 2013, Cros et al., 2010). They are therefore likely to play a role in other aspects of the immune response. In particular, gene expression analysis indicates that these cells may have a prominent role in wound healing and tissue repair (Wong et al., 2011).

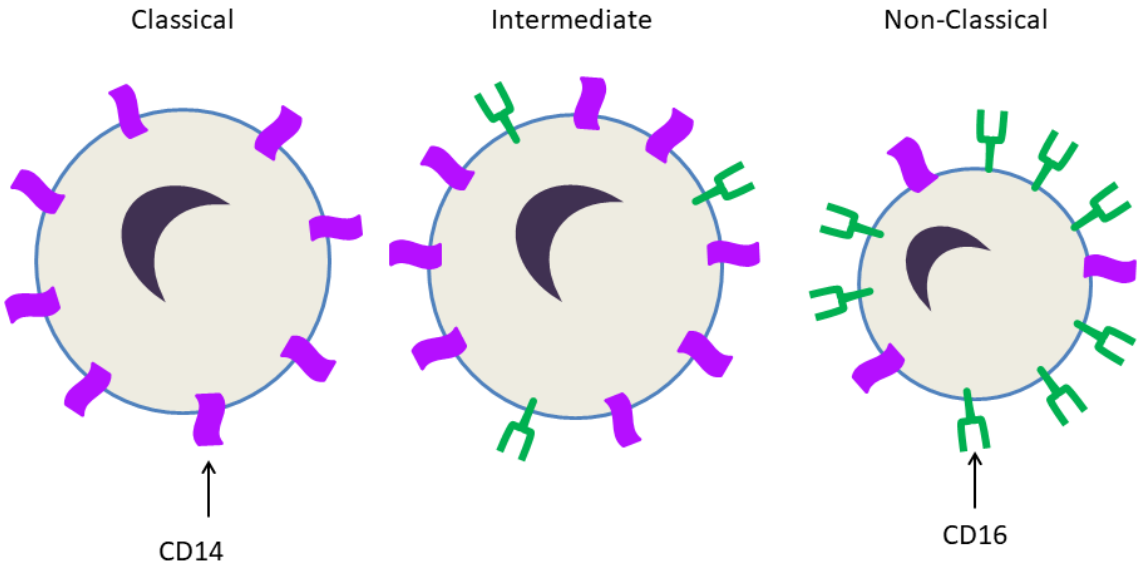

Figure 1.3 Identifying markers for monocyte subsets
Surface markers used to identify classical (CD14++CD16-), intermediate (CD14++CD16+) and non-classical (CD14+CD16++) monocytes.

1.3.2.2 Intermediate monocytes

The intermediate monocyte subset was initially thought of as a transitional stage in monocyte development however, recently, this subset has become the subject of increased scrutiny in disease. The suggestion that cells are transitional is largely based on genetic analysis which showed that some aspects of their gene expression profile was somewhere between that of the classical and non-classical subsets (Wong et al., 2011). On the other hand, these cells have an interesting collection of genes which were expressed at higher levels than those seen in either of the other two subsets. These included antigen processing genes, such as CD40, CD74 and HLA-DR, and inflammation related genes such as TGFβ1, AIF1 and PTPN6 (Zawada et al., 2011). These variations in gene expression suggest possible unique functions for this cell type. Intermediate monocytes have phagocytic capacities similar to those seen in the classical subset (Cros et al., 2010). They have also been shown to produce a different cytokine profile in response to LPS signalling particularly showing an increase in IL-1β and TNF-α production (Cros et al., 2010). This increased proinflammatory cytokine production from these cells was also found using low density lipoprotein (LDL) uptake assays, indicating that they may have a more pro inflammation phenotype than classical or non-classical monocytes. Conflicting studies regarding this proinflammatory cytokine production have emerged with variability between research groups possibly due to non-standardised protocols for isolating these individual cell types (Wong et al., 2011, Thiesen et al., 2014).

1.3.2.3 Non-classical monocytes

The final, non-classical, subset has been referred to as patrolling monocytes. These cells are thought of as being highly differentiated due to their increased persistence in circulation in comparison to the other subsets (Liaskou et al., 2013). The patrolling nature of these cells is derived from their ability to adhere to and move along endothelial surfaces (Cros et al., 2010, Thomas et al., 2015). This movement mechanism allows these cells to sample antigens passing in the circulation more readily and for an increased period to allow activation. One of the distinguishing features of this subset is their smaller size when compared to the other two subsets (Stansfield and Ingram, 2015, Boyette et al., 2017). Interestingly, monocytes which differentiate into macrophages have been shown to increase in size suggesting that the non-classical subset may have a role in this regard in the immune response (Visioli et al., 2000). The exact immune functions of non-classical monocytes remains unclear with studies showing they have only weak phagocytic ability as well as little or no inflammatory cytokine production (Cros et al., 2010). This subset is therefore likely to have a role in sensing pathogens and injury rather than having a major role in the effector response.

1.3.2.4 Monocytes in AAV

While neutrophils have been the main cell studied in AAV, monocytes have also been implicated in the disease since its first description. In fact, when the antibodies of interest were first discovered they were known as anti-cytoplasmic antibodies (ACPA) to reflect their binding to different cell types (van der Woude, 1985). As neutrophils become the primary focus of study the term ANCA became more predominantly used. The importance of monocytes in disease is indicated by several clinical characteristics of patients with AAV. In patients with kidney involvement, monocytes/macrophages are the predominant infiltrating immune cell found in the glomeruli in biopsies from early stages of disease (Zhao et al., 2015). MCP-1 levels are also found to be increased in patient kidney biopsies indicating a mechanism by which monocytes may be recruited to the areas of damaged tissue (Tam et al., 2004).

The presence of these cells in the early lesions along with the fact macrophages are the dominant cell type in the later stages of ANCA GN suggests they are important throughout the course of disease (Jennette and Falk, 2015). Monocytes are likely to be particularly important in GPA due to their involvement in granuloma formation. Monocytes, along with neutrophils, make up the centre of the granuloma with other immune cells being present around the periphery (Csernok and Gross, 2013). The interaction of monocytes with T cells in the granuloma is likely to be an important mediator of pathology in granulomatous disease, although the exact mechanism and interactions are yet to be fully elucidated (Brunini et al., 2016). Aberrant T cell populations are thought to be involved in AAV and are discussed below. Briefly, monocytes are thought to interact with CD4+ T cells in the granuloma of GPA patients, which can lead to a polarisation to T_H17 cells (Evans et al., 2009). Therefore, monocytes could be important in driving the transition from more localised inflammation of the respiratory tract to systemic disease often seen in later stage GPA. More recently, monocytes have also been heavily implicated in crescent formation in anti-MPO driven disease, with depletion of these cells resulting in loss of disease in mice (Rousselle et al., 2017). These data emphasise the potentially important role for these cells in disease.

1.3.3 **Other immune cells**

Other immune cells are also thought to be involved in the pathogenesis of AAV. As would be expected in a disease thought to be driven by autoantibody production, B cells have been implicated. The key role for B cells, and ANCA, in disease pathogenesis is emphasised by the success of Rituximab treatment in patients (Rhee et al., 2010). Rituximab treatment results in depletion of CD20+ B cells and therefore prevents ANCA production. In addition to their role in antibody production in the normal immune response, B cells also have a role in antigen presentation to T cells. A subset of these cells produce IL-10 and are involved in the regulation of T cells. The role of these IL-10 producing regulatory B cells (B_{reg}) cells has been implicated in the pathogenesis of disease, with one study showing that AAV patients have impaired functionality in these cells (Wilde et al., 2013). There are however conflicting results with regard to this loss of functionality with another study showing that only the frequency, but not the functionality, of B_{reg} cells is reduced in AAV patients (Todd et al., 2014). This understudied cell type requires further research to fully establish its importance in disease.

Along with B cells, T cells are the other major arm of the adaptive immune response. These cells have also been implicated in AAV pathogenesis with T cells being found in the inflammatory lesions in kidney and lung of patients, as well as being present in granulomas found in GPA (Wilde et al., 2010). The role of T cells in disease is likely to mainly involve T helper (T_H) cell activation of B cells to produce antibody. This role, along with defects in regulatory T (T_{reg}) cell functions which suppress autoimmunity (Lepse et al., 2011) and even direct damage to the endothelial surface by a subset of these cells (de Menthon et al., 2011), is likely to be important in disease. T_H cells are mainly divided into three subtypes based on cytokine production and inflammatory phenotype. These are; pro-inflammatory T_H1 cells, anti-inflammatory T_H2 cells and IL-17 producing T_H17 cells. The role of these cells in AAV is thought to vary, with T_H1 cells being found mainly in lesions in localised disease while T_H2 cells are more associated with systemic manifestations (Lepse et al., 2011, Sanders et al., 2006, Csernok et al., 1999).

T_H17 cells are of particular interest in AAV as these cells have been implicated in several other autoimmune diseases (Tabarkiewicz et al., 2015) and have been shown to be present in increased frequencies in AAV patients (Abdulahad et al., 2008). IL-17A, the predominant cytokine produced by Th17 cells, has also been shown to induce IL-1β and TNF-α production from macrophages as well as to recruit neutrophils (Chen et al., 2013) which may play a role in developing a proinflammatory environment at sites of vascular damage in patients. Interestingly, cytokines produced by neutrophils in response to anti-MPO stimulation, such as IL-6, IL-17 and IL-23, have all been shown to promote T_H17 cells indicating a possible feedback mechanism (Gan et al., 2010).

T_{reg} cells function to inhibit aberrant immune responses and maintain self-tolerance in a normal immune system. These cells have been shown to be dysfunctional in AAV patients which may help to explain how autoreactive cells develop (Free et al., 2013). Studies reporting the proportion of T_{reg} cells found in AAV patients have shown conflicting results, however, each study has found a similar lack of functionality in these cells (Abdulahad et al., 2007, Rimbert et al., 2011, Morgan et al., 2010). T_{reg} cells are involved in suppression of T_H17 cell responses and this lack of function may explain the increased proportion of the later cell type in patients (Fletcher et al., 2009). T cells are emerging as important cells in the pathogenesis of AAV and more research is required to elucidate the exact role these cells play both in the development and progression of the disease.

1.3.4 **Complement in AAV**

The complement system is a series of proteins, mainly protease enzymes, which aid in the immune response to pathogens. The effects of this pathway are mediated in three main ways; opsonisation of bacteria and target cells, pore formation in bacterial plasma membranes and chemoattractant effects. The proteins in the complement system are present mainly as inactive membrane bound precursors. These proteins are then activated by proteolytic cleavage in a cascade leading to their effector functions. The complement system consists of three main pathways of initial activation; the classical, mannose binding lectin (MB), and alternative pathways. Although initial activation may differ in each pathway they each converge when the C3 convertase enzyme is activated. Two of the main components of the complement system are C3a and C5a. These two proteins act as chemokines and have strong chemoattractant effects on neutrophils (Ehrengruber et al., 1994).

Complement is also important in the clearance of antibody-antigen complexes, known as immune complexes. In a normal immune response complement binds to immune complexes to increase their opsonisation and solubility. When complement proteins are not functioning correctly, such as in some autoimmune diseases, there is a reduction of this solubility and this can lead to immune complex deposition (Markiewski and Lambris, 2007). Due to the lack of immune deposits associated with AAV, complement had largely been thought of as being unimportant in disease. Recently, however, *in vivo* experiments have indicated that complement is important in disease. *Xiao et al* have shown that depletion of complement completely abrogates the pathogenic effect of anti-MPO antibodies passively transferred into $MPO^{-/-}$ mice (Xiao et al., 2007). These data have been supported by human studies where complement components have an increased prevalence in renal biopsies from AAV patients compared to controls (Xing et al., 2009, Chen et al., 2009). ANCA stimulated neutrophils have been shown to be primed by C5a (Xiao et al., 2014), as well as to activate

the complement pathway (Xiao et al., 2007), which may result in a positive feedback loop recruiting more neutrophils which can then be activated.

1.3.5 Inflammatory cytokines

Cytokines are a group of structurally diverse, small proteins which are involved in signalling between cells and can be released by many different cell types in the body. Cytokines can be involved in cell proliferation, activation, apoptosis, and in the recruitment of cells to sites of infection or injury. In the context of immunity the recruitment of cells to the site of infection is particularly important. This occurs through specific cytokines known as chemokines (Rollins, 1997). Chemokines are released by immune cells in response to antigen and also by epithelial cells in response to pro-inflammatory cytokines.

1.3.5.1 IL-1β

IL-1β is a member of the IL-1 family of cytokines. It is produced as a non-biologically active 30kDa protein (pro-IL-1β) and requires cleavage in order to carry out its effector functions (Dinarello, 2009). Once the pro form has been cleaved a 17kDa active IL-1β protein can be secreted by the cell where it has a role in activation of other immune cells as well as inducing further cytokine release from endothelial cells (Johnson et al., 2005). IL-1β is often seen as a danger signal to the immune system due to its release from innate immune cells such as monocytes and macrophages. Levels of IL-1β have been shown to be increased in several autoimmune diseases such as rheumatoid arthritis, type-2 diabetes and psoriasis (Kay and Calabrese, 2004, Dinarello et al., 2010, Schon et al., 2001). Systemic levels of IL-1β have been shown to be unchanged in AAV patients (Nogueira et al., 2010), however, this cytokine is found to be produced by cells in the kidneys of patients with GPA suggesting a more localised function in disease (Noronha et al., 1993). The production of this cytokine is heavily linked to changes in cellular metabolism which will be discussed later.

1.3.5.2 IL-6

IL-6 is a pleiotropic cytokine with several functions in the immune response. Initially, this cytokine was described based on its ability to differentiate and expand T cells and cause B cell differentiation (Klimpel, 1980, Yasukawa et al., 1987). As well as this role in immune cell function, IL-6 has since been described as having ‘hormone-like’ effects affecting lipid metabolism, insulin resistance and mitochondrial activities (Hunter and Jones, 2015). IL-6 production is induced from both immune and stromal cells by other cytokines such as IL-1β (Tosato and Jones, 1990). IL-6 also has important functions in neutrophil activation (Wright et al., 2014) and trafficking (Fielding et al., 2008) suggesting it may have a role in AAV. This

hypothesis is supported by data showing that blocking the IL-6 receptor is beneficial as a treatment (Berti et al., 2015).

1.3.5.3 Other cytokines

Other cytokines have also been suggested to have a role in the pathogenesis of AAV. IL-8 is a chemokine which induces neutrophil chemotaxis and can increase phagocytosis in these cells (Dixit and Simon, 2012, Harada et al., 1994). IL-8 production has been shown to be upregulated by monocytes *in vitro* in response to ANCA stimulation (Ralston et al., 1997). Tumour necrosis factor (TNF)-α is another cytokine which has been implicated in disease. Similar to IL-1β, TNF-α production occurs *in situ* in the lesions of patients (Noronha et al., 1993). This cytokine is involved in regulation of the immune system and can be induced by several stimuli such as lipopolysaccharide (LPS), bacterial products and IL-1. The main immune cell functions of TNF-α derive from its interactions with endothelial cells (Bradley, 2008). This results in the upregulation of adhesion molecules which allows for transmigration of cells to sites of infection (Munro et al., 1989). The role of TNF in AAV is thought to be as a result of increased trafficking of neutrophils and other immune cells to the sites of vascular damage as well as providing priming effects on neutrophils (Hess et al., 2000, Harper et al., 2001b). *In vivo* models of disease have shown that TNF-α levels are increased in diseased animals compared to controls and that inhibition of this cytokine results in reduced disease severity (Ishida-Okawara et al., 2004, Huugen et al., 2005). In patients, inhibiting TNF-α resulted in a slight improvement in patient outcomes however, this improvement was not as consistent as that seen in patients treated with rituximab (Jarrot and Kaplanski, 2014). These data indicate a potential role for TNF-α in disease however, this is unlikely to be pivotal for disease progression.

1.4 Animal models of AAV

1.4.1 Anti-MPO models

The availability of murine models of disease has greatly increased our knowledge of a wide variety of conditions from cancer and autoimmune diseases to infection and obesity (Cheon and Orsulic, 2011, Lee et al., 2012, Lutz and Woods, 2012). The elucidation of anti-MPO antibody driven AAV has been aided greatly by the availability of several *in vivo* models (**Table 1.1**). These models have helped to provide evidence for the pathogenic effects of anti-MPO and have allowed for a greater understanding of the mechanisms behind disease. No one model perfectly replicates disease and therefore each model has advantages and disadvantages depending on the research question being asked. Some of these models are discussed in detail below.

1.4.1.1 Spontaneous cresentic glomerulonephritis/Kinjoh (SCG/Kinjoh)

SCG/Kinjoh mice are an inbred strain which have been selectively bred to have high glomerular crescent formation. These mice spontaneously produce anti-MPO antibodies and develop necrotising vasculitis and crescentic glomerulonephritis (Neumann et al., 2003). The main advantage of this model is the autoimmune nature of disease similar to human disease. There are however several drawbacks to using these mice to study disease. These include the presence of anti-nuclear antibodies which may contribute to kidney injury and the presence of immune complex deposition which is not seen in the human disease.

1.4.1.2 Experimental autoimmune vasculitis

Unlike the majority of the models used to study AAV to date the experimental autoimmune vasculitis (EAV) model uses rats as opposed to mice. This model was developed using WKY rats which are susceptible to the induction of glomerulonephritis (Little et al., 2005). The susceptibility of these rats to disease induction derives from a specific polymorphism in the *Fcgr3* gene. This gene encodes FcγRIII CD16. This polymorphism leads to increased activation of the CD16 receptor which leads to macrophage overactivity and susceptibility to glomerulonephritis (Aitman et al., 2006). Immunisation of WKY rats with human MPO results in the generation of antibodies directed against hMPO. These antibodies can also cross react with rat MPO which generates the pathogenic phenotype. Pauci-immune crescentic GN develops in approximately 60% of animals within 6-8 weeks of immunisation. The lack of total disease induction is a particular drawback of this model along with the relatively mild form of disease developed. In order to improve the number of animals developing disease, complete Freund's adjuvant and pertussis toxin has been used (Little et al., 2009). While this approach did improve the susceptibility of the animals to disease it also introduces additional variables reducing the ability of this model to mirror the human disease. This model has also been only shown to induce disease in WKY rats with other strains showing no signs of disease. This indicates a strong genetic component which may confound the design of some experiments in these animals (Coughlan et al., 2012a).

Model		Advantages	Disadvantages
SCG-Kinjoh mice		• Spontaneous autoimmune disease • Robust disease observed (Crescents present)	• Other autoantibodies present besides ANCA • Not Pauci-immune
Experimental autoimmune vasculitis		• Model is autoimmune	• Only WKY rats susceptible • Relies on human rather than rat MPO
Passive transfer models	Transfer of IgG from $MPO^{-/-}$ mice	• Simple controllable model for studying direct effect of ANCA • Quick readout	• Not autoimmune • No cellular immunity to MPO • Mild disease
	Transfer of splenocytes from $MPO^{-/-}$ mice	• Robust disease	• Immune deposits in kidney
$MPO^{-/-}$ Bone marrow transplant mice		• Allows the study of direct effects of ANCA • Disease is induced by circulating antibody without need for IgG isolation	• Not autoimmune • No cellular immunity to MPO • Mild disease

Table 1.1: Animal models of Anti-MPO ANCA vasculitis.
Some of the models used in the study of AAV. (Adapted from (Coughlan et al., 2012a))

1.4.1.3 Passive transfer models

The passive transfer model of AAV involves the generation of anti-MPO antibodies by immunising $MPO^{-/-}$ mice and the transfer of these antibodies into wild-type mice to induce disease. These antibodies have been shown to generate a focal necrotising crescentic GN in the recipient mice 1 week post injection (Xiao et al., 2002). This model was one of the first to show a direct pathogenic effect of ANCA in an *in vivo* setting. While the disease seen in these mice was mild (~5% glomeruli affected), the impact this finding had on the field was considerable. The same group also showed that disease severity can be improved in this model by transferring splenocytes from the MPO immunised $MPO^{-/-}$ mice into recombinase activating gene (RAG)-$2^{-/-}$ mice. $RAG2^{-/-}$ mice lack T and B cells and this system resulted in crescent development in 80% of glomeruli (Xiao et al., 2002). Unfortunately, this model also resulted in significant immune complex deposition which limits its suitability to model the human condition.

1.4.1.4 Bone marrow transplant model

Similar to the passive transfer model described above, this model involves the immunisation of $MPO^{-/-}$ mice with MPO. However, rather than transferring the anti-MPO antibodies produced into wild-type animals, the immunised mice are irradiated prior to receiving wild-type bone marrow (Schreiber et al., 2006). Due to the radio resistant nature of plasma cells, anti-MPO antibody levels remain high following irradiation. These antibodies can then activate cells produced from the new bone marrow which express MPO, leading to the induction of disease. The main advantage of this model over the previous model is the presence of cells which constitutively produce antibody rather than the transient administration of IgG (Coughlan et al., 2012a). The biggest hindrance to the use of this model to study disease is that crescentic GN does not develop until 8 weeks post bone marrow transplant.

1.4.2 **Anti-PR3 models**

All of the models outlined above use MPO in order to induce disease with varying degrees of similarity to that seen in humans. These models have allowed for greater elucidation of the mechanisms behind anti-MPO antibody driven disease and have been important in the development of new drug targets. *In vivo* models of anti-PR3 driven disease have proven much more difficult to establish. This difficulty is thought to be as a result of differences between the structure and expression of human and mouse PR3. Antibodies raised against human PR3 target epitopes not present on rodent PR3 (Pfister et al., 2004). Interestingly, Pfister et al found that immunising PR3 and neutrophil elastase double deficient mice with murine PR3 led to anti-PR3 specific antibodies but no disease. This lack of disease is thought to be due to PR3 not being expressed on the surface of isolated mouse neutrophils in the same way as it is on human cells (Pfister et al., 2004). Other studies have shown that immunisation of mice with chimeric human/mouse PR3 leads to high titres of anti-PR3 antibodies however, again no disease was observed in these animals (van der Geld et al., 2007).

1.4.3 **Humanised mice**

The models described previously have provided a valuable surrogate for experimentation using human subjects which has several ethical, moral and financial constraints. The benefit of these model organisms largely derives from the similar biology of mice and humans. While there are numerous similarities between the two species the divergence of evolution has resulted in differences in the some responses which can limit the translational value of using a mouse model (Constantinescu et al., 2011), as seen in attempts to generate anti-PR3 models of AAV. In order to compensate for the differences between these two organisms, the concept of mice which could be given more human-like characteristics was theorised. Initial experiments in this regard proved largely unsuccessful. These experiments, attempted in nude mice which lack T cells, failed to support the growth of human cells (Ganick et al., 1980).

Following this, it was shown that low levels of human cell engraftment could be obtained in mice which had severe combined immunodeficiency (SCID). These mice lacked both T and B cells which reduced the rejection of the injected human cells. The next breakthrough in creating humanised mice came when these SCID mice were crossed onto non-obese diabetic (NOD) mice which have defects in NK cell, macrophage and complement activity (Shultz et al., 1995). These mice dramatically improved engraftment levels, however, problems remained with residual NK cells being present and with these mice having a short lifespan (Lowry et al., 1996, Shultz et al., 2007). The final piece of the humanised mouse puzzle came with the development of NOD-SCID mice which were also deficient for the IL-2 receptor gamma (IL-2rγ) chain. This deficiency led to a complete loss of NK cells resulting in an improved

environment for human cell engraftment (Cao et al., 1995). These mice also had increased lifespans compared to the previous NOD-SCID strain allowing for increased potential for their use as an experimental model (Shultz et al., 2007).

While NOD-SCID IL-2rγ$^{-/-}$ (NSG) mice are the most commonly used strain to create humanised mice, other immunocompromised strains containing the IL-2rγ$^{-/-}$, such as BALB/c-RAG-2$^{-/-}$ IL-2rγ$^{-/-}$ (RAG$^{-/-}$) mice, can also be used (Brehm et al., 2010). The predominant use of the NSG strain is as a result of increased engraftment levels in these mice when compared to RAG$^{-/-}$ mice (Brehm et al., 2010, Stoddart et al., 2011). Recently, studies have attempted to increase the levels of human engraftment using mouse strains based on NSG or RAG$^{-/-}$ backgrounds which have inserted human cytokine genes. The use of NSG mice with genes for human cytokines is described in **Chapter 5**. Two main strains of RAG$^{-/-}$ mice have been used to increase engraftment by insertion of human genes. Mice with knocked in human M-CSF, IL-3 GM-CSF and thrombopoietin (Tpo), named MITRG, or M-CSF, IL-3, GM-CSF, Tpo and bacterial SIRPα (MISTRG) have been shown to increase human cell engraftment in RAG$^{-/-}$ background animals (Rongvaux et al., 2014). These different strains have different advantages and disadvantages as model systems outlined in Table 1.2 The reconstitution of a human immune system in these mice involves the administration of human cells or tissue to the immunocompromised animals. The cells and methods used can therefore vary. The most commonly used methods are outlined in **Figure 1.4** and the main advantages and disadvantages are summarised in **Table 1.3**.

The first method involves the intravenous (I.V.) injection of human peripheral blood leukocytes. NSG mice are the strain most commonly used to develop this model largely due to the difficulties associated with conditioning BALB/c-RAG-2$^{-/-}$ IL-2rγ$^{-/-}$ mice to accept the peripheral blood leukocytes (van Rijn et al., 2003). The most common human cell type found in mice engrafted in this way are T cells. These mice are therefore useful in the study of effector T cell functions, however, the lack of interaction between the human leukocyte antigen (HLA) restricted T cells and the mouse major histocompatibility complex (MHC) provides a limitation to the work which can be performed using this model (Shultz et al., 2011).

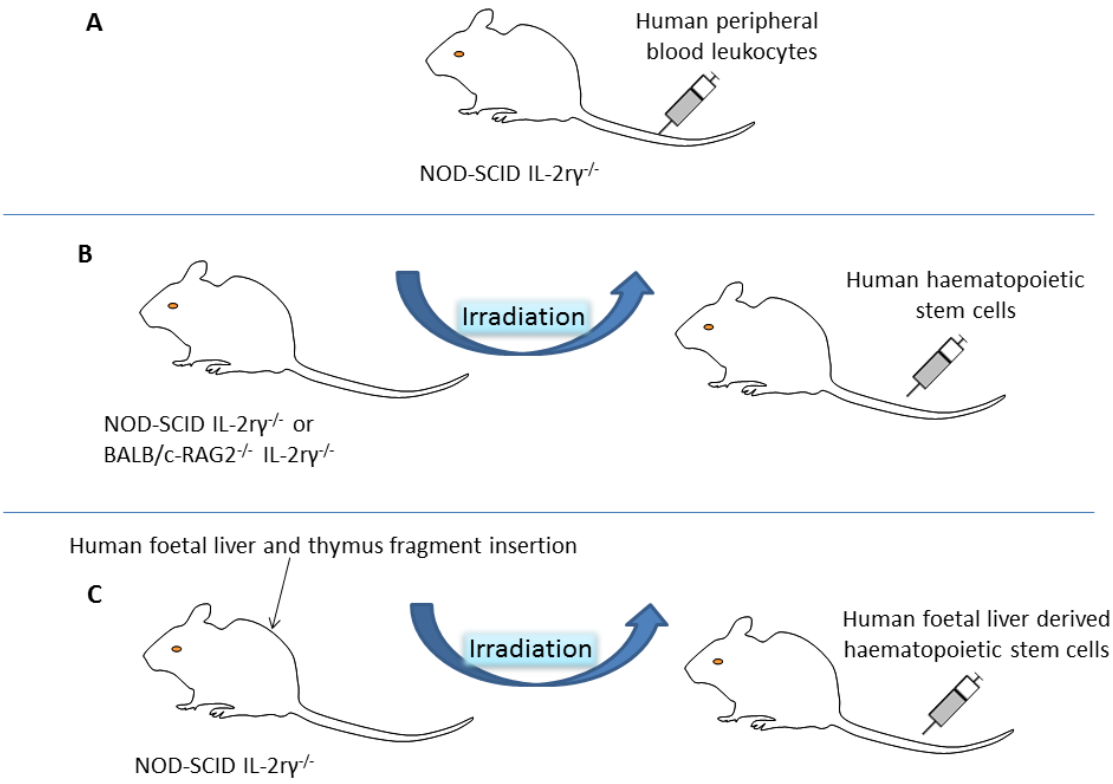

Figure 1.4 Methods for generating humanised mice.
The most commonly used methods for generating humanised mice are shown. NSG mice are injected with human peripheral blood leukocytes (**A**), NSG of BALB/c-RAG2$^{-/-}$ IL-2rγ$^{-/-}$ mice are irradiated and injected with human HSCs (**B**) or human foetal liver and thymus fragments are inserted beneath the kidney capsule of NSG mice before they are irradiated and injected with human foetal liver derived HSCs (**C**).

The second model commonly used involves the injection of human haematopoietic stem cells (HSCs) in place of peripheral blood leukocytes. These HSCs have the potential to develop into numerous cell types and therefore should provide a broader range of human immune cell types. These cells are also self-renewing meaning that model systems can be extended for longer periods of time (Metcalf, 2007). The HSCs used in this model are usually CD34+ cells isolated from either peripheral blood, bone marrow, foetal liver or umbilical cord blood. Mice humanised in this way require sub lethal irradiation to remove bone marrow cells before injection with the HSCs (Pearson et al., 2008). This is the most commonly used model in humanised mouse research due to the presence of human T, B, and NK cells along with myeloid lineage cells such as monocytes, granulocytes and dendritic cells (DCs) (Ito et al., 2012).

Strain	Advantages	Disadvantages
NSG	Efficiently engraft human cells (mainly T cells)	Low levels of myeloid engraftment
RAG-2$^{-/-}$	Can engraft human cells	Levels of engraftment are much lower than NSG mice
MITRG	Show increased human cell engraftment vs RAG$^{-/-}$ and NSG mice	Use of foetal tissue to engraft mice
MISTRG	Show increased human cell engraftment vs RAG$^{-/-}$ and NSG mice	Use of foetal tissue to engraft mice

Table 1.2 Advantages and disadvantages of humanised mouse strains.
Some of the mouse strains which have successfully engrafted human immune cells

The final model used to humanise mice involves the implantation of human foetal liver and thymus beneath the renal capsule of adult NSG mice. These mice are then irradiated and injected with foetal liver CD34+ cells. These mice have been shown to develop B cells, monocytes, DCs and T cells (Lan et al., 2006). In contrast to the previous models the T cells present in this model can be class I and class II restricted due to the presence of a human thymus like organ (Wege et al., 2008). The primary disadvantage of this model is the requirement for foetal tissue stem cells which can have ethical implications as well as being difficult to acquire.

The value of humanised mice as a model system for human disease is increasing. These animals have proven particularly useful in the study of diseases which have no murine equivalent such as HIV and Epstein-Barr virus (EBV), as well as in cancer and autoimmunity. HIV was one of the first pathogens studied in humanised mice due to the inability of this virus to infect mice. These mice acquire a similar phenotype to humans infected with HIV with a reduction in CD4+ T cells and a proliferation of CD8+ cells (Sun et al., 2007, Sato et al., 2010). The human foetal liver and thymus mice have been shown to be susceptible to HIV infection via a mucosal route further increasing the translational value of these mice (Sato and Koyanagi, 2011). Humanised mice have

Model	Human cells present	Advantages	Disadvantages
Peripheral blood leukocyte injection	T, B, and NK cells, monocytes/macrophages	Easy to reconstitute human cell populations, Strong effector T cell engraftment	Mainly T cells present, Human T cells don't interact with mouse MHC, Poor myeloid engraftment
HSC injection	T, B, and NK cells, monocytes/macrophages, DCs, granulocytes	Widest variety of human cells present, Self-renewing populations	Poor myeloid and T cell engraftment
Foetal liver and thymus transfer	T, B, and NK cells, DCs, monocyte/macrophages	Human thymic organoid development allows for HLA restricted T cell generation	Foetal tissue difficult to work with, Requires surgery, Poor myeloid engraftment

Table 1.3 Humanised mouse models.
Advantages and disadvantages of methods commonly used for the generation of humanised mice.

provided a mechanism where by not only the pathogenesis of HIV could be investigated but have also allowed for new therapeutic trials in this area (Choudhary et al., 2009). EBV is another interesting virus which only infects human cells. For this reason humanised mice are currently the only animal model of this disease (Ramer et al., 2011). The use of humanised mice in the study of this disease has led to the discovery that EBV plays an important role in development of B cell lymphomas (Ma et al., 2011) along with the discovery of a virally encoded tumour suppressor gene, EBNA3B, which reduces viral evasion and lymphomagenesis (White et al., 2012).

In the context of AAV, it has been suggested that humanised mice would provide a model for anti-PR3 disease. Cells in these mice should display human PR3 and therefore may be susceptible to disease following immunisation with anti-PR3 antibodies. *Little et al* have shown that mild disease can be induced in these animals and possible avenues to increase the severity of this disease are discussed in **Chapter 5**.

1.5 Immunometabolism

1.5.1 Cellular metabolism

Cells require adenosine triphosphate (ATP) in order to meet their energy needs. This ATP is generated by two mechanisms, namely oxidative phosphorylation (ox phos), a multistep, oxygen-dependent pathway leading to the generation of 32 ATP molecules for each glucose molecule taken into the cells, and glycolysis, which converts glucose to pyruvate and then lactate generating 2 ATP molecules per glucose molecule. Ox phos is generally employed by quiescent cells under normoxic conditions while glycolysis has been traditionally associated with hypoxic conditions. While the ATP yield from glycolysis is much lower than ox phos, the rate of production is much higher through this pathway (Pfeiffer et al., 2001). Certain cells have been shown to become more reliant on glycolysis for the production of ATP despite the presence of normal oxygen levels. This process of aerobic glycolysis has been particularly well studied in cancer cells where it is termed the “Warburg effect” (Warburg, 1956). The Warburg effect is thought to occur in these cells due to their need to rapidly proliferate. Using glycolysis to produce ATP allows for intermediates usually required for ox phos to be sequestered into producing biosynthetic precursors. These precursors can then be used to allow the cells to grow.

1.5.2 Metabolic changes in immune cells

In recent years it has become evident that changes in immune cell metabolism is important for these cells to function (Pearce and Pearce, 2013). Immune cells are largely inactive under resting conditions, however, they require rapid activation in response to immune stimuli and this activation has significant metabolic demands. The majority of the research into this area of immune cell metabolism, termed immunometabolism, has investigated changes in macrophages, DCs, and T cells in response to various stimuli. Macrophages and DCs have been shown to decrease ox phos along with a concomitant increase in glycolysis in response to lipopolysaccharide (LPS) stimulation (Tannahill et al., 2013). This reduction in ox phos occurs as a result of nitric oxide (NO) production which leads to inhibition of a number of electron transport chain (ETC) complexes (Beltran et al., 2000). This reduction in the ETC results in an upregulation of glycolysis in order to maintain mitochondrial membrane potential ($\Delta\psi_m$) and produce energy to ensure cell survival (Everts et al., 2012). Similar to cancer cells, these activated immune cells require increased biosynthetic precursors to proliferate and produce cytokines (Palsson-McDermott and O'Neill, 2013).

The classification of macrophages has proved contentious with suggestions that a new paradigm for describing these cells is required (Murray et al., 2014). The majority of studies on these cells discuss activated macrophages as being broadly classified into 2 groups, pro-

inflammatory M1 macrophages and anti-inflammatory M2 macrophages. While the concept M1 and M2 polarisation is important as a mechanism to study macrophage function, physiologically, macrophages are likely to exist along a spectrum of activation states. The phenotype of these cells is therefore likely to vary between tissue types as well as in response to different stimuli. Recently, the awareness of this spectrum has led to the suggestion that macrophages should be reclassified to better reflect their varying roles (Murray et al., 2014).

Although a new paradigm regarding the classification of these cells may be required, the majority of research in this area has used the M1 and M2 phenotypes. This is largely due the the ease of generation of these cells and the increased homogeneity of polarised populations. These cells have differing functions with M1 macrophages having important roles in the clearance of infection and damaged cells, and production of inflammatory cytokines such as IL-12, IL-1β and TNF-α, while M2 macrophages are involved in tissue repair and regulation of inflammation. As well as these functional differences these cells have been shown to have differing metabolic signatures. M1 macrophages switch to aerobic glycolysis upon activation where as M2 macrophages maintain ox phos similar to quiescent cells. The changes in metabolism between these two cell types are likely due in part to the differing time scales in which they perform their effector functions; M1 macrophages respond within hours to days while M2 macrophages have a longer-term resolution role (Galvan-Pena and O'Neill, 2014). As mentioned above, glycolysis is a much faster form of energy production than ox phos, and the need for the quick activation of M1 macrophages therefore makes this pathway seem the more logical option for energy production in these cells.

Although the rate of energy production is important, metabolic pathways have been shown to have other roles within these cells and therefore this change is likely to be functional on multiple levels. The link between shifting metabolic pathways and the polarisation of macrophages is emphasised by the fact that forcing an M1 macrophage into oxidative metabolism results in a more M2-like phenotype and like-wise making an M2 macrophage more glycolytic leads to an M1-like response (Rodriguez-Prados et al., 2010, Vats et al., 2006). The manner in which these metabolic changes can be translated to macrophages when viewed as a spectrum remains to be elucidated, however, it is likely that physiologically these cells also have a spectrum of metabolic profiles depending on the stimuli and tissue in which they reside and more research into the true nature of how macrophages respond in a physiological setting is required in order to contextualise the importance of these responses. The ways in which metabolic changes influence T cell fate and effector functions have also been extensively studied. In these cells, changes in metabolic profile have been shown to be required both in development and in mature cells (Ciofani and Zuniga-Pflucker, 2005, Janas et al., 2010, MacIver et al., 2013). During development, T cells upregulate glycolysis in order to begin differentiation into CD4+ or CD8+ cells (Rodriguez-Borlado et al., 2003). Inhibition of

this upregulation results in an increase in double positive or double negative T cells being released from the thymus demonstrating the instructive role that these metabolic pathways have on the cell (Rodriguez-Borlado et al., 2003). Upon their release from the thymus, naïve T cells have switched back to ox phos similar to the majority of quiescent cells (Buck et al., 2015). In secondary lymphoid organs, upon stimulation by antigen presenting cells (APCs), T cells upregulate both glycolysis and ox phos (MacIver et al., 2013). T helper cells subsequently switch to a glycolytic phenotype in order to carry out their effector functions while T_{reg} cells become more reliant on ox phos and fatty acid oxidation (FAO) (Michalek et al., 2011). Plasticity between T cell subtypes has been well documented and it is thought that metabolic changes play an important role in these changes (Buck et al., 2015). In fact inhibition of mechanistic target of rapamycin (mTOR), a key mediator in the upregulation of glycolysis, leads to the generation of T_{reg} cells despite the presence of other inflammatory signals (Kopf et al., 2007). Interestingly, while switches to aerobic glycolysis have been the focus of the majority of study on activated T cells mitochondrial-driven activities are emerging as having an important role in these cells (Sena et al., 2013). In particular, ROS production from the ETC has been shown to be important for T cell responses and this production has been linked to changes in ox phos (Devadas et al., 2002).

Since initial observations by *Oren et al* in 1963 that alveolar monocyte metabolism differs from pathways used by peritoneal monocytes (Oren et al., 1963), metabolic changes associated with activation of monocytes have been relatively understudied. The few studies which have been performed in this regard have either focused mainly on HIV infected cells, with the role of the monocyte relegated to a side note in a predominantly T cell focused literature (Palmer and Crowe, 2014, Palmer et al., 2016) or have conflated monocytes and macrophages as the same cell type despite obvious differences in their phenotype (Kramer et al., 2014).

1.6 Hypothesis and aims

The hypothesis of this study is that monocytes play a key role in mediating the pathogenic effects seen in AAV and that these effects are directly linked to changes in intracellular metabolism in these cells. The aims of this study were:

- To characterise the proportions of monocyte subsets in patients with AAV
- To identify the inflammatory response of monocyte subsets to ANCA stimulation
- To determine the effect of ANCA on monocyte metabolism
- To develop a robust and reproducible animal model of anti-PR3 AAV in order to test the effects of monocytes on disease *in vivo*

Chapter 2: Materials and Methods

2.1 Reagents

Name	Company
0.2µm filter	BD Biosciences, Oxford, UK
10ml syringe	BD Biosciences, Oxford, UK
19G needle	BD Biosciences, Oxford, UK
27G needle	BD Biosciences, Oxford, UK
2-Deoxyglucose (2-DG)	Sigma Aldrich, Wicklow, Ireland
2-(N-(7-nitrobenz-2-oxa-1,3-diazol-4-yl)amino)-2-deoxyglucose (2-NBDG)	Cayman Chemicals, Michigan, USA
3, 3', 5, 5' – tetramethylbenzindine (TMB) substrate solution	Sigma Aldrich, Wicklow, Ireland
4% paraformaldehyde (PFA)	Santa Cruz, Texas, USA
Anti-CD14 microbeads	Miltenyi Biotec, Bergisch Gladbach, Germany
BD FACS lysing solution	BD Biosciences, Oxford, UK
Bio-Scale MT high-resolution column	Bio-Rad, Sundbyberg, Sweden
Bovine Serum Albumin (BSA)	Thermo Fisher Scientific, Loughborough, UK
Brefeldin A	Sigma Aldrich, Wicklow, Ireland
CaCl	Sigma Aldrich, Wicklow, Ireland
CD14 Negative selection beads	Miltenyi Biotec, Bergisch Gladbach, Germany
CellTak	Thermo Fisher Scientific, Loughborough, UK
CM-H_2DCFDA	Thermo Fisher Scientific, Loughborough, UK

Cord blood Stem cells	Lonza, Basel, Switzerland
CountBright Absolute Count Beads	Molecular Probes, Oregon, USA
CPI-613	Bio-Techne, Minnesota, USA
Cytochalasin B	Sigma Aldrich, Wicklow, Ireland
Dasa-58	Merk Millipore, Massachusetts, USA
D-Glucose	Sigma Aldrich, Wicklow, Ireland
Dichloroacetate (DCA)	Sigma Aldrich, Wicklow, Ireland
Dihydrorhodamine 123 (DHR123)	Molecular Probes, Oregon, USA
Dimethyl sulfoxide (DMSO)	Sigma Aldrich, Wicklow, Ireland
DPX mountant for histology	Sigma Aldrich, Wicklow, Ireland
Dulbecco's modified eagle medium (DMEM)	Thermo Fisher Scientific, Loughborough, UK
Ethanolamine-HCL	Sigma Aldrich, Wicklow, Ireland
Ethylenediaminetetraacetic acid (EDTA)	Sigma Aldrich, Wicklow, Ireland
FACS tubes	BD Biosciences, Oxford, UK
Foetal calf serum (FCS)	Greiner Bio-One, Kremsmunster, Austria
Carbonyl cyanide-p-trifluoromethoxyphenylhydrazone (FCCP)	VWR International, Dublin, Ireland
Fc Block (Human)	BD Biosciences, Oxford, UK
Fc Block (Mouse)	BD Biosciences, Oxford, UK
Formalin	Sigma Aldrich, Wicklow, Ireland
Glasstic Slides	KOVA International, California, USA
Glycine	Sigma Aldrich, Wicklow, Ireland

H_2SO_4	Sigma Aldrich, Wicklow, Ireland
Hanks buffered salt solution (HBSS)	Thermo Fisher Scientific, Loughborough, UK
Hepes	Thermo Fisher Scientific, Loughborough, UK
HiTrap Protein G column	GE Healthcare Life Sciences, Buckinghamshire, UK
Hoechst dye	Thermo Fisher Scientific, Loughborough, UK
IL-1β DuoSet	R&D Systems, Minnesota, USA
IL-6 DuoSet	R&D Systems, Minnesota, USA
IL-8 DuoSet	R&D Systems, Minnesota, USA
Isopentane	Sigma Aldrich, Wicklow, Ireland
JC-1	Thermo Fisher Scientific, Loughborough, UK
$KHCO_3$	Sigma Aldrich, Wicklow, Ireland
L-glutamine	Gibco
Lipopolysaccharide (LPS)	Sigma Aldrich, Wicklow, Ireland
Live/Dead Aqua stain	Invitrogen, Loughborough, UK
LS Columns	Miltenyi Biotec, Bergisch Gladbach, Germany
Lymphoprep	Axis-Shield, Oslo, Norway
Maxisorb ELISA plates	Thermo Fisher Scientific, Loughborough, UK
Mini Leak gel	Kem-En-Tec, Taastrup, Denmark

MitoSox Red	Thermo Fisher Scientific, Loughborough, UK
MitoTempo	Sigma Aldrich, Wicklow, Ireland
Mitotracker Green	Thermo Fisher Scientific, Loughborough, UK
Multistix 10G urine dipstick	Siemens Healthcare, Dublin, Ireland
NaOH	Sigma Aldrich, Wicklow, Ireland
$(NH_4)_2SO_4$	Sigma Aldrich, Wicklow, Ireland
NH_4Cl	Sigma Aldrich, Wicklow, Ireland
Nile Red fluorescent beads	Spherotech, Illinois, USA
Normal Goat serum	Thermo Fisher Scientific, Loughborough, UK
Oligomycin	Sigma Aldrich, Wicklow, Ireland
OneComp Beads	eBiosciences, California, USA
Osmotic pump	Alzet, California, USA
Paediatric blood collection tube-LiHep	Sarstedt, Numbrecht, Germany
PD10 desalting column	GE Healthcare Life Sciences, Buckinghamshire, UK
Pegylated filgrastim	Amgen, Cambridge, UK
PermaFluor	Thermo Fisher Scientific, Loughborough, UK
Penicillin	Thermo Fisher Scientific, Loughborough, UK
Periodic acid	Sigma Aldrich, Wicklow, Ireland
Phosphate buffered saline (PBS)	Thermo Fisher Scientific, Loughborough, UK

PMSF	Sigma Aldrich, Wicklow, Ireland
Proteinase-3	Wieslab, Lund, Sweden
Pre separation filters	Miltenyi Biotec, Bergisch Gladbach, Germany
Propidium iodide (PI)	Miltenyi Biotec, Bergisch Gladbach, Germany
Recombinant human C5a	Peprotech, New Jersey, USA
Recombinant human M-CSF	Peprotech, New Jersey, USA
Recombinant human TNF-α	Peprotech, New Jersey, USA
Rotenone	Sigma Aldrich, Wicklow, Ireland
Roswell Parks Memorial Institute Medium (RPMI)	Thermo Fisher Scientific, Loughborough, UK
Saponin	Sigma Aldrich, Wicklow, Ireland
Schiff stain	Sigma Aldrich, Wicklow, Ireland
Sodium azide	Sigma Aldrich, Wicklow, Ireland
Sodium bicarbonate	Sigma Aldrich, Wicklow, Ireland
Sodium pyruvate	Sigma Aldrich, Wicklow, Ireland
Streptomycin	Thermo Fisher Scientific, Loughborough, UK
Tepp-46	Cayman Chemicals, Michigan, USA
Tris	Sigma Aldrich, Wicklow, Ireland
Tris-HCL	Sigma Aldrich, Wicklow, Ireland
Trypan Blue	Sigma Aldrich, Wicklow, Ireland
Tween-20	Sigma Aldrich, Wicklow, Ireland
Vacuette EDTA tubes	Greiner Bio-One, Kremsmunster, Austria

Vivaspin Column	Sartorious, Goettingen, Germany
XF media	Agilent Technologies, Copenhagen, Denmark
XFe24 cell culture plates	Agilent Technologies, Copenhagen, Denmark
XFe24 FluxPak	Agilent Technologies, Copenhagen, Denmark
Xylene	Sigma Aldrich, Wicklow, Ireland

Table 2.1.1 Reagents used

Buffer	Components
1% BSA	1mg/ml BSA in PBS
ACK lysis buffer	H_2O + 8.3g/L NH_4Cl + 1g/L $KHCO_3$ + 0.037g/L EDTA
Blocking buffer	PBS + 20% FCS
cRPMI	RPMI + 10%FCS + 100U/ml streptomycin + 1mg/ml penicillin
ELISA wash buffer	PBS + 0.05% Tween-20
FACS buffer	PBS + 0.1% sodium azide + 3%FCS
HBH buffer	HBSS + 10mM Hepes
MACS buffer	PBS + 2mM EDTA + 0.5%BSA
XF+ media	XF media + 4mM L-glutamine
XF+++ media	XF media + 5.5mM D-Glucose + 4mM L-glutamine + 1mM sodium pyruvate

Table 2.1.2 Solutions and buffers used

Name	Clone	Company
Anti-MPO mAb	2C7	Acris Antibodies, Herford, Germany
Anti-PR3 mAb	CLB-12.8	HiSS Diagnostics GmbH, Freiburg, Germany
Isotype mAb	IgG1	Acris Antibodies, Herford, Germany

Table 2.1.3 Antibodies used for cell stimulations

Target antigen	Flurochrome	Clone	Species targeted	Company
CD1c	FITC	L161	Human	Biolegend
CD3	FITC	UCHT1	Human	Biolegend
CD14	APC	RMO52	Human	Beckman Coulter
CD14	Pacific Blue	RMO52	Human	Beckman Coulter
CD14	PE-Cy7	M5E2	Human	Biolegend
CD16	APC	3G8	Human	Biolegend
CD19	APC-Cy7	H1B19	Human	Biolegend
CD45	APC	2D1	Human	Biolegend
CD45	VioBlue	30-F11	Mouse	Miltenyi Biotec
CD56	PE-Cy7	B159	Human	BD Pharmingen
CD66b	PerCP-Cy5.5	G10F5	Human	BD Biosciences
CD177	PE	MEM-166	Human	Molecular Probes
MPO	PE	2C7	Human	Serotec
PR3	FITC	W6M2	Human	Abcam
TNF-α	PE	MAb11	Human	BD Pharmingen

Table 2.1.4 Antibodies used for flow cytometry staining

2.2 Methods

2.2.1 Patient and control individual samples

Blood samples from patients and both healthy and disease control individuals were obtained through the Rare Kidney Disease (RKD) Biobank and University Medical Center Groningen. Written consent was obtained from all individuals. The RKD Biobank has full approval from the Trinity College Dublin Institutional Review Board and Ethics Committee, and approval from each of the individual hospitals from which samples were obtained (St. James' hospital, Tallaght hospital and Beaumont hospital). Similarly, collection of samples at the University Medical Center Groningen was conducted according to local ethical guidelines and approved by the ethical committee of the University Medical Center Groningen, and in accordance with the Declaration of Helsinki. All AAV patients fulfilled the Chapel Hill Consensus Conference (CHCC) classification criteria (Jennette et al., 2013). Active vasculitis was defined as a Birmingham vasculitis activity score (BVAS) >3. Where possible, blood was collected from active patients prior to commencement of immunosuppression therapy. Antibodies against MPO and PR3 were determined by ELISA. The disease control group comprised patients with anti-glomerular basement membrane (anti-GBM) disease (n=2), Takayasu's arteritis (n=1), uveitis (n=1), isolated leukocytoclastic vasculitis (n=1), IgA nephropathy (n=1), lupus nephritis (n=1), non-immune chronic kidney disease (n=4), triple vessel coronary artery disease (n=1), pyelonephritis (n=1), cirrhosis (n=1), megaloblastic anaemia (n=1), end stage kidney disease due to ischemic nephropathy (n=1), vascular dementia (n=1) and minimal change glomerulonephritis (n=1).

2.2.2 Flow cytometry

2.2.2.1 Whole blood staining

Blood was collected in vials containing anticoagulant; ethylenediametetraacetic acid (EDTA) for patient samples or lithium heparin for humanised mouse blood. For humanised mouse experiments blood was blocked for 10min by the addition of 1µl human Fc block (BD Biosciences, Oxford, UK) and 1µl mouse Fc block (BD Biosciences, Oxford, UK) per 100µl blood. Whole blood was stained by adding 5µl of the relevant antibodies shown in **Table 2.1.4** followed by incubation at room temperature for 20min in the dark. Red cells were lysed by addition of 2ml 1X BD FACS lysing solution (BD Biosciences, Oxford, UK) and incubation in the dark for 10min at room temperature. Cells were spun at 400g for 5min, supernatant was discarded and cells were washed with 500µl FACS buffer (PBS + 0.1% sodium azide + 3%FCS). Cells were spun again at 400g for 5min and the supernatant discarded. Cells were washed again before being resuspended in 500µl FACS buffer if being run immediately or 2% paraformaldehyde (PFA) (Santa Cruz, Texas, USA) if being stored overnight at 4°C. For

humanised mouse experiments 25µl of CountBright Absolute Counting beads (Molecular Probes, Oregon, USA) were added to each tube prior to analysis.

2.2.2.2 Cell surface marker staining of isolated cells

$1x10^5$ cells were added to each tube. Cells were incubated in the dark with a 1:1000 dilution of Live/Dead aqua dye for 30 min before being spun at 400g for 5min and washed with FACS buffer. Cells were blocked by incubation with blocking buffer (PBS + 20% FCS) for 10min at room temperature before 2 washes using FACS buffer. Cells were then resuspended in 100µl FACS buffer and incubated with 2µl of relevant antibodies shown in **Table 2.1.4** for 20min at room temperature. Cells were then washed X2 with FACS buffer and resuspended in 500µl FACS buffer if being analysed immediately or 2% PFA if being stored overnight at 4°C. Propidium iodide (PI) staining was performed in the appropriate experiments by addition of 5µl 10µg/ml PI immediately before the sample was run on the flow cytometer.

2.2.2.3 Intracellular cytokine staining

Cells were stained for surface markers as outlined above before being in 96-well plates and fixed by addition of 120µl 4% PFA and incubated in the dark for 10min at room temperature. Cells were then washed with FACS buffer and spun at 500g for 3 min. The supernatant was carefully discarded and cells were permeabilised by incubation with 120µl FACS buffer containing 0.2% saponin for 10min at room temperature. Cells were then washed by addition of 120µl FACS buffer and spun at 500g for 3 min before the supernatant was discarded. Cells were stained by addition of anti-TNFα PE (BD Pharmingen, MAb11) diluted in 100µl 0.2% saponin and incubated for 10min at room temperature in the dark. Cells were then washed with 300µl FACS buffer and spun at 500g for 3 min. Supernatant was discarded and cells were resuspended in FACS buffer and transferred to FACS tubes. Tubes were topped up to 500µl with FACS buffer if being analysed immediately or 2% paraformaldehyde (PFA) if being stored overnight at 4°C

2.2.2.4 Flow cytometry analysis

Flow cytometry was performed using a CyanADP analyser using Summit software. Compensation controls were included in each run using OneComp beads (eBiosciences, California, USA) stained with appropriate antibodies. At least 10000 events were collected for each sample and analysis was performed using Kaluza analysis software (Beckman Coulter, Clare, Ireland).

2.2.3 Isolation of cells

2.2.3.1 Isolation of mononuclear cells

Peripheral blood mononuclear cells (PBMCs) were isolated by density gradient centrifugation from EDTA anti-coagulated fresh samples or buffy coat samples obtained through the Irish Blood Transfusion Service. All steps were performed in aseptic conditions under a laminar flow hood. For buffy coats, blood was diluted 1:1 with phosphate buffered saline (PBS) (Thermo Fisher Scientific, Loughborough, UK) by injection into the buffy coat bag. The buffy coat was then mixed well and diluted blood was removed to a sterile container. For fresh samples blood was diluted 1:1 with PBS. Diluted blood was layered slowly onto Lymphoprep (Axis-Shield, Oslo, Norway) at a ratio of 2:1. Tubes were spun at 400g for 25 min without acceleration and brake. Plasma layer was aspirated and discarded. The PBMC layer was aspirated off and saved. The red cell pellet was saved for isolation of granulocytes if required. PBMCs were washed with PBS and centrifuged at 800g for 5 minutes. Supernatant was discarded and cells were again washed with PBS before being spun at 400g for 10 minutes. Cells were resuspended in appropriate buffer or media. Cells were counted by Trypan blue (Sigma Aldrich, Wicklow, Ireland) exclusion as detailed in **Chapter 2.2.3.3**.

2.2.3.2 Isolation of granulocytes

Red cells in pellets from the PBMC isolation were lysed by 10:1 dilution with ACK lysis buffer (H_2O + 8.3g/L NH_4Cl + 1g/L $KHCO_3$ + 0.037g/L EDTA) and incubation a room temperature for 10 min. Cells were then washed with 20ml PBS and spun at 400g for 5 min. Cells were resuspended in Hanks buffered salt solution (HBSS) (Thermo Fisher Scientific, Loughborough, UK) supplemented with 10mM Hepes (Thermo Fisher Scientific, Loughborough, UK) (HBH buffer). Cells were counted by Trypan blue exclusion as detailed in **Chapter 2.2.3.3**.

2.2.3.3 Cell counts and viability

In order to count cells and establish initial viability Trypan blue dye was used. Cells were diluted in Trypan blue between 1:2 and 1:50 as appropriate for the initial volume of blood. 10µl of cells/Trypan blue solution was transferred to a chamber of a Glasstic slide (KOVA international, California, USA). Slides were visualised using a light microscope. Glasstic chambers consist of a 3 X 3 layout of large squares each containing a 3 X 3 layout of smaller squares as shown in **Figure 2.1**. The number of cells in 3 large squares was counted and the average number was found. Cells touching the bottom and right border of each large square were not counted to avoid duplication. The average number of cells in one large square was multiplied by 10^4 and by the dilution factor to calculate the number of cells per ml. Trypan blue is excluded from live cells and therefore dead cells could be excluded from the counted.

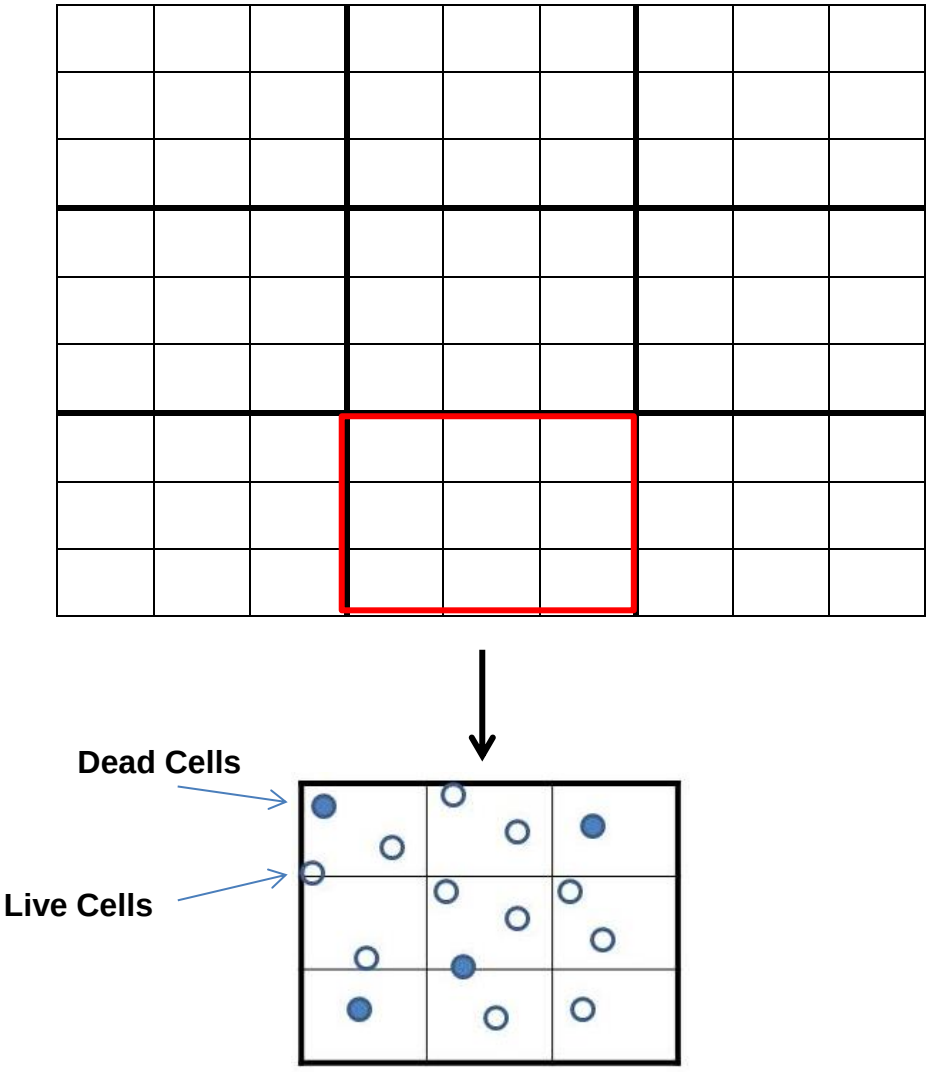

Figure 2.1 Counting of viable cells using a Glasstic haemocytometer slide and trypan blue.

2.2.3.4 MACS isolation of monocytes

CD14+ monocytes were isolated by magnetic associated cell sorting (MACS). Isolated PBMCs were resuspended in MACS buffer (PBS + 2mM EDTA + 0.5%BSA) and incubated for 15min at 4°C with 10µl anti-CD14 microbeads (Miltenyi Biotec, Bergisch Gladbach, Germany) per 10^7 cells. CD14+ cells were isolated using an LS column (Miltenyi Biotec, Bergisch Gladbach, Germany) on a quadroMACS separator (Miltenyi Biotec, Bergisch Gladbach, Germany). A pre-separation filter was placed in the column and the column was washed with 3mls of MACS buffer. PBMCs were then added and washed through three times with 3mls MACS buffer per wash. The column was removed from the separator and bound cells were eluted using 5mls MACS buffer. Cells were spun at 400g for 5 minutes. Supernatant was discarded and cells were resuspended in 1ml Roswell Park Memorial Institute (RPMI) media (Thermo Fisher Scientific, Loughborough, UK,) supplemented with 10% fetal calf serum (FCS) (Greiner Bio-One, Kremsmunster, Austria), 100U/ml streptomycin and 1mg/ml penicillin (cRPMI). Cells were counted by Trypan blue exclusion as detailed in **Chapter 2.2.3.3**. CD14+ monocyte purity was assessed by flow cytometry.

For monocytes isolated by –ve selection PBMCS were first incubated for 15min at 4°C with 20µl beads from a CD14 negative selection kit (Miltenyi Biotec, Bergisch Gladbach, Germany) per 10^7 cells. Columns were prepared as above. Cells were added and the run through from the column was saved. The column was washed 3 times with MACS buffer and washes were saved. Run through and washes were pooled and spun at 400g for 5 minutes. Supernatant was discarded and cells were resuspended in 1ml cRPMI. Cells were counted by Trypan blue exclusion as detailed in **Chapter 2.2.3.3**. CD14+ monocyte purity was assessed by flow cytometry.

2.2.3.5 Isolation of specific monocyte subsets

Specific monocyte subsets were isolated by fluorescence associated cell sorting (FACS). Isolated CD14+ cells were stained with 2.5µl/1x10^5 cells of anti-CD14 PE-Cy7 (M5E2, Biolegend) and 2.5µl anti-CD16 APC (3G8, Biolegend) and incubated for 20 min at room temperature. Cells were washed X2 with PBS + 3%FCS and resuspended in PBS + 3%FCS at a concentration of 10^7/ml. Cells were then sorted based on CD14 and CD16 expression using a MoFlo XDP analyser with a 70µm nozzle (Beckman Coulter) (**Figure 3.3.15)**.

2.2.4 Stimulation of cells with ANCA

2.2.4.1 Stimulation of cells for cytokine analysis

Cells were seeded at a density of $2x10^6$ cells/ml in 250µl for total monocytes, or $1.2x10^6$ cells/ml in 500µl for sorted subsets. The cells were incubated with 5 ng/ml TNF-α (Peprotech, London, UK) at 37 ^{0}C with 5% CO_2 for 30 minutes as used previously (Schreiber et al., 2012) for initial experiments and then stimulated with 5µg/ml of either monoclonal antibody (mAb) directed against MPO (2C7, Acris Antibodies), PR3 (CLB-12.8, HiSS Diagnostics GmbH), isotype control antibody (IgG1, Acris Antibodies), or 100µg/ml protein G purified IgG from anti-MPO+ (n=3), anti-PR3+ (n=3) patients or healthy controls (n=4) for 4 hours at 37 ^{0}C with 5% CO_2. Supernatants were removed and IL-1β, IL-6 or IL-8 ELISA (R&D Systems, Minnesota, USA) was performed as described in **Chapter 2.2.5**

2.2.4.2 Fc blocking of stimulated monocytes

Monocytes were incubated with 2.5µg Fc block (BD Biosciences, Oxford, UK)/$1x10^6$ cells @ 37 ^{0}C with 5% CO_2 for 30 minutes and then stimulated with 5µg/ml of either monoclonal antibody (mAb) directed against MPO (2C7, Acris Antibodies) or isotype control antibody (IgG1, Acris Antibodies) for 4 hours at 37 ^{0}C with 5% CO_2. Supernatants were removed and IL-1β ELISA (R&D Systems, Minnesota, USA) was performed as described in **Chapter 2.5**.

2.2.4.3 Stimulation of humanised mouse blood

Humanised mouse blood was diluted 1:1 with cRPMI and stimulated @ 37°C with 5% CO_2 with 2ng/ml lipopolysaccharide (LPS) for 4hrs in the presence of 10ng/ml brefeldin A to prevent cytokine secretion. Cells were then stained as in **Chapter 2.2.2.3**

2.2.4.4 Stimulation of monocytes for measurement of 2-NBDG uptake analysis

Monocytes were plated at a density of $2x10^6$ cells/ml in 250µl cRPMI and treated with 5µg/ml anti-MPO or isotype mAb for 60min. Cells were then removed and placed in FACS tubes. Tubes were spun at 400g for 5min before supernatant was discarded and the cells resuspended in blocking buffer for 10min. Cells were then spun and supernatant was discarded before being resuspended in 200µl of 86.5µg/ml 2-(N-(7-nitrobenz-2-oxa-1,3-diazol-4-yl)amino)-2-deoxyglucose (2-NBDG) (Cayman Chemicals, Michigan, USA). Cells were incubated in the dark for 60min @ 37°C with 5% CO_2. Anti-CD14 antibody was added for the last 10min of the incubation. Following incubation, cells were washed and resuspended in 100µl FACS buffer. Cells were analysed immediately on a Cyan ADP analyser.

2.2.4.5 Measurement of ROS production in neutrophils using DHR123

Monocytes and granulocytes were isolated as outlined above. Cells were incubated with 17µg/ml Dihydrorhodamine 123 (DHR123) (Molecular probes, Oregon, USA) together with 5µg/ml cytochalasin B and 2mM sodium azide for 10min at 37°C with 5% CO_2 in the dark. Cells were then treated with 2ng/ml TNF-α for 15min at 37°C with 5% CO_2 before stimulation with 5µg/ml anti-MPO mAb or isotype mAb for 60min at 37°C with 5% CO_2. The reaction was then stopped by the addition of cold 1% BSA. Cells were then stained for CD14 and CD66b as outlined in **Chapter 2.2.2.2** and analysed immediately on a Cyan ADP analyser.

2.2.4.6 Measurement of cellular and mitochondrial ROS in monocytes

Monocytes were isolated and stimulated with 5µg/ml anti-MPO, anti-PR3 or isotype mAb or 5ng/ml LPS for 1 hour at 37°C with 5% CO_2. For the final 30min of the incubation cells were treated with either 5µM CM-H2DCFDA (Thermo Fisher Scientific, Loughborough, UK), 2.5µM MitoSOX red (Thermo Fisher Scientific, Loughborough, UK), or 10µg/ml JC-1 (Thermo Fisher Scientific, Loughborough, UK). Anti-CD14 antibody was added for the final 10min of the incubation. Cells were washed X2 with FACS buffer and run immediately on a Cyan ADP analyser.

2.2.4.7 Treatment of monocytes with inhibitors and cell death assay

Monocytes were plated at a density of $2x10^6$ cells/ml in 250µl cRPMI. Cells were treated with 10mM 2-deoxyglucose (2-DG) (Sigma Aldrich, Wicklow, Ireland), 8µM oligomycin (Sigma Aldrich, Wicklow, Ireland), 20mM dichloroacetate (DCA) (Sigma Aldrich, Wicklow, Ireland), 100µM CPI613 (Bio-Techne, Minnesota, USA) or varying concentration of Dasa-58 (Merk Millipore, Massachusetts, USA), Tepp-46 (Cayman Chemicals Michigan, USA), or MitoTempo (Sigma Aldrich, Wicklow, Ireland) and incubated @ 37°C with 5% CO_2 for 20min before the addition of 5µg/ml anti-MPO mAb, isotype control or vehicle for 4hr @ 37°C with 5% CO_2. Plates were then spun @ 400g for 3min. Supernatant was removed and IL-1β levels were assessed by ELISA. Cells were washed with PBS and placed in FACS tubes and stained with PI and antibodies as described in **Chapter 2.2.2.2**.

2.2.5 Enzyme linked immunosorbent assay (ELISA)

Duoset ELISA kits (R&D Systems, Minnesota, USA) were used to measure cytokine production from ANCA stimulated monocytes. Each kit contained a capture antibody, biotin conjugated detection antibody, a known amount of the cytokine to be measured (standard) and a streptavidin-horseradish peroxidase (HRP) solution. All reagents were diluted based on the manufactures instructions.

Maxisorb ELISA plates (Thermo Fisher Scientific, Loughborough, UK) were coated with 50µl per well of capture antibody diluted in PBS. Plates were then covered and incubated overnight at 4°C. Plates were then washed by being submerged in wash buffer (PBS + 0.05% Tween-20) and then emptied and dried using blotting paper. This wash was repeated X2 times. Plates were blocked by the addition of 300µl 1mg/ml BSA in PBS (1%BSA) per well for 2 hours at room temperature. Plates were then washed X3 times. A 7 point standard curve was made up by serial dilution of recombinant cytokine in 1%BSA. Samples were diluted in 1%BSA as required to appear on the linear section of the standard curve (1 in 25 for IL-1β, 1 in 20 for IL-6 and 1 in 50 for IL-8). 50µl standards, samples or blank (1%BSA alone) were added to the plate in duplicate. Plates were covered and incubated overnight at 4°C. Cells were then washed X3 times and 50µl detection antibody diluted in 1%BSA was added to each well. Plates were covered and incubated at room temperature for 2 hours before being washed X3 times. 50µl HRP solution diluted in PBS was then added to each well and the plate was incubated for 20min in the dark at room temperature. Plates were then washed X3 times before 50µl 3,3',5,5' – tetramethylbenzidine (TMB) (Sigma Aldrich, Wicklow, Ireland) was added to each well. Plates were incubated in the dark until the colour of unknown samples matched the colour of the middle of the standard curve (40min for IL-1β, 1 hour for IL-8 and 2 hours for IL-6). The reaction was then stopped by addition of 25µl 2M H_2SO_4 to each well. Absorbances from each well were then read at 450nm using a VERSAmax microplate reader (Molecular Devices, California, USA). Standard curves were drawn using GraphPad prism software (GraphPad Inc., California, USA) to determine unknown concentrations.

2.2.6 **Seahorse extracellular flux technology**

Seahorse extracellular flux analysis is a technology which allows for the simultaneous real time measurement of extracellular acidification rate (ECAR) and oxygen consumption rate (OCR). These readings are used as correlates of glycolytic activity and oxidative phosphorylation respectively. This technology involves the use of plates specifically designed to aid binding of cells in an even monolayer coupled with an XFe FluxPak (Agilent Technologies, Copenhagen, Denmark). These plates contain a series of probes which have embedded fluorophores which measure H+ or O_2 levels. These probes are lowered onto cells in the plate to form a microchamber which allows for readings to be made. The small volume of the microchamber allows for great sensitivity in the assay. The FluxPak also contains 4 ports which can be used to inject various compounds into the cell culture well so that responses can be measured in real time. FluxPaks cartridges are hydrated by emersion in calibration solution overnight at 37°C with no CO_2 prior to an experiment. In this study a 24 well XFe24 Seahorse extracellular flux analyser (Agilent Technologies, Copenhagen, Denmark) was used.

Using this technology and the addition of several compounds which affect metabolic pathways in the cell a number of readouts of cellular metabolism can be obtained. These compounds and their functions are outlined in **Table 2.2.1.**

Compound	Effect on metabolism
Oligomycin	Inhibits complex V of electron transport chain
FCCP	Uncouples mitochondria
Rotenone	Inhibits oxidative phosphorylation
2-DG	Inhibits glycolysis

Table 2.2.1 Compounds used to alter metabolism in Seahorse analysis.

For oxidative respiration Seahorse analysis can give readouts of the basal respiration, non-mitochondrial respiration, proton leak, spare respiratory capacity and maximum respiratory capacity. This type of experiment is known as a mitochondrial stress test and an example OCR trace showing how these values can be calculated is shown in **Figure 2.2**. A similar glycolytic stress test can be performed to provide readings for glycolysis, non-glycolytic acidification, spare glycolytic capacity and maximum glycolytic capacity. An example of the ECAR trace used in this test is shown in **Figure 2.3**.

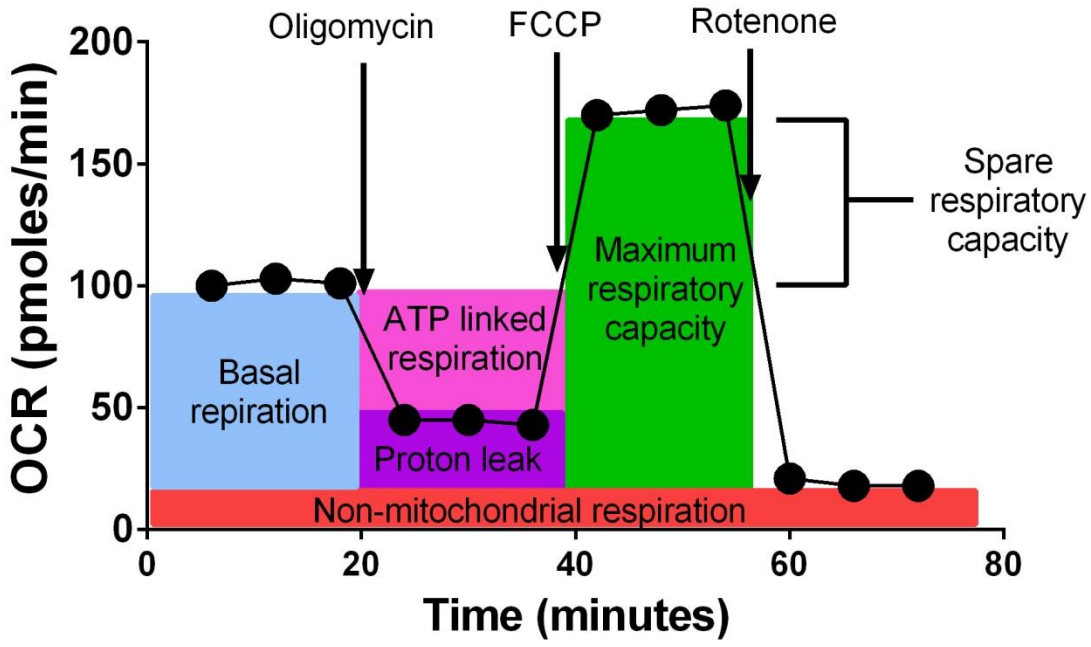

Figure 2.2 Sample mitochondrial stress test trace.

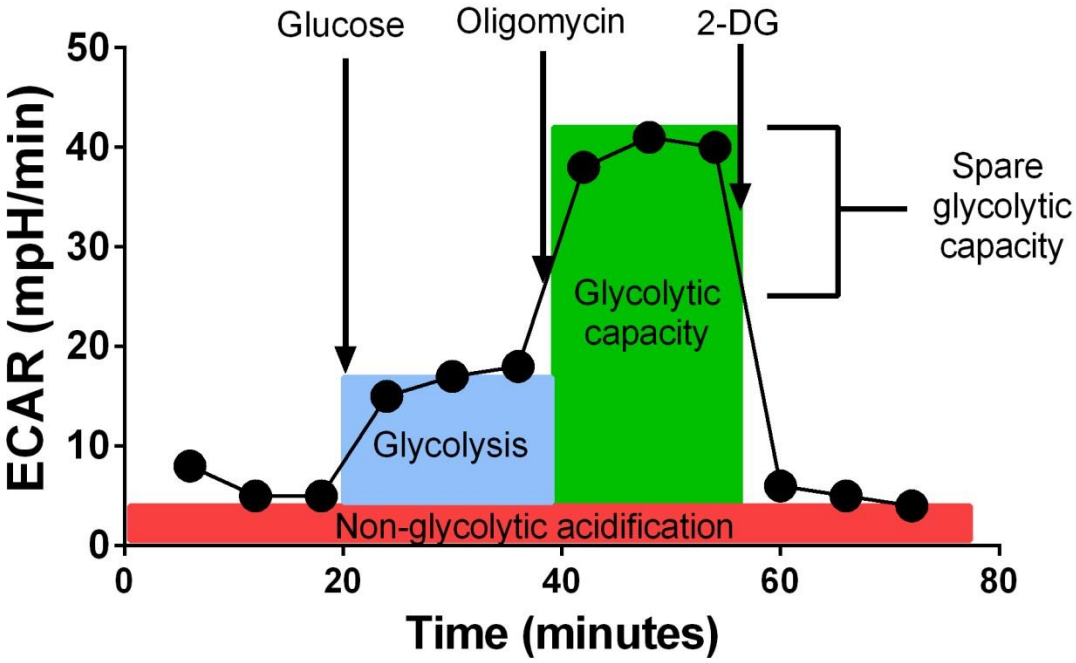

Figure 2.3 Sample glycolytic stress test trace.

2.2.6.1 Adherence of cells to Seahorse plate

Prior to Seahorse analysis non adherent cells such as monocytes must be immobilised to the base of the XF cell culture plate wells. CellTak (Thermo Fisher Scientific, Loughborough, UK) was diluted in 0.1M sodium bicarbonate pH=8 and 2mM NaOH to give a final concentration of 2.85µg/ml. 200µl diluted CellTak was then immediately added to each well of the XF24 well cell culture plate. CellTak was allowed to adsorb to the plate for 30min at room temperature. Unbound CellTak was removed by washing by addition of 500µl sterile H_2O. The plate was then emptied and the wash step repeated before the plate was allowed to air dry. Plates were either used immediately or covered and stored at 4°C. Plates were brought to room temperature before adherence of cells.

$1x10^6$ cells were plated in 100µl cRPMI per well. Plates were pulse centrifuged up to 40g with acceleration = 4 and no brake. The plate was then turned 180° and pulsed up to 80g with acceleration = 4 and no brake. This assists with even layering of the cells on the plate. Cells were then allowed to adhere during incubation at 37°C with 5% CO_2 for 30min. 200µl cRPMI was then added to each well prior to stimulations.

2.2.6.2 Optimisation of Seahorse cell numbers and mitochondrial stress test concentrations

$0.25x10^6$, $0.5x10^6$, $1x10^6$ or $1.5x10^6$ monocytes were plated per well onto CellTak coated plates. One cell concentration was used per row. The media on the cells was then changed from cRPMI to XF media. In order to prevent disturbing the adhered cells, this was achieved by removal of cRPMI leaving 50µl and addition of 450µl XF media (Agilent Technologies, Copenhagen, Denmark) supplemented with 5.5mM D-glucose (Sigma Aldrich, Wicklow, Ireland), 4mM L-glutamine (Sigma Aldrich, Wicklow, Ireland) and 1mM sodium pyruvate (Sigma Aldrich, Wicklow, Ireland) (XF+++ media). This process was then repeated. The plate was then left to equilibrate for 45 min at 37°C with no CO_2. To determine the optimum concentration of each compound to be used in the mitochondrial stress test a number of concentrations were investigated for each. These compounds were prepared in a 10X solution and added to the relevant ports on the XFe24 FluxPak. For each cell concentration duplicate wells were used to determine oligomycin, rotenone (Sigma Aldrich, Wicklow, Ireland) and Carbonyl cyanide-p-trifluoromethoxyphenylhydrazone (FCCP) (VWR International, Dublin, Ireland) concentrations. Final concentrations after addition from each port are shown in **Figure 2.4**. Optimal concentrations of 2-DG used for the glycolysis stress test were chosen based on the cytokine stimulation experiments described in **Chapter 2.2.4.7**.

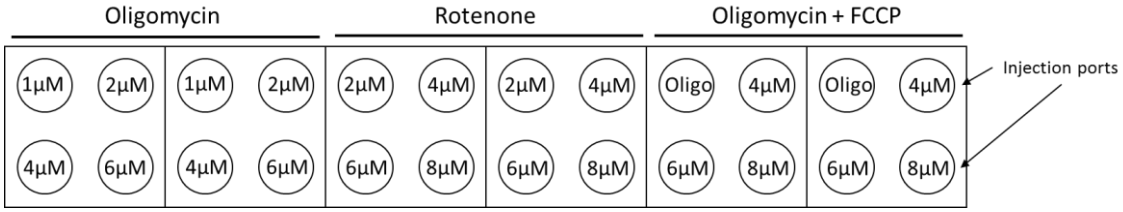

Figure 2.4 Layout of Seahorse optimisation plate

2.2.6.3 Mitochondrial stress test and glycolysis stress test

Monocytes were adhered to CellTak-coated 24 well plates at a concentration of $1x10^6$ per well as described above. Cells were stimulated with 5µg/ml anti-MPO, anti-PR3, isotype or vehicle for 4 hours at 37°C with 5% CO_2. The media was then changed from cRPMI to XF+++ media, for mitochondrial stress test, or XF+ media (XF media + 4mM L-glutamine) for glycolysis stress test as described above in Section 2.2.6.2. The removed cRPMI was frozen for later cytokine analysis. The plate was then left to equilibrate for 45 min at 37°C with no CO_2. Compounds were then prepared to give final concentrations as shown in **Table 2.2.2.** Compounds were added to the appropriate ports of the FluxPak and the plate was then left to equilibrate for 10 min at 37°C with no CO_2.

Compound	Test used in	Final concentration used
Oligomycin	Mitochondrial stress test	2µM
FCCP	Mitochondrial stress test	4µM
Rotenone	Mitochondrial stress test	4µM
D-glucose	Glycolytic stress test	5.5mM
Oligomycin	Glycolytic stress test	4µM
2-DG	Glycolytic stress test	10mM

Table 2.2.2 Concentrations of compounds used for mitochondrial and glycolytic stress tests.

The FluxPak was then placed in the Seahorse XFe24 analyser and calibration was performed. The plate containing the cells was then added to the analyser. Each XFe24 measurement was set to: mix for 3min, wait for 3min, measure for 3min. 3 initial basal measurements were performed followed by 3 measurements after injection of each compound.

2.2.6.4 Measurement of real time metabolic changes in response to ANCA

Monocytes were adhered to Seahorse plates as described above. Cells were washed with XF+++ media or XF+ media for OCR and ECAR measurements respectively and the plate was then left to equilibrate for 45 min at 37°C with no CO_2. Anti-MPO, anti-PR3 or isotype antibodies were added to port A of an XFe24 FluxPak. For ECAR measurements, D-glucose was added to port B. For OCR measurements rotenone or vehicle was added to port B. The FluxPak was then left to equilibrate for 10 min at 37°C with no CO_2 before being placed in the Seahorse XFe24 analyser and calibration performed. The plate containing the cells was then added to the analyser. Each XFe24 measurement was set to: mix for 3min, wait for 3min, measure for 3min. 6 initial basal measurements were performed followed by injection of antibody. For ECAR experiments 3 more measurements were performed before injection of glucose followed by 9 further measurements. For OCR experiments 1 measurement was performed before rotenone injection followed by 9 further measurements.

2.2.7 Purification of ANCA

2.2.7.1 Total IgG purification by FPLC

Plasma stored at -80°C was thawed in a water bath at 37°C. In order to remove fibrin, plasma was diluted 1:50 with 1M CaCl (Sigma Aldrich, Wicklow, Ireland) and left to precipitate overnight at 4°C. Plasma was then spun at 1000g for 30min and the supernatant was removed and saved. The supernatant was diluted 1:1 in sterile PBS before being passed through a 0.2µm filter. A 1ml protein G column (GE Healthcare Life Sciences, Buckinghamshire, UK) was set up on an AKTA fast pressure liquid chromatography (FPLC) apparatus (GE Healthcare Life Sciences, Buckinghamshire, UK). The column was washed with 50ml sterile PBS at 3ml/min. Sample was then injected through the column at a flow rate of 3ml/min. The column was washed with 4ml sterile PBS. Bound IgG was eluted in 1ml fractions by passing 0.1M glycine pH 2.7 (Sigma Aldrich, Wicklow, Ireland) through the column at a rate of 3ml/min and collected into tubes containing 100µl 1M Tris pH 9 (Sigma Aldrich, Wicklow, Ireland). Sample OD was measured at 280nm and fractions >0.5 were pooled and buffer exchanged into PBS using PD10 desalting columns (GE Healthcare Life Sciences, Buckinghamshire, UK). Concentration of antibody was found by measurement at A280 using a ND-8000 nanodrop spectrophotometer (Thermo Fisher Scientific, Loughborough, UK). Samples were concentrated to 2mg/ml using Vivaspin 20 columns (Sartorious, Goettingen, Germany) and stored at -20°C.

2.2.7.2 Binding of PR3 to Bio-Scale MT high resolution column

2mg PR3 (Wieslab, Lund, Sweden) was dialysed overnight against PBS + 1mM PMSF (Sigma Aldrich, Wicklow, Ireland) to remove Tris. The next day, Mini-Leak gel (Kem-En-Tec, Taastrup, Denmark) was washed on a glass filter with 2 volumes of H_2O. Excess water was removed by suction. 1.5g of gel was added to the dialysed PR3. The volume was measured and 0.53ml of 3.5M $(NH_4)_2SO_4$ pH 8.8 (Sigma Aldrich, Wicklow, Ireland) was added per ml of mixture. This was then incubated overnight with gentle rocking. The gel was then washed with 3.5M $(NH_4)_2SO_4$ pH 8.8. Active groups were then blocked with 0.1M ethanolamine-HCL pH 8.5 (Sigma Aldrich, Wicklow, Ireland) for 3hrs. The gel was then washed with 50mM Tris-HCL pH 7.5 0.5M NaCl 0.02%NaN_3 (Sigma Aldrich, Wicklow, Ireland) and poured into a Bio-Scale MT high-resolution column (Bio-Rad, Sundbyberg, Sweden).

2.2.7.3 Purification of anti-PR3 IgG

IgG was thawed and diluted 1:10 with PBS. The PR3 bound column was washed with 5 volumes of 0.1M glycine pH 2.7 to remove unbound antigen before being blocked by injection of 1%BSA and incubation for 30min at room temperature. Antibody was then circulated through

the column using a peristaltic pump for 1 hr. The column was then added to the FPLC machine before being washed with 10 column volumes of 1% BSA. Bound IgG was eluted in 1ml fractions by passing 5 column volumes 0.1M glycine pH 2.7 through the column and collection into tubes containing 100µl 1M Tris pH 9. Sample OD was measured at 280nm and fractions >0.5 were pooled and buffer exchanged into PBS using PD10 desalting columns. Concentration of antibody was found by measurement at A280 on a ND-8000 nanodrop spectrophotometer. Samples were filtered and stored at -20°C.

2.2.8 Humanised mice

2.2.8.1 Sources of stem cells

CD34+ stem cells were sourced through 3 different routes. Commercially derived cord stem cells were purchased from Lonza (Basel, Switzerland) and were used at a concentration of $1x10^5$ per mouse. Locally isolated cord blood stem cells were isolated by CD34+ MACS isolation from cord blood samples obtained from patients undergoing elective caesarean section in the Coombe Maternity Hospital, Dublin and were used at a concentration of $1.5x10^5$ per mouse. Adult peripheral blood stem cells were isolated from granulocyte colony stimulating factor (G-CSF) mobilized apheresis products obtained from normal healthy adult donors on d5 & 6 after stimulation. CD34+ cells were isolated from the apheresis product using ISOLEX 300i Magnetic Cell Positive Selection System (version 2.5, Baxter Healthcare, Deerfield, IL, USA) as per the manufacturer's instructions and were used at a concentration of 8 $x10^5$ per mouse.

2.2.8.2 Generation of human chimeric mice

All experiments involving animals were conducted in accordance with Irish Health Products Regulatory Authority (HPRA) regulations and had full approval from Trinity College Dublin ethics board. Non-obese diabetic (NOD) severe combined immunodeficiency (Scid) IL-2 receptor γ-chain-/- (NSG) mice, NSG mice transgenic for human membrane stem cell factor (hu-mSCF) and NSG mice transgenic for human IL-3, GM-CSF and soluble SCF (SGM3) were purchased from Jackson Laboratories (Maine, USA) or bred in house from a breeding pair purchased from Jackson Laboratories. All animals were housed in specific pathogen free (SPF) conditions in individually ventilated cages. 6-8 week old mice were irradiated with 2.4Gy using a Cs-source irradiator. Within 24 hr mice were injected intravenously (i.v.) via the lateral tail vein with CD34+ stem cells from sources outlined in **Chapter 2.2.8.1**. Engraftment of human cells in the peripheral blood was assessed using flow cytometry 12 weeks post injection. 1 week later mice which had > 15% engraftment were injected i.v. with 50µg pegylated filgrastim (Amgen, Cambridge, UK). 4 days later mice were bled and changes in number of monocytes were assessed by flow cytometry.

2.2.8.3 Immunisation of mice with anti-PR3 antibodies

13 weeks post engraftment mice which had > 15% engraftment were injected sub cutaneously (s.c.) with 1µg LPS followed by i.v. 1mg of IgG isolated from either anti-PR3 +ve patients or disease control individuals or 500µg of affinity purified anti-PR3 IgG from anti-PR3 +ve patients. 7 days later the mice were anaesthetised using Isoflurane and spot urines were collected by gently massaging the bladder. Mice were then culled by terminal bleed before collection of samples.

2.2.8.4 Insertion of C5a osmotic pump

An osmotic pump (Alzet, California, USA) containing 4032ng of human recombinant C5a (Peprotech, New Jersey, USA) with a release rate of 24ng/hr was inserted s.c. between the scapula of each mouse 12 weeks post engraftment. 1 day later mice were immunised with anti-PR3 antibodies as above.

2.2.8.5 Sample collection culled animals

Blood from the terminal bleed was collected in Paediatric Li-Hep tubes (Sarstedt, Numbrecht, Germany) for flow cytometry. Upon initially opening the chest cavity and before any subsequent manipulations, lungs were observed for punctate haemorrhage. Haemorrhage scores were based on the number of petechiae counted on the left lung. All counts were performed blinded to treatment.

Mice were perfused through the heart by injection of 10ml cold PBS. The kidneys were then removed and bisected using a scalpel blade. Kidney sections were placed in formalin for fixation. The other half of the kidney was placed in phosphate-lysine-periodate (PLP) and incubated for 4hrs at 4°C. They were then transferred to 13% sucrose and incubated overnight at 4°C before being frozen in isopentane and stored at -80°C. Lungs were inflated by injection of 1ml cold PBS and immediately removed and placed in formalin. Spleen was removed and placed in formalin. Hind legs were removed by cutting above the hip and below the ankle.

Haematuria levels were measured by addition of 10µl urine to a Multistix 10G urine dipstick (Siemens Healthcare, Dublin, Ireland).

2.2.8.6 Periodic acid-Schiff staining of kidney sections

Kidney tissue was processed using an automatic tissue processor before being embedded in paraffin wax. Tissue sections were cut to 1µm thickness and incubated in an oven for 30min. Kidney sections were then stained with periodic acid-Schiff (PAS) staining. This was done by first placing the section in xylene for 10min and followed by 20 seconds each in 100%, 90% and 70% alcohol. They were then washed with H_2O for 2 minutes before incubation with 1% periodic acid for 10min followed by a 3 min was with H_2O. They were then incubated with Schiff reagent for 20min followed by a further 3min wash with H_2O. Slides were then moved back through the graded alcohol concentrations for 20sec each and placed in xylene before being mounted using DPX mountant for histology (Sigma Aldrich, Wicklow, Ireland) and left to dry. Evidence of tissue damage was analysed using a light microscope.

2.2.8.7 Immunofluorescent staining of kidney sections

Frozen Kidney sections were cut to 5µm thickness using an automatic tissue processor. Sections were blocked by incubation with 20% normal goat serum for 15min at 4°C. Sections were then stained with FITC anti-human CD45 (eBioscience, HI30) or isotype control (FITC anti-mouse IgGκ, Abcam). Nuclei were stained with Hoechst dye and sections were mounted in PermaFluor mounting reagent (Thermo Fisher Scientific, Loughborough, UK). Cell numbers were taken from the average counts of 5 high-powered fields using a Nikon Eclipse 90i (Nikon Instruments, Amsterdam, Netherlands) fluorescent microscope.

2.2.8.8 Culture of bone marrow derived macrophages and Phagocytosis assay

Muscle tissue and fat was removed from legs and the femur and tibiae were removed. The ends of each bone were opened using a scissors and a 27G needle was inserted into the orifice. Bones were each flushed with 10ml into a petri dish. Aggregates were broken by passing the bone marrow through a 19G needle. Cells were then spun at 1500rpm for 5min. Supernatant was discarded and the pellet was resuspended in 2ml ACK lysis buffer. Cells were incubated at room temperature for 5min before addition of 50ml media to stop the reaction. Cells were spun at 1500rpm for 5min. Isolated bone marrow cells were resuspended in 10mL Dulbecco's modified Eagle's medium (DMEM) (Thermo Fisher Scientific, Loughborough, UK) containing 20 ng/mL recombinant human macrophage colony-stimulating factor (M-CSF) (Peprotech, New Jersey, USA) and cultured at 37°C with 5% CO_2 for 7 days. Cells were harvested and counted.

Cells were then loaded with Nile Red fluorescent particles (Spherotech, Illinois, USA) at a concentration of 50 particles/cell and incubated for 2 h at 37°C with 5% CO_2. Cells were spun at 400g for 5 min and resuspended in FACS buffer to remove unphagocytosed beads. Cells

were then stained as described in **Chapter 2.2.2** with APC anti-human CD14 (Beckman Coulter, clone: RMO52) and VioBlue anti-mouse CD45 (Miltenyi Biotec; Clone: 3F11) and analysed by flow cytometry on a CyanADP analyser.

Chapter 3: Intermediate monocytes express increased cell-surface ANCA antigens and produce highest amounts of pro-inflammatory cytokines in response to anti-MPO antibodies

3.1 Introduction

To date, most of the studies into the cellular mechanism behind AAV pathogenesis have focused on neutrophils as the main cell type of interest. As mentioned in **Section 1,** monocytes have also been implicated in disease pathogenesis. Monocytes, along with macrophages, are the first cell type to infiltrate the kidney of patients (Zhao et al., 2015). While macrophages do not express MPO or PR3 on their surface (Ohlsson et al., 2012), it has been shown that monocytes do express these antigens and therefore have the potential to be activated by autoantibodies (Yang et al., 2000). While macrophages cause the majority of damage at the lesion site, the lack of surface MPO and PR3 on these cells means that peripheral blood monocytes must be the cells on which ANCA can have effects and therefore are an important cell type to study in the context of this disease. The response of neutrophils is well characterised in disease and monocytes are now re-emerging as a cell of interest in the pathogenesis of AAV. I therefore wanted to better characterise these cells in patients and to investigate their response to ANCA.

In particular, I wanted to characterise the monocyte subsets present in patients and to investigate the differential responses that may occur in these monocyte subsets in response to ANCA. As outlined in **Chapter 1**, monocytes can be divided into three subsets based on their surface expression of CD14 and CD16. These subsets, an overview of their functions, and the proportion of each found in blood are shown in **Table 3.1.1**. The current consensus for identifying the three subsets has yet to provide an unequivocal definition of the intermediate subset (Ziegler-Heitbrock, 2015), however, the use of CD14 and CD16 is thought to be the best currently available method to distinguish these populations (Ziegler-Heitbrock and Hofer, 2013).

Due to their short half-life and ability to move in and out of the circulation the study of monocytes in humans can prove difficult. To address this issue several studies have attempted to characterise monocytes and their subsets in mice. Similar populations of monocyte subsets have been identified in the mouse with differing levels of Ly6c and CD43 being used to distinguish between each cell type similar to CD14 and CD16 in humans (Ziegler-Heitbrock, 2014). Ly6C^{hi} murine monocytes show a number of similarities with classical human monocytes, sharing their pro-inflammatory and anti-microbial characteristics. There are however some differences between the two species such as differential gene expression in these cells (Ingersoll et al., 2010). These Ly6C^{hi} cells have also been shown to leave the circulation and differentiate into macrophages (Shi and Pamer, 2011). The non-classical subset in humans is thought to correspond to the ly6C^{low} population found in mice. These cells appear to have a similar patrolling role and also may be involved in tissue repair (Nahrendorf et al., 2007, Auffray et al., 2007). Currently there is not thought to be a murine subset which

corresponds exactly to the intermediate subset found in humans, whether this population is absent from the mouse or whether further markers would help to identify them remains the subject of study. The proportion of each subset found in mice varies dramatically to that seen in humans (Palframan et al., 2001, Burke et al., 2008). This fact, along with the lack of a direct intermediate subset, suggests that the murine system may not be suitable for translational studies on monocyte subsets.

It is not yet clear whether monocyte subsets in humans are developmentally linked, however, a link between the classical and non-classical populations has been suggested (Weiner et al., 1994, Ziegler-Heitbrock and Hofer, 2013) although the exact relationship between these cells remains unclear.

Monocyte Subset	**CD14/CD16 expression**	**Inflammatory role**	**% in peripheral blood median (IQR)**
Classical	$CD14^{high}CD16^{neg/low}$	Pro-inflammatory, antimicrobial	84.3 (81.4- 88.8)
Intermediate	$CD14^{high}CD16^{high}$	Pro-inflammatory	9.4 (7.4-13.7)
Non-classical	$CD14^{low}CD16^{high}$	Patrolling, Anti-viral	4.8 (2.8-7.3)

Table 3.1: Monocyte subset markers and phenotype (adapted from (Shi and Pamer, 2011)) '% in peripheral blood' refers to the median and interquartile range (IQR) of all samples included in my study.

Before being distinguished as two separate populations CD16+ monocytes were mainly thought to be pro- inflammatory TNF-α producing (Schlitt et al., 2004, Belge et al., 2002). While these roles have yet to be fully attributed to either the intermediate or non-classical subtype the intermediate monocytes appear to have a more proinflammatory role as evidenced by their production of IL-1β and TNF-α in response to LPS stimulation (Cros et al., 2010), while the non-classical subset have a more patrolling and anti-viral function (Shi and Pamer, 2011). ANCA stimulation of neutrophils has been shown to require the Fc portion of the autoantibody for full effect (Mulder et al., 1994), suggesting that ANCA may interact with CD16 on monocytes and therefore, distinct monocyte subsets may play a role in the pathogenesis of the disease. Interestingly, human Fc receptors have been shown to bind to

murine Fc, albeit with reduced affinity, and this interaction may allow for stimulation of these cells with murine monoclonal antibodies which have high affinity for the ANCA antigens (Lubeck et al., 1985, Stewart et al., 2014). On the other hand some studies have shown that monocytes may not require Fc binding at all, with Fab fragment stimulation being sufficient to induce a response (Weidner et al., 2001). Differences in the proportion of monocyte subsets, particularly an increase in intermediate cells, have previously been shown in several autoimmune diseases including rheumatoid arthritis (Rossol et al., 2012), sarcoidosis (Heron et al., 2008), and severe asthma (Moniuszko et al., 2009). This subset has also been shown to increase after excessive exercise or stress (Steppich et al., 2000). I therefore postulated that distinct monocyte subsets, particularly the CD16+ subsets, may exhibit differential responses to the autoantibodies associated with ANCA vasculitis.

3.2 Design and rational

3.2.1 Hypothesis

Monocyte subset populations have been shown to be altered in a number of autoimmune conditions. These subsets are characterised in part by their expression of CD16 which is important for activation of neutrophils by ANCA. I therefore hypothesised that:

I. The proportion of each monocyte subset is altered in ANCA associated vasculitis
II. ANCA stimulation of monocytes induces a pro-inflammatory response
III. The response to ANCA varies between monocyte subsets due to differing CD16 expression

3.2.2 Methods:

Patients and controls were recruited from two cohorts; from Ireland and The Netherlands, which are defined in **Figure 3.2.1** and **Figure 3.2.2**. The methods used to investigate the hypothesis outlined in **Section 3.2.1** are outlined in **Figure 3.2.3**.

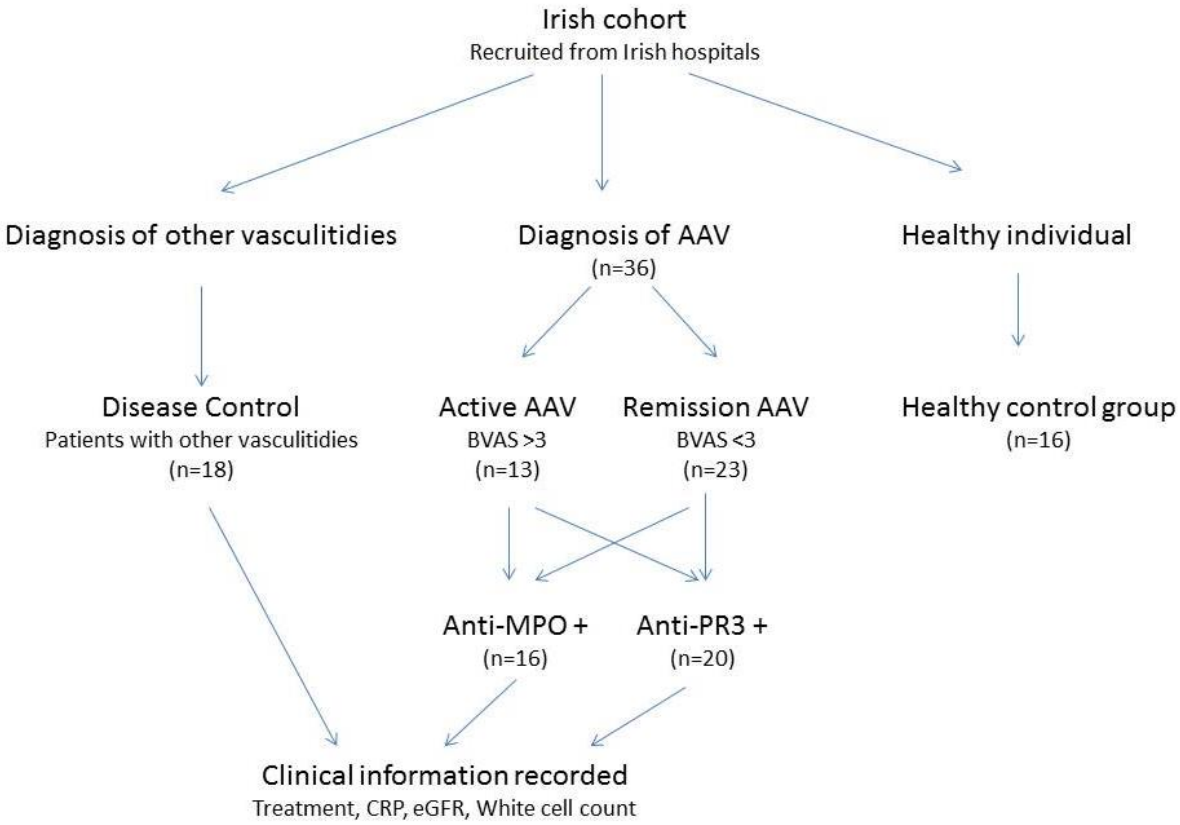

Figure 3.2.1 Patient and control breakdown of Irish Cohort

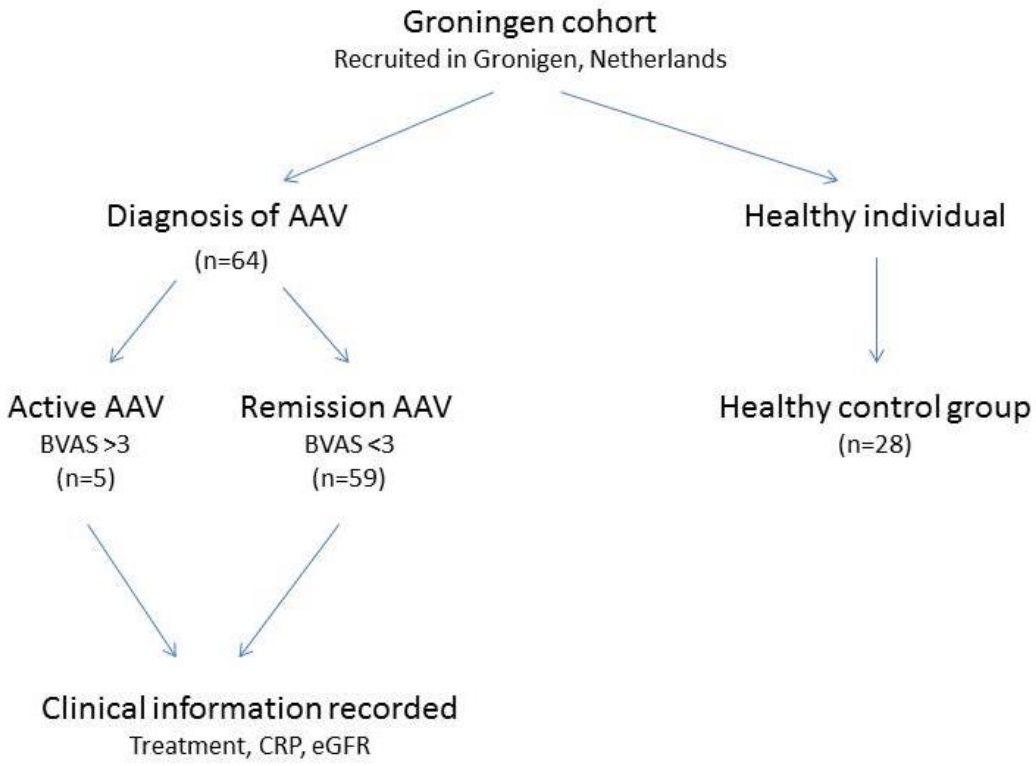

Figure 3.2.2 Patient and control breakdown of Groningen Cohort

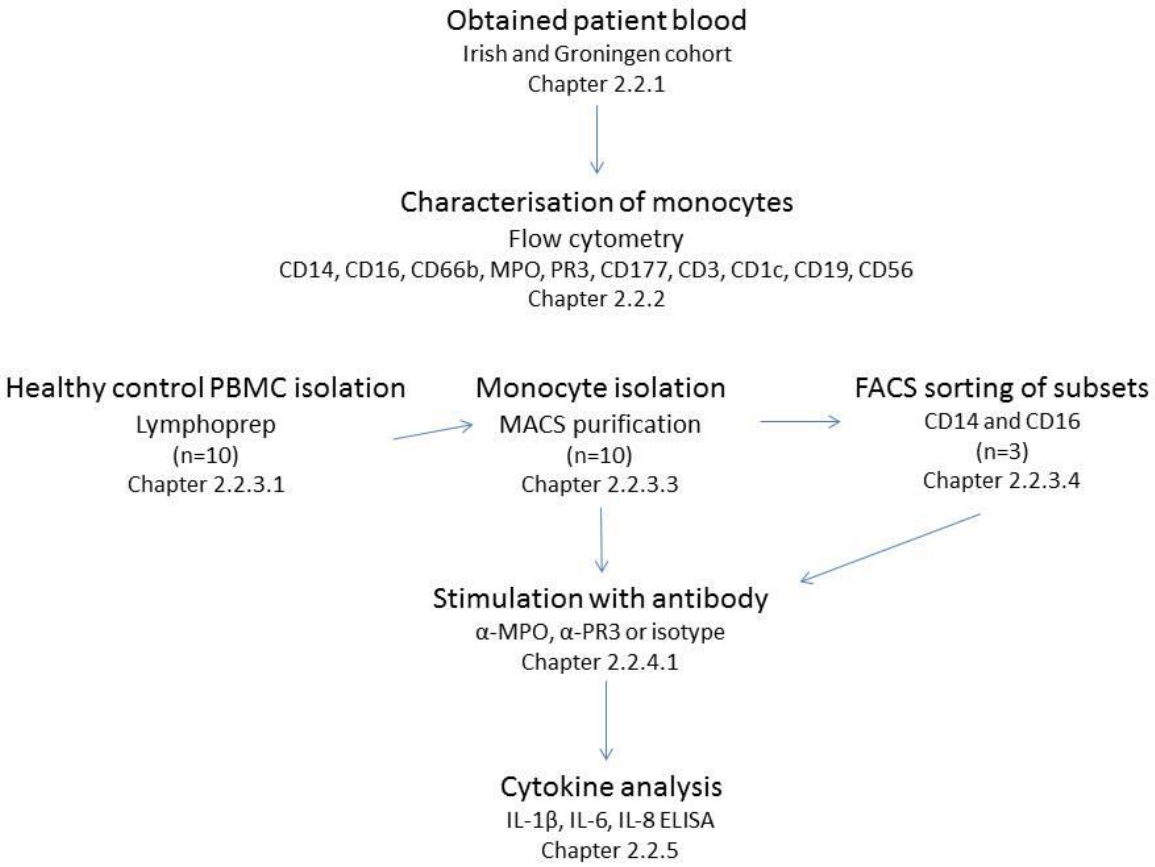

Figure 3.2.3 Diagramtic representation of techniques used.
Overview of experimental plan and techniques used to: investigate and phenotype monocyte subsets in patients with AAV, and to investigate the response of monocytes to ANCA stimulation. Detailed methods are provided in the section number shown below each technique.

3.3 Results

3.3.1 Optimisation of monocyte subset staining

Individual monocyte subsets were identified based on cell surface expression of CD14 and CD16 as measured by flow cytometry (**Fig 3.3.1**). Gating monocytes in this way resulted in a small population of $CD14^{low}CD16^{low}$ cells (**Figure 3.3.1 E**) In order to get an accurate percentage of the monocyte subsets as a percentage of total CD14+ monocytes I identified the cells contained in this $CD14^{low}CD16^{low}$ population (**Figure 3.3.2**). These cells were comprised mainly of $CD1c^{+}$ dendritic cells (**Figure 3.3.2 A**) with smaller proportions of $CD3^{+}$ T cells (**Figure 3.3.2 B**), $CD19^{+}$ B cells (**Figure 3.3.2 C**) and $CD56^{+}$ NK cells (**Figure 3.3.2 D**). This population was therefore removed from future analysis to allow for correct monocyte subset proportions.

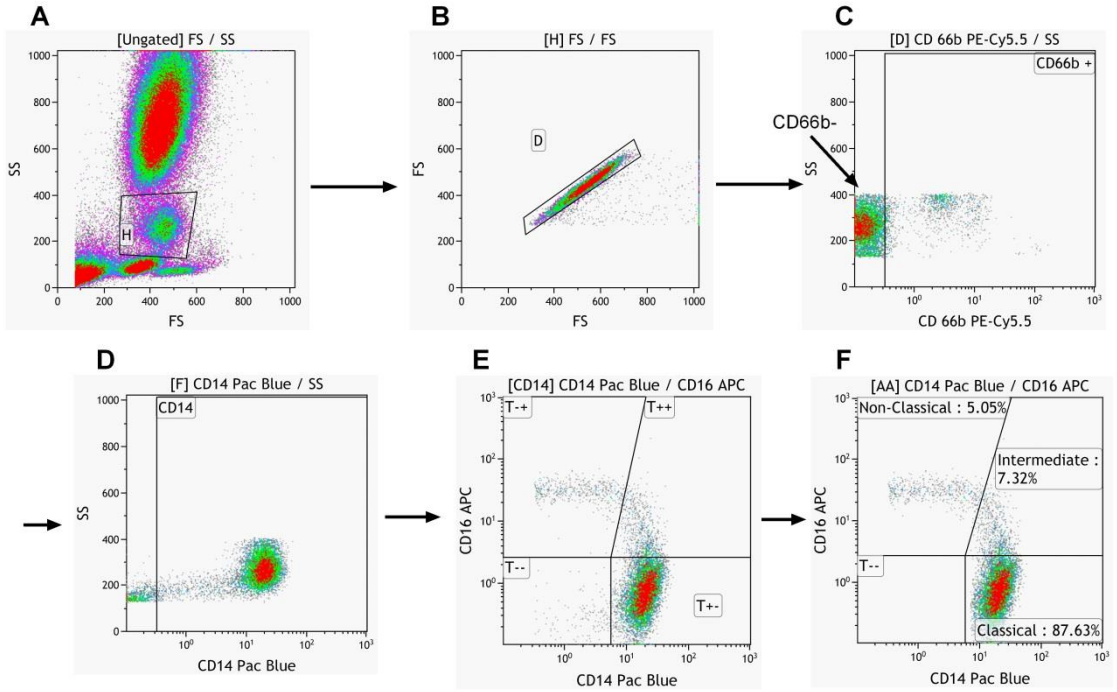

Figure 3.3.1 Gating of monocyte subsets.
Monocytes were initially gated based on size (FS) and granularity (SS) (**A**). Doublets were excluded (**B**). Granulocytes were excluded based on positive CD66b staining (**C**). CD14+CD66b- monocytes (**D**) were gated on and the contaminating CD14lowCD16- population was removed (**E**) and the pure CD14+ cells were subdivided into classical, intermediate and non-classical subsets based on CD14 and CD16 staining (**F**). Flow plots represent a typical AAV patient.

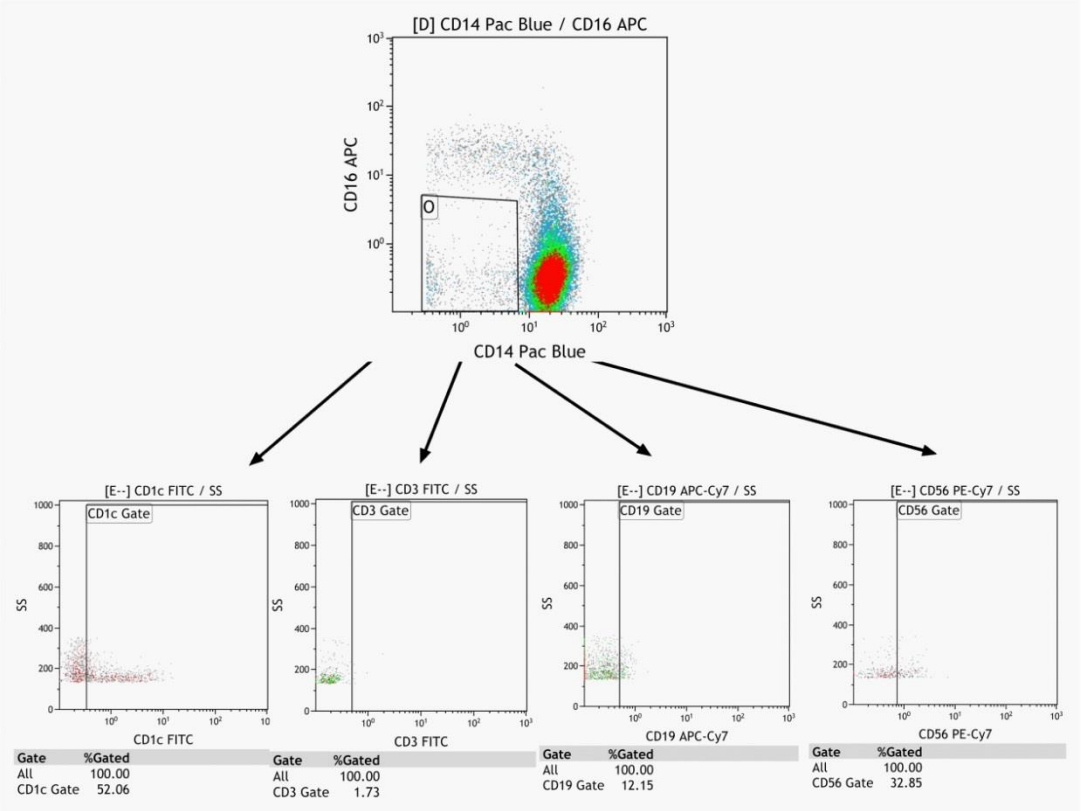

Figure 3.3.2 Characterisation of CD14^{low} CD16^{low} population.
Monocytes were gated as shown in **Figure 3.3.1**. CD14^{low}CD16^{low+} cells were gated and identified using antibodies directed against CD1c, CD3, CD19 and CD56 to remove contaminating cell populations.

3.3.2 The proportion of intermediate monocytes is increased in AAV patients

Patients were recruited from hospitals in two locations; Ireland and Groningen, The Netherlands. Patient cohorts are described in **Figure 3.2.1** and **Figure 3.2.2**. A detailed breakdown of the patient characteristics and demographics is described in **Table 3.3.1**. These patients were matched for steroid and immunosuppressive treatment across the three disease groups in order to account for variations in cell numbers as a result of these treatments. Monocyte subset populations for each cohort were identified by flow cytometry. I observed no significant difference in the proportion of classical and non-classical monocytes, as a percentage of total monocytes, between healthy controls, disease controls and AAV patients (remission or active) (**Figure 3.3.3 A, C**). Intermediate monocytes were significantly increased in both remission and active AAV patients when compared to healthy control individuals (**Figure 3.3.3 B**).

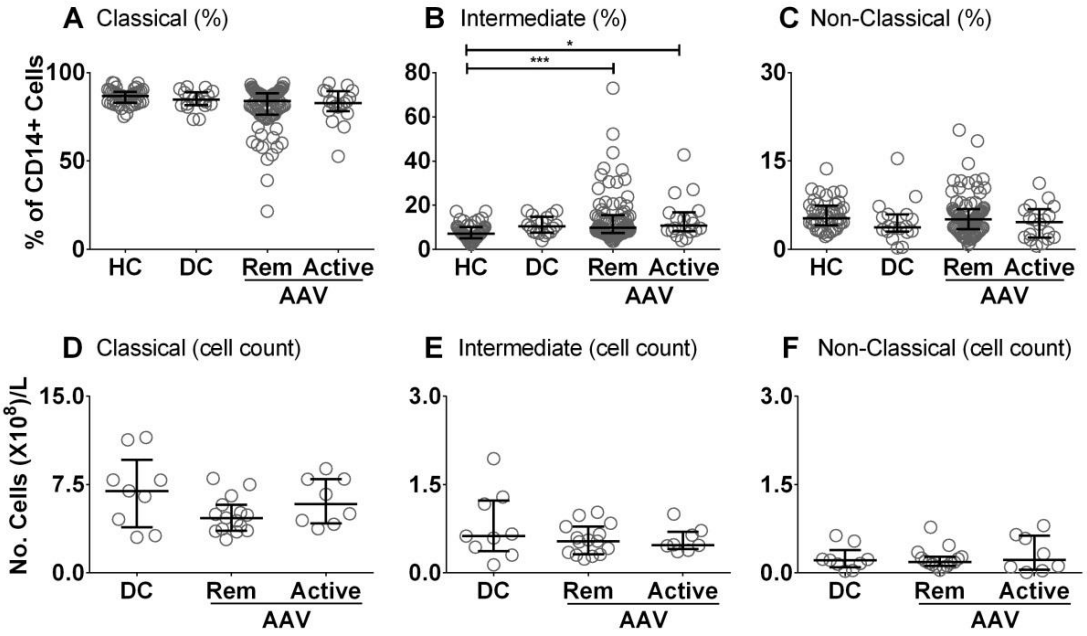

Figure 3.3.3 Intermediate monocyte subsets are increased in both active and remission AAV patients compared to healthy control individuals.
Peripheral blood was collected from healthy control individuals, AAV patients (both patients with active disease and those in remission), and patients with other renal disease (disease controls). Percentages of monocytes in each subset (**A-C**) were established by flow cytometry based on CD14 and CD16 staining. Total monocyte counts from the Irish cohort (**D-F**) were determined based on available clinical data. Each symbol represents a separate individual. Data are presented as the median and interquartile range (*p<0.05, ***p<0.005). HC: healthy control; DC: disease control; Rem: remission. A-C N=44, 18, 81 and 19 for HC, DC, Rem and Active respectively. D-E N= 9, 15 and 8 for DC, Rem and Active respectively.

The fraction of intermediate monocytes in the disease control group was numerically similar to the vasculitis groups, but the increase was not significantly different from the healthy control group (**Figure 3.3.3 B**). The absolute cell counts between the three subsets did not vary across the patient and control groups (**Figure 3.3.3 D-F**) however, these counts are available for the Irish cohort only. No difference was found between the percentage or cell number of each subset in this Irish cohort when patients were stratified based on ANCA specificity (either MPO or PR3) (**Figure 3.3.4**).

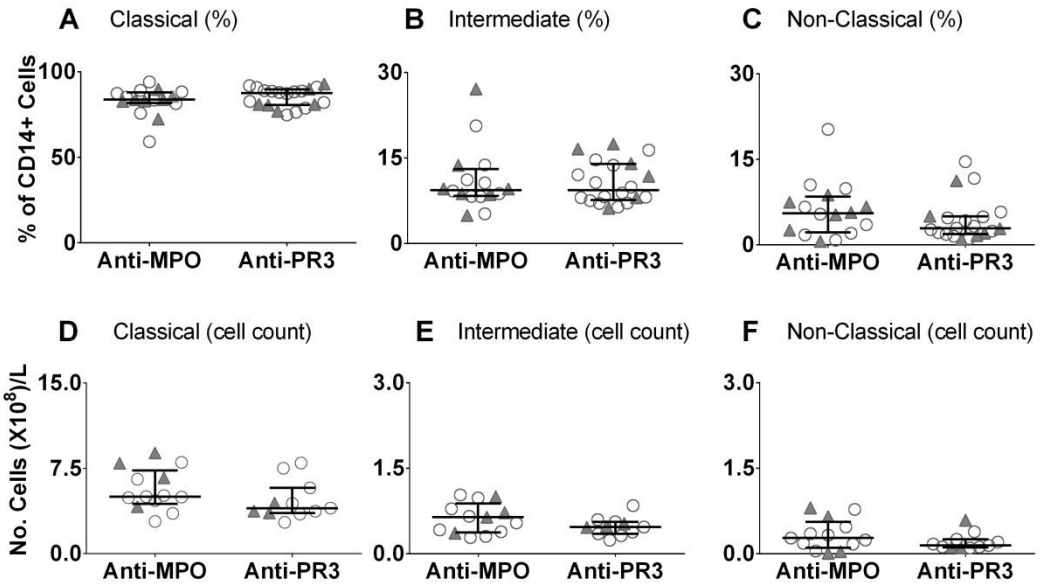

Figure 3.3.4 Patient ANCA type does not affect the proportion of each monocyte subset. AAV patients were divided based on their ANCA type. Percentages of monocytes in each subset (**A-C**) were established by flow cytometry based on CD14 and CD16 staining. Total monocyte counts from the Irish cohort (**D-F**) were determined based on available clinical data. Each symbol represents a separate individual. Data are presented as the median and interquartile range. Circles represent patients in remission and triangles represent patients with active disease. N= 16 Anti-MPO and N=20 Anti-PR3

	Vasculitis (n=100)	*Active (n=19)*	*Remission (n=81)*	Disease Controls (n=18)	Healthy Controls (n=44)
Age: Median (Range)	59 (50-70)	*55 (51-73)*	*59 (49-70)*	54 (17-87)	39 (22-75)
Gender	51 male 49 female	*14 male 5 female*	*37 male 44 female*	13 male 5 female	19 male 25 female
ANCA type at diagnosis	17 anti-MPO 83 anti-PR3	*7 anti-MPO 12 anti-PR3*	*10 anti-MPO 71 anti-PR3*	N/A	N/A
Proportion of patients on immunosuppression	72%	*76%*	*72%*	65%	0%
Proportion of patients on steroids	53%	*68%*	*32.4%*	43%	0%
Median CRP (mg/dL, interquartile range)	3 (1-12)	*15 (10-64)*	*2 (1-7)*	9 (1-34)	N/A
eGFR (ml/min, interquartile range)	63 (42-80)	*49 (35-87)*	*64 (42-80)*	64 (18-87)	N/A
Proportion eGFR <60ml/min	40%	*47%*	*38%*	44%	N/A

Table 3.2 Demographic and clinical information for patients and controls
All clinical data were obtained on the same date as analysis of monocytes. CRP=C reactive protein, GFR=Glomerular filtration rate

3.3.3 MPO and PR3 antigens are preferentially expressed on intermediate monocytes

As MPO and PR3 expression on neutrophils has been shown to localise with CD16 (David et al., 2005), and due to the variability in CD16 expression on monocyte subsets, I hypothesised that cell surface expression of the MPO and PR3 autoantigens may vary between these subsets. Using the Irish cohort, I divided the AAV patients into anti-MPO and anti-PR3 positive groups. Following gating on each subset, the percentage of monocytes within that subset expressing cell-surface MPO or PR3 was determined by flow cytometry. MPO expression was significantly increased on intermediate monocytes when compared to the classical and non-classical subsets (**Figure 3.3.5 A, C**). Similarly, cell-surface PR3 expression was also increased on intermediate monocytes (**Figure 3.3.5 B, D**).

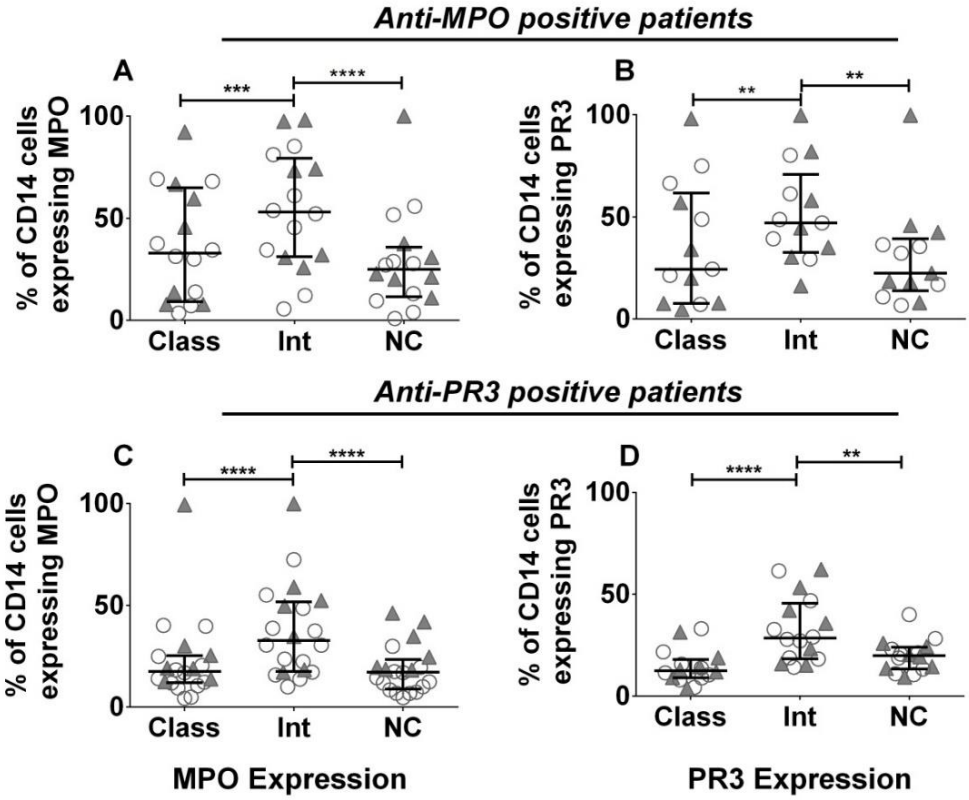

Figure 3.3.5 ANCA autoantigens are preferentially expressed on intermediate monocytes.
Peripheral blood was collected from patients with AAV and the percentage of cells expressing cell-surface MPO and PR3 was examined by flow cytometry. The percentage of MPO and PR3 positive cells in each subset is shown for anti-MPO+ AAV patients (**A-B**) and anti-PR3+ AAV patients (**C-D**). Each symbol represents a separate individual. Open circles represent patients in remission and filled triangles patients with active disease. Data are presented as the median and interquartile range. Non-parametric one-way ANOVA (Friedman test) and Dunn's post-test were used to test for significance (*p<0.05, **p<0.01; ****p<0.0001). Class: classical; Int: intermediate: NC: non-classical. N= 16 Anti-MPO and N=20 Anti-PR3

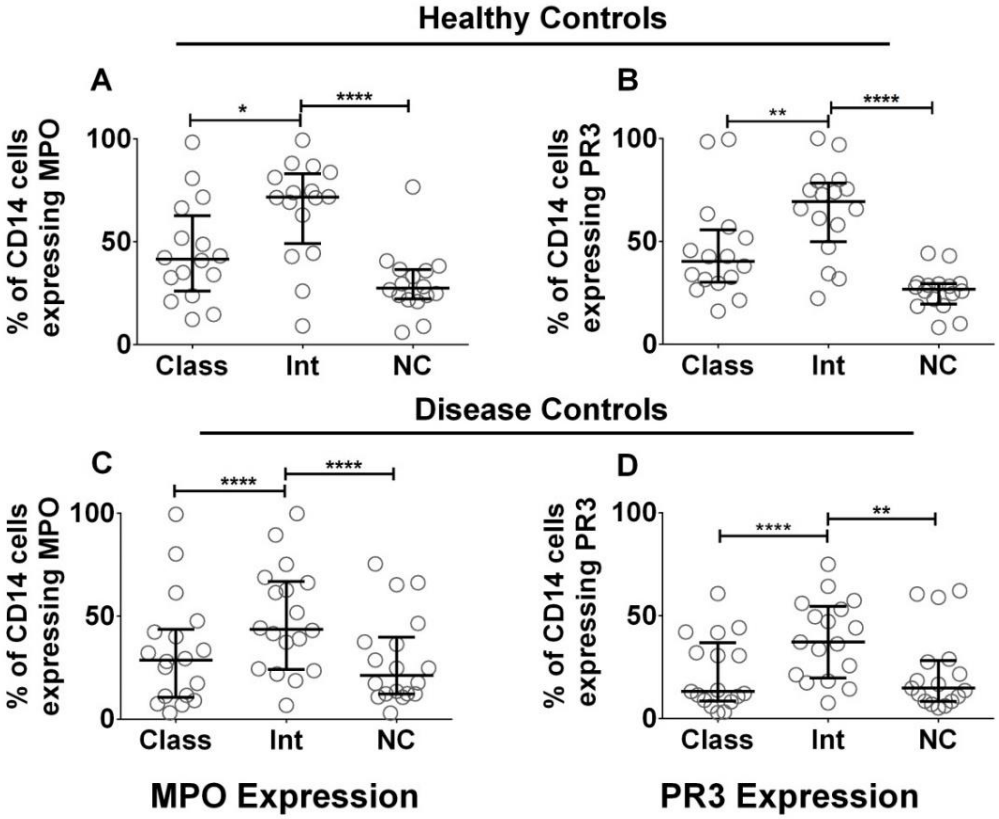

Figure 3.3.6 Intermediate monocytes from control individuals also express increased levels of MPO and PR3.
Peripheral blood was collected from healthy and disease control individuals and the percentage of cells expressing cell-surface MPO and PR3 was examined by flow cytometry. The percentage of MPO and PR3 positive cells in each subset is shown for healthy controls (**A-B**) and disease controls (**C-D**). Each symbol represents one individual. Data are presented as the median and interquartile range. Non-parametric one-way ANOVA (Friedman test) and Dunn's post-test were used to establish significance (*p<0.05, **p<0.01; ***p<0.001; ****p<0.0001). Class: classical; Int: intermediate: NC: non-classical. N= 17 Healthy controls and N=18 Disease controls

This increase was observed in both AAV patient categories (anti-MPO and anti-PR3) and was also found in the intermediate subset of both disease control patients and healthy control individuals, indicating that this is not a disease specific phenomenon but rather a fundamental feature of the intermediate monocyte subset (**Figure 3.3.6**). I next looked at the relative amount of MPO and PR3 on the surface of each monocyte subset. Following gating of MPO/PR3 positive cells in each subset I found a small but significant increase in the median fluorescence intensity of MPO and PR3 on intermediate monocytes (**Figure 3.3.7**) indicating that not only are more of these cells MPO and PR3 positive, each positive cell also has an increased proportion of both antigens on their surface when compared to classical and non-classical monocytes. This change appeared quite subtle and more work is required to ascertain the biological significance of this finding.

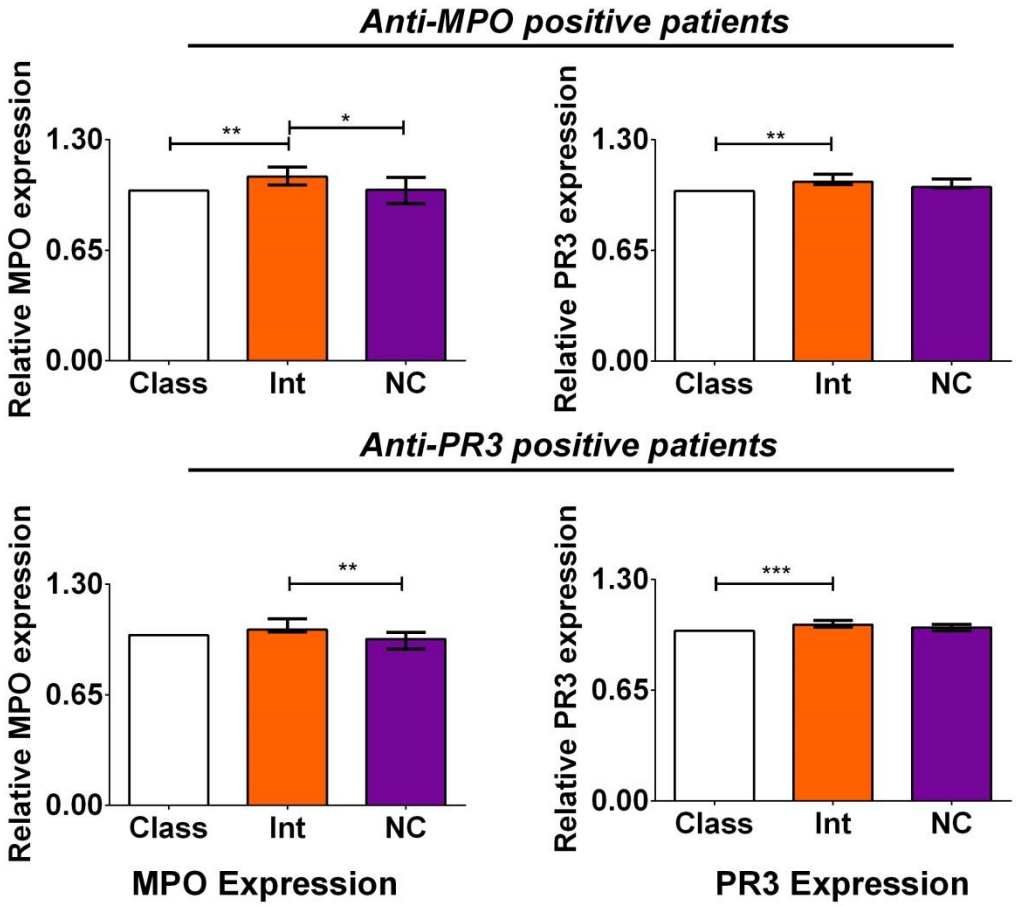

Figure 3.3.7 The MFI of MPO and PR3 expression is increased on intermediate monocytes in patients.

Peripheral blood was collected from patients with AAV. Cells were stained as described in methods and analysed by flow cytometry. Following gating on MPO or PR3 positive cells in each monocyte subset, the median fluorescence intensity (MFI) of MPO and PR3 was determined. For each individual these values were corrected by subtraction of the MFI for the fluorescence minus one (FMO) control and expressed relative to the corrected MFI for classical monocytes in that individual. Relative expression of cell-surface MPO or PR3 in each monocyte subset is shown for (**A-B**) anti-MPO+ AAV patients and (**C-D**) anti-PR3+ AAV patients. Data are presented as the median and interquartile range. Non-parametric one-way ANOVA (Friedman test) and Dunn's post-test were used to establish significance (*p<0.05, **p<0.01; ***p<0.001). Class: classical; Int: intermediate: NC: non-classical. N= 16 Anti-MPO and N=20 Anti-PR3

3.3.4 **Monocyte surface expression of MPO and PR3 is not linked.**

As cell-surface expression of both MPO and PR3 was increased on intermediate monocytes I investigated whether expression of the two autoantigens was linked in this cell type. However, I found that the majority of autoantigen expressing monocytes were positive for either MPO or PR3 alone, indicating that expression of MPO and PR3 on the monocyte cell surface occur independently of each other (**Figure 3.3.8**).

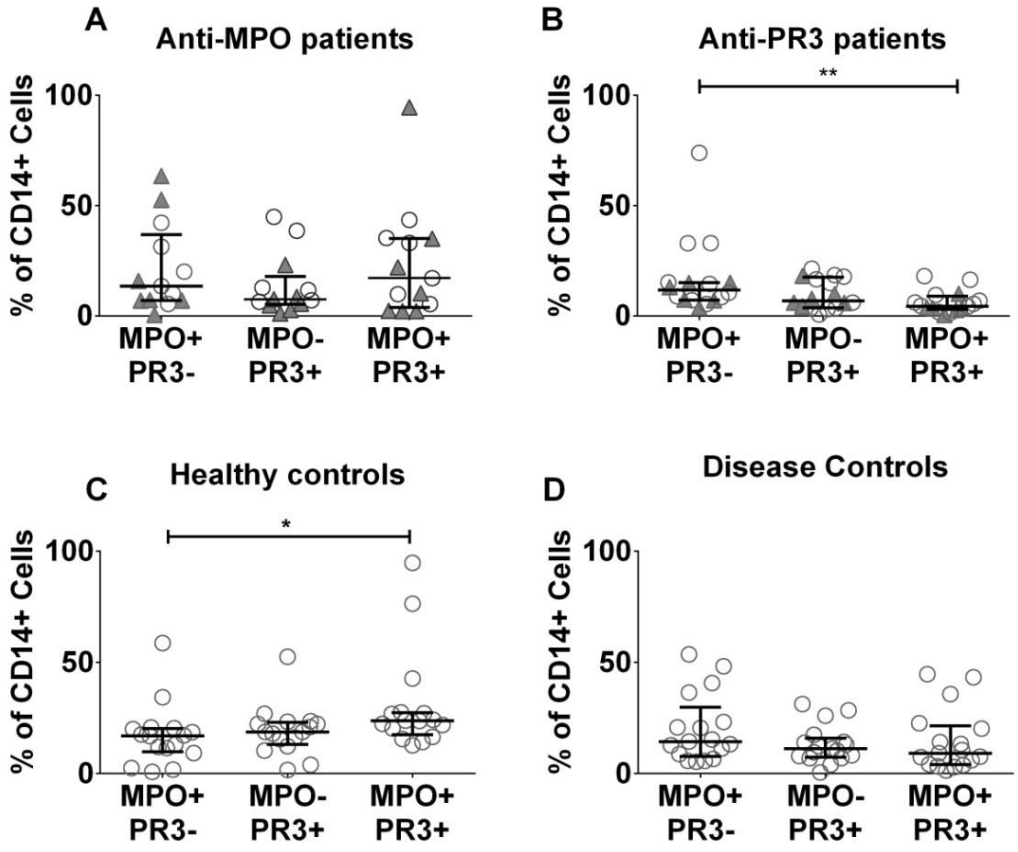

Figure 3.3.8 Cell-surface expression of MPO and PR3 is not linked on monocytes.
Peripheral blood was collected from patients with AAV and the percentage of cells expressing surface MPO and PR3 was examined by flow cytometry. Cells were classified as being MPO+PR3-, MPO-PR3+, MPO+PR3+. Data are presented for anti-MPO+ patients (**A**), anti-PR3+ patients (**B**), healthy control individuals (**C**) and disease control patients (**D**). Each symbol represents an individual patient. Open circles represent patients in remission and filled triangles patients with active disease. Data are presented as the median and interquartile range. Non-parametric one-way ANOVA (Friedman test) and Dunn's post-test were used to test for significance (**p<0.01). N= 16 Anti-MPO, N=20 Anti-PR3, N= 17 Healthy controls and N=18 Disease controls

These data suggest that the mechanism for anchoring the antigen to the plasma membrane is different for MPO and PR3. In neutrophils, surface expression of CD177 is linked to PR3 expression, with increased membrane expression of PR3 dependent on CD177 (Abdgawad et al., 2010). I investigated whether the same mechanism accounted for surface PR3 expression

on monocytes. I found little expression of CD177 on monocytes and no association between CD177 and PR3 (**Figure 3.3.9**). As demonstrated previously a high proportion of PR3+ granulocytes co-expressed CD177 (**Figure 3.3.9**).

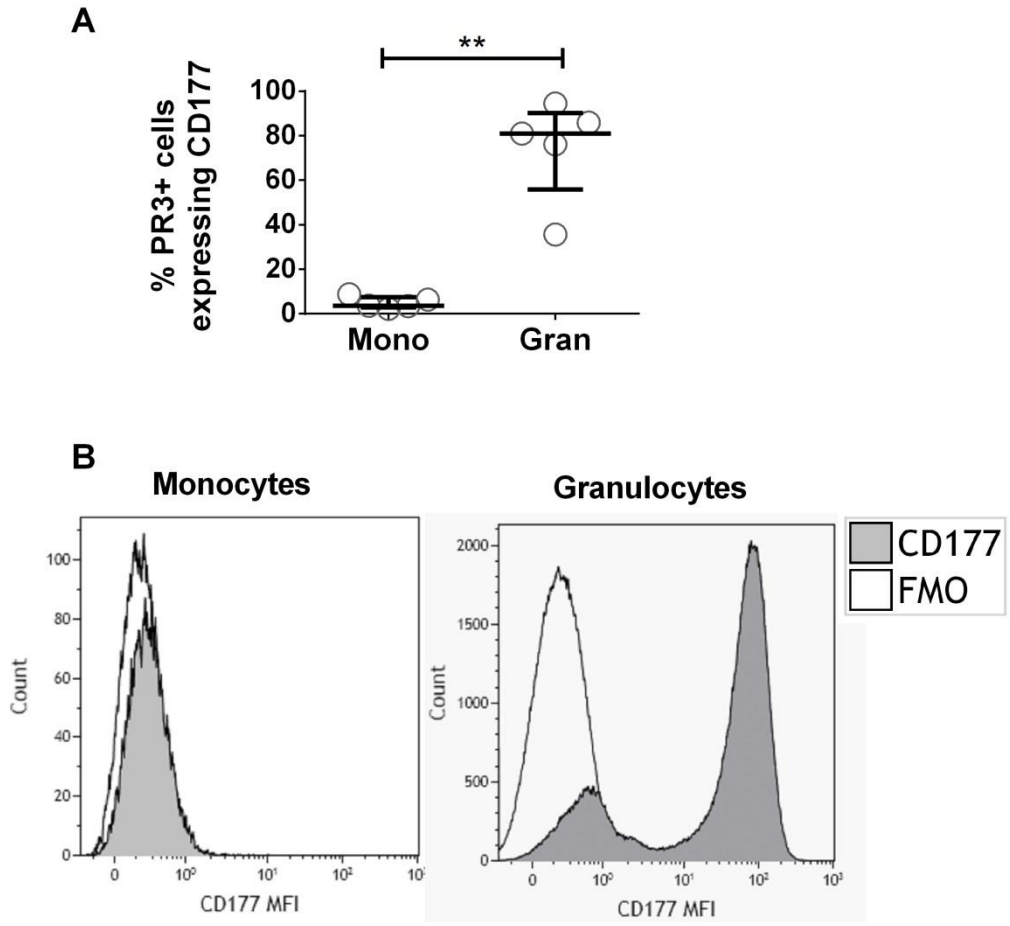

Figure 3.3.9 PR3+ monocytes do not co-express CD177.
Peripheral blood was collected from healthy control individuals, patients with AAV and disease controls and analysed by flow cytometry. Following gating on monocytes or granulocytes the percentage of PR3+ cells in each population which co-express CD177 was determined (**A**). Representative histograms show the median fluorescence intensity (MFI) of CD177 on monocytes and granulocytes (**B**). Data represent the median and interquartile range. Paired t-test was used to test for significance (**p<0.01). Mono: monocytes; Gran: granulocytes; FMO: fluorescence minus one control. N=5

3.3.5 CD16 expression correlates with cell-surface MPO but not PR3 expression on intermediate monocytes

As CD16 positivity is the criterion for differentiation between classical and intermediate monocytes, as well as being a potential signalling mechanism for ANCA in monocytes, I investigated the relationship between CD16 and MPO/PR3. Following gating on intermediate monocytes, I assessed whether the MPO/PR3 median fluorescence intensity was correlated with that of CD16. I found that surface MPO (**Figure 3.3.10 A, C**), but not PR3 (**Figure 3.3.10 B, D**), was significantly correlated with CD16 in both anti-MPO+ and anti-PR3+ AAV patients. Neither antigen was correlated with CD16 in

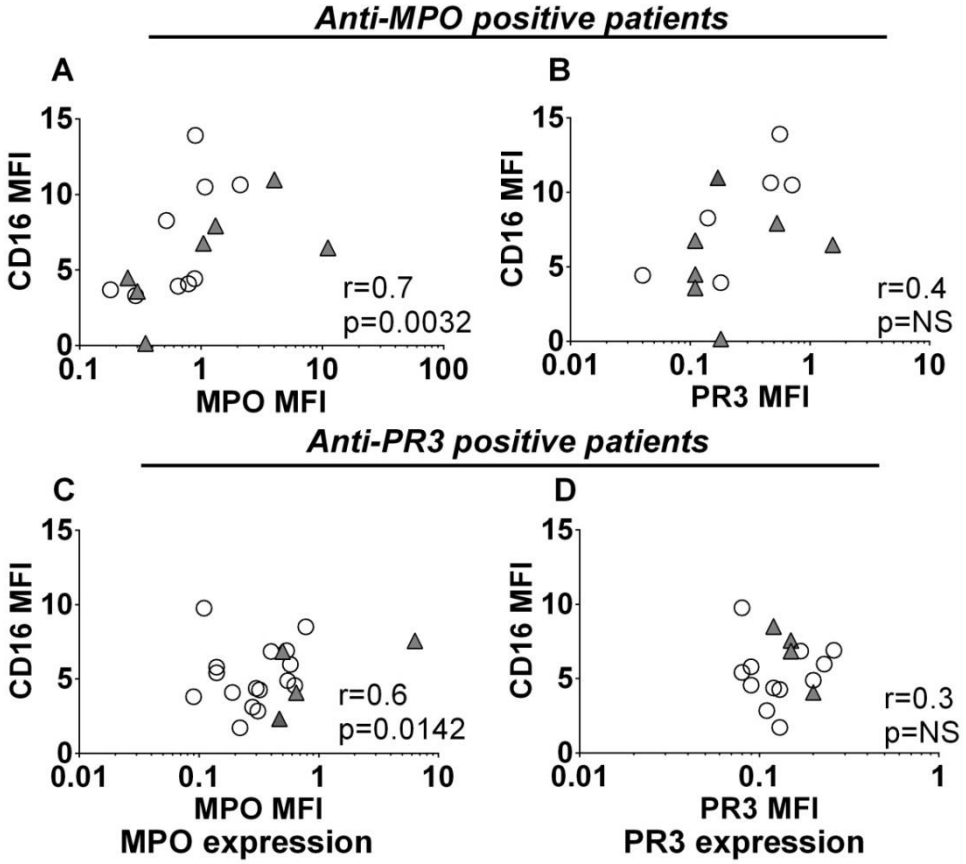

Figure 3.3.10 CD16 expression correlates with MPO but not PR3 expression on monocytes.
Peripheral blood was collected from patients with AAV and analysed by flow cytometry. Following gating on intermediate monocytes the MFI of CD16 was plotted against that of MPO or PR3. Data presented show (**A-B**) anti-MPO+ AAV patients, (**C-D**) anti-PR3+ AAV patients. Each symbol represents an individual patient. Open circles represent patients in remission and filled triangles show patients with active disease. Correlation was tested by Spearman Rank Test. NS=not significant. N= 16 Anti-MPO, N=17 Anti-PR3

healthy controls (**Figure 3.3.11 A, B**). Interestingly, both MPO and PR3 expression correlated with that of CD16 in disease control patients (**Figure 3.3.11 C, D**), suggesting that this may be a feature of either renal dysfunction or systemic inflammation.

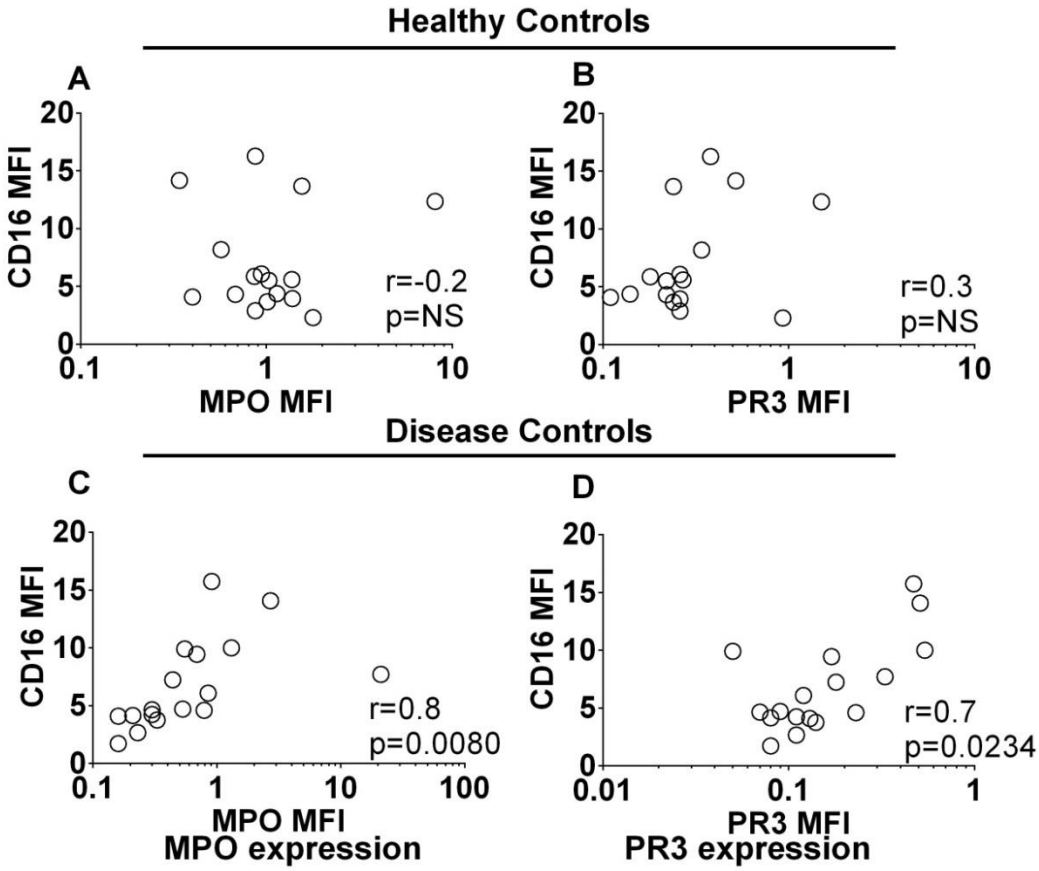

Figure 3.3.11 CD16 expression correlates with MPO and PR3 on disease controls but is not correlated in healthy individuals.
Peripheral blood was collected from healthy and disease control individuals. Following gating on intermediate monocytes the MFI of CD16 was plotted against that of MPO or PR3. Data presented show (**A-B**) healthy controls and (**C-D**) disease controls. Each symbol represents an individual patient. Correlation was tested by Spearman Rank Test. NS=not significant. N= 16 Healthy controls and N=17 Disease controls

3.3.6 Antibodies directed against MPO stimulate IL-1β, IL-6 and IL-8 production in monocytes

To investigate activation of monocytes following binding of ANCA to surface antigen, I measured release of pro-inflammatory cytokines; IL-1β, IL-6 and IL-8 from isolated monocyte populations. In order to isolate the required numbers of monocytes healthy donor blood obtained from the Irish Blood Transfusion Service was used in the following sections. First, I compared a number of different techniques which had been used in the literature for the isolation of monocytes from peripheral blood mononuclear cells (PBMCs). These techniques were adhesion to plastic (Schreiber et al., 2012), positive selection MACS (+ve MACS) (Yoon

et al., 2014) and negative selection MACS (-ve MACS) (Gelinas et al., 2011). I found that using +ve MACS based on CD14 expression provided a much higher purity level than either adherence of PBMCs to plastic or -ve MACS based on CD14 (**Figure 3.3.12 A**). While I did see a slight reduction in the percentage of viable cells using the +ve MACS isolation (**Figure 3.3.12 B**), I concluded that the dramatic increase in purity meant that this method was the most appropriate to elucidate mechanisms of monocyte activation. Although +ve MACS purity levels were ~80%, contaminating cells were found to be T and B cells which do not normally produce the cytokines of interest here and therefore should not interfere with the interpretation of these results

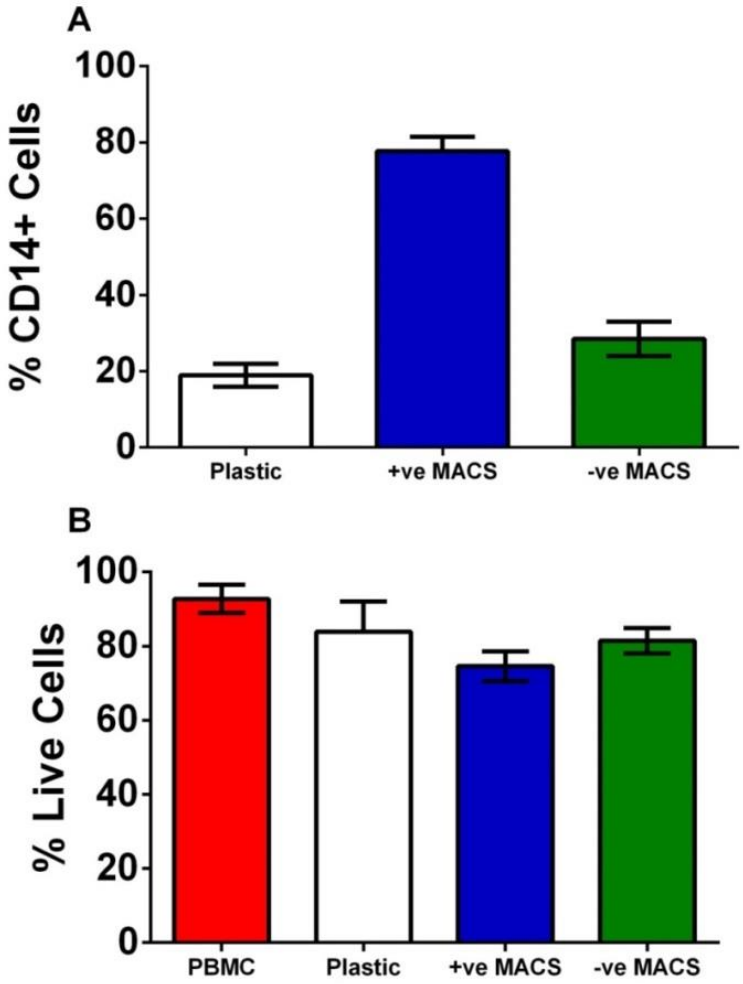

Figure 3.3.12 Positive selection provides the highest level of monocyte purity.
PBMCs were isolated from healthy control individuals. The purity of monocytes was measured using flow cytometry and the %CD14 positive cells is shown for three different isolation methods, adherence to plastic, positive selection MACS (+ve MACS) and negative selection MACS (-ve MACS) (**A**). The percentage of live cells before and after isolation using the three methods was determined using live/dead staining and flow cytometry (**B**). N=7

Based on previously described models of monocyte activation by ANCA,, monocytes were primed with tumour necrosis factor (TNF)-α in order to ensure antigen surface expression (Schreiber et al., 2012), before being stimulated with either monoclonal antibodies (mAb) directed against MPO or PR3 or with immunoglobulin G (IgG) purified from the plasma of patients with AAV as described in **Section 3.2.4**. Treatment with anti-MPO mAb resulted in significantly increased IL-1β, IL-6 and IL-8 production (**Figure 3.3.13 A-C**).

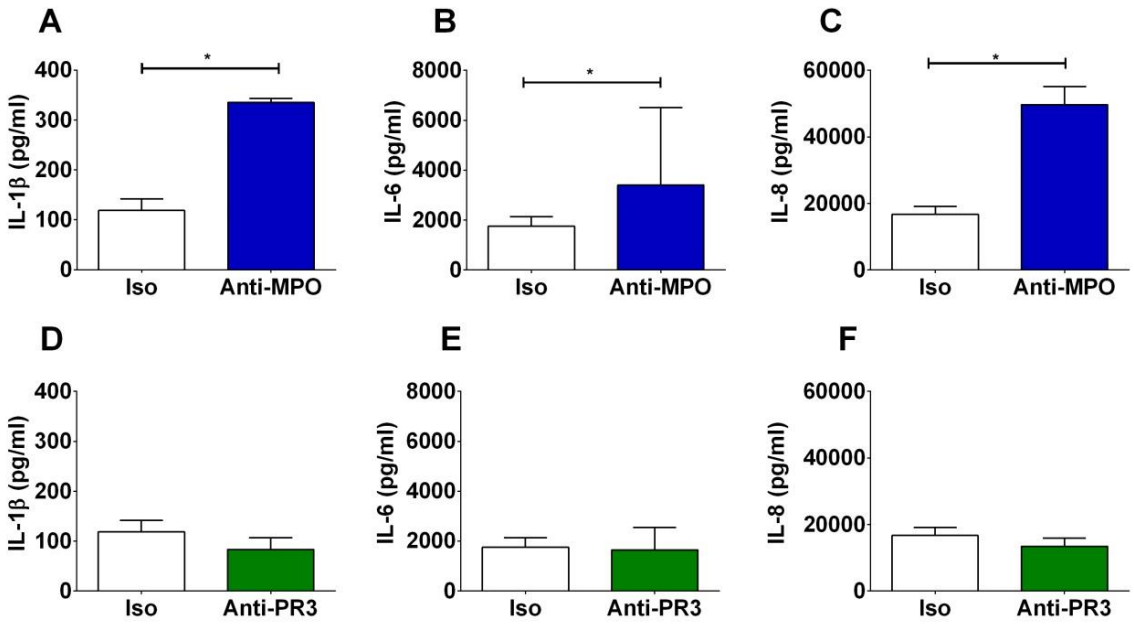

Figure 3.3.13 Stimulation of monocytes with anti-MPO mAb leads to an increase in IL-1β, IL-6 and IL-8 secretion.
CD14+ monocytes were isolated from the PBMCs of healthy controls by MACS separation. The cells were plated and incubated with 5 ng/ml TNF-α @ 37 ^{0}C for 30 minutes and then stimulated for 4 hours with 5μg/ml of either monoclonal antibody (mAb) directed against MPO or mAb against PR3 Supernatants were then removed and levels of IL-1β (**A, D**), IL-6 (**B, E**) and IL-8 (**C, F**) measured by ELISA. Data are presented as the median and interquartile range. Statistical analysis was performed using Wilcoxon signed rank test (*p<0.05,). Iso: isotype control. N=7

This increase in inflammatory cytokine production was also observed when monocytes were stimulated with IgG purified from anti-MPO+ AAV patients (**Figure 3.3.14 A-C**). Interestingly, this effect was not seen in monocytes stimulated with either mAb directed against PR3 (**Figure 3.3.13 D-F**) or protein G purified IgG from anti-PR3+ AAV patients (**Figure 3.3.14 D-F**).

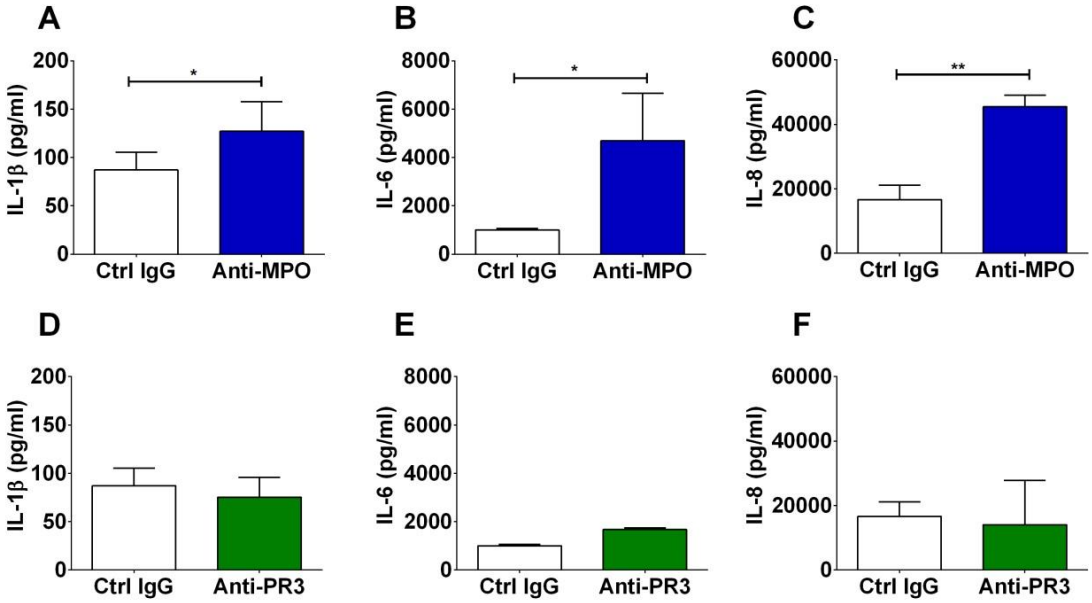

Figure 3.3.14 Stimulation of monocytes with IgG from anti-MPO+ patients leads to an increase in IL-1β, IL-6 and IL-8 secretion.
CD14+ monocytes were isolated from the PBMCs of healthy controls by MACS separation. The cells were plated and incubated with 5ng/ml TNF-α @ 37 ^{0}C for 30 minutes and then stimulated for 4 hours with 5μg/ml of either protein G purified IgG from anti-MPO+ patients or IgG purified from anti-PR3+ patients. Supernatants were then removed and levels of IL-1β (**A, D**), IL-6 (**B, E**) and IL-8 (**C, F**) measured by ELISA. Data are presented as the median and interquartile range. Statistical analysis was performed using Wilcoxon signed rank test (*p<0.05, **p<0.01). CTRL: Control. N=7

3.3.7 Cytokine production in response to stimulation with anti-MPO mAb varies between monocyte subsets

As I found MPO to be differentially expressed on different monocyte subsets, I next investigated if the production of pro-inflammatory cytokines IL-1β, IL-6 and IL-8 observed following stimulation of total monocytes differed in a subset-specific manner. Classical, intermediate and non-classical cells were sorted from MACS purified monocytes based on CD14 and CD16 expression (**Figure 3.3.15**). Sorted cells were primed with TNF-α and treated with anti-MPO mAb. This stimulation failed to induce secretion of any of the cytokines tested (IL-1β; IL-6; IL-8) from non-classical (NC) monocytes (**Figure 3.3.16 A-C**). IL-1β production was found to vary most between monocyte subsets, with intermediate monocytes producing higher quantities than classical monocytes both basally and in response to anti-MPO stimulation (**Figure 3.3.16 A**). IL-6 production was found to be similar in classical and intermediate monocytes and to be increased in both subsets following incubation of cells with anti-MPO (**Figure 3.3.16 B**). Conversely only classical monocytes were found to secrete IL-8 in response to anti MPO mAb (**Figure 3.3.16 C**).

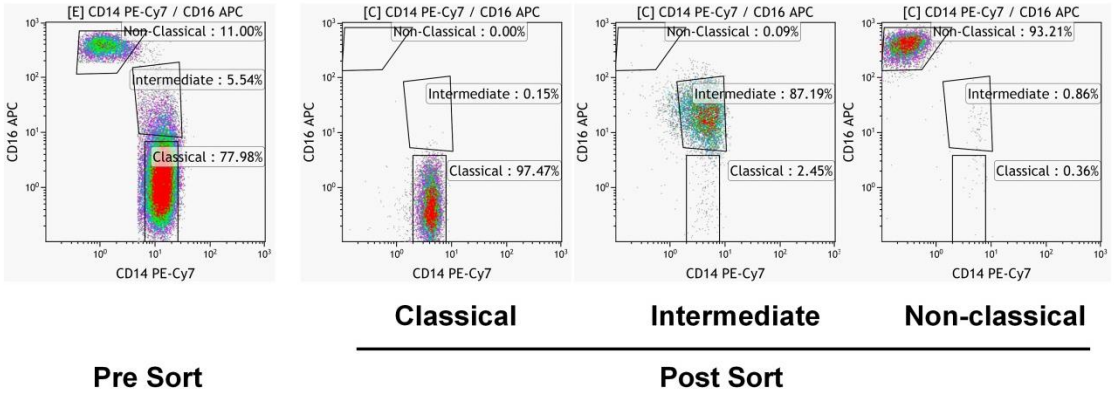

Figure 3.3.15 Purity of monocyte subsets following sorting.
Monocytes were gated based on size (FS) and granularity (SS). Doublets were excluded. Purity of sorted subsets was found by subdividing CD14+ monocytes into classical, intermediate and non-classical subsets based on CD14 and CD16 staining. Flow plots show typical pre- and post-sort monocyte subsets proportions.

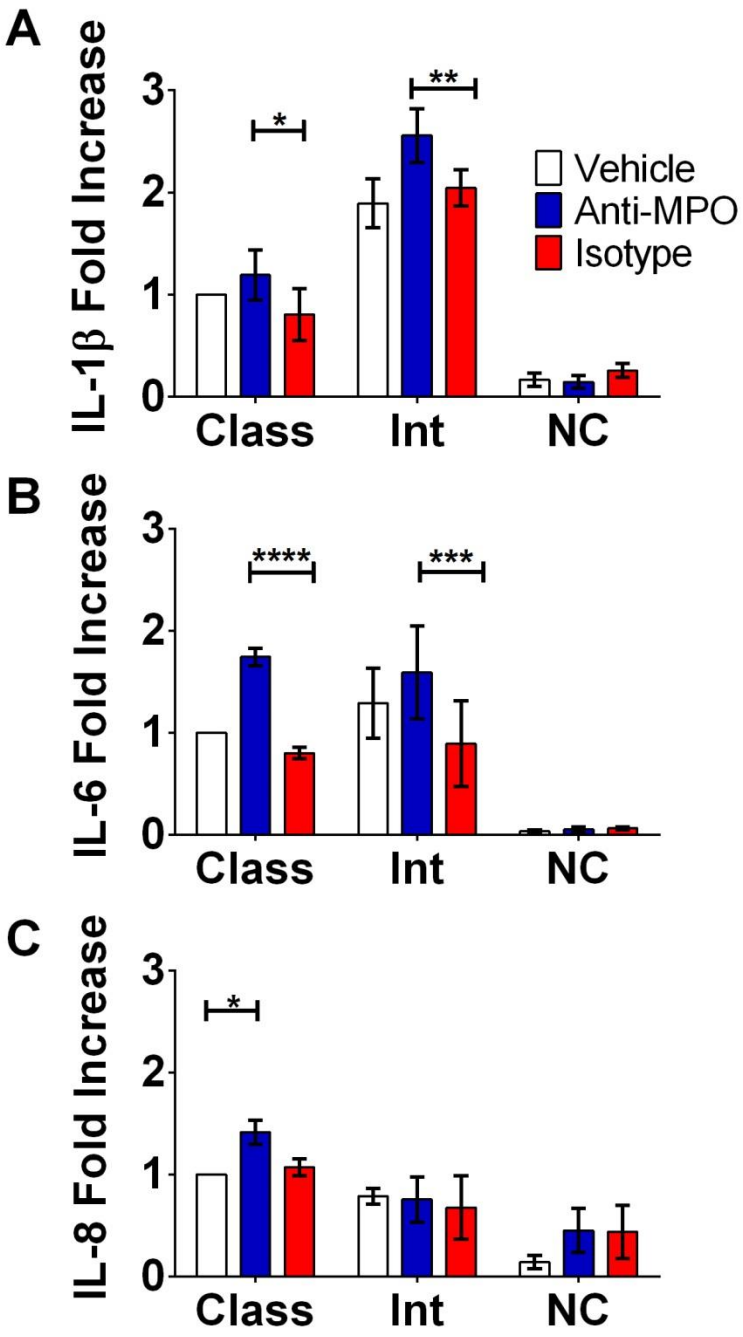

Figure 3.3.16 Intermediate monocytes produce increased amounts of IL-1β and IL-6 both basally and in response to stimulation with anti-MPO mAb.
CD14+ monocytes were isolated from PBMCs of healthy control individuals by MACS separation. Monocyte subsets were then sorted from CD14+ cells based on CD14 and CD16 expression. Sorted subsets of monocytes were incubated with 5ng/ml TNF-α @ 37 ^{0}C for 30 minutes followed by stimulation for 4 hours with 5μg/ml of either monoclonal antibody (mAb) directed against MPO or an isotype control. Supernatants were then removed and levels of (**A**) IL-1β, (**B**) IL-6 and (**C**) IL-8 measured by ELISA. Data are presented as the median and interquartile range of the fold increase over control. Statistical analysis was performed using Two-way ANOVA and Sidak test to correct for multiple comparisons (*p<0.05, **p<0.01, ***p<0.001, ****p<0.0001). Class: Classical; Int: Intermediate; NC: Non-Classical. N=4

3.3.8 IL-1β production in response to anti-MPO is not dependent on Fc binding in monocytes

It has been shown previously that the binding of the Fc portion of ANCA antibodies to neutrophils is required for their activation (Mulder et al., 1994). This finding, along with our own finding that the Fc receptor (CD16) expression on monocytes correlates with expression of MPO led us to investigate whether blocking the Fc receptor would abrogate the effect of anti-MPO stimulation in monocytes. In order to test this hypothesis I treated cells with anti-MPO mAb after pre-treatment with either Fc blocking solution or vehicle. Monocyte activation was measured by IL-1β production. Treatment with Fc blocking solution had no effect on the ability of anti-MPO mAb to activate monocytes (**Figure 3.3.17**).

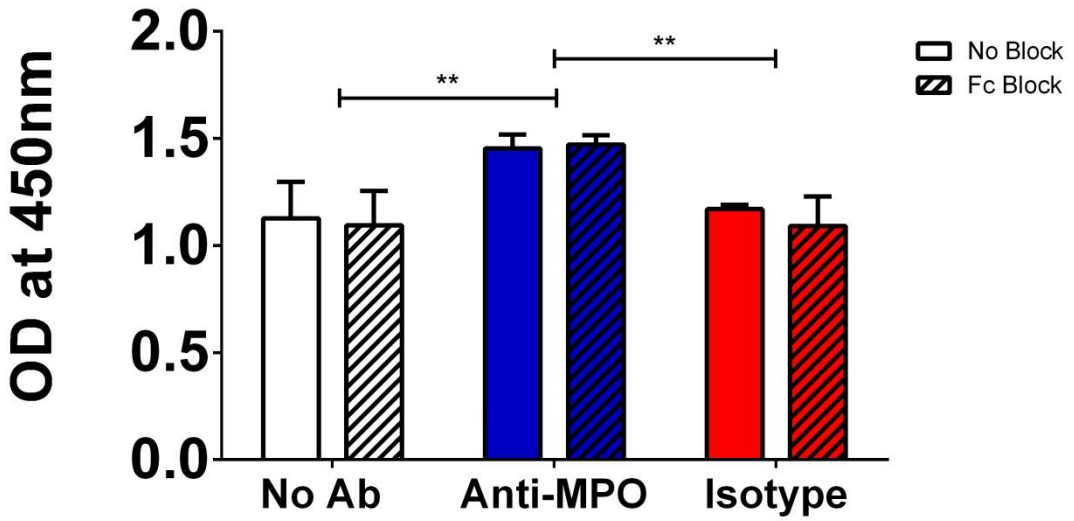

Figure 3.3.17 Fc receptor binding is not required for anti-MPO-induced IL-1β production by monocytes.
CD14+ monocytes were isolated from PBMCs of healthy control individuals by MACS separation. Cells were incubated with 2.5μg/10^6 cells Fc Block @ 37^{o}C for 30 minutes followed by stimulation for 4 hours with 5μg/ml of either monoclonal antibody (mAb) directed against MPO or an isotype control. Supernatants were then removed and levels of IL-1β measured by ELISA. Data are presented as the median and interquartile range. Statistical analysis was performed using Two-way ANOVA and Sidak test to correct for multiple comparisons (**p<0.01). N=3

3.4 Discussion

At the time that the stimulatory effect of ANCA on neutrophils was first described, a similar phenomenon was described in monocytes (Charles et al., 1992). ANCA were shown to stimulate oxygen radical production (Weidner et al., 2001) and to induce production of inflammatory cytokines such as IL-8 from monocytes (Ralston et al., 1997). Following these initial studies, the focus of research has been almost exclusively on neutrophils. As several other autoimmune diseases are characterised by an expansion of intermediate monocytes, I postulated that ANCA vasculitis would also display this phenotype. I have shown for the first time that the proportion of intermediate monocytes found in AAV patients is increased when compared to healthy control individuals. A recent paper by *Tarzi et al* found no difference in the proportion of each monocyte subset in patients (Tarzi et al., 2015). The change which I found in the proportion of intermediates is subtle and therefore the differences between these two results may just be a result of the increased number of patients captured in my study (100 vs 60). In addition, I have demonstrated that the autoantigens associated with ANCA vasculitis (MPO and PR3) are differentially expressed on distinct monocyte subsets, with the highest expression being seen on intermediate cells. Interestingly, *Tarzi et al* found that intermediate monocytes only preferentially expressed MPO and it was the classical subset which had the highest prevalence of surface PR3 expression (Tarzi et al., 2015). The reason for discrepancy between these two sets of results is unclear as similar staining protocols were used in both studies. Minor differences such as the type of lysis buffer used or the different fluorescent antibodies used may play a role in these differences however this is unlikely to be the only reason behind them. More study into the surface expression of ANCA antigens, particularly PR3, may therefore be needed in order to fully characterise these cells. In concordance with cell surface expression of MPO on monocytes I confirmed that stimulation with anti-MPO antibodies results in monocyte activation, as measured by IL-1β, IL-6 and IL-8 production, although anti-PR3 antibodies did not have this effect. Importantly, I also demonstrated that monocyte subsets respond differently to anti-MPO antibodies, with intermediate monocytes producing the highest amount of IL-1β and increased IL-6 following stimulation.

I first divided the AAV patients into those with active disease and those who were in remission based on the hypothesis that those patients with active disease would have increased inflammatory monocytes. I found that both remission and active patients had an increased proportion of intermediate monocytes when compared to the proportions observed in healthy control individuals. This indicates that this cell type is expanded in patients and therefore may play a role in disease pathogenesis or pathophysiology.

I also analysed the expression of the autoantigens targeted by ANCA on monocyte subsets. It has been reported that monocytes express both MPO and PR3 on their cell surface (Owen et al., 1994, Hattar et al., 2002) although their expression on different monocyte subsets has not been reported. I found that both of these antigens are expressed preferentially on intermediate monocytes when compared to the classical and non-classical populations. Although intermediate cells account for a relatively small fraction of total monocytes in peripheral blood (6-11% in healthy individuals), the proportion of this monocyte subset is increased in ANCA patients as I have shown. This increase, in combination with increased expression of the autoantigens, suggests that this subset may be the monocyte target of ANCA. Not only do an increased proportion of intermediate monocytes express these antigens, but these cells express a greater amount of MPO or PR3 on their surface than their classical or non-classical equivalents. Taken together these data suggest that the intermediate subset is the monocyte population which is most susceptible to ANCA stimulation.

In anti-MPO+ AAV patients the correlation between surface MPO and CD16 on intermediate monocytes indicates that expression of these two molecules may be linked. In neutrophils, ANCA have been shown to induce the activation of the cell through first binding to MPO or PR3 and subsequent signalling through their Fc region (Mulder et al., 1994). As CD16 is an Fc receptor its expression on the same cells as MPO may provide an insight into the possible activation of these cells by anti-MPO ANCA. The differential nature of surface MPO and PR3 expression is highlighted by the fact that in AAV patients CD16 is only correlated with MPO but not PR3. The significance of this finding remains to be determined as I have found that Fc receptor binding is not required for the induction of IL-1β by anti-MPO. This finding, along with the similar response to vehicle and isotype treated cells further emphasises the lack of requirement for CD16 binding in these cells.

It has been shown that CD16 expression occurs in lipid rafts (Cherukuri et al., 2001). While CD16 is not directly required for signalling in response to anti-MPO stimulation, the correlation between MPO and CD16 may indicate that lipid raft formation is occurring and therefore other glycosylphosphatidylinositol (GPI)-linked proteins may be involved in the response to anti-MPO antibodies. Another way in which monocytes appear to differ from neutrophils is the way in which they express PR3 on their surface. In neutrophils, surface translocation of PR3 usually occurs through an association with CD177 (Abdgawad et al., 2010). This does not appear to be the mechanism in monocytes; elucidation of how both PR3 and MPO traffic and remain on the plasma membrane of monocytes, as well as presumably facilitating an outward-in signalling process, will need to be examined closely. CD177 is thought to form a signalling complex through which neutrophils are stimulated following binding of antibodies to PR3 (Jerke et al., 2011). As I have shown, monocytes lack CD177 on their

surface and this may explain why stimulation with PR3 antibodies does not lead to IL-1β production in these cells.

It has been shown previously that mAbs directed against both MPO and PR3 lead to the production of IL-1β from monocytes (Schreiber et al., 2012). However, my data demonstrate that only anti-MPO and not anti-PR3 stimulation leads to the activation and subsequent IL-1β production from monocytes. The discrepancy between these two results may be due to the fact that monocytes were isolated by different methods. I have used a positive magnetic bead selection method, whereas Schreiber *et. al.* used a plastic adherence method in order to purify their monocytes. As I have shown here, this plastic adhesion method resulted in poorer monocyte purity. It has also been shown previously that adherence of monocytes to plastic can result in partial activation of the cells (Kelley et al., 1987). This presence of impure monocytes or possible prior activation of these cells may account for the differences in IL-1β production in response to ANCA stimulation. While positive selection produced purer monocyte populations than the other methods this process may also partially activate these cells (Beliakova-Bethell et al., 2014). Interestingly, monocyte gene expression was only slightly altered between positive and negative selection in this study suggesting a minimal role for isolation method in activating the cells. However, due to the potential trade-off between purity and activation, the inclusion of isotype and vehicle control stimulations are vital for the interpretation of these results. I have shown a similar result when mAbs were replaced with IgG derived from anti-MPO+ and anti-PR3+ patients, with only IgG from anti-MPO+ patients leading to IL-1β production, further verifying the specificity of the response. This specific anti-MPO response is also observed when I investigated other inflammatory cytokines, IL-6 and IL-8. The production of these cytokines mirrored the pattern observed in IL-1β production from the stimulated total monocyte population.

In order to investigate the hypothesis that the intermediate subset of monocytes, by virtue of their increased antigen expression, would have the greatest response to anti-MPO antibodies I used a similar system of stimulation to that used for total monocytes. For these experiments I went a step further and sorted the individual monocyte subsets based on their CD14 and CD16 expression. This allowed me to analyse the individual subsets and therefore show how each group was contributing to the response to antibody stimulation which I had seen previously. Stimulation of the intermediate subset led to the highest production of IL-1β. The magnitude of the increase in anti-MPO induced IL-1β in sorted monocytes was not as high for any of the subsets as had been observed in total monocytes. This is likely a consequence of the additional MoFlo sorting procedure, which may have partially activated the cells prior to stimulation. Intermediate monocytes have previously been shown to produce a number of cytokines in response to LPS (Cros et al., 2010); however, their response to ANCA has not been studied until now. I have shown that the three monocyte subsets each have a different

cytokine profile following stimulation with anti-MPO antibodies. While the intermediate monocytes showed the greatest increase in IL-1β production, the amount of IL-6 produced in these cells was comparable to that seen in the classical subset. Conversely, the IL-8 production observed in response to ANCA stimulation of monocytes was shown to be exclusively a product of the classical subset. Interestingly, secretion of each of these cytokines was unchanged in the non-classical subset in response to ANCA stimulation. Previous studies have attempted to classify the three monocyte subsets based on their differential cytokine production, which also serve to underline the complex nature of cytokine release by each subset (Skrzeczynska-Moncznik et al., 2008, Cros et al., 2010).

It is unclear whether intermediate monocytes represent a transitional cell type or whether they are a functionally distinct cell population. While the current consensus of monocytes is that there are three distinct subsets as discussed above, recent studies have suggested that these cells may in fact exist on a continuum rather than distinct subsets (Villani et al., 2017). This study used unbiased RNA-seq in order to characterise monocytes and dendritic cells from human samples. When using this approach, monocytes could be classified into 4 subsets rather than the three currently used. The classical and non-classical cells appeared to form two separate clusters with the intermediate subset being split into two categories based on gene expression. This study suggests that, similar to macrophages, monocytes may exist in a continuum rather than the polarised subsets discussed in the majority of the literature. The fact that myself and others have shown that monocyte subsets have distinct functions and how these data could be translated to monocytes described on a spectrum remains unclear. In reality monocytes likely have various activation states depending on the tissue in which they are situated and the stimuli they have encountered. This research indicates the importance of further study into this cell type and the exact mechanisms through which different monocyte types may respond to stimuli.

My data clearly support a distinct functional role for these cells as they differ from both classical and non-classical monocytes in terms of autoantigen expression, production of the pro-inflammatory cytokine IL-1β, and response to ANCA. For all of these parameters, non-classical cells were more similar to the classical subset than they were to the intermediate, suggesting that intermediate monocytes are not a transitional population.

The production of IL-1β has been shown to play a critical role in disease pathogenesis, with the IL-1 receptor antagonist anakinra protecting against glomerulonephritis in an anti-MPO-induced mouse model (Schreiber et al., 2012). By sorting of individual monocyte subsets I have shown that intermediate monocytes preferentially express the autoantigens associated with AAV and that these cells produce the highest levels of IL-1β in response to anti-MPO, suggesting a possible key role for these cells in AAV. It is likely that while neutrophils are

responsible for initial pathologic responses to ANCA in patients, monocyte interactions with neutrophils may have a role in this early stage of disease. In this context, IL-1β has been shown to prime neutrophils for activation (Sullivan et al., 1989), suggesting a feedback loop in which monocytes and neutrophils continuously activate one another to propagate disease.

My data demonstrating the induction of IL-1β, IL-6 and IL-8 by anti-MPO but not anti-PR3 antibodies highlights differences between the two primary autoantigens associated with AAV. It is increasingly appreciated that MPO-ANCA and PR3-ANCA vasculitis are different diseases both genetically and phenotypically (Lyons et al., 2012). The presence of anti-PR3 antibodies portends a high relapse rate (Sanders et al., 2004) and granulomatous disease affecting the upper and lower respiratory tract (Franssen et al., 1998, Goldschmeding et al., 1990), while the presence of anti-MPO antibodies is associated with a more “vasculitic” phenotype with a high incidence of scarring in kidney and lung at the time of diagnosis (Goldschmeding et al., 1990, Falk and Jennette, 1988). While mechanistic explanations linking the current work with these observations are beyond the scope of this body of work, monocytes and macrophages are important in both the generation of granuloma (Mukhopadhyay et al., 2012) and progression of fibrosis, so it is conceivable that the differential effect of anti-PR3 and anti-MPO antibodies on these cells is important in cellular pathogenesis. For example, the MCP1 / CCR2 chemokine axis is known to be pro-fibrotic (Distler et al., 2006) and may be preferentially activated by anti-MPO antibodies. Further investigation to understand this differential effect and its link to clinical phenotype is ongoing.

Chapter 4: The pro-inflammatory effects of ANCA on monocytes are linked to changes in cellular metabolism

4.1 Introduction

Cellular metabolism has been the subject of extensive study in cancer. The “Warburg effect” which occurs in many cancer cells results in a large increase in glycolysis despite non limiting levels of oxygen (Warburg, 1956, Lopez-Lazaro, 2008). Cancer cells are thought to activate this pathway in order to produce materials which are vital for growth (Lopez-Lazaro, 2008). For many years the realm of cellular metabolism was largely ignored by immunologists. This was despite the fact that it had been shown as far back as 1962 that certain immune cells such as macrophages have an increase in their glycolytic rate upon activation (Evans and Karnovsky, 1962). In many ways immune cells in the early stages of activation have similar characteristics to cancer cells; increased requirement for cellular building blocks, ability to proliferate quickly and need to proliferate in multiple environments, such as in areas of high pH (Zheng, 2012). Immune cells such as monocytes, macrophages and T cells can often be polarised to perform a number of different functions. This polarisation within cell types requires tight control to allow for an adequate and appropriate response to stimuli. Recent studies have shown that changes in intracellular metabolism play a major role in immune cell function and polarisation (Galvan-Pena and O'Neill, 2014). These changes are more than just responsive but rather they have been shown to instruct cell function (Gleeson et al., 2016) and have recently been implicated in several autoimmune conditions (Yang et al., 2013, Wahl et al., 2010). Functionally distinct metabolic profiles have been established for a number of cell types. Some of these are shown in **Figure 4.1.1**.

The majority of cells in the body, both stromal and resting immune cells, rely mainly on oxidative phosphorylation (ox phos) for energy production. This efficient metabolic pathway allows for the production of 36 ATP molecules for each molecule of glucose consumed by the cell (Rich, 2003). Anti-inflammatory cells such as M2 macrophages and memory T cells rely on ox phos to meet their energy needs (Jha et al., 2015, O'Sullivan et al., 2014). This pathway, while extremely efficient, can often be relatively slow to be activated (Pfeiffer et al., 2001). For this reason cancer cells and immune cells which are considered to be pro inflammatory, such as LPS activated M1 macrophages or effector T cells, rely mainly on glycolysis for energy production (Rodriguez-Prados et al., 2010, Michalek et al., 2011). Interestingly, CD4+ T cells also upregulate ox phos when activated however glycolysis is the more predominant pathway (Palmer et al., 2016).

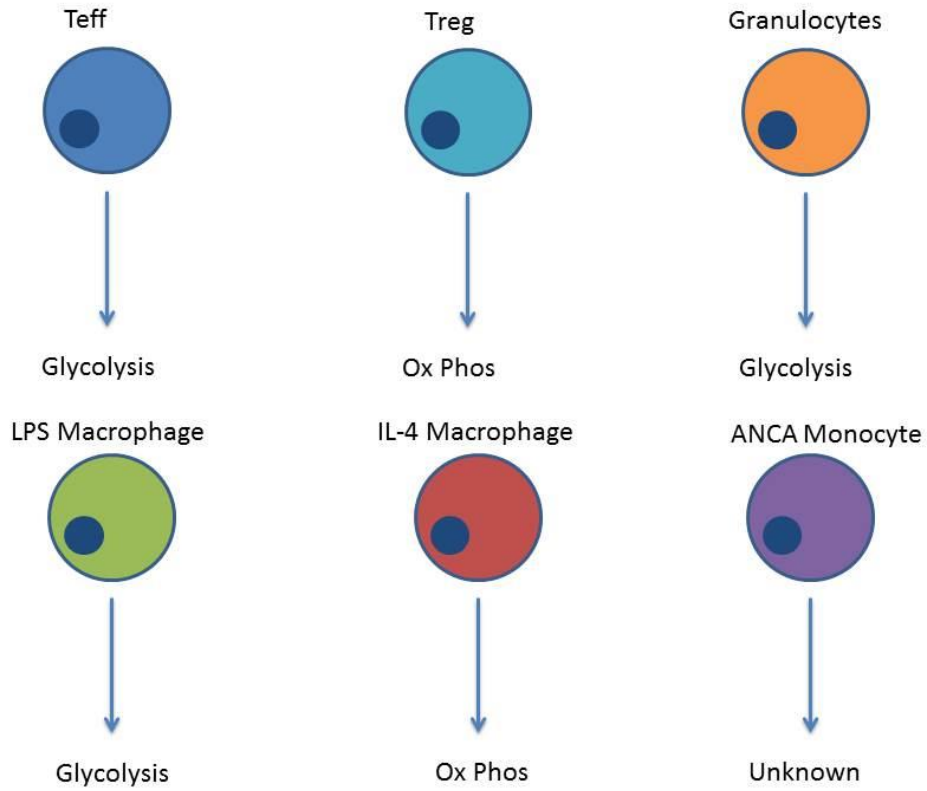

Figure 4.1.1 Predominant metabolic pathways in activated cell types

While the main output of these metabolic pathways is energy in the form of ATP they also produce a number of intermediates which are used to create the building blocks needed for cell growth and division (Lopez-Lazaro, 2008). Cells which use glycolysis as their main source of energy can therefore divert intermediates, such as citrate, which would usually be used in the TCA cycle into other pathways such as fatty acid synthesis (Martin and Vagelos, 1962). While glycolysis and ox phos are often considered to be the main metabolic pathways in the cell, other pathways such as the pentose phosphate pathway or glutaminolysis are also important in immune cell function (Haschemi et al., 2012, Wallace and Keast, 1992). The interactions between all of these pathways are beginning to emerge as having important roles in immune cell functionality (O'Neill et al., 2016). In this initial study into the effect of ANCA stimulation on monocyte metabolism I have focussed on glycolysis and oxidative phosphorylation.

Monocytes have been less well studied than either macrophages or T cells when it comes to metabolic shifts upon activation. Some studies have shown that monocytes also undergo a metabolic shift from ox phos to glycolysis in response to lactate (Dietl et al., 2010). Other data, using HIV as the stimulus, have however shown the opposite effect with glycolysis being decreased in activated monocytes (Hollenbaugh et al., 2011). These data show that

metabolic response of monocytes varies depending on stimulus and therefore specific work on diseases in which monocytes are thought to play a role is necessary. Monocytes activated with HIV also display increased levels of the glucose transporter Glut-1 and have increased glucose uptake (Palmer et al., 2014). These studies show that increased study on the metabolic changes involved in monocyte activation is required in order to correctly phenotype this cell type.

IL-1β is a key inflammatory cytokine which has a number of effects both locally and systemically. These include induction of cyclooxegenase type 2 (COX-2), nitric oxide production, increase in adhesion molecules, fever induction and polarisation of T cells (reviewed in (Dinarello, 2009)). In **Chapter 3** I observed increased IL-1β production from monocytes in response to anti-MPO. This result has also been shown by other groups with IL-1β being used as a signal for monocyte proinflammatory activation (Schreiber et al., 2012). A number of recent studies have shown links between the production of IL-1β from bone marrow derived macrophages (BMDMs) and changes in the cellular metabolism of those cells (Tannahill et al., 2013, Palsson-McDermott et al., 2015). In these studies IL-1β production was linked to a switch to aerobic glycolysis in these cells and also to an increase in fatty acid oxidation (Mills et al., 2016, Tannahill et al., 2013). The molecular changes involved in this pathway have been the subject of extensive study in macrophages. In these cells activation with a pro inflammatory signal such as LPS results a complex set of changes which allow for an upregulation of proinflammatory pathways. The primary change in these cells is a downregulation of oxidative metabolism through the inhibition of succinate dehydrogenase (SDH) which results in an accumulation of succinate. Succinate then acts to stabilise Hif-1α which leads to the production of IL-1β. In macrophages treated with LPS there is also an upregulation of enzymes associated with glycolysis such as hexokinase 1(HK1) (Tannahill et al., 2013) and enolase (Bae et al., 2012). The primary role of these enzymes is in the conversion of glucose to pyruvate in glycolysis. HK1 can also act outside of the glycolytic pathway by activating the NLRP3 inflammasome which increases IL-1β levels while enolase can increase proinflammatory cytokines such as TNF and IFN-γ. As members of the myeloid lineage changes in macrophages have provided the basis for my work into monocytes. In comparison to these cells the elucidation of metabolic shifts in monocytes is in its infancy however the pathways involved are beginning to become clearer.

The ability to detect changes in cellular metabolism in real time has been greatly aided by Seahorse extracellular flux technology. This relatively new technology allows for the real time measurement of extracellular acidification rate (ECAR) and oxygen consumption rate (OCR). These measurements act as surrogate markers for glycolysis and ox phos respectively. In recent years the literature has become more and more reliant on using this technology to explore changes in cellular metabolism. The real time nature of Seahorse measurements,

compared to techniques such as using oxygen electrodes to measure oxygen consumption, and the ability to add inhibitors directly to cells of interest provides a more robust method of elucidating pathways and changes involved in immune cell metabolism. Here I have investigated the metabolic changes involved in the response of monocytes to ANCA stimulation.

4.2 Hypothesis and methods

4.2.1 Hypothesis

Activation of immune cells has been shown to be dependent on switches in cellular metabolism. In particular IL-1β production from innate immune cells has been shown to be reliant on a switch to aerobic glycolysis. I therefore hypothesised that:

I. Activation of monocytes in response to ANCA results in a switch to glycolytic metabolism
II. Metabolic changes in monocytes are required for their pro-inflammatory response to ANCA

4.2.2 Methods:

The methods used to investigate the hypothesis outlined in Chapter 4.2.1 are outlined in Figure 4.2.1.

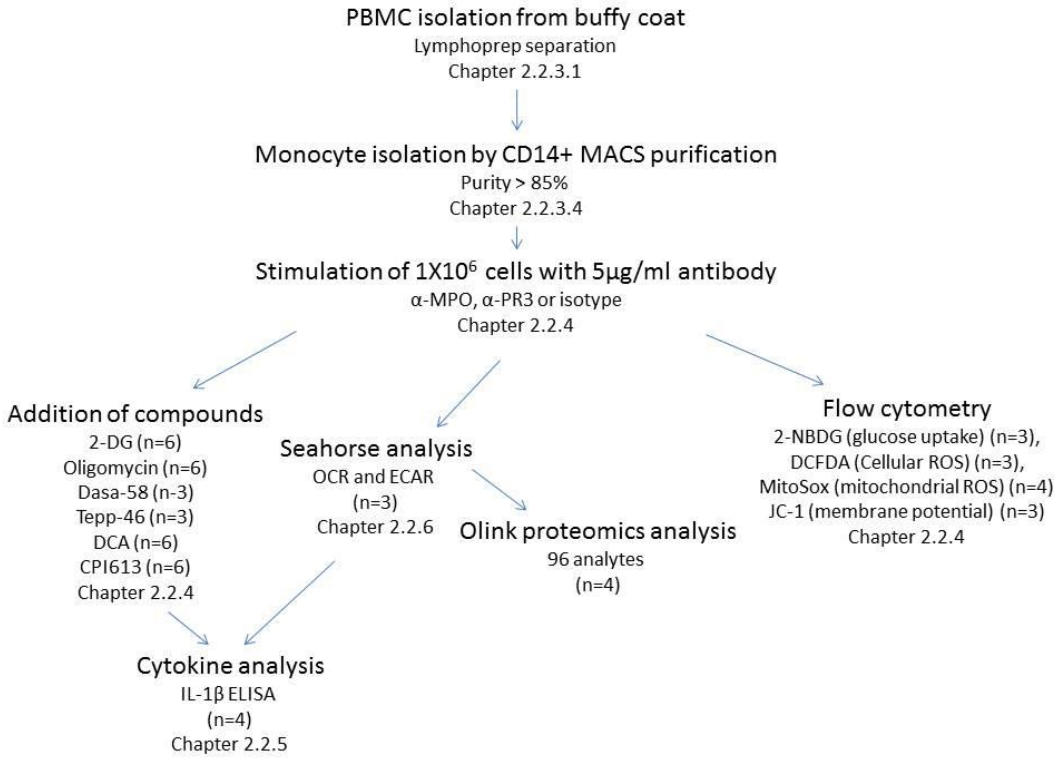

Figure 4.2.1 Diagramtic representation of techniques used.
Overview of experimental plan and techniques used to investigate metabolic changes involved in ANCA stimulated monocytes. Detailed methods are provided in the chapter number shown below each technique.

4.3 Results

4.3.1 TNF-α priming is not required for monocyte activation by ANCA

Previous studies, including Chapter 3 of this work, had used TNF-α to prime monocytes before ANCA stimulation (Schreiber et al., 2012). This step was performed as a result of previous data from neutrophil studies which showed that priming was required for neutrophil activation by ANCA (Csernok et al., 1994, Harper et al., 2001a). This priming step is required in neutrophils as they do not basally express MPO and PR3 on their surface. As I have shown in Chapter 3.3.2, monocytes in unstimulated whole blood have MPO on their surface. In order to assess whether priming with TNF-α was necessary in purified monocytes I measured the amount of MPO on the surface of these cells with and without TNF-α stimulation and also examined the ability of these cells to produce IL-1β in response to ANCA under the same conditions. I found that TNF priming did not increase the proportion of monocytes with MPO on their surface (**Figure 4.3.1 A**). There was also no significant difference in the amount of IL-1β produced by ANCA stimulated monocytes which had not been primed when compared to those which were pre-treated with TNF-α (**Figure 4.3.1 B**). These results allowed me to remove the TNF priming step and therefore allow for this important cytokine to be measured in future work.

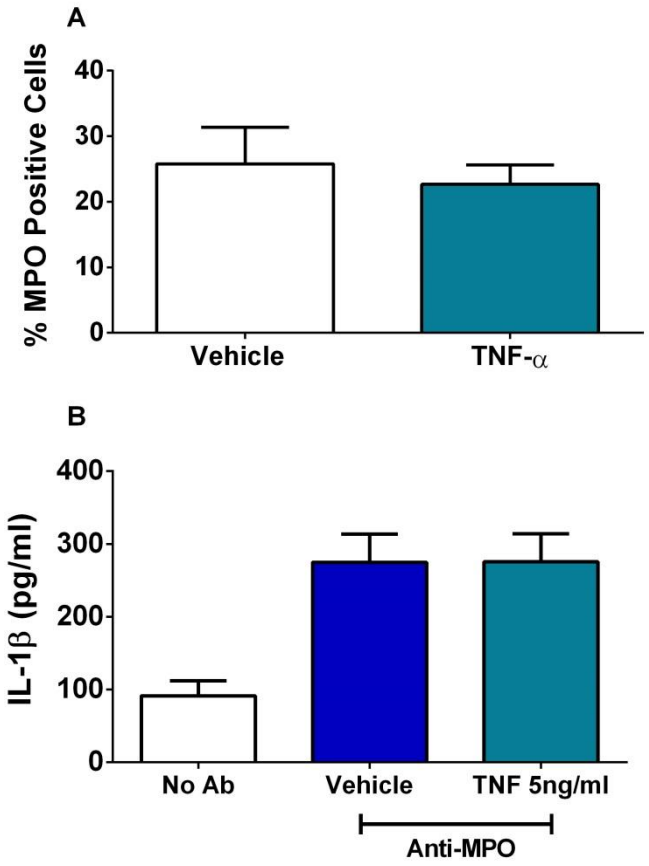

Figure 4.3.1 TNF-α priming is not required for the monocyte response to anti-MPO antibodies.
CD14+ monocytes were isolated from the PBMCs of healthy controls by MACS separation. The cells were plated and incubated with vehicle or 5ng/ml TNF-α @ 37 ^{0}C for 30 minutes and then stimulated for 4 hours with 5μg/ml monoclonal antibody (mAb) directed against MPO. Cells were removed and stained for surface MPO (**A**) or PR3 (**B**). Supernatants were removed and levels of IL-1β (**C**) measured by ELISA. Data are presented as the median and interquartile range (n=4).

4.3.2 **Anti-MPO stimulated monocytes have increased glucose uptake**

As IL-1β production had been linked to changes in intracellular metabolism I next wanted to investigate if similar changes were occurring in the anti-MPO stimulated monocytes which produce this cytokine (**Chapter 3.3.13**) and to establish whether differences in metabolism could be involved in the differential reaction of monocytes to anti-MPO and anti-PR3 antibodies. Firstly I wanted to look at the overall glucose uptake by these cells. To do this I used 2-[N-(7-nitrobenz-2-oxa-1,3-diazol-4-yl) amino]-2-deoxy-D-glucose (2-NBDG), a non-metabolisable fluorescent analogue of glucose. This molecule is taken up in the same way as glucose but is not broken down by the cell and it's fluorescence can therefore be used as a surrogate marker for glucose uptake (Zou et al., 2005). I have found that anti-MPO stimulation of monocytes results in an increase in glucose uptake (**Figure 4.3.2 A and C**).

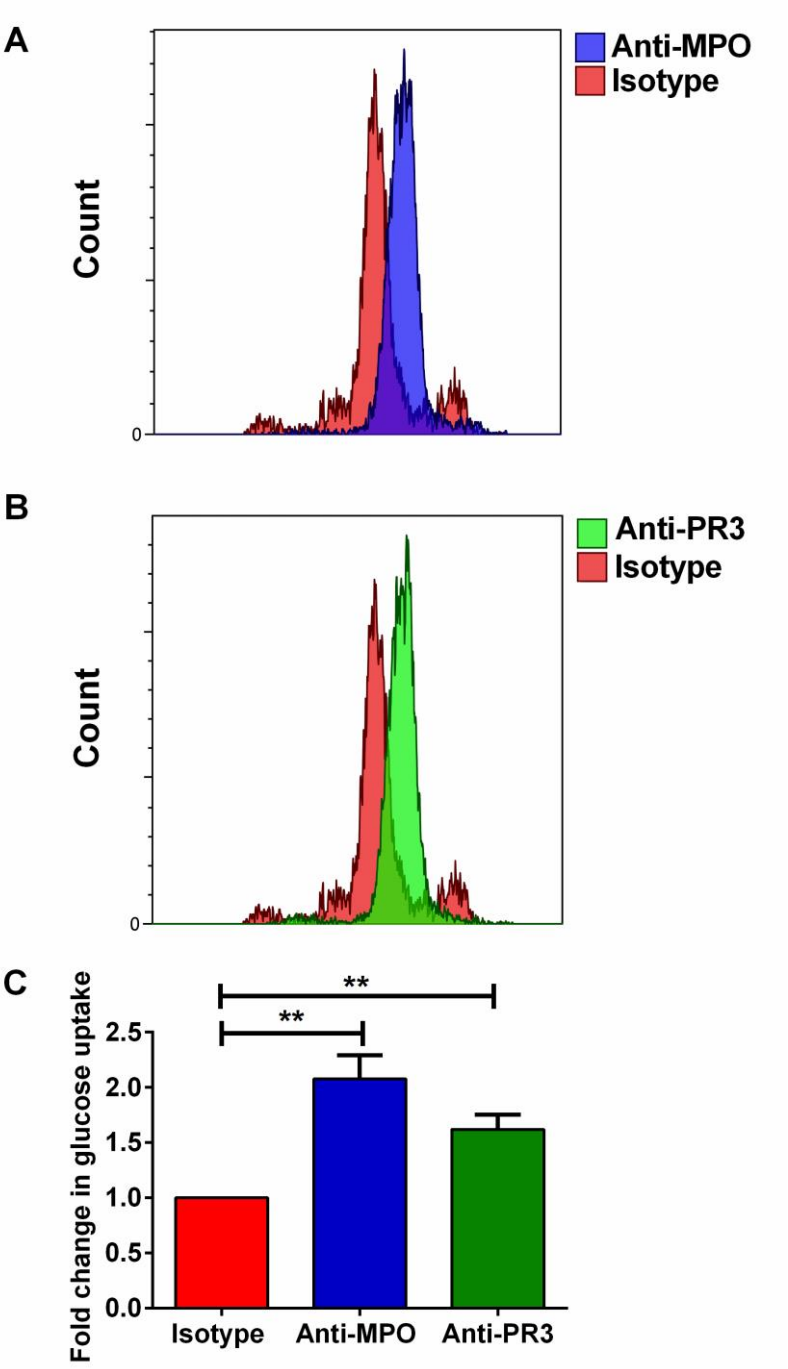

Figure 4.3.2 Anti-MPO stimulation of monocytes results in increased glucose uptake. CD14+ monocytes were isolated from the PBMCs of healthy controls by MACS separation. The cells were plated and stimulated @ 37 ^{0}C for 60min with 5µg/ml monoclonal antibody (mAb) directed against MPO or isotype control antibody. Cells were then incubated with 86.5µg/ml 2-NBDG for @ 37 ^{0}C for 60min. The median fluorescence intensity (MFI) was compared for isotype, anti-MPO and anti-PR3 stimulated cells. Representative overlays are shown for anti-MPO (**A**) and anti-PR3 treatments (**B**). The fold changes in 2-NBDG uptake after antibody stimulation are shown for 3 independent donors (**C**). Data are presented as the median and interquartile range. Students T-test was used to establish significance (**p<0.01).

Interestingly, unlike the inflammatory cytokine production, I also found an increase in glucose uptake from anti-PR3 stimulated cells (**Figure 4.3.2 B and C**). This result indicated that the cells were responding to both antibodies however only anti-MPO resulted in IL-1β production. While this increase in glucose uptake was interesting, I wanted to further investigate the role of glycolysis and other metabolic pathways in the activation of monocytes by ANCA. In particular I wanted to investigate whether the changes in cytokine production in response to anti-MPO stimulation were linked to changes in metabolism. To do this I used 2-deoxyglucose (2-DG) to block hexokinase and therefore block glycolysis in the cell and oligomycin to block the electron transport chain. When monocytes were treated with 2-DG I found a dramatic reduction in IL-1β indicating that glycolysis is required for IL-1β production in these cells (**Figure 4.3.3 A**). Treatment with oligomycin resulted in a trend for increased IL-1β production however this increase did not reach statistical significance (**Figure 4.3.3 B**). Neither of these treatments resulted in an increase in cell death (**Figure 4.3.3 C**).

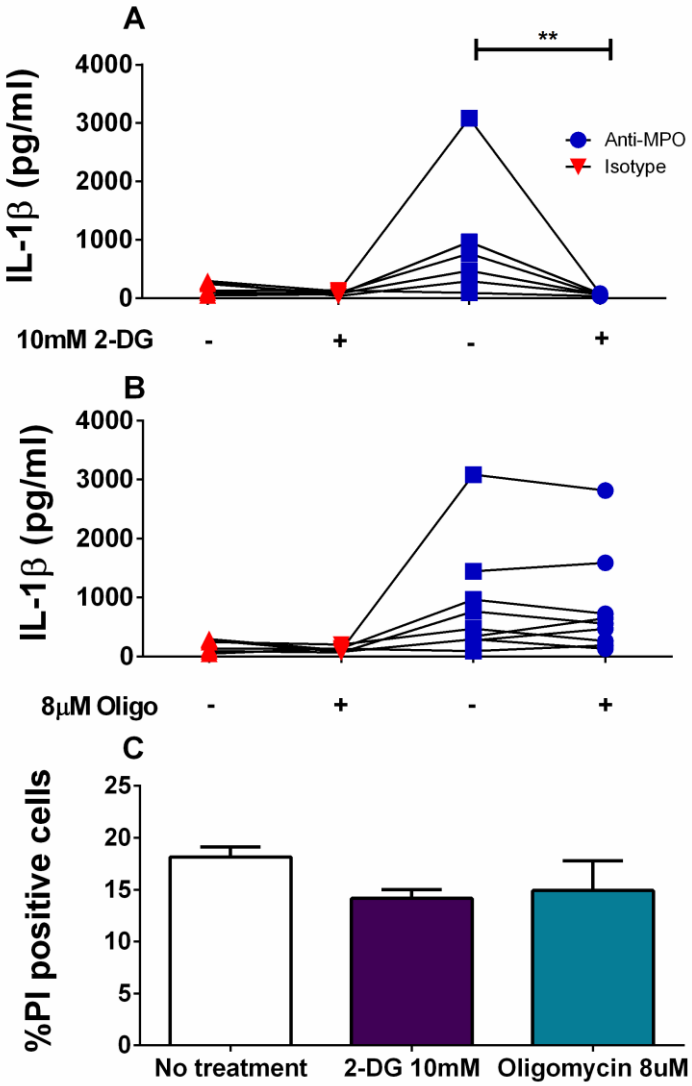

Figure 4.3.3 Glycolysis is required for IL-1β production from monocytes in response to anti-MPO antibodies.
CD14+ monocytes were isolated from the PBMCs of healthy controls by MACS separation. The cells were plated and incubated for 20min with either 10mM 2-DG (**A**) or 8μM oligomycin (**B**) and then stimulated @ 37 ^{0}C for 4hr with 5μg/ml monoclonal antibody (mAb) directed against MPO or isotype control antibody. Supernatants were removed and IL-1β was measured by ELISA. Cells were then removed and cell death was measured by flow cytometry using propidium iodide (PI) uptake (**C**). Data are presented as the median and interquartile range. Statistical analysis was performed by one-way ANOVA with Friedman's post-test (**p<0.01) (n=6).

4.3.3 **Optimisation of Seahorse extracellular flux analyser for monocytes**

In order to further investigate changes in the metabolic profile of monocytes in response to ANCA I used a seahorse extracellular flux analyser. This allowed for real time measurements of the extra cellular acidification rate (ECAR), a measure of glycolysis, and oxygen consumption rate (OCR), a measure of oxidative phosphorylation. I first wanted to optimise the number of cells that would be used in each well (**Figure 4.3.4 A)**. The manufacturers recommend that an optimal cell density should yield a basal OCR of ~250pmoles/min. For this reason, $1x10^6$ cells per well was chosen as the concentration for future experiments. Next, I wanted to optimise the concentration of the compounds which would be added to the seahorse in order to allow for the maximum respiratory capacity, spare respiratory capacity and non-mitochondrial respiration to be calculated.

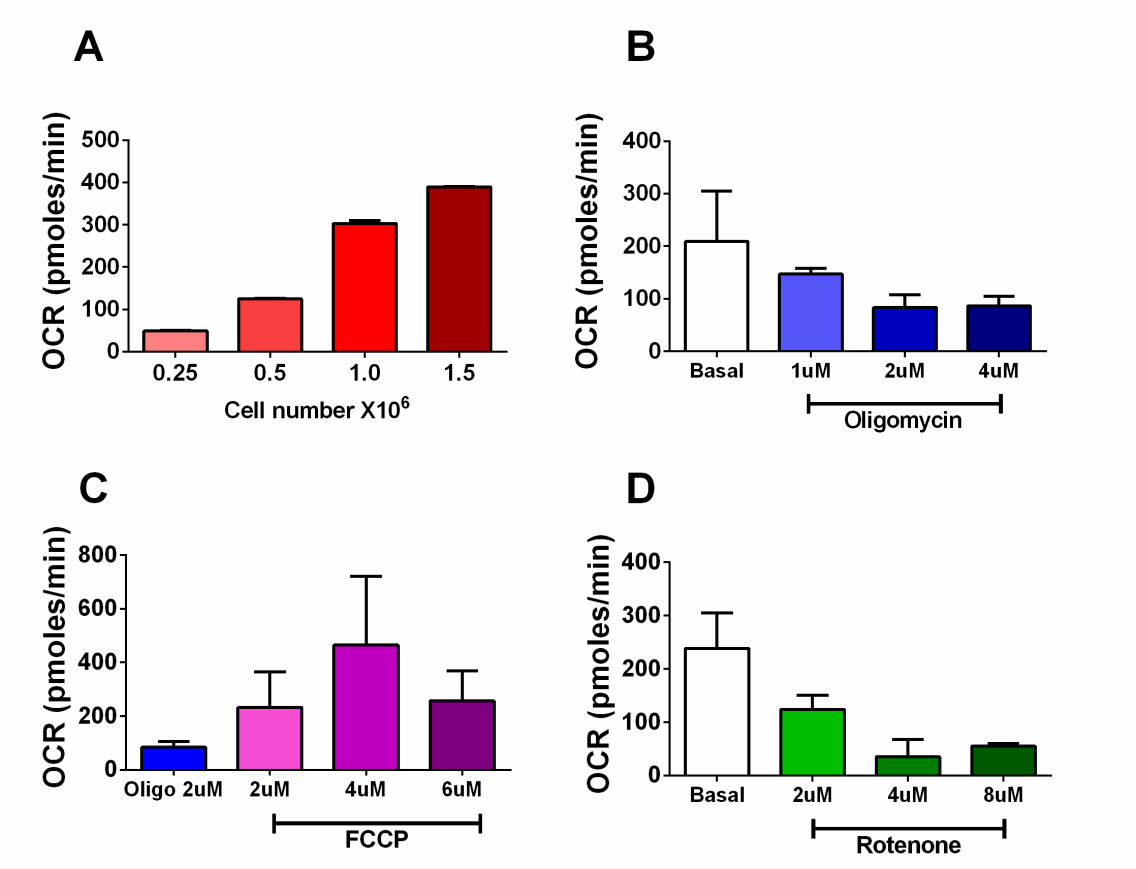

Figure 4.3.4 Optimisation of cell numbers and compounds for Seahorse.
CD14+ monocytes were isolated from the PBMCs of healthy controls by MACS separation. Cells were plated in CellTak coated XFe24 cell culture plates at various concentrations and oxygen consumption rate (OCR) was measured using Seahorse extracellular flux analysis (**A**). Cells were then treated with increasing concentrations of oligomycin (**B**), FCCP (**C**) or rotenone (**D**) and OCR was measured to determine optimum concentrations of each compound. Data are presented as the median and interquartile range (n=5).

These compounds were oligomycin, which inhibits complex VI in the electron transport chain (ETC), Carbonyl cyanide-4-(trifluoromethoxy)phenylhydrazone (FCCP), which uncouples the mitochondria, and rotenone, which blocks complex I of the ETC. This process is described in detail in **Chapter 2.6**. Using multiple concentrations of each compound I found that the recommended concentrations of 2µM oligomycin, 4µM FCCP and 4µM rotenone had most consistent effect (**Figure 4.3.4 B-D**).

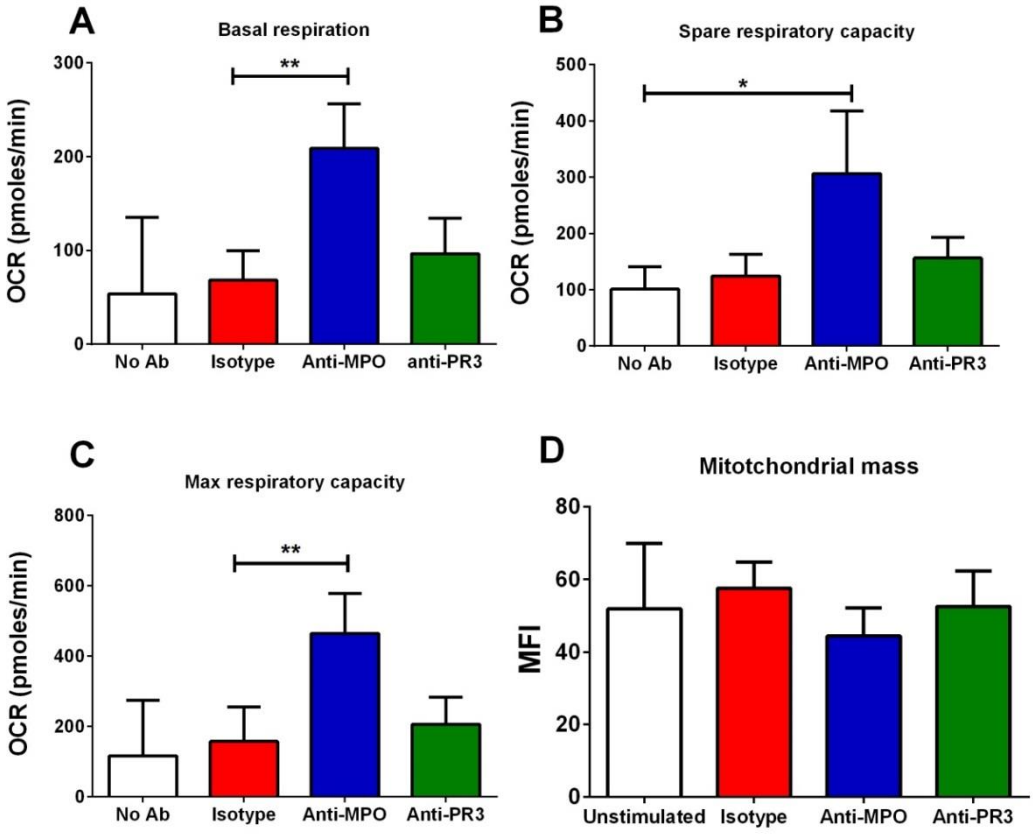

Figure 4.3.5 Anti-MPO, but not anti-PR3 stimulation of monocytes leads to increased oxidative respiration and respiratory capacity.
CD14+ monocytes were isolated from the PBMCs of healthy controls by MACS separation. Cells were plated in CellTak coated XFe24 cell culture plates and stimulated @ 37 ^{0}C for 4hr with 5µg/ml monoclonal antibody (mAb) directed against MPO, PR3 or isotype control antibody. Initial OCR was measured followed by addition of 4µM oligomycin, 2µM FCCP and 4µM rotenone. Basal respiration levels were found by subtracting the non-mitochondrial respiration from the initial OCR readings (**A**). Spare respiratory capacity was calculated by subtracting the basal respiration from the OCR value after FCCP addition (**B**). Maximum respiratory capacity was calculated by subtracting the OCR value after rotenone addition from the post FCCP value (**C**). For mitochondrial mass experiments cells were plated in 24 well plates and stimulated as above before incubation with 50nM Mitotracker green for 30min @ 37 ^{0}C. Cells were then removed and the MFI of Mitotracker green was determined by flow cytometry for each treatment (**D**). Data are presented as the median and interquartile range. Statistical analysis was performed by one-way ANOVA with Friedman's post-test (*p<0.05, **p<0.01) (A, B, C n=6, D n=3).

4.3.4 **Anti-MPO stimulation of monocytes results in an increase in OCR**

The Seahorse analyser allows for measurements of both glycolysis (ECAR) and oxidative phosphorylation (OCR). These two readouts require differing experimental conditions in order to achieve a fully accurate representation of each pathway. I initially examined the OCR. My initial hypothesis was that the increase in glucose uptake was associated with a switch to aerobic glycolysis which would be associated with a decrease in OCR. However, I found that monocytes treated with anti-MPO for 4hr had increased basal OCR (**Figure 4.3.5 A**) as well as an increase in their spare respiratory capacity and maximum respiratory capacity (**Figure 4.3.5 B, C**). This increase was not found in anti-PR3 stimulated cells further illustrating the differential response of monocytes to these two stimuli. The increase in maximum respiratory capacity in response to anti-MPO stimulation is particularly interesting due to the relatively short stimulation time. This increase implies that there may be an increase in the number of mitochondria present in the cell or an increase in the amount of machinery capable of using oxygen. To test the hypothesis that the increase in respiratory capacity was due to an increase in the number of mitochondria present in the cell I used mitotracker green to measure the mitochondrial mass of the cell. I found no increase in the amount of mitochondria present after treatment with anti-MPO antibodies (**Figure 4.3.5 D**). I also looked at the effect of ANCA stimulation on ECAR. Using the method described in Chapter 2. I measured basal glycolysis, glycolytic capacity and non-glycolytic acidification. The concentration of 2-DG and oligomycin used in these experiments was established based on data from **Chapter 4.3.2** and **4.3.3** respectively. In contrast to results seen for OCR, both anti-MPO and anti-PR3 treatment resulted in an increase in basal glycolysis (**Figure 4.3.6 A**). I also found an increase in the glycolytic capacity and non-glycolytic acidification in these cells (**Figure 4.3.6 B, C**).

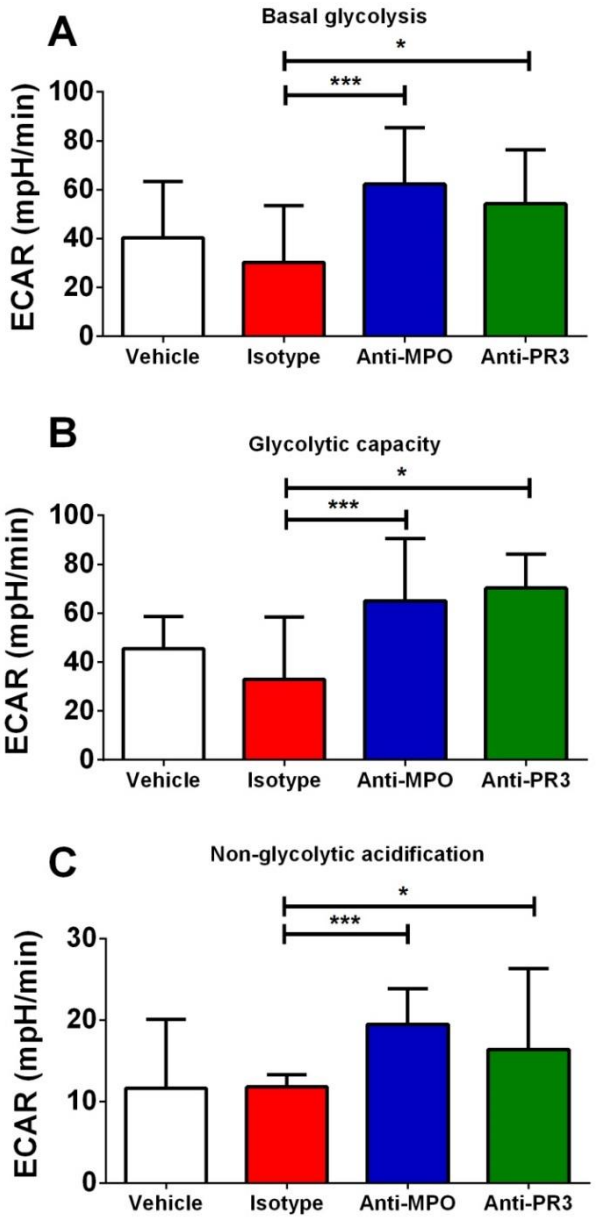

Figure 4.3.6 Anti-MPO and anti-PR3 stimulation results in an upregulation of glycolysis in monocytes.
CD14+ monocytes were isolated from the PBMCs of healthy controls by MACS separation. Cells were plated in CellTak coated XFe24 cell culture plates and stimulated @ 37 0C for 4hr with 5µg/ml monoclonal antibody (mAb) directed against MPO, PR3 or isotype control antibody. Extra cellular acidification rate (ECAR) was measured in glucose free media at basal levels followed by addition of 4.5mM D-glucose, 4µM oligomycin and 10mM 2-DG. Glycolytic rate was measured after addition of glucose (**A**) Glycolytic capacity was calculated by subtraction of the non-glycolytic acidification rate from the post oligomycin ECAR reading (**B**). Non-glycolytic acidification was defined as the ECAR rate after 2-DG (**C**). Data are presented as the median and interquartile range. Statistical analysis was performed by one-way ANOVA with Friedman's post-test (*p<0.05, ***p<0.001) (n=11).

4.3.5 Changes in monocyte cellular metabolism in response to ANCA occur immediately after stimulation

The changes observed in the monocyte response to ANCA occur just 4hr after stimulation. This relatively short time led me to investigate the real time kinetics of these responses. In order to achieve this anti-MPO and anti-PR3 were added directly to the cells using the Seahorse analyser and changes in OCR were measured in real-time immediately following stimulation (**Figure 4.3.7**). Interestingly I found that both anti-MPO and anti-PR3 stimulation resulted in an immediate increase in OCR of similar magnitude. While this response was sustained in the anti-MPO treated cells, anti-PR3 resulted in a transient increase in OCR.

Figure 4.3.7 Anti-MPO and anti-PR3 stimulated monocytes have divergent OCR kinetics

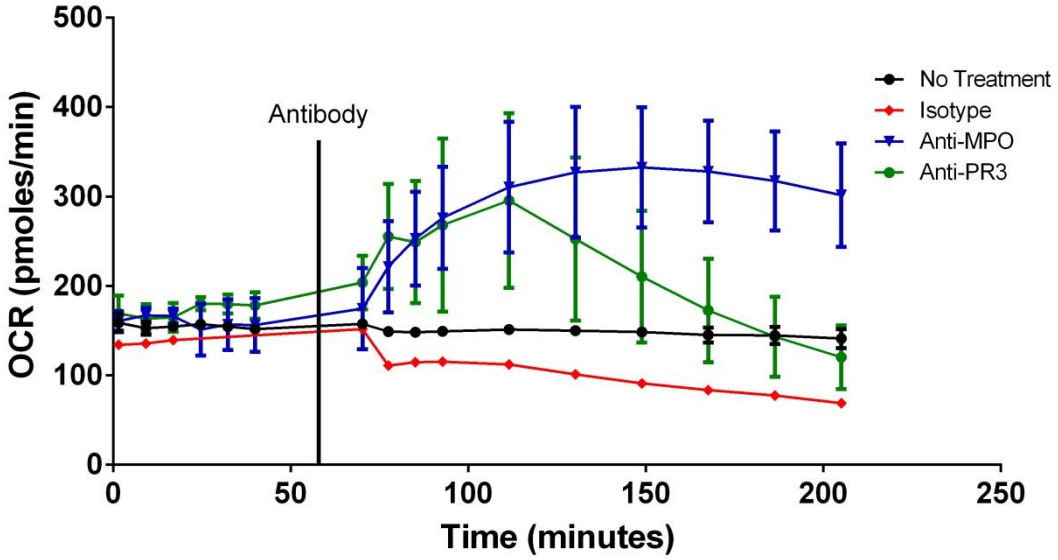

patterns.
CD14+ monocytes were isolated from the PBMCs of healthy controls by MACS separation. Cells were plated in CellTak coated XFe24 cell culture plates. Cells were then placed in the Seahorse extracellular flux analyser and basal measurements were recorded. Cells were then stimulated with 5µg/ml monoclonal antibody (mAb) directed against MPO, PR3 or isotype control antibody and OCR was measured at regular intervals. Data represent three independent experiments.

Such an immediate increase in oxygen consumption raised the possibility that this change in OCR was due to non-mitochondrial oxygen consumption, such as through NADPH oxidase ROS production. I used the oxidative phosphorylation inhibitor rotenone to investigate the possible role of non-mitochondrial oxygen consumption. I found that inhibiting ox phos in this way resulted in a marked decrease in OCR from both anti-MPO (**Figure 4.3.8 A**) and anti-PR3 (**Figure 4.3.8 B**) stimulated monocytes,

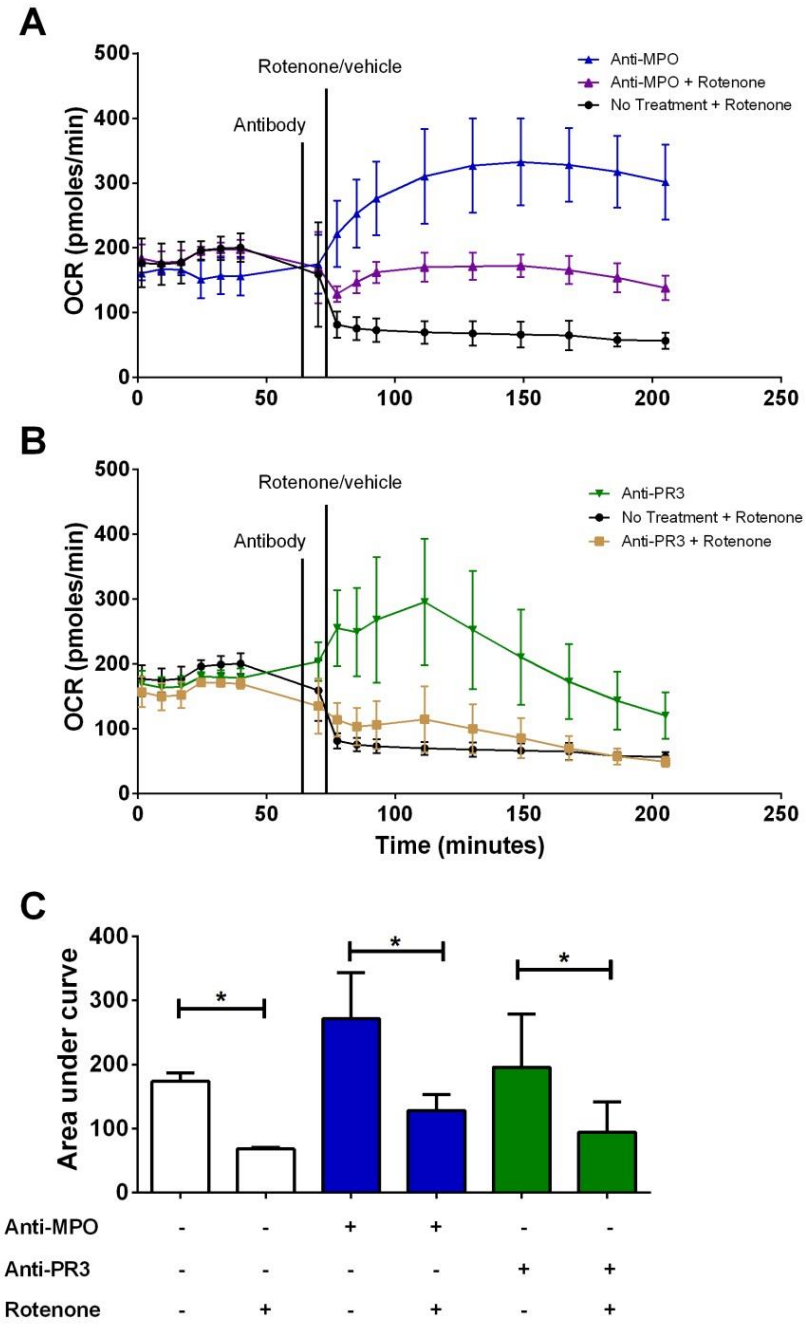

Figure 4.3.8 Anti-MPO and anti-PR3 OCR is primarily due to mitochondrial respiration. CD14+ monocytes were isolated from the PBMCs of healthy controls by MACS separation. Cells were plated in CellTak coated XFe24 cell culture plates. Cells were then placed in the Seahorse extracellular flux analyser and basal measurements were recorded. Cells were then stimulated with 5µg/ml monoclonal antibody (mAb) directed against MPO (**A**) or PR3 (**B**) before immediate addition of rotenone or vehicle and OCR was measured The area under the curve for each stimulation type was found using Graph Pad Prism and the OCR for each treatment with or without rotenone was found (**C**). Data are presented as the median and interquartile range. Statistical analysis was performed by one-way ANOVA with Friedman's post-test (*p<0.05). Data represent three independent experiments.

indicating that the observed effect was a result of increased mitochondrial respiration and not another oxygen consuming pathway (**Figure 4.3.8 C**). In order to more accurately provide ECAR readings I also used an experimental model in which monocytes were stimulated in glucose free media. Under these conditions I saw a small but significant increase in ECAR after anti-MPO and anti-PR3 stimulation (**Figure 4.3.9 A**).

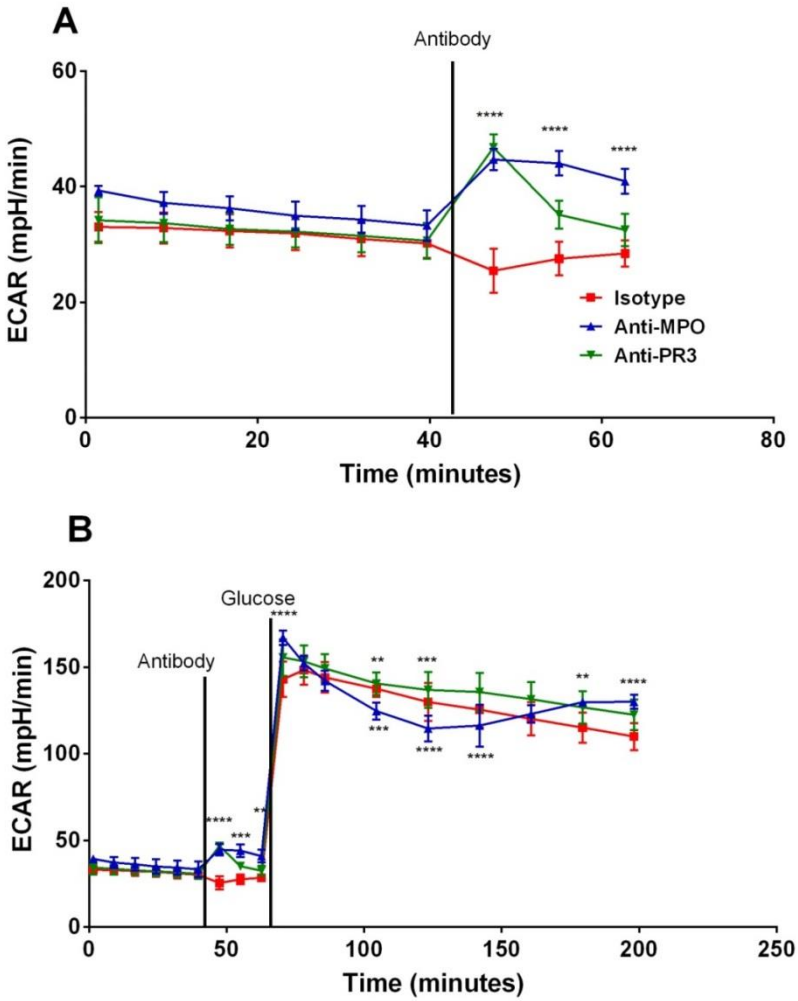

Figure 4.3.9 Anti-MPO and anti-PR3 stimulated monocytes have differing initial glycolytic kinetics.
CD14+ monocytes were isolated from the PBMCs of healthy controls by MACS separation. Cells were plated in CellTak coated XFe24 cell culture plates in XF media without glucose. Cells were then placed in the Seahorse extracellular flux analyser and basal measurements were recorded. Cells were then stimulated with 5µg/ml monoclonal antibody (mAb) directed against MPO, PR3 or isotype control antibody and ECAR was measured (**A**). Glucose was the added to each well and ECAR was measured (**B**). Statistical analysis was performed by Two-way ANOVA with Tukey's multiple comparrisons test (**p<0.01, ***p<0.001, ****p<0.0001) Data represent 3 independent experiments.

Similar experiments were carried out in order to examine the immediate effects of ANCA on ECAR. After the addition of glucose, I observed a significant increase in ECAR as a result of both ANCA stimulations (**Figure 4.3.9 B**). When the acidification was tracked over time following this addition the two ANCA stimulations showed markedly different patterns with anti-MPO ECAR declining quickly before rebounding and anti-PR3 showing a slower rate of steady decline.

4.3.6 PDH activity may be important for the proinflammatory effect of ANCA

In an attempt to further elucidate the pathway through which anti-MPO antibodies resulted in IL-1β production I used a number of pharmacological compounds. These compounds allowed me to inhibit or activate specific parts of the glucose metabolism pathway (**Figure 4.3.10**).

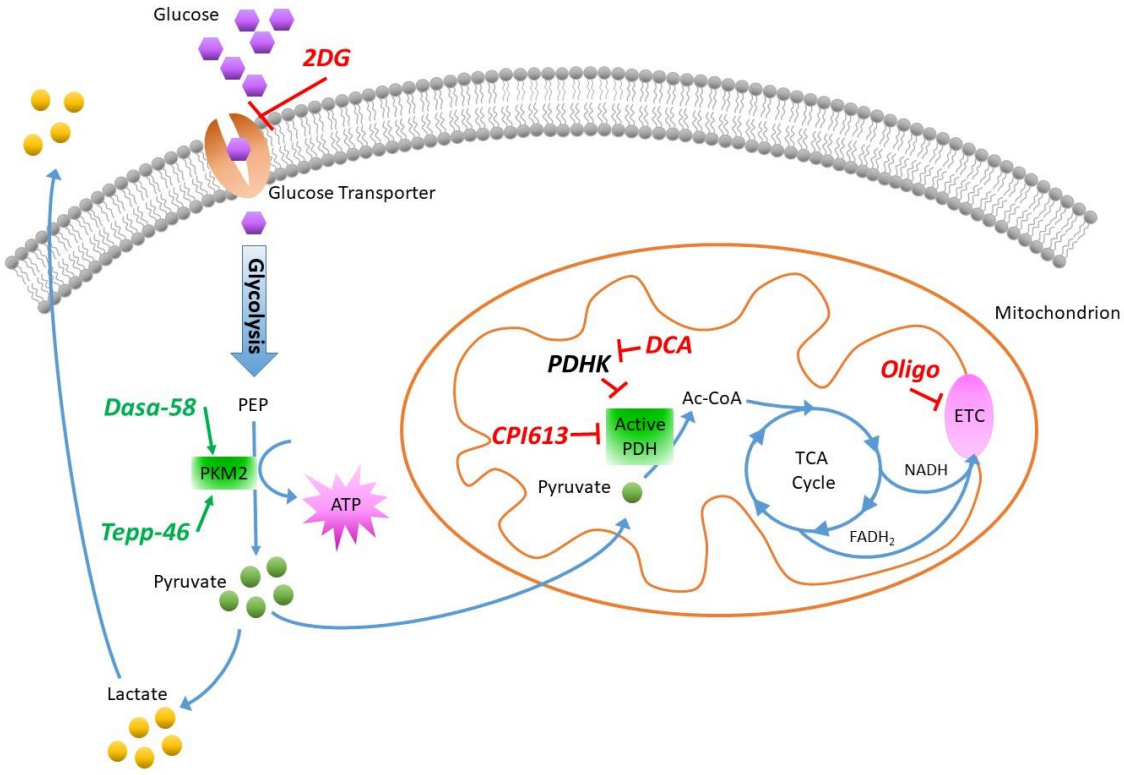

Figure 4.3.10 Pharmacological compounds used to alter glucose metabolism.

I first looked at the effect of activating PKM2, a key step in the glycolytic pathway. Using two small molecule activators I found no change in the production of IL-1β in response to either Dasa-58 (**Figure 4.3.11 A**) or Tepp-46 (**Figure 4.3.11 B**).

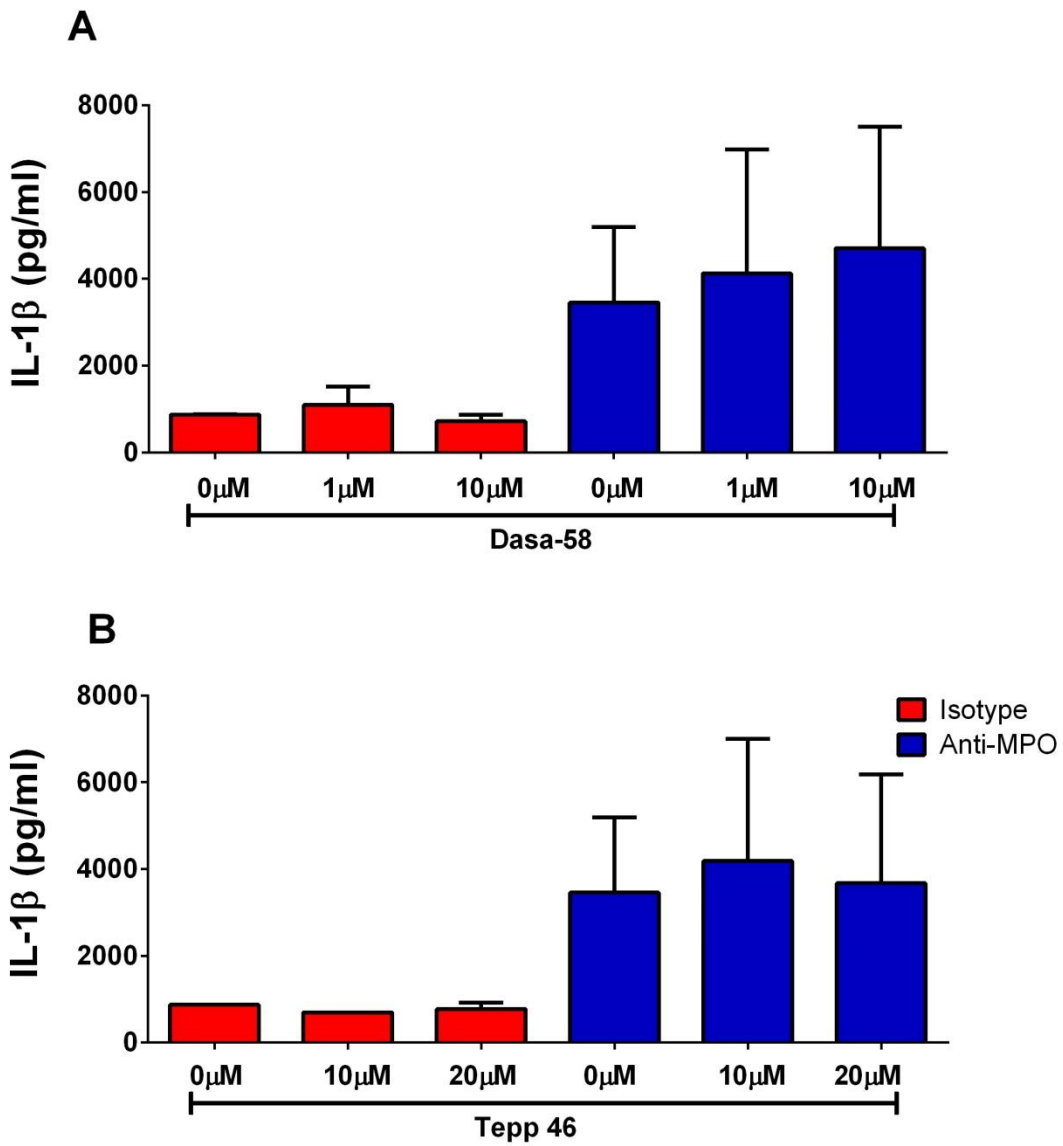

Figure 4.3.11 PKM2 activation does not alter anti-MPO induced IL-1β secretion from monocytes.
CD14+ monocytes were isolated from the PBMCs of healthy controls by MACS separation. The cells were plated and incubated for 20min with varying concentrations of either Dasa-58 (**A**) or Tepp-46 (**B**) and then stimulated for 4hr with 5μg/ml monoclonal antibody (mAb) directed against MPO or isotype control antibody. Supernatants were removed and IL-1β was measured by ELISA (n=4).

Pyruvate dehydrogenase (PDH) is the enzyme responsible for moving pyruvate into the TCA cycle and works downstream of PKM2. To investigate the role of this important bridge between glycolysis and the TCA cycle I used dichloroacetate (DCA), an inhibitor of PDH kinase (PDHK). PDHK phosphorylates PDH which leads to its inhibition; as such inhibition of PDHK should result in increased PDH activity and therefore increased flux of pyruvate into the TCA cycle. I hypothesised that this activation of PDH would increase the flux of pyruvate into the TCA cycle which would provide insight into the role of this pathway in the pro inflammatory effects of

ANCA stimulation on monocytes. I found that activation of PDH using DCA caused a significant reduction in IL-1β production in these cells (**Figure 4.3.12 A**).

Figure 4.3.12 PDH may be involved in the production of IL-1β by monocytes induced by anti-MPO antibodies.
CD14+ monocytes were isolated from the PBMCs of healthy controls by MACS separation.

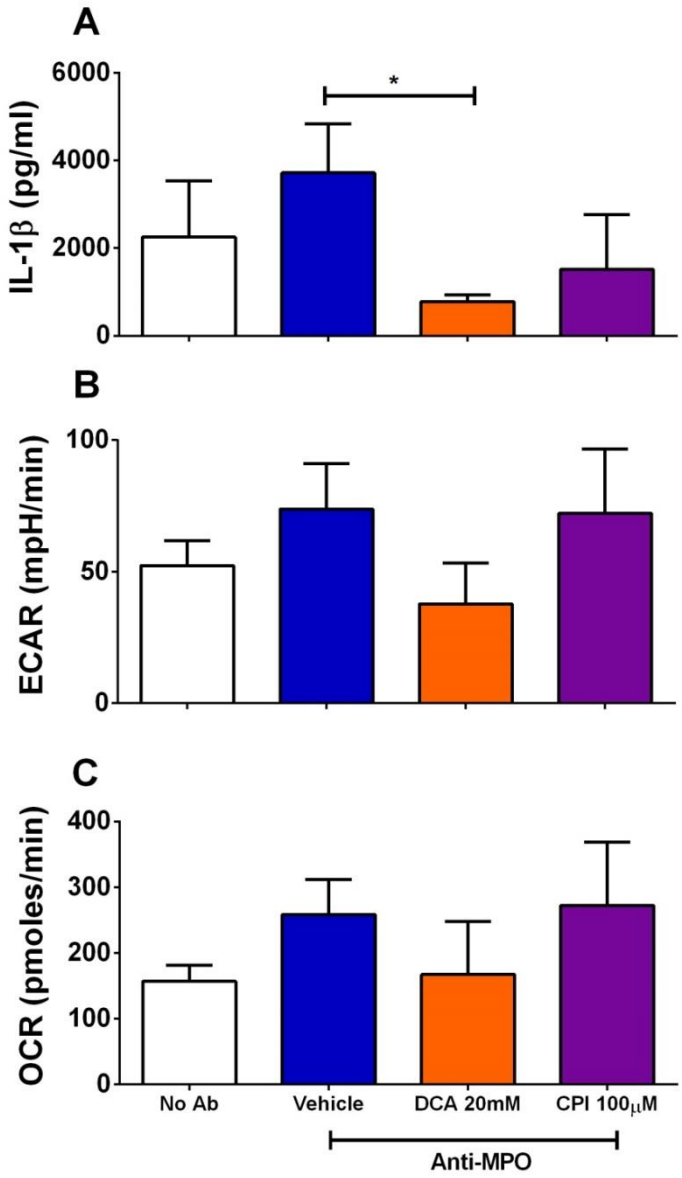

Cells were plated in Cell-Tak coated XFe24 cell culture plates and incubated for 20min with either 20mM DCA or 100μM CPI613 and then stimulated for 4hr with 5μg/ml monoclonal antibody (mAb) directed against MPO or isotype control antibody. Supernatants were removed and IL-1β was measured by ELISA (**A**). Cells were then analysed on Seahorse and ECAR (**B**) and OCR (**C**) were measured for each treatment. Statistical analysis was performed by one-way ANOVA with Friedman's post-test (*p<0.05) (n=4).

Activation of PDH in this way resulted in a marked decrease in glycolysis as expected (**Figure 4.3.12 B**). Unexpectedly, I also observed a decrease in OCR in these cells (**Figure 4.3.12 C**).While PDHK inhibition should result in increased PDH activity, and therefore increased

oxidative metabolism, these cells may already have upregulated PDH to maximal levels and so no further increase is possible. The reduction in OCR may also be as a result of other pathways responding to the inhibition of PDHK and these may be causing inhibition further down the TCA cycle before oxidative phosphorylation occurs. As this result did not provide a clear indication of the role of PDH in this pathway I next blocked PDH activity hypothesising that this would have an opposing effect to DCA on the cytokine production from these cells. Using CPI-613 to inhibit PDH I found a reduction in IL-1β production (**Figure 4.3.12 A**) however I saw no change in the rates of glycolysis or oxygen consumption (**Figure 4.3.12 B, C**) in these cells. This IL-1β reduction by CPI-613 may therefore have been a result of off target effects of this compound.

4.3.7 Mitochondrial reactive oxygen species are induced by anti-MPO stimulation

Recently the concept of reverse electron transport (RET) and its ability to induce mitochondrial ROS (mROS) production has been shown to promote a proinflammatory phenotype in some immune cells. I next tested the hypothesis that mROS were involved in the effect of ANCA on monocytes. Using the specific mROS scavenger MitoTempo I found that the IL-1β produced by monocytes in response to ANCA could be completely inhibited (**Figure 4.3.13 A**) indicating a role for mROS in this pro-inflammatory pathway. I also looked at the amount of cellular ROS and mROS in these cells after ANCA stimulation. I found an increase in cellular ROS in anti-MPO treated cells and to a lesser extent anti-PR3 treated cells (**Figure 4.3.13 B**). Interestingly, I found that the mROS was not significantly induced in response to these stimuli with only a slight upward trend in ANCA stimulated cells (**Figure 4.3.13 C**). ANCA stimulation also resulted in no change in the percentage of monocytes with high mitochondrial membrane potential as measured by JC-1 uptake (**Figure 4.3.13 D**). High membrane potential indicates functional mitochondria and capacity for oxidative phosphorylation.

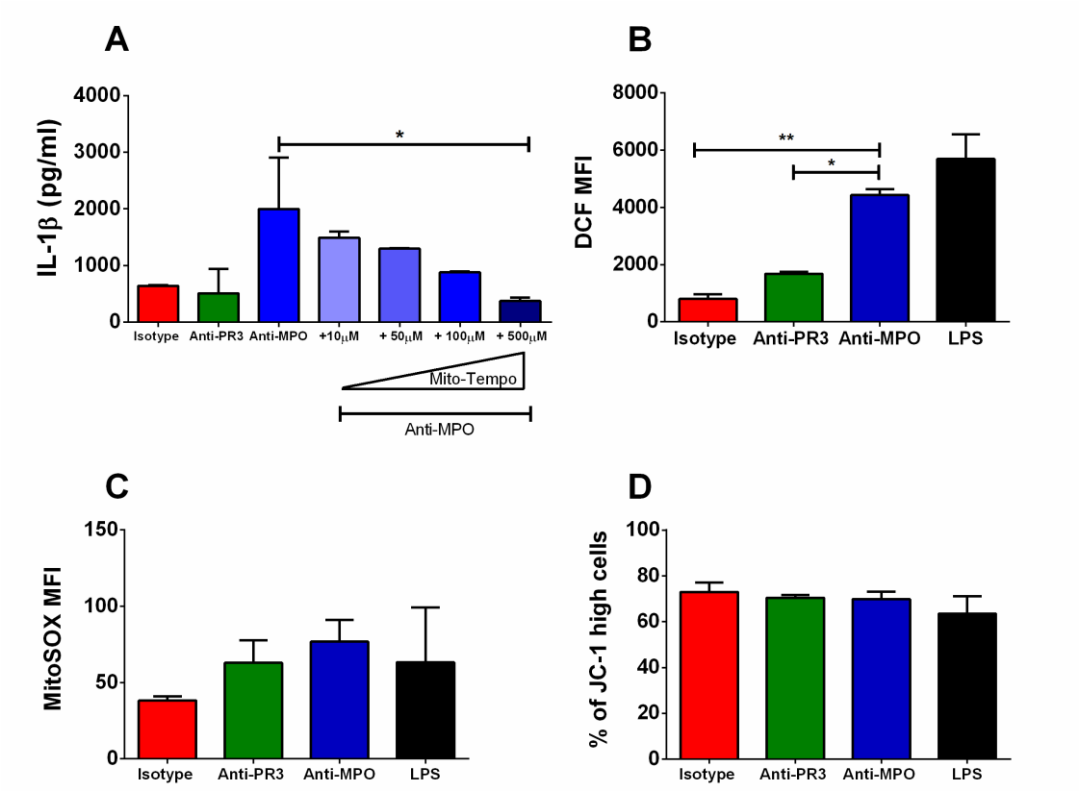

Figure 4.3.13 Anti-MPO induced IL-1β production is abrogated by the mitochondrial ROS scavengers MitoTempo.
CD14+ monocytes were isolated from the PBMCs of healthy controls by MACS separation. The cells were plated and incubated for 20min with MitoTempo and then stimulated for 4hr with 5µg/ml monoclonal antibody (mAb) directed against MPO, PR3 or isotype control antibody. Supernatants were removed and IL-1β was measured by ELISA (**A**). For flow cytometry experiments monocytes were plated as above and stimulated for 4hr with 5µg/ml monoclonal antibody (mAb) directed against MPO, PR3 or isotype control antibody or 5ng/ml LPS. DCF (**B**), MitoSox Red (**C**) or JC-1 (**D**) dyes were added to the cells for the final 30min of antibody treatment. Cells were stained with 5µl anti-CD14 Pacific Blue antibody for the last 10min of incubation before being analysed on an ADPCyan analyser.

4.3.8 Anti-MPO and anti-PR3 stimulation leads to differential protein secretion from monocytes

As I had previously shown a difference between anti-MPO and anti-PR3 stimulated monocytes in terms of cytokine production (**Chapter 3**), and have now shown that differences are also present in the metabolic response to these antibodies, I next wanted to determine if these metabolic differences were linked to the production of other proteins in the cell and therefore form a clearer picture of how each antibody activates these cells. To attempt to answer this question I used a proteomic screening panel provided by Olink Proteomics. This panel allowed for the simultaneous testing of 92 inflammation related proteins in the supernatants of stimulated monocytes. Of these, 55 were detectable in the supernatants of monocytes treated with ANCA. These proteins are outlined in **Table 4.3.1**. Significance values of anti-MPO and anti-PR3 stimulation compared to isotype control are

shown in **Table 4.2** and **4.3**. Using this method I have found a significant increase in Oncostatin M (OSM), IL-10 receptor subunit A (RA), vascular endothelial growth factor (VEGF), hepatocyte growth factor (HGF), CXCL5 and matrix metalloproteinase (MMP)-10 (**Figure 4.3.14**) from anti-MPO treated monocytes. I also found a decrease in some proteins such as MCP-1, 2, and 3, CXCL-10, CXCL-11 and IL-12B in response to this stimulus. The response to anti-PR3 stimulation was less pronounced, with only HGF and IL-18 receptor 1 levels being significantly altered. I did, however, see similar trends for OSM, IL-10RA, MCP-1, IL-12B and the lack of a significant response may be due to the small number of donors tested.

Cytokines	Chemokines	Surface receptors	Growth Factors	Enzymes and other proteins
Flt3L	CCL-3	CD5	DNER	4E-BP1
IL-1α	CCL-4	CD6	FGF-21	ADA
IL-6	CCL-19	CD40	HGF	AXIN1
IL-8	CCL-20	CD244	M-CSF	CASP-8
IL-10	CCL-23	IL-10RA	VEGF	EN-RAGE
IL-12β	CCL-28	IL-10RB		MMP-1
IL-18	CXCL-1	IL-18R		MMP-10
IL-20	CXCL-5	OPG		SIRT2
LIF	CXCL-6	TNFRSF9		ST1A1
OSM	CXCL-9			STAMPB
TGF-α	CXCL-10			uPA
TGF-β	CXCL-11			
TNFSF14	MCP-1			
TNFα	MCP-2			
TRAIL	MCP-3			
TWEAK				

Table 4.1 Proteins analysed from Olink proteomic screening.
List of proteins measured using Olink proteomics inflammation panel which were above the limit of detection.

Cytokines	Anti-MPO p-value	Anti-PR3 p-value	Chemokines	Anti-MPO p-value	Anti-PR3 p-value
Flt3L	0.200	0.343	CCL-3	0.200	0.114
IL-1α	0.200	0.686	CCL-4	0.343	0.886
IL-6	0.486	0.686	CCL-19	0.114	0.114
IL-8	0.486	0.343	CCL-20	0.200	0.029
IL-10	0.114	1.000	CCL-23	0.057	0.114
IL-12β	0.029	0.057	CCL-28	0.057	0.057
IL-18	0.486	0.686	CXCL-1	0.114	0.686
IL-20	0.384	0.306	CXCL-5	0.029	0.114
LIF	0.114	0.686	CXCL-6	0.200	0.200
OSM	0.029	0.200	CXCL-9	0.057	0.114
TGF-α	0.486	1.000	CXCL-10	0.029	0.200
TGF-β	0.343	0.686	CXCL-11	0.029	0.343
TNFSF14	0.200	0.057	MCP-1	0.029	0.057
TNFα	0.486	0.343	MCP-2	0.029	0.114
TRAIL	0.886	1.000	MCP-3	0.029	0.114
TWEAK	0.686	0.057			

Table 4.2 Significance values vs isotype control for cytokines and chemokines.
List of significance values measured by two sample Wilcoxon t-test. Red indicates an increase and blue indicates a decrease vs isotype control values

Surface receptors	Anti-MPO p-value	Anti-PR3 p-value	Enzymes and other proteins	Anti-MPO p-value	Anti-PR3 p-value
CD5	0.343	0.886	4E-BP1	0.057	0.343
CD6	0.686	0.486	ADA	0.343	0.343
CD40	0.686	0.200	AXIN1	0.114	0.886
CD244	0.486	0.486	CASP-8	0.343	0.686
IL-10RA	0.029	0.200	EN-RAGE	0.486	0.200
IL-10RB	0.200	0.114	MMP-1	0.114	1.000
IL-18R	0.057	0.029	MMP-10	0.029	0.686
OPG	0.114	0.886	SIRT2	0.114	0.486
TNFRSF9	0.343	1.000	ST1A1	0.057	1.000
			STAMPB	0.114	0.686
			uPA	0.200	1.000
Growth Factors					
DNER	1.000	0.200			
FGF-21	0.686	0.114			
HGF	0.029	0.029			
M-CSF	0.486	0.686			
VEGF	0.029	0.686			

Table 4.2 Significance values vs isotype control for Surface receptors, growth factors and other proteins.
List significance values measured by two sample Wilcoxon t-text

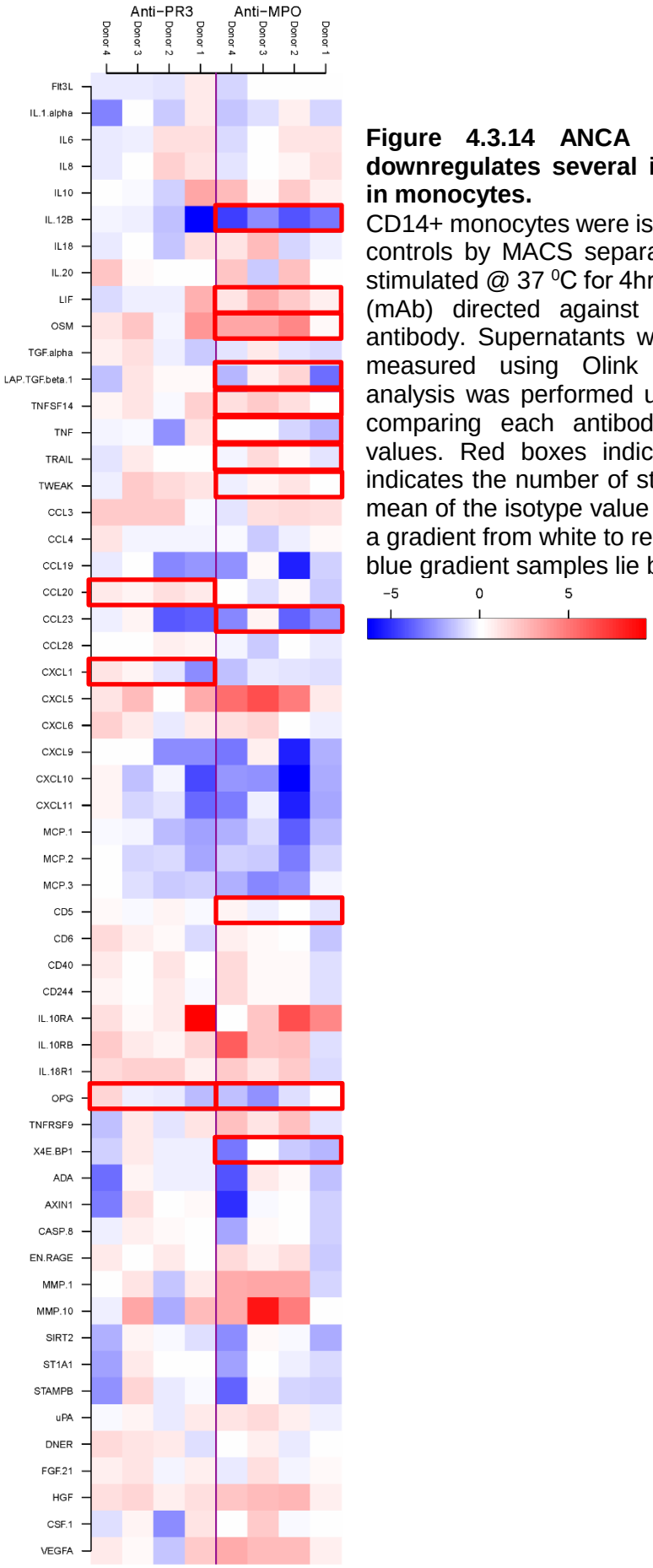

Figure 4.3.14 ANCA stimulation upregulates and downregulates several inflammation related pathways in monocytes.

CD14+ monocytes were isolated from the PBMCs of healthy controls by MACS separation. The cells were plated and stimulated @ 37 ^{0}C for 4hr with 5µg/ml monoclonal antibody (mAb) directed against MPO, PR3 or isotype control antibody. Supernatants were removed and samples were measured using Olink proteomic analysis. Statistical analysis was performed using two sample Wilcoxon t-test comparing each antibody treatment to isotype control values. Red boxes indicate p = 0.029 (n=4). The plot indicates the number of standard deviations away from the mean of the isotype value for each treatment. Samples with a gradient from white to red lie above isotype, while white to blue gradient samples lie below.

4.4 Discussion

The vital importance of metabolic changes in immune cells is quickly becoming a key area of interest in the study of immunology. The processes involved in these pathways are complex and often interwoven with multiple pathways changing in a particular cell type in response to a specific stimulus (Smith et al., 2014). While it is important to look at these changes as a whole in order to understand the mechanism behind immune cell phenotypes it is also just as important to first tease out the specific workings of each pathway. My research is focused on the latter area and looks mainly at the glycolytic and oxidative respiration pathways. As stated in the introduction, macrophages have become the subject of intense study in terms of their metabolic profile in response to stimuli such as LPS. These studies have often focused on either murine bone marrow derived macrophages (BMDMs) or tissue resident macrophages (Fei et al., 2016, Freemerman et al., 2014, Gleeson et al., 2016) and have largely neglected myeloid lineage cells in blood, specifically monocytes. While these cells can translocate to tissues and differentiate into macrophages or dendritic cells they can also have effects while still in the circulation (Munoz et al., 2005, Jia et al., 2008). These effects may be particularly important in diseases where part of the mechanism of action is not always localised to a specific tissue but rather to the vasculature such as the case in AAV. For this reason I believe that studying monocytes as opposed to macrophages would allow for a greater understanding of the pathogenesis of disease. This work was performed in order to expand on my previous studies on monocytes and to further develop this emerging area of interest.

As glucose is the main fuel used in the production of ATP from cells, increases in glucose uptake are indicative of an increase in glycolysis. 18-F-Fluorodeoxyglucose Positron Emission Tomography with Computed Tomography (PET) can be used to identify glucose uptake in patients and has been used clinically in the diagnosis of Alzheimer's disease (Wang et al., 2017), cancer (Flanagan et al., 1997) and cardiovascular disease (Ziegler et al., 2016). Patients with AAV show increased rates of glucose uptake in affected organs as measured by PET (Soussan et al., 2014) indicating a likely upregulation of glycolysis in these immune cell rich areas. I have shown that monocytes treated with ANCA have an increase in their glucose uptake as measured by the fluorescent glucose analogue 2-NBDG. This compound has been shown to be a useful measure of glucose uptake (Zou et al., 2005) although some recent studies have indicated that this uptake may be lower than that of radiolabelled glucose (Tao et al., 2016). This potential lowering in uptake of 2-NBDG indicates that our ANCA stimulated monocytes may actually be increasing their glucose uptake to an even greater extent than I have observed here. Recently, unpublished data suggests uptake of 2-NBDG may occur through a different pathway than the glucose transporter (Clair Gardner, personal communication) and therefore may nay be a suitable readout of glucose uptake. The

conclusion that ANCA increase glucose uptake may therefore need to be re-evaluated in future using more accurate glucose uptake assays.

Increased glucose uptake is a requirement for increases in cellular metabolism and this, along with the IL-1β production from the anti-MPO treated monocytes, led me to further investigate the metabolic changes in these cells. The development of Seahorse extracellular flux analysis technology has greatly aided the expansion of the field of immunometabolism in recent years. As monocytes have not been well studied using this technology I first optimised the ideal conditions to assess metabolic changes in this cell type. This then allowed me to be confident in characterising the response of monocytes to ANCA stimulation. As mentioned previously the current paradigm for immune cell pro-inflammatory activation is that these cells shift to a more glycolytic phenotype. While this is the case in most cell types it is also true that some plasticity between pathways exists in cells depending on their level of activation. Treg cells for example, require ox phos for long term survival (Huynh et al., 2015) however in the initial stages of activation these cells have enhanced glycolysis (Wei et al., 2016). I have shown here that unlike macrophages which show an increase in reliance on a particular metabolic pathway depending on their polarisation, monocytes treated with ANCA show an upregulation of metabolism as a whole. These changes are likely a result of the monocyte having pro-inflammatory effector functions of its own as well as beginning the process of differentiation into macrophages found in the lesion site of AAV patients (Zhao et al., 2015).

Some of the proinflammatory effect of monocytes in response to ANCA appear to be similar to the proinflammatory macrophage response where blocking glycolysis and mitochondrial ROS (mROS) results in a downregulation of proinflammatory cytokines (Mills et al., 2016) suggesting a role for these two pathways. In LPS stimulated macrophages, which have switched to glycolytic metabolism, mROS are produced through complex I (West et al., 2011). This mROS production has been shown to require an increase in membrane potential (Mills et al., 2016). It has been hypothesised that one reason for the switch to glycolysis in activated macrophages is the need to maintain mitochondrial membrane potential to allow for activation of this pathway (O'Neill and Hardie, 2013). Interestingly, I have shown here that cellular ROS but not mROS are significantly increased in monocytes stimulated with anti-MPO antibodies for 1 hour. These cells also showed no change in mitochondrial membrane potential at the same time point. While these data appear to show a divergence in the mitochondrial responses to stimulation in monocytes and macrophages it may be that later timepoints are necessary for mROS and membrane potential changes to be observed Some activated T cells also increase both glycolysis and oxidative respiration upon activation and it is thought that the oxidative respiration may be needed in order to produce ROS (Sena et al., 2013). ANCA activated monocytes may therefore be more similar to T cells than macrophages in this regard.

While IL-1β has been shown by our lab and others to increase in response to ANCA, other markers of immune cell activation can also be upregulated by ANCA stimulation (Popat et al., 2017, Ralston et al., 1997). My use of Olink proteomic analysis allowed me to screen a large number of proteins produced in response to ANCA stimulation. This unbiased approach allowed for the discovery of a number of upregulated or downregulated proteins which may be important in the overall cellular response to ANCA stimulation. Of particular interest was the increased level of IL-10 receptor subunit A (IL-10RA) from anti-MPO stimulated monocytes. This protein is part of the IL10 receptor and is vital for the signalling of this cytokine and its downstream anti-inflammatory effects. As a receptor this protein is usually found bound to the cell surface. The dramatic increase in IL-10RA levels in supernatants from monocytes in response to anti-MPO stimulation indicates shedding from the cell surface. This loss of the IL-10 receptor increases the proinflammatory phenotype of these cells. Interestingly, anti-PR3 stimulated cells did not increase IL-10RA secretion to the same degree which may partially explain why we do not see a similar proinflammatory cytokine induction in these cells. OSM is also upregulated in response to anti-MPO stimulation. This protein is a member of the IL-6 cytokine superfamily and has several proinflammatory effects such as increasing IL-6 production from endothelial cells as well as increasing adhesion molecules such as p-selectin. These proteins could therefore have a role in the propagation of disease and recruitment of neutrophils to the site of inflammation.

Interestingly, I also found a number of cytokines were downregulated in response to anti-MPO stimulation. The reduction in MCP-1, 2 and 3 levels is interesting as it appears to indicate a more anti-inflammatory phenotype in these cells. The reason for reducing the recruitment of monocytes is unclear and further time course studies may help in elucidating these pathways. The fact that I have seen effects in other proteins secreted from monocytes stimulated with anti-PR3 antibodies indicates that, while these cells are responsive to these antibodies, they cannot activate the same proinflammatory pathways which are induced by anti-MPO antibodies. This interesting divergence in these pathways further emphasises the dramatic differences between the way monocytes and neutrophils respond to ANCA and shows how this cell type is of interest to the study of disease.

Chapter 5: Development of a murine model of ANCA associated vasculitis

5.1 Introduction

While *in vitro* studies have proven valuable in establishing the mechanisms by which ANCA can activate immune cells, systemic interactions are often lost in these isolated systems. Therefore, *in vivo* models of disease are required to fully elucidate the complex cellular and cytokine interactions underlying disease as well as to allow future drug development. Currently, several models of AAV exist which are described in detail in **Chapter 1**. The majority of the models developed to date focus on anti-MPO driven disease (Salama and Little, 2012). This is largely due to differences in human and murine biology, particularly the fact that mice do not express PR3 on the surface of their neutrophils in the same way humans do (Schreiber et al., 2005). This lack of antigen is thought to be one of the key obstacles in the development of a murine anti-PR3 driven disease model. Due to the variation in monocyte responses to anti-MPO and anti-PR3 antibodies I found in **Chapters 3** and **4**, and as anti-MPO models are already available, I wanted to develop a functional *in vivo* model of anti-PR3 driven disease to further tease out the different responses of monocytes to these antibodies.

In recent years the use of strains of immunocompromised mice to study disease has increased. Non obese diabetic (NOD) mice are one such strain which have been developed to aid in the study of autoimmune disease and cancer (Atkinson and Leiter, 1999). These mice have defects in their T lymphocyte populations and NK cell function (Anderson and Bluestone, 2005). This strain of mice have also been shown to be deficient in the complement system specifically in complement component C5 due to a homozygous gene deletion (Baxter and Cooke, 1993). NOD mice have been used in attempts to create a PR3 driven *in vivo* model of AAV. Immunisation of these mice with recombinant PR3 led to the development of PR3 ANCA but no disease (Primo et al., 2010), this lack of disease was likely due to the absence of surface PR3 in murine cells as discussed above. However, when splenocytes from these mice were transplanted into NOD-severe combined immunodeficiency (SCID) mice these mice developed severe renal disease. These data indicate a possible anti-PR3 mediated response however, as these mice should have a similar lack of surface PR3 expression the exact mechanism of disease induction is unclear. As disease was not established in the NOD mice it was concluded that some form of immunological protection was occurring in these animals which prevented their use as a model organism for this disease. Although the NOD-SCID mice did develop disease this disease was not granulomatous and therefore was not a true representation of the human condition.

Mice which are chimeric for human cells have recently become more readily available and the use of these ‘humanised’ mice has become important in the study of diseases which have no murine equivalent such as HIV (Stoddart et al., 2011) as well as in cancer research (Shiokawa et al., 2010, Ninomiya et al., 2004). Studies using humanised mice allow for a more

accurate model of disease as they provide real human cell interactions as opposed to murine surrogates. These mice may prove valuable in the study of vasculitis as they could allow for the differences between PR3 expression in mouse and human to be overcome. With this in mind *Little et al* humanised NOD-SCID mice which were also lacking the IL-2 receptor γ chain (NSG) using adult peripheral blood CD34+ stem cells (Little et al., 2012). The addition of the IL-2Rγ knockout has been shown to greatly increase haematopoietic stem cell engraftment (Shultz et al., 2007, Manz, 2007). These humanised NSG mice have been shown to develop functional human immune cells particularly cells important in AAV such as neutrophils (Coughlan et al., 2012b). *Little et al* successfully induced mild disease in mice injected with total IgG purified from patients with anti-PR3 ANCA. The disease was manifested in the form of crescentic and abnormal glomeruli and lung haemorrhage (Little et al., 2012). This disease phenotype is much more closely related to the disease seen in human when compared with the previous NOD-SCID model. While this model may be valuable in the study of this disease, the lack of a severe disease phenotype indicates that improvements can still be made.

NSG mice are an extremely immunodeficient strain which lack functional T cells, B cells, NK cells, and have impaired dendritic cells and macrophages (Shultz et al., 2005). These mice have been shown to engraft moderate levels of human CD45 cells when injected with CD34+ stem cells. Since they were developed in 2005 a number of other transgenic NSG strains have been designed in an attempt to increase the levels of haematopoietic stem cell engraftment. The main reason for this lack of high engraftment levels is thought to be the lack of a suitable human cytokine environment with a number of important cytokines involved in immune cell differentiation having no cross reactivity between humans and mice (Hara and Miyajima, 1992, Shanafelt et al., 1991). In particular, two NSG strains which are transgenic for human cytokines have been shown to be important in myeloid differentiation:

- NSG mice transgenic for human membrane stem cell factor (hu-mSCF)
- NSG mice transgenic for human interleukin-3 (IL-3), granulocyte macrophage colony stimulating factor (GM-CSF) and soluble stem cell factor (SCF) (SGM3).

The presence of hu-mSCF has been shown to aid human cell engraftment in these mice, in particular the differentiation of granulocytes (Takagi et al., 2012). The triple transgenic nature of SGM3 mice is designed to aid engraftment in several ways; IL-3 stimulates myeloid lineage cell proliferation (Hara and Miyajima, 1996), GM-CSF stimulates macrophages, monocytes and granulocytes to be produced from stem cells (Root and Dale, 1999) and SCF has a role in haematopoiesis similar to GM-CSF (Broudy, 1997). These cytokines are secreted consistently in SGM3 mice and therefore should aid in human cell differentiation and development. The majority of research involving these mice has focused on lymphocytes with myeloid lineage cells being less well studied (Coughlan et al., 2012b). Here I investigate the human monocyte engraftment of these humanised mouse models and differences in disease

induction in different NSG strains. I have also attempted to increase the suitability of this model to display a disease phenotype more closely related to that seen in human by the addition of C5a, through the use of affinity purified anti-PR3 antibodies and through a comparison of engraftment levels based on human stem cell source.

5.2 Methods

5.2.1 Hypothesis

Previous work to humanise NSG mice has resulted in low levels of myeloid cell engraftment. These mice also displayed only mild disease phenotypes in response to ANCA challenge. I therefore hypothesised that:

I. NSG mice transgenic for human cytokines will result in increased monocyte engraftment levels
II. Transgenic NSG mice will allow for greater disease induction than traditional NSG strains

5.2.2 Methods

The methods used to investigate the hypothesis outlined in **Chapter 5.2.1** are outlined in **Figure 5.2.1** and **Figure 5.2.2**. Stem cells were sourced through 3 different routes outlined in **Table 5.1**. The process used for engraftment and disease induction is shown in **Figure 5.2.3**.

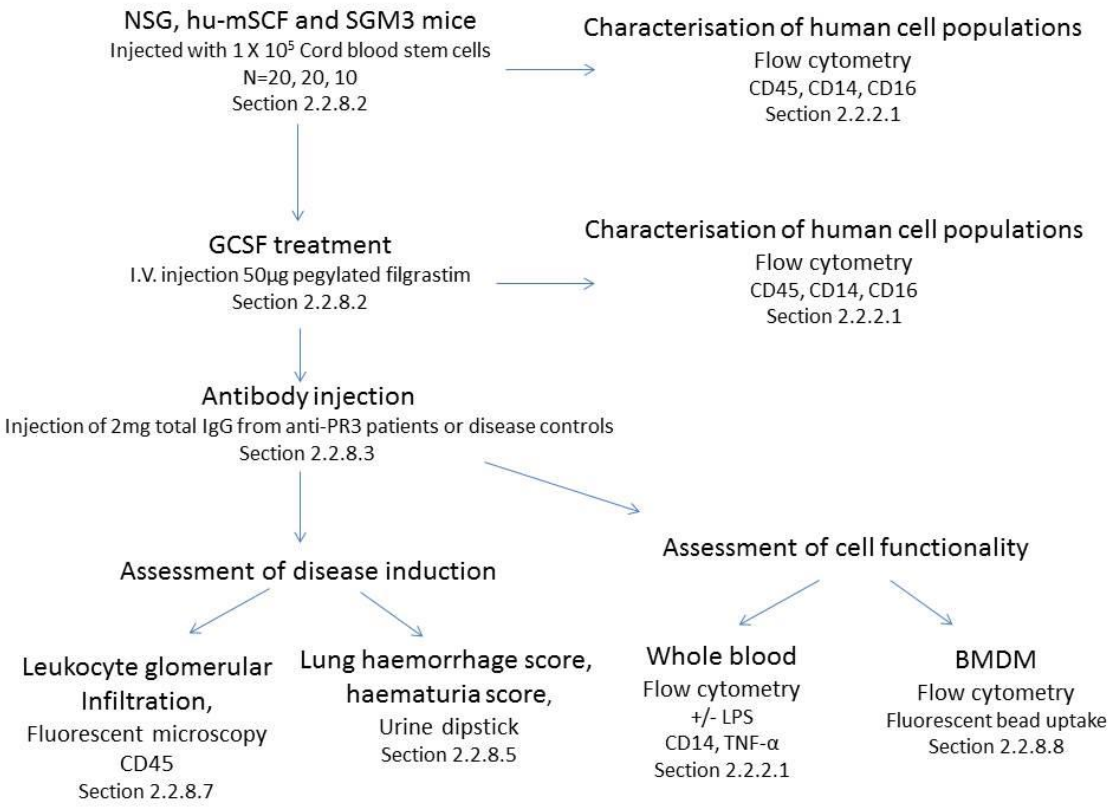

Figure 5.2.1 Diagrammatic representation of NSG strain comparison.
Overview of experimental plan and techniques used to compare engraftment and disease induction in different NSG strains. Detailed methods are provided in the chapter number shown below each technique.

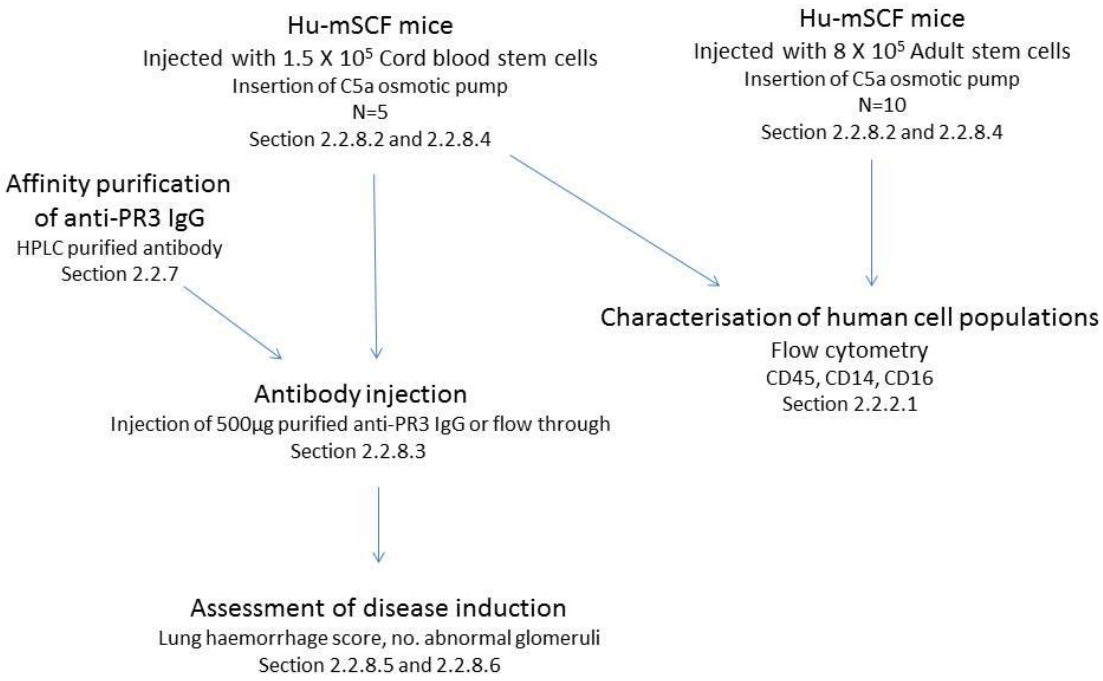

Figure 5.2.2 Diagrammatic representation of experimental plan to enhance disease phenotype in humanised mice.
Overview of experimental plan and techniques used to induce disease in hu-mSCF mice. Detailed methods are provided in the chapter number shown below each technique.

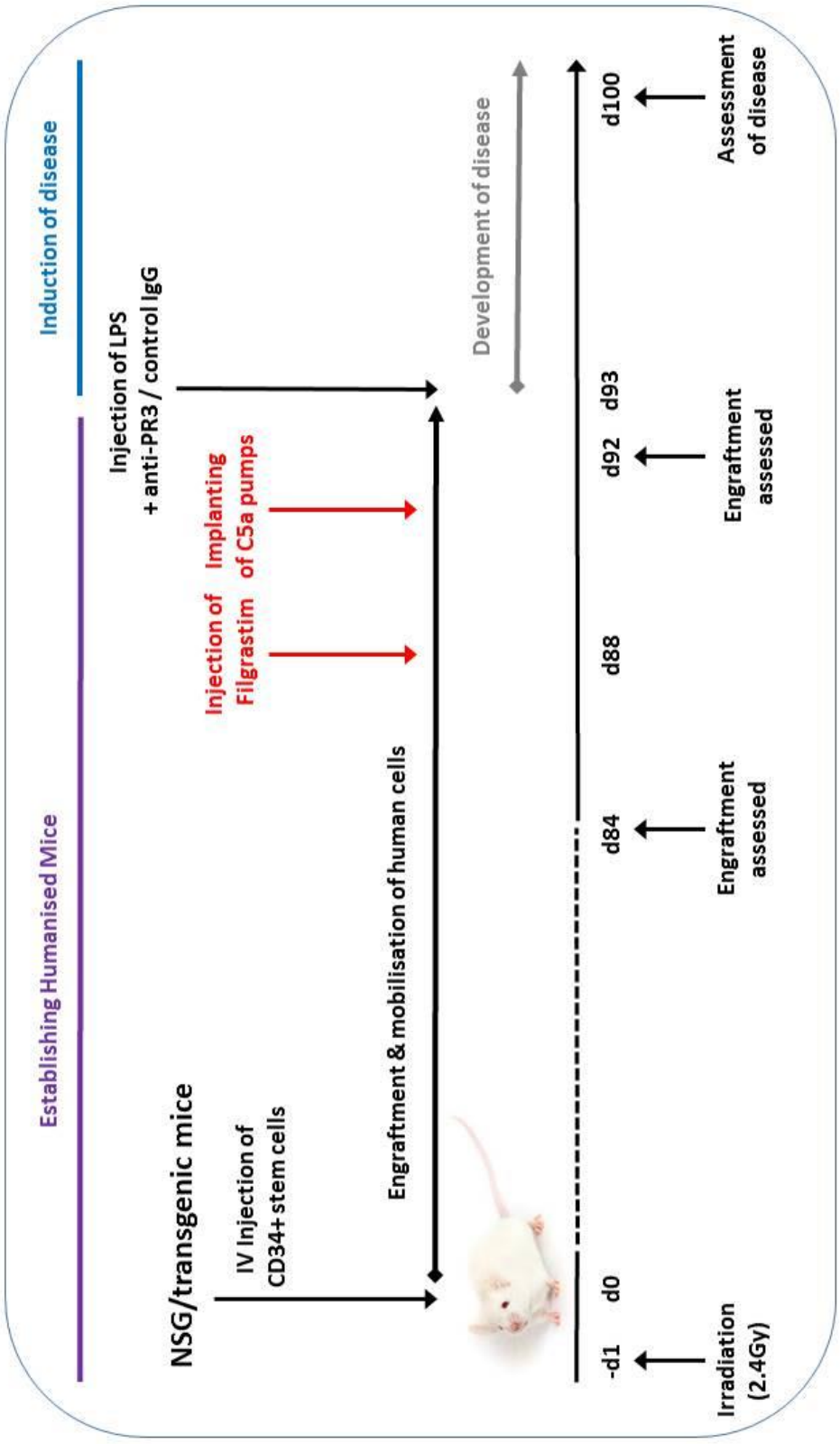

Figure 5.2.3 Procedure for engrafting humanised mice and subsequent disease induction.

Stem cell source	Isolation method	Concentration used	Experiments
Commercial sourced cord blood	Commercially isolated	1 X 10^5	Figure 5.2.1 - 5.2.5, 5.2.8 and 5.2.9
Locally sourced cord blood	Miltenyi MACS isolation	1.5 X 10^5	Figure 5.2.7 and 5.2.8
Adult peripheral blood	Baxter positive selection	8 X 10^5	Figure 5.2.8

Table 5.1 Source and numbers of stem cells used to engraft humanised mice

5.2.3 Acknowledgments

Due to their complexity humanised mouse experiments were performed with assistance from a group of individuals in the lab. I would like to thank Dr Alice Coughlan, Dr Vincent O'Reilly and Dr Dearbhaile Dooley for their assistance in various aspects of the analysis of these experiments. In particular I would like to thank Dr Coughlan and Dr Dooley for the staining of sections for histology.

5.3 Results

5.3.1 Transgenic NSG mice have increased myeloid cell engraftment compared to control NSG mice

In order to investigate whether transgenic NSG mice would provide a better model system for AAV than the model described previously I determined the engraftment levels for hu-mSCF and SGM3 transgenic mice along with NSG mice as a control. Adult NSG, hu-mSCF and SGM3 mice were irradiated with a sub-lethal dose of irradiation before I.V. injection of commercially available cord blood derived CD34+ human stem cells from two donors. Engraftment levels were established by flow cytometry 12 weeks post stem cell injection. I found a significant increase in the fraction and number of human CD45+ cells in both transgenic strains when compared to the NSG control mice (**Figure 5.3.1 A and B**).

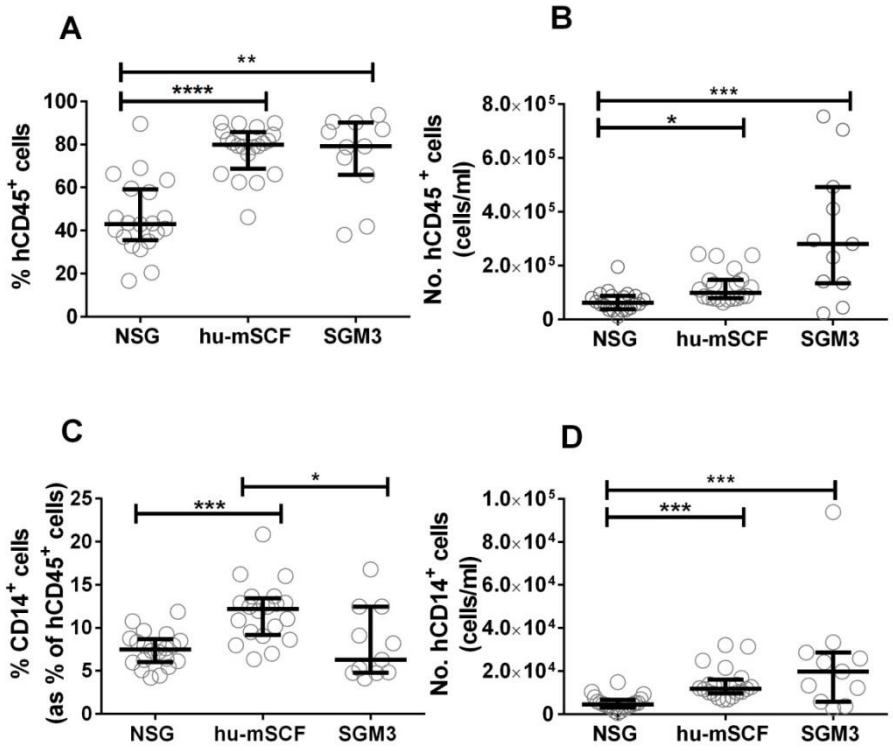

Figure 5.3.1 Transgenic NSG mice have increased human monocyte engraftment.
NSG, hu-mSCF or SGM3 mice were irradiated with 2.4Gy before I.V. injection of 1 X 10^5 human cord blood-derived CD34+ cells. Mice were allowed to engraft for 13 weeks before reconstitution was assessed by flow cytometry. The percentage and absolute number of cells are shown for CD45 (A and B), CD14 (C and D). Each symbol represents a separate mouse. Data are presented as the median and interquartile range (*p<0.05, **p<0.01, ***p<0.001, ****p<0.0001).

Importantly the proportion of monocytes was also increased in the hu-mSCF strain but not the SGM3 mice (**Figure 5.3.1 C).** Interestingly, both strains had an increase in total monocyte numbers with the SGM3 mice having the highest absolute number of these cells (**Figure 5.3.1 D**).

5.3.2 hu-mSCF mice reconstitute monocyte subsets with the greatest efficiency

Monocytes can be divided into 3 subsets as outlined in **Chapter** 1. In combination with *in* vitro studies on these cells shown in **Chapter 3** I next investigated whether different monocyte subsets were established in humanised mice. I found that all three monocyte subsets (Classical: CD14+ CD16-; Intermediate: CD14+ CD16+; Non-classical: CD14lo CD16+) were detectable in blood from each of the three mouse strains (**Figure 5.3.2 A-C**). The NSG (**Figure 5.3.2 A**) and hu-mSCF (**Figure 5.3.2 B**) mice had similar proportions of classical monocytes with SGM3 mice having the highest proportion of this subset (**Figure 5.3.2 C**). The highest proportion of intermediate and non-classical monocytes were found in the hu-mSCF mice (**Figure 5.3.2 B**) and this strain best represented the proportion of each subset seen in humans. Interestingly, we found that CD14 expression was highest on the intermediate subset across the three strains (**Figure 5.3.2 D-F**). We also found only a moderate (but consistent and significant) increase in CD16 expression on the intermediate cells compared to classical indicating a possible deficiency in the differentiation of this cell type (**Figure 5.3.2 G-I**).

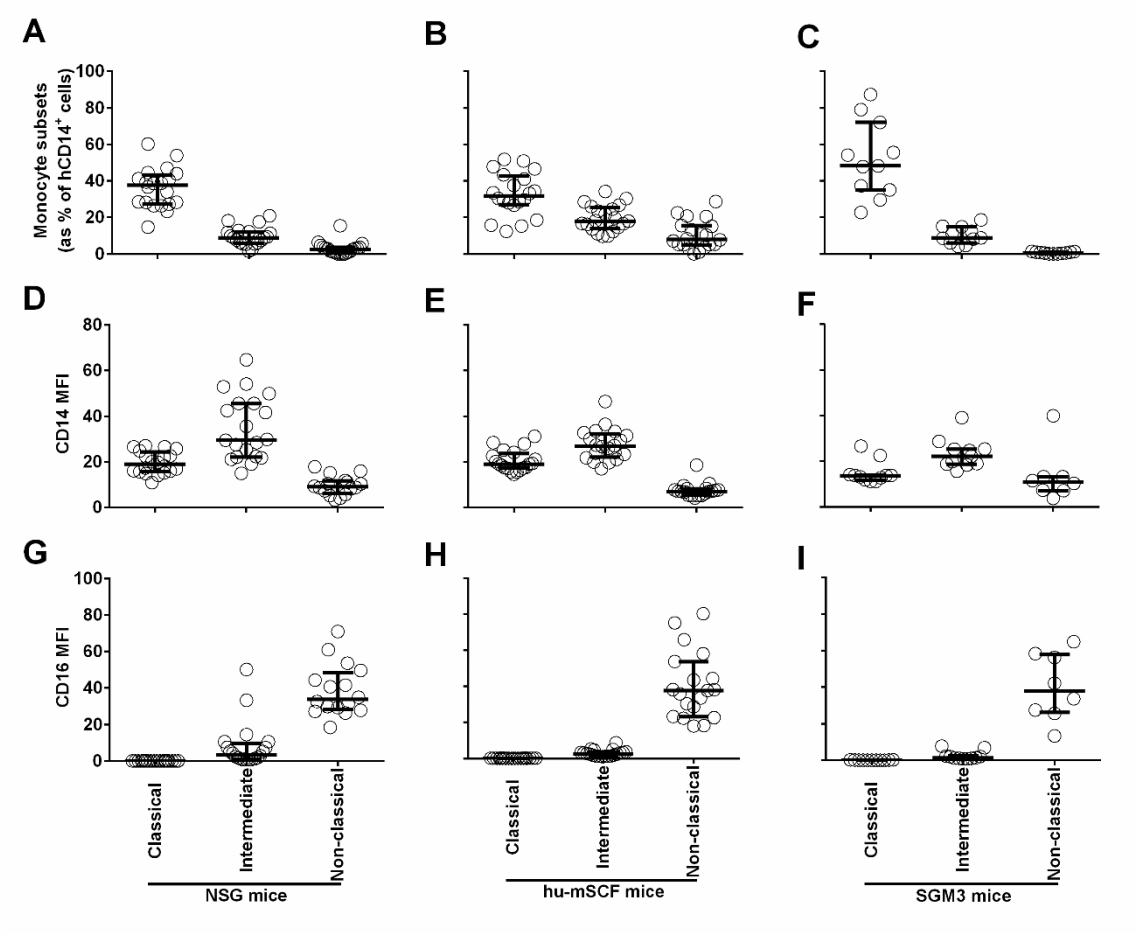

Figure 5.3.2 Humanised mice reconstitute human monocyte subsets.
NSG, hu-mSCF or SGM3 mice were irradiated with 2.4Gy before I.V. injection of 1 X 10^5 human cord blood-derived CD34+ cells. After 13 weeks mice were bled and stained for flow cytometry with antibodies against CD14 and CD16. Monocyte subsets were defined as CD14++CD16- (Classical), CD14++CD16+ (Intermediate) and CD14+CD16++ (Non-classical). The percentage of each subset as a proportion of total CD14+ cells is shown for NSG (**A**), hu-mSCF (**B**) and SGM3 (**C**) mice. The median fluorescence intensity (MFI) of CD14 (**D-F**) and CD16 (**G-I**) is shown for each strain. Each symbol represents a separate mouse. Data are presented as the median and interquartile range.

5.3.3 GCSF treatment had differential effects on monocyte proportions in different NSG strains

While I had found a reasonable level of myeloid engraftment in our transgenic mice I wanted to improve this further. Granulocyte colony stimulating factor (GCSF) has been shown to increase myeloid cell mobilisation from the bone marrow to the periphery. I hypothesised that administering GCSF to the humanised NSG mice would increase the proportion of myeloid cells, particularly monocytes, in the peripheral blood. I used filgrastim, an analogue of human GCSF, to try to mobilise cells from the myeloid compartment to the periphery. Mice were treated with 50µg pegylated filgrastim and four days later the proportion of human cells in their peripheral blood was established by flow cytometry. Filgrastim treatment resulted in a significant increase in the number of CD14+ monocytes in NSG and hu-mSCF mice (**Figure 5.3.3 A**). The change in monocyte numbers in response to filgrastim was most striking in the hu-mSCF mice with a doubling in numbers compared to the NSG mice (**Figure 5.3.3 B**). Interestingly, while we did see an increase in neutrophils as expected (**Figure 5.3.3 C**) this increase was similar across the three strains (**Figure 5.3.3 D**).

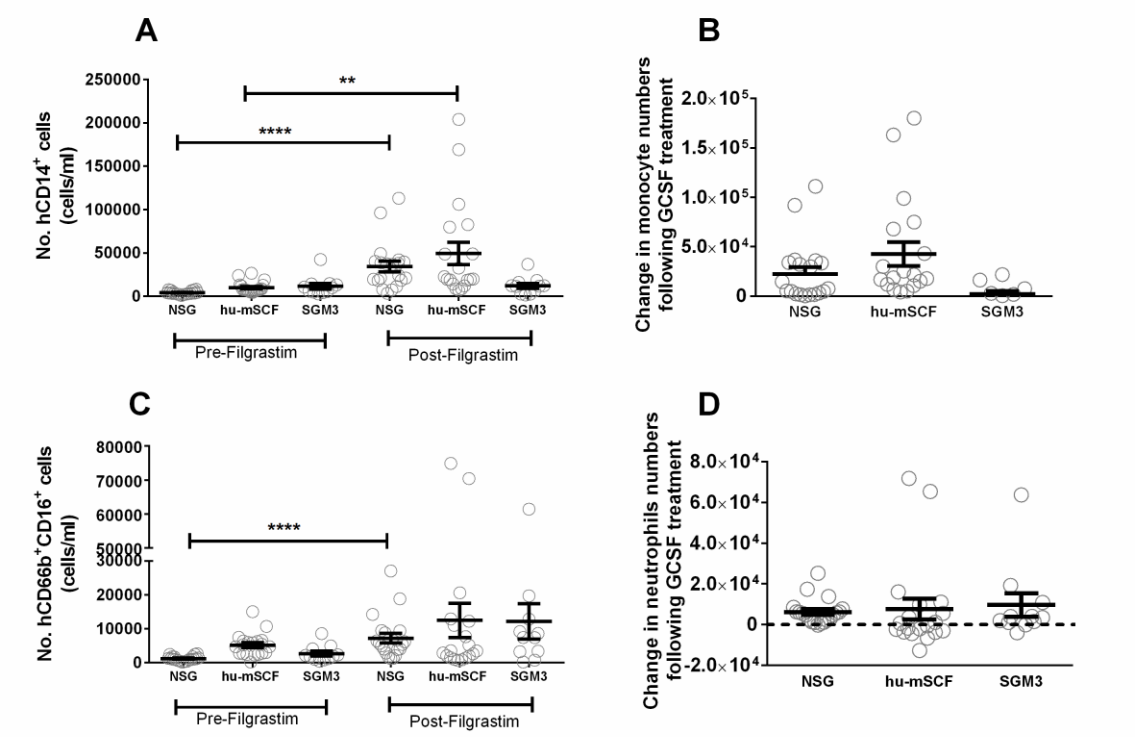

Figure 5.3.3 GCSF increases monocytes in NSG and transgenic NSG mice.
NSG, hu-mSCF or SGM3 mice were irradiated with 2.4Gy before I.V. injection of 1 X 10^5 human cord blood-derived CD34+ cells. After 13 weeks mice were injected with 50µg pegylated filgrastim (GCSF). 4 days later the mice were bled and number of monocytes (**A**). The overall change in monocyte numbers following GCSF treatment is shown for each strain (**B**). Each symbol represents a separate individual. Data are presented as the median and interquartile range (**p<0.01, ****p<0.0001).

5.3.4 GCSF treatment significantly altered the proportion of each monocyte subset in humanised mice

While GCSF treatment had led to a significant increase in the overall monocyte numbers in our humanised mice (**Figure 5.3.3 A**) I next determined if this increase occurred in each monocyte subset or if one subset was being preferentially expanded. I found that GCSF treatment resulted in significant expansion of the non-classical subset in both NSG and hu-mSCF mice with a concomitant reduction in the other subsets (**Figure 5.3.4 A, B**). Subsets in SGM3 mice were mainly unaffected by the addition of GCSF (**Figure 5.3.4 C**) as expected based on the lack of response in total monocyte numbers in this strain. My *in vitro* studies had shown that the intermediate monocyte subset was important in AAV (**Chapter 3**) and due to the reduction in this population GCSF was not used for subsequent experiments. Based on their levels of human cell engraftment and the proportions of monocyte subsets present in their peripheral blood, hu-mSCF mice were chosen as the most suitable strain to use for further work to improve the AAV model.

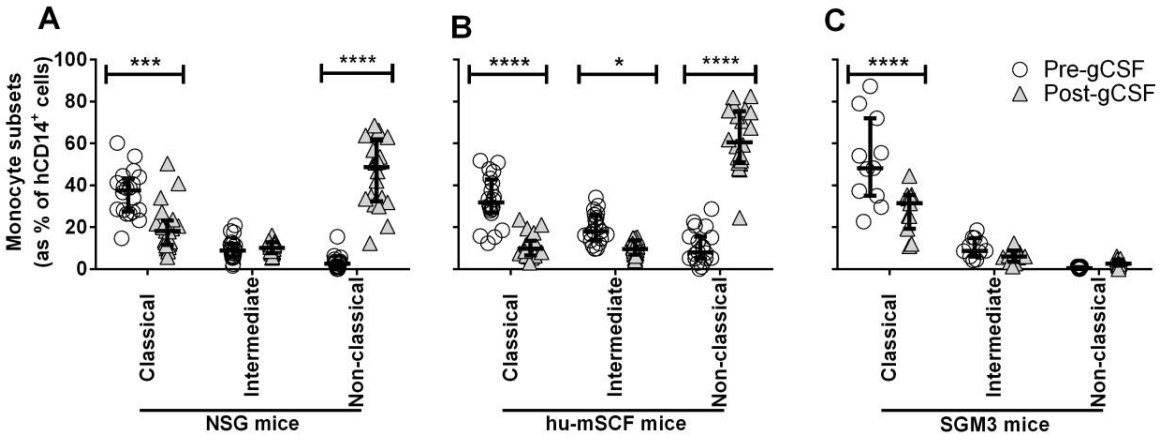

Figure 5.3.4 Monocyte subsets in humanised mice are altered by GCSF treatment.
NSG, hu-mSCF or SGM3 mice were irradiated with 2.4Gy before I.V. injection of 1 X 10^5 human cord blood-derived CD34+ cells. After 13 weeks mice were injected with 50µg pegylated filgrastim (GCSF). 4 days later the mice were bled and stained for flow cytometry with antibodies against CD14 and CD16.Monocyte subsets were defined as CD14++CD16- (Classical), CD14++CD16+ (Intermediate) and CD14+CD16++ (Non-classical). The percentage of each subset as a proportion of total CD14+ cells before and after filgrastim treatment is shown for NSG (**A**), hu-mSCF (**B**) and SGM3 (**C**) mice. Each symbol represents a separate mouse. Data are presented as the median and interquartile range (*p<0.05, ***p<0.001, ****p<0.0001).

5.3.5 Engraftment levels may be insufficient as a readout of human immune system reconstitution in humanised mice

Throughout this study humanised mice showed good human cell engraftment however the lack of disease induction led us to question the functionality of these cells. In order to assess functionality of the human monocytes found in humanised mice I stimulated peripheral blood monocytes and investigated their ability to produce TNF-α. I found that human monocytes from NSG and hu-mSCF mice were capable of producing TNF-α (**Figure 5.3.5 A**). I also isolated bone marrow from each mouse strain and expanded bone marrow derived macrophages (BMDMs). The ability of these BMDMs to phagocytose was established by incubation with fluorescent beads (**Figure 5.3.5 B**). I found that despite the increased levels of monocytes in hu-mSCF mice it is the NSG mice which can develop macrophages with the best functionality (**Figure 5.3.5 C**).

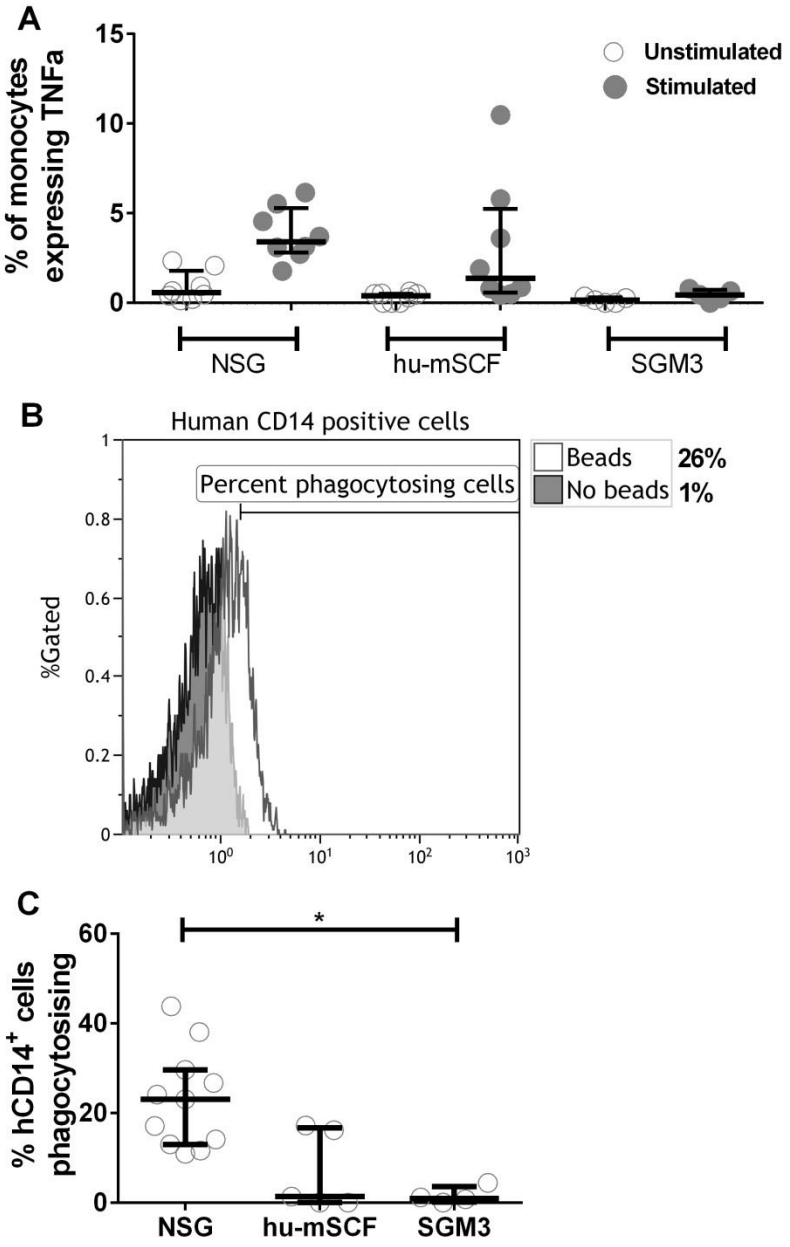

Figure 5.3.5 NSG and hu-mSCF humanised mice can develop functional monocytes and macrophages.

NSG, hu-mSCF or SGM3 mice were irradiated with 2.4Gy before I.V. injection of 1 X 10^5 human cord blood-derived CD34+ cells. After 13 mice received 1µg lipopolysaccharide (LPS) and 1mg IgG from purified from anti-PR3 patients or disease control individuals. 7 days later the mice were culled by terminal bleed. Peripheral blood was treated with or without 2ng/ml LPS and stained for CD14 and intracellular TNF-α (**A**). Bone marrow was isolated and cultured in DMEM supplemented with human M-CSF for 1 week to expand BMDMs. Cells were harvested and incubated with fluorescently labelled polystyrene beads before staining with anti-CD14 antibody. Representative histogram depicting the fraction of human CD14+ cells which successfully phagocytosed beads is shown (**B**) The proportion of BMDMs capable of phagocytosing beads was established for each strain (**C**). Each symbol represents a separate mouse. Data are presented as the median and interquartile range (*p<0.05).

5.3.6 Humanised mice injected with anti-PR3 patient IgG did not develop vasculitis

After characterising the cells present in the periphery of humanised mice, I next wanted to investigate whether I could induce disease in the different transgenic NSG strains. I injected IgG purified from either patients with anti-PR3 disease or disease control patients. In order to identify the presence of disease I looked at lung damage in the form of haemorrhage, and renal impairment by haematuria and presence of human CD45 cells in glomeruli. I found that there was no significant difference in the amount of lung haemorrhage observed after anti-PR3 injection in any of the three strains tested (**Figure 5.3.6 A-C**). The amount of haematuria compared to disease control IgG treated animals also remained the same across the three strains (**Figure 5.3.6 D-F**). Infiltrating human cell numbers into glomeruli were similar in each strain between anti-PR3 and disease control IgG treated animals, however the two transgenic strains had markedly increased numbers of these cells in each glomerulus counted when compared to the NSG mice (**Figure 5.3.6 G-I**).

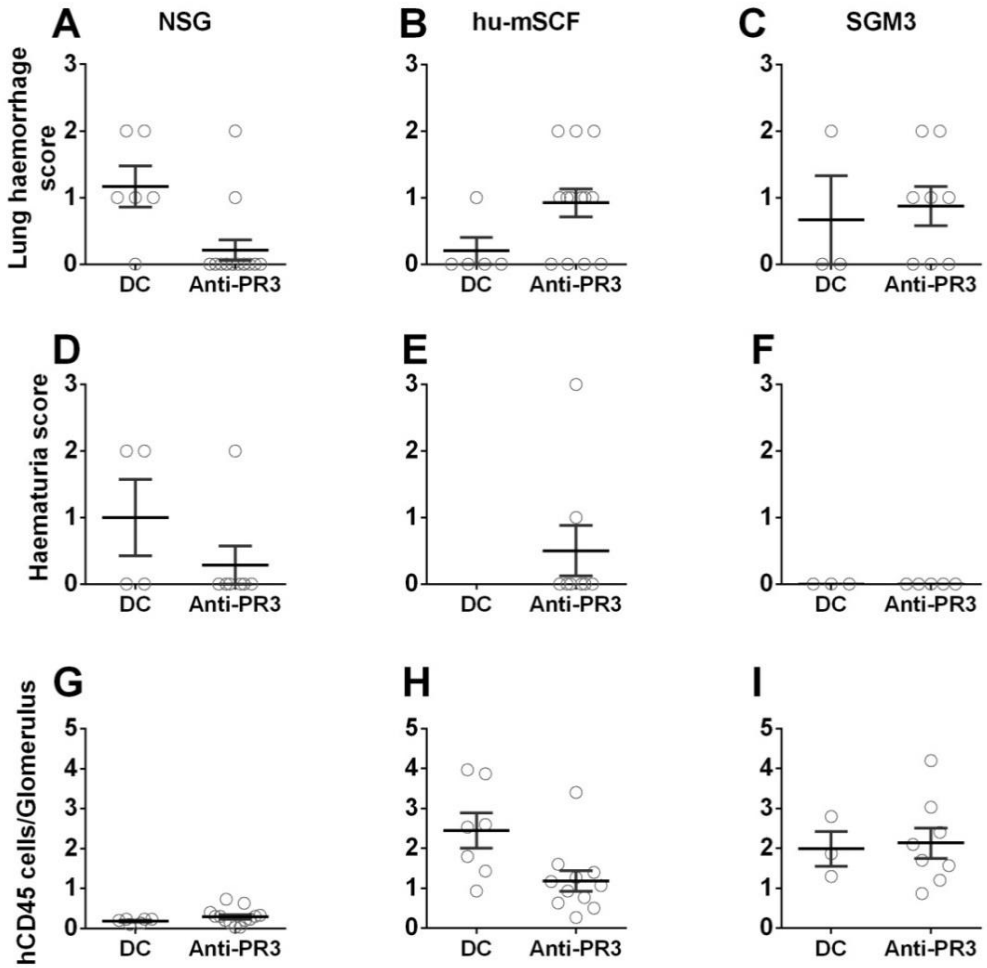

Figure 5.3.6 Anti-PR3 patient total IgG did not induce disease in humanised mice.
NSG, hu-mSCF or SGM3 mice were irradiated with 2.4Gy before I.V. injection of 1 X 10^5 human cord blood-derived CD34+ cells. After 13 weeks mice were injected with 50µg pegylated filgrastim. 1 day later mice received 1µg lipopolysaccharide (LPS) and 1mg IgG purified from anti-PR3 patients or disease control individuals. 7 days later the mice were culled by terminal bleed. Lung haemorrhage score was recorded based on the number of observed haemorrhages on the right lung immediately following opening of the chest cavity for each strain (**A-C**). Spot urines were collected where possible and the degree of haematuria was measured using a urine dipstick (**D-F**). Kidney tissue was frozen in liquid nitrogen before being fluorescently stained for hCD45. The number of hCD45 cells in each glomerulus was counted (**G-I**). Each symbol represents a separate individual. Data are presented as the median and interquartile range.

5.3.7 Affinity purified anti-PR3 antibodies did not induce disease in hu-mSCF humanised mice.

I hypothesised that the failure to induce disease in the previous model may have been due to the concentration of specific antibody being too low in the total IgG preparation used from patients. Previous work in our lab had shown that anti-PR3 monoclonal antibodies would be unsuitable for inducing disease due to the presence of murine Fc portion. To address the issue of specificity I affinity purified anti-PR3 specific antibodies from patient IgG in collaboration with Thomas Hellmark's group in Lund, Sweden. Affinity purification was performed on pooled total IgG from 12 anti-PR3 positive patients. The purity of anti-PR3 IgG in the eluted fraction was assessed by ELISA. Anti-PR3 specific antibodies were enriched to a 6-fold higher concentration in the eluted fraction compared to the flow through (**Figure 5.3.7 A**).

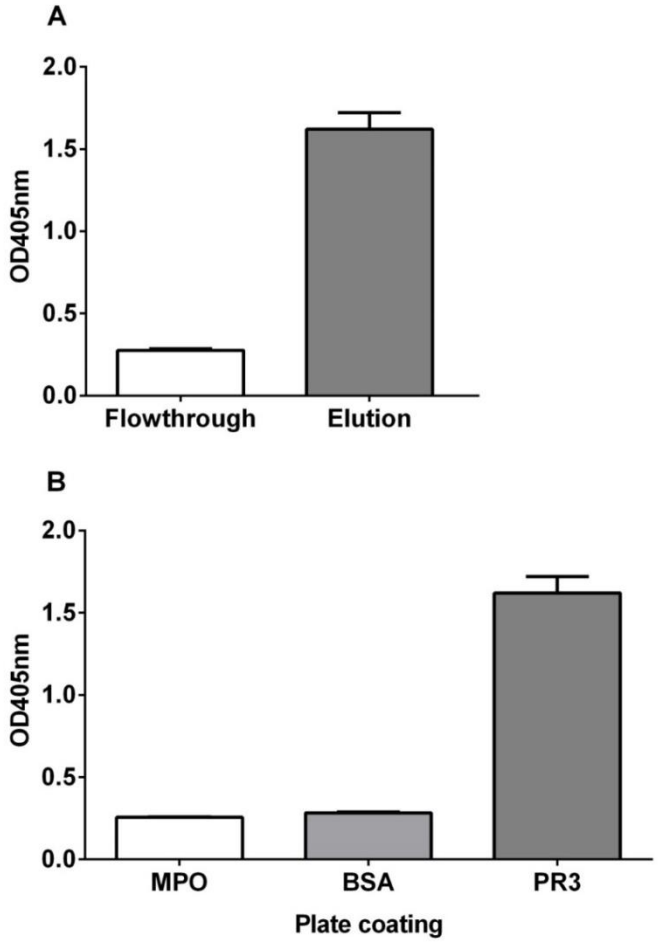

Figure 5.3.7 Isolation of anti-PR3 specific antibodies from total patient IgG.
IgG was isolated using protein G from plasma exchange samples from 12 patients with anti-PR3 positive disease. IgG was pooled and anti-PR3 antibodies were affinity purified using fast pressure liquid chromatography (FPLC). The level of anti-PR3 antibodies in the eluted fraction was compared to levels in the flow through using an anti-PR3 ELISA (**A**). Specificity of the antibodies for PR3 was measured by addition of the eluted fraction to ELISA plates coated with MPO, BSA and PR3 (**B**).

These antibodies were found to be specific for anti-PR3 with minimal binding to MPO or BSA coated plates (**Figure 5.3.7 B**). hu-mSCF mice were humanised by injection with locally isolated CD34+ cord blood stem cells. Affinity purified anti-PR3 antibodies were injected into humanised mice as above. Flow through IgG was injected into control animals. As discussed in the **Chapter 1**, complement has recently been implicated in the pathogenesis of disease. In order to compensate for the lack of complement in these NSG mice, C5a loaded osmotic mini pumps were inserted subcutaneously. These pumps provide consistent release of C5a at a concentration similar to that found in humans. I found no difference between anti-PR3 IgG and flow through treated animals in terms of lung haemorrhage (**Figure 5.3.8 A**). I also assessed the number of normal, abnormal and crescentic glomeruli present in each mouse. Representative normal and abnormal glomeruli are shown in **Figure 5.3.8 B and C**. I found no difference in the number of abnormal glomeruli between anti-PR3 IgG and flow through treated animals (**Figure 5.3.8 D**).

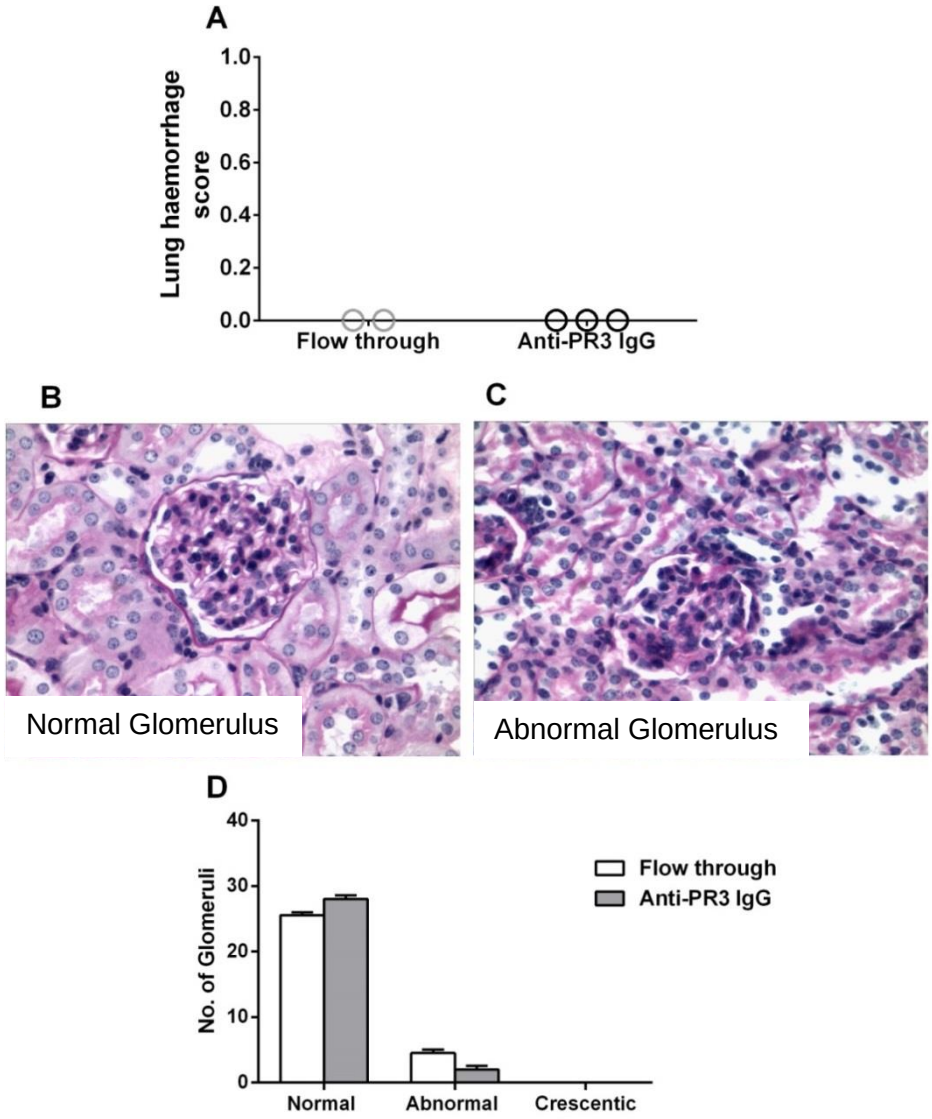

Figure 5.3.8 Affinity purified anti-PR3 antibody did not induce disease in humanised mice.

hu-mSCF mice were irradiated with 2.4Gy before I.V. injection of 1.5 X 10^5 cord blood-derived CD34+ cells. After 12 weeks an osmotic pump containing 4032ng C5a was inserted subcutaneously with a release rate of 24ng/hr. 1 day later mice received 1µg lipopolysaccharide (LPS) and 500µg affinity purified anti-PR3 antibody or flow through IgG. 7 days later the mice were culled by terminal bleed. Lung haemorrhage score was recorded based on the number of observed haemorrhages on the right lung immediately following opening of the chest cavity (**A**). Kidney tissue was frozen in liquid nitrogen before periodic acid-Schiff (PAS) staining. The normal (**B**) and abnormal (**C**) glomeruli were counted and are shown based on IgG received (**D**). Each symbol represents a separate mouse. Data are presented as the median and interquartile range.

5.3.8 Adult peripheral blood stem cells and cord blood stem cells did not increase engraftment or disease induction

In the previous humanised mouse model published by *Little et al* adult peripheral blood stem cells were used to reconstitute a human immune system. I therefore investigated whether the lack of disease induction I observed was due to the use of cord blood derived stem cells. I compared engraftment levels using adult stem cells with two sources of cord blood stem cells, commercially sourced and locally isolated through collaboration with the Coombe maternity hospital. I found significantly lower levels of human CD45+ cells in mice injected with adult stem cells when compared to the commercial cord cells used previously while the locally isolated cells had an intermediary level (**Figure 5.3.9 A**). These adult cells also showed a reduction in the proportion of monocytes present compared to both the previous commercial stem cell source and the locally isolated cells (**Figure 5.3.9 B**).

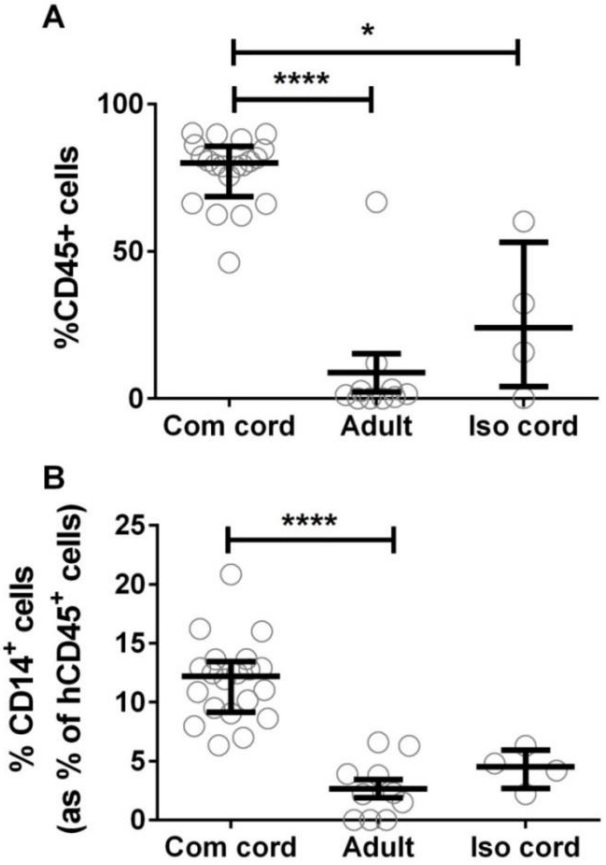

Figure 5.3.9 CD34+ stem cell source influences total leukocyte and myeloid engraftment of humanised mice.
hu-mSCF mice were irradiated with 2.4Gy before I.V. injection of 1 X 10^5 commercially sourced human cord blood-derived (Com cord), 8 X 10^5 adult peripheral blood-derived (Adult) or 1.5 X 10^5 locally isolated human cord blood-derived CD34+ cells (Iso cord). After 13 weeks mice were bled and blood was stained for CD45, CD14 and CD66b. The percentage of human CD45 cells (**A**) and CD14+ monocytes (**B**) is shown. Data are presented as the median and interquartile range (*p<0.05, ****p<0.0001).

5.4 Discussion

In vivo models of disease are vital for the elucidation of the immunological interactions in complex diseases such as AAV. The previous work in this area by *Little et al* found that anti-PR3-induced glomerulonephritis could be successfully established using a humanised NSG model (Little et al., 2012), although the severity of disease in these mice was relatively mild. The mild nature of disease was thought to be a result of insufficient human CD45+ cell engraftment. I therefore investigated mechanisms through which human CD45+ cell engraftment could be improved using different transgenic strains. Our results, in agreement with the literature (Brehm et al., 2012, Billerbeck et al., 2011), indicate that transgenic NSG strains do have better human cell engraftment than the parental NSG strain. Transgenic NSG mice also displayed an increase in monocyte engraftment as expected. Importantly, I was able to identify individual human monocyte subsets in these mice at proportions similar to humans and show that GCSF leads to marked changes in this subset profile. These subsets and their potential role in disease are discussed further in **Chapter 3**. As expected, I found an increase in the number of neutrophils in response to G-CSF, however, unlike the monocyte data, the three strains had broadly similar changes in neutrophil numbers in response to G-CSF treatment. Interestingly, I found that while the SGM3 mice appeared to have the greatest proportion of human cells overall, the proportion of monocytes present in these mice was not expanded compared to the NSG strain. This lack of increased monocyte engraftment in SGM3 mice, together with both the apparent inability of the monocytes present to respond to GCSF and the lack of distinct monocyte subset populations, led to hu-mSCF mice being chosen as the strain to best allow elucidation of monocytes in disease.

In this study we used three strains of NSG background mice, however, as discussed in **Chapter 1,** cytokine knock in mice based on a $RAG^{-/-}$ background are also available (Rongvaux et al., 2014). Similar to the SGM3 strain, these mice have human IL-3 and GM-CSF genes knocked in and also include genes for M-CSF and thrombopoietin (Tpo) (MITRG) and bacterial SIRPα (MISTRG). These gene insertions have been shown to increase human cell engraftment in $RAG^{-/-}$ background animals. Previously, functional monocyte subsets have been identified in these mice however, this study found that only a small proportion of monocytes were of a non-classical phenotype (<1%) whereas a high fraction (>20%) were non-classical (Rongvaux et al., 2014). These percentages do not reflect the human system where classical monocytes are the most numerous population. The proportion of monocytes found in our model better reflects the proportions found in humans.

MITRG and MISTRG mice showed increased engraftment when injected with human fetal liver tissue. Due to the unavailability of this tissue in Ireland our study must be compared

to the cord blood and adult CD34+ groups used. In this regard, we found considerably higher engraftment levels when using cord blood derived stem cells when compared to the same group in the *Rongvaux et al* study (80% vs 40%) (Rongvaux et al., 2014). These data suggest that when fetal tissue is not readily available NSG background mice provide a more suitable model system for humanisation.

I was unable to replicate the results of *Little et al* in terms of disease phenotype, namely lung haemorrhage; however, I did find a statistically insignificant trend towards increased haemorrhage in the hu-mSCF mice treated with anti-PR3 antibodies compared to those injected with control IgG. I found similar levels of leukocytes infiltrating the kidneys between both treatment groups. In human disease leukocytes infiltrate the kidneys and lead to crescent formation and vascular damage (Weidner et al., 2004). While I found no evidence of vascular damage, the presence of leukocytes in this area indicates that these cells have received migratory signals to move out of the vasculature and are therefore in the ideal location to be activated to induce disease. The discrepancies between the previously published model and our own may be as a result of differences in stem cell source; I used a commercially available source of cord blood stem cells where as *Little et al* used adult peripheral blood stem cells. Cord blood stem cells have been previously shown to provide increased levels of human cell engraftment when compared to adult cells (Lepus et al., 2009). While our results showed consistently increased human cell engraftment in cord vs adult cell recipients other differences in these cells may explain the lack of disease in our model. For example, cord blood stem cells differ from peripheral blood stem cells, such as those from the adult donors, in their composition and properties (Hordyjewska et al., 2015). These cells display higher proliferative potential, capable of forming colonies (HPP-CFC) cells (Stojko and Witek, 2005, Brunet de la Grange et al., 2002) than those found in peripheral blood meaning they should in theory have greater potential to differentiate into cells of interest. However, these sources also have differing T and NK cell repertoires. The T cell compartment of cord blood stem cells has a greater CD4+/CD8+ ratio than that seen in peripheral blood while NK cell proportion is also reduced (Zeman et al., 1996). These cord blood cells are generally considered to be more “naïve” than their adult counterparts (Kaminski et al., 1996). Indeed, cord blood cells have been shown to be tolerant to endotoxin stimulation indicating a possible more overall inert phenotype for these cells (Gessler et al., 1999, O’Hare et al., 2016). This “naivety” may help to explain the differences in these two models.

It has been shown previously that neutrophils from humanised mice can express PR3 on their surface (Coughlan A. unpublished) and therefore we did not investigate the expression of these antigens in our model. The administration of LPS was designed to aid in antigen expression however, the lack of PR3 staining means that a lack of surface antigen expression cannot be ruled out as the cause of our lack of disease phenotype.

One of the major features of mice which are based on the NOD background is the lack of a functional complement system (Baxter and Cooke, 1993). Recently it has emerged that complement may play a role in the pathogenesis of AAV (Kallenberg and Heeringa, 2013) with complement blockers currently undergoing clinical trials (Jayne et al., 2017). As discussed in Chapter 1, complement has recently been shown to be important in the pathogenesis of AAV with clinical trials of anti-C5a mAb currently underway. The lack of functional complement in NOD mice may therefore play a role in the failure of this model to induce disease, although it is worth noting that complement was also absent in the previously published model. To combat this lack of complement I inserted an osmotic pump containing the complement component C5a in a subset of animals. However, these mice also failed to develop disease. Further studies with larger numbers of animals would be required to determine the potential benefit of adding complement.

Another potential cause of the lack of disease observed in the previous humanised mice was the unknown quantity of anti-PR3 specific IgG in the total IgG preparation used. To overcome this, I hypothesised that monoclonal antibodies against PR3 may improve disease induction. However, other work from our lab indicated that the lack of human Fc portion on these monoclonal antibodies, and therefore the reduction in any potential crosslinking which may be required, would counteract any potential benefits of the increased specificity. In order to increase the amount of specific antibody being used to induce disease, I established a collaboration with a group in Lund university which allowed me to purify anti-PR3 specific antibodies from patient total IgG. This approach was designed to overcome the lack of specific antibodies in the total IgG prep used previously as well as the lack of human Fc receptors in monoclonal antibodies. Using these purified antibodies and the mice humanised with cord blood derived stem cells I was again unable to induce any disease in these animals. The reason for this lack of replication of the previously published disease model is unclear and requires further study. One possibility is that differential housing conditions in the different animal facilities may influence this model. A recent study by *Beura et al* showed that mice housed in different environments have drastically different immune cell phenotypes (Beura et al., 2016). This model requires an immune system boost of LPS administration in order to achieve disease (Little et al., 2012) however the exact mechanism through which disease is induced is not known. Other factors, such as environmental conditions, may be important in establishment of disease and differences in these factors between facilities may result in differing outcomes. The lack of reproducibility in these models is not isolated to this model but rather is a problem for the scientific community as a whole (Jilka, 2016). A robust *in vivo* model of disease is required to allow for future drug design and therefore further work to improve the effectiveness and reproducibility of this model is vital.

Interestingly, I have shown a marked difference in the ability of CD34+ cells from different sources to reconstitute a human immune system. When using adult peripheral blood derived stem cells I found very few human CD45 cells in these mice. This lack of human cells was striking when compared to the impressive levels I had achieved using commercially sourced cord cells and further highlights the differences between the mice used in our studies and the previous work. I established a collaboration with the Coombe maternity hospital which could provide us with cord blood to allow isolation of stem cells from multiple donors. This approach was taken in order to reduce the potential for donor specific interactions as well as having significant reduction in the costs involved compared to the previously used commercial cord cells. While these cells did not provide the same level of engraftment commercially sourced cord cells I did establish a significantly increased human CD45+ population compared to the adult stem cells.

The presence of human CD45+ cells is used as the main readout for successful engraftment in humanised mice however, these data show that high engraftment levels do not always equate to the best model of a human immune system. The lack of functionality which I found in SGM3 macrophages and the only partially functional macrophages found in hu-mSCF mice are of concern in the use of these mice going forward, both in the study of AAV and other conditions. Further research is required into the role of strain in the ability to train and differentiate functional cells as well as the role that stem cells from different sources may play in this regard. The effect of GCSF on monocyte subsets is also of particular interest and the way in which this may affect the treatment of patients must be explored further. Finally the role of C5a in disease and its effects in humanised mice must be elucidated in order to establish an accurate and reproducible model of the human disease.

Chapter 6: General discussion

6.1 Monocytes in AAV: A remerging field

The prevailing current model of AAV pathogenesis, as discussed in **Chapter 1,** places the neutrophil as the central cell in causing disease. While neutrophils do play a major role in disease, this model fails to account for the myriad of other immune cells in the circulation which can encounter ANCA and how these cells may interact with their environment and each other. Here, I have investigated how another important innate immune cell type, monocytes, are implicated in this disease. Although implicated in early AAV research, focus subsequently largely moved away from these cells. However, thanks to research by myself and others in this field a new paradigm is beginning to emerge for how we interpret the role of monocytes in AAV. The role of monocytes in this disease is likely to be multifactorial, acting at both the initial stages of disease development and also having long term functions.

In the early stages of disease it has been suggested that the development of AAV may be linked to infection (Brunini et al., 2016). The breakdown of tolerance which leads to the generation of autoantibodies and subsequent disease in patients is still not well understood. It has been suggested that infection may trigger this breakdown with high levels of S. *aureus* being found in AAV patients and postulated as having a role in this process (Stegeman et al., 1994, Cartin-Ceba et al., 2010). As monocytes are one of the first cells to respond to infection their role in propagating an immune response is likely to be important in the development of disease. The major role which monocytes play in providing inflammatory signals which not only activate neutrophils but also increase inflammation via interactions with B cells and T cells is also likely to drive the long-term pathogenesis of disease. Here I have shown that several pro-inflammatory cytokines which can drive the immune response are upregulated in monocytes following ANCA stimulation. Secretion of these cytokines could drive a positive inflammatory feedback loop in patients.

One of the primary pathological features in patients is the presence of crescents in the glomeruli. These crescents are a result of aberrant immune cell infiltration and result in a loss of function and necrosis of the surrounding glomerular tissue. Macrophages are the main cell type present in crescents and it has been shown previously that the majority of these macrophages are derived from circulating monocytes (Clarke et al., 1983) further highlighting the important role of this cell type in disease progression. Interestingly my research has shown a marked divergence in the response of monocytes to anti-MPO and anti-PR3 antibodies, the two primary autoantibodies associated with AAV. However, both of these antibodies elicit similar effects in neutrophils. As such the differential response in monocytes may be important in understanding when monocytes should be targeted in disease.

6.2 Unanswered questions

The research presented in this thesis has helped to increase our understanding of AAV by establishing a role for metabolic changes in monocytes in response to ANCA stimulation and by characterising changes in monocyte subset proportions in ANCA patients. However, a number of key questions remain unanswered:

1. Why do anti-MPO and anti-PR3 have such differing effects on monocytes?
2. Can targeting monocyte metabolism be used as a target for treatment of AAV?
3. Why were we unable to induce disease in the humanised mouse model?

6.2.1 Anti-MPO vs anti-PR3 effects

Treatment of MPA and GPA is largely similar for most patients as the two conditions share numerous clinical symptoms. As discussed in **Chapter 1**, MPA and GPA are associated mainly with anti-MPO and anti-PR3 antibodies respectively. Using genome wide association studies *Lyons et al* found that anti-MPO and anti-PR3 driven disease are genetically distinct syndromes (Lyons et al., 2012). These differences have led to suggestions that AAV should be divided based on ANCA specificity rather than the clinical diagnosis. Interestingly, these antibodies have broadly similar effects on neutrophil activation *in vitro.* Here, I have shown that anti-MPO and anti-PR3 stimulation of monocytes results in differing proinflammatory responses in these cells. As these diseases are genetically distinct this may indicate that monocytes are more important to the inflammatory events seen in anti-MPO+ patients as opposed to anti-PR3+ patients. In this regard, the association of anti-PR3 with GPA is of specific interest as the formation of granulomas, the hallmark of the disease, depends on the presence of macrophages. The lack of a strong monocyte response to these antibodies suggests that granulomas formed in GPA patients with anti-PR3 antibodies may be as a result of some other process or perhaps through stimulation of tissue resident macrophages rather than the recruitment of circulating monocytes.

The role of resident cells vs peripheral blood monocytes may also be important in elucidation of the mechanism through which these cells result in vascular damage, Recently, Rousselle et al demonstrated that depleting circulating monocyte populations results in a reduction, but not complete abrogation, of pathogenic effects in a passive transfer model of AAV (Rousselle et al., 2017). This model found reduced crescent formation and glomerular necrosis in the monocyte depleted mice suggesting an important role for these cells in these processes. This result emphasises the importance of studying peripheral blood monocytes in the context of AAV pathogenesis. Interestingly, the finding that some pathology remains in these monocyte depleted mice indicates that other cells are still causing damage to the kidneys (Rousselle et al., 2017). These cells are likely neutrophils, however, tissue resident

monocytes/macrophages may be having a role in this damage. Studies which identify these populations and their role in disease are therefore required to aid in our understanding of monocyte induced damage.

The elucidation of the signalling pathways activated in monocytes in response to anti-MPO and anti-PR3 antibodies is vital to understanding the differences in the response to these antibodies. These pathways are well established in neutrophils, particularly the mechanism of activation by anti-PR3. As discussed in **Chapter 1**, CD177 is thought to be important in mediating anti-PR3 signalling through Mac-1 on the neutrophil cell surface. My work showing that monocytes expressing PR3 on their surface do not co-express CD177 demonstrates an important difference between these two cell types. The lack of CD177 expression on monocytes may help to explain why a reduced proinflammatory effect was seen in response to anti-PR3 when compared with anti-MPO. Interestingly, the changes in the secretion of other proteins which I have shown using Olink proteomic analysis demonstrates that anti-PR3 antibodies are having a similar effect on monocytes, albeit at a lower level. Elucidating the role, if any, of Mac-1 in monocyte signalling and the mechanism through which PR3 is displayed and mediates a signal are therefore important questions to be answered in the future (**Figure 6.1**).

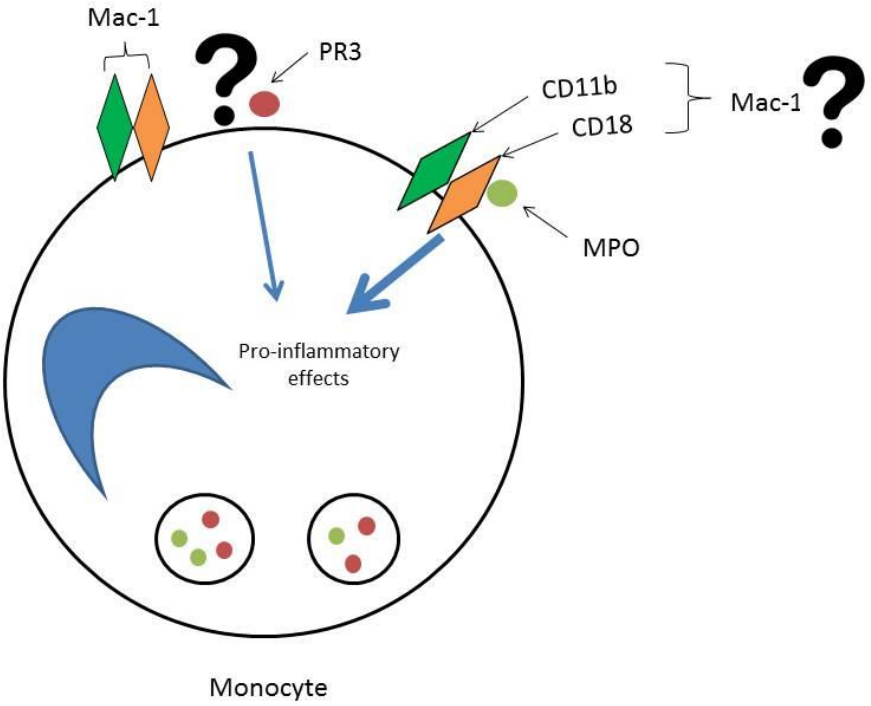

Figure 6.1 Important questions involved in monocyte activation by ANCA.

6.2.2 **Targeting metabolism**

Immunometabolism is fast emerging as a key potential target to alter aberrant immune phenotypes in patients. Currently, the majority of research in this area is focused on T cells and investigating the potential to switch on immune cells *ex vivo* and to use these cells to combat cancer. The manipulation of these cells has the potential to not only increase the immune response to fight cancer but using the correct stimulus could also be used to dampen this response to benefit patients with autoimmune disease. Due to the paucity of data concerning monocyte metabolism I will outline some of the recent advances and therapeutic targets identified in other cell types and discuss how similar approaches could potentially be developed to target monocytes in AAV based on my results.

While the concept of activating most immune cells in autoimmune disease may seem counter intuitive, if specific regulatory cells such as T_{reg} or B_{reg} cells could be activated these cells could then have a role in reducing the immune response. As these cells have been implicated in AAV, their regulation in this way may have potential in the treatment of disease. While this approach may be advantageous in longer lived cells of the adaptive immune system, it is likely that innate cells, such as monocytes and neutrophils, will require a different approach due to their more transient nature. Therefore, the possibility of therapeutically altering cellular metabolism, and consequently cell phenotype, is more promising in targeting these cells in disease.

Due to the distinct metabolic pathways used by particular effector cells, treatments which broadly affect these pathways have been studied. For example, in graft versus host disease (GVHD), where T cells are mainly dependant on ox phos, targeting mitochondrial ATP production is thought to be a potential treatment (Park et al., 2016). Metformin has been suggested as one such therapeutic agent as it inhibits complex I of the ETC and therefore disrupts ATP production. Targeting metabolic pathways has been shown to be effective in various disease models summarised in **Table 6.1.** The application of metabolic alteration has been made possible in these settings by the myriad of research into the pathways involved in T cell metabolism. As changes in glycolysis and ox phos as a result of monocyte activation are not well known, the ability to target metabolism in these cells is unlikely in the immediate future. However, my research has shown that altering metabolic pathways in these cells does affect their inflammatory phenotype suggesting a potential for these kinds of treatments in future.

Interestingly, the upregulation of the two metabolic pathways which I have shown here appears to indicate that the metabolic pathways involved in monocyte activation may differ from those previously described in other cell types. The simultaneous increase in glycolysis and ox phos which I have found is an interesting divergence from the most commonly studied innate lymphoid cell; the macrophage. In M1 macrophages, breaks are formed in the TCA

cycle which results in a build-up of intermediates leading to proinflammatory phenotype in these cells. These key molecules include citrate and succinate. Succinate accumulation stabilises Hif-1α leading to an increase in IL-1β production (Palsson-McDermott et al., 2015), while citrate can be converted to itaconate via immune responsive gene-1 (Irg1) which is activated in these cells (Michelucci et al., 2013, Meiser et al., 2016). Itaconate inhibits succinate dehydrogenase (SDH) and therefore reduces ox phos. This increase in glycolysis therefore usually results in a negative feedback loop further inhibiting ox phos. Whether similar events occur in monocytes is yet to be elucidated, although, at least in ANCA stimulated cells, some divergence from this model must occur as both pathways

Drug		**Pathway targeted**	**Disease model**	**Effect**
2-DG		Glycolysis	Systemic Lupus Erythematosus (SLE)	Decrease clinical score while leaving normal immune function unaffected (in combination with metformin)
DCA		PDHK	Experimental autoimmune encephalitis	Decrease clinical score and pathogenic Th17 formation while promoting Tregs
Metformin		Electron transport chain (complex I)	SLE	Decrease clinical score while leaving normal immune function unaffected (in combination with 2DG)
Etomoxir		Lipid metabolism	GVHD	Decrease clinical score while preserving graft reconstitution

Table 6.1 Drugs used to target metabolic pathways.
Adapted from (Bettencourt and Powell, 2017). 2-DG: 2-Deoxyglucose, DCA: Dichloroacetate, PDHK: Pyruvate dehydrogenase kinase, GVHD: Graft versus host disease

are upregulated simultaneously. Interestingly, I have shown here that NADPH oxidase and respiratory burst are also at least partially involved in this activation. The mechanism behind the combined activation of both of these metabolic pathways in ANCA stimulated monocytes, along with the role of respiratory burst and NADPH oxidase, is therefore of major interest. These differences suggest that the treatments used for other cell types may not be appropriate for treating monocyte driven diseases and more research is required into the role of metabolism in this cell type.

6.2.3 Lack of disease induction

I was unable to replicate the disease model previously published by Little *et al* where crescentic GN and lung haemorrhage were induced in humanised mice after injection with anti-PR3 IgG. The exact reason for the lack of disease is unclear and a number of possible explanations exist as outlined in **Chapter 5.4**. The most likely explanation is the different facilities used in my study and the previous work. In order to improve both the levels of human cell engraftment and disease induction in this model there are a number of possible avenues which could be investigated. Firstly, we added C5a secreting osmotic mini pumps in order to compensate for the lack of complement in the NOD background strains. The experiments incorporating these pumps included small numbers of animals due to a number of mice failing to survive until the end of the experiment. Further research into the role of complement in disease induction and the effect which administration of C5a has would be beneficial for this model going forward. In particular, the use of C5 which has an increased half-life compared to C5a may benefit in the longer term. Using C5 is dependent on the presence of other complement components, namely C4, which are required for its cleavage. The presence of these factors, or the possibility for their co-administration, must therefore first be established for C5 treatment to work correctly.

Another aspect which could be investigated is the strain of mice chosen. I have used 3 different strains of mice to compare engraftment levels; however, each of these strains was created on the same genetic background, NSG. The use of immunocompromised mice from a different genetic background such as $Rag2^{-/-}$ could help to shed more light on the best model in which to induce this disease. These mice are also complement sufficient meaning that the addition of human complement would not be required.

Despite the lack of disease development, other aspects of this study unrelated to AAV may help to improve our knowledge of the mechanisms involved in the immune response. Of particular interest in the context of the other results chapters in this thesis is the identification of monocyte subsets in these humanised mice. As there is no direct correlate for all three human monocyte subsets in wild-type mice this finding provides a potential for studying the responses of these subsets *in vivo*.

6.3 Future work

The work presented in this thesis has helped to better define monocytes and their role in AAV. Further work is needed to better understand the contribution of this important cell type in the pathogenesis of disease. The finding that the proportion of intermediate monocytes is increased in patients with AAV represents the first report of differences in monocyte subsets in this population. However, the discrepancy between my results and those of Tarzi *et al*, where no change in the proportion of each subset was observed, requires further study. Elucidating the reasons behind these differences would be greatly aided by a more robust mechanism of defining the monocyte subsets. In this regard, the addition of new markers which are specific for each subset would greatly assist not only this field but other areas in which these subsets are becoming the focus of study. This study has shown for the first time that monocyte subsets have differential responses to ANCA stimulation. This research could be expanded to investigate differential roles for these cells in disease. In particular, it would be beneficial to distinguish if one subset, such as the intermediate monocytes, is found more frequently in the kidneys and granulomas of patients. This could then lead to more focused research and targeted therapies in future.

With regards to changes in monocyte metabolism, this study has provided initial data into the response of these pathways to ANCA. More research is required to fully identify whether increased glycolysis, ox phos or both are critical in the activation of these cells by ANCA. Other metabolic pathways also require further study to establish their relevance in this cell type and specifically, their importance in responses to ANCA stimulation. In this context the role of fatty acid oxidation (FAO) may be important. This pathway has been shown to be important in other activated immune cells, such as Treg cells, and is often upregulated in cells which are more reliant on ox phos (Buck et al., 2015, O'Neill et al., 2016). The response of this pathway to ANCA stimulation could therefore provide further insight into the monocyte effector function. The results which I have shown here regarding metabolic changes would also benefit from more molecular biological data such as investigating the effect of ANCA stimulation on the mTOR pathway and whether Hif-1α is affected by this stimulation. The role of these proteins is well defined in other cell types and understanding their role in this context would help to better define the metabolic pathways involved in monocyte activation.

Another area of monocyte metabolism which requires further study is the differences in the metabolic profile of the distinct monocyte subsets. The main limitation of this kind of study is in the number of each subset which can be isolated from an individual donor. The study of these pathways therefore may not be possible using the Seahorse technology used in this thesis although other surrogate markers of metabolic changes, such as flow cytometric read outs, may provide insight into differences between these subset populations.

One of the most important findings of this thesis has been the widely divergent response between anti-MPO and anti-PR3 stimulated monocytes. One of the biggest obstacles in establishing the mechanisms behind these differences is the lack of data concerning the display of these antigens and potential signalling pathways activated in these cells. I have shown here that PR3 expression differs in monocytes from that seen in neutrophils. However, anti-PR3 antibody stimulation does result in several changes to these cells indicating some form of signalling is occurring. The exact signalling pathways involved in this response and how they compare to the pathways activated by anti-MPO stimulation must therefore be established to further phenotype these cells in the context of this disease. In particular, the potential to alter the response of anti-MPO treated monocytes to resemble the less inflammatory anti-PR3 phenotype could provide a valuable target for therapeutic intervention.

My work on humanised mice has shown that distinct monocyte subsets can be identified in these mice. This finding provides the potential to study the function of each of these cells in more detail and may allow for the elucidation of their role in several other models of disease. Although I was unable to successfully induce vasculitis in these mice, future avenues to optimise this disease model have emerged from this work. In particular the use of C5a requires further study using groups with larger N numbers. This along with the potential to use C5 rather than C5a could allow for an environment in which disease can be more readily induced.

6.4 Final remarks

The role of monocytes in AAV is likely to be complex with differing functions depending on the disease type, patient and stage of disease. In this thesis I have attempted to increase our understanding of these cells and how they may function in disease. This work has however only begun to unravel the functions of this interesting and understudied cell type. The key results which I have found are outlined below:

- The intermediate monocyte subset is increased in AAV patients and these cells have increased ANCA antigen presentation

- Monocyte subsets have differential responses to ANCA stimulation with the intermediate subset having the most pro inflammatory phenotype

- Anti-MPO and anti-PR3 stimulation of monocytes have significantly different effects *in vitro* both on inflammatory cytokine production and intracellular metabolism

- ANCA stimulation of monocytes leads to changes in their cellular metabolism and these changes differ from previously described “Warburg” like metabolism seen in other activated immune cells

- Monocyte subsets populations can be successfully reconstituted in humanised mice providing a valuable *in vivo* tool for the study of their function

These results have helped to add to the working model of AAV pathogenesis. Although these data have advanced our understanding of these cells in disease they have also opened new avenues for future studies both in AAV and the understanding of monocyte biology as a whole.

References:

ABDGAWAD, M., GUNNARSSON, L., BENGTSSON, A. A., GEBOREK, P., NILSSON, L., SEGELMARK, M. & HELLMARK, T. 2010. Elevated neutrophil membrane expression of proteinase 3 is dependent upon CD177 expression. *Clin Exp Immunol,* 161**,** 89-97.

ABDULAHAD, W. H., STEGEMAN, C. A., LIMBURG, P. C. & KALLENBERG, C. G. 2008. Skewed distribution of Th17 lymphocytes in patients with Wegener's granulomatosis in remission. *Arthritis Rheum,* 58**,** 2196-205.

ABDULAHAD, W. H., STEGEMAN, C. A., VAN DER GELD, Y. M., DOORNBOS-VAN DER MEER, B., LIMBURG, P. C. & KALLENBERG, C. G. 2007. Functional defect of circulating regulatory CD4+ T cells in patients with Wegener's granulomatosis in remission. *Arthritis Rheum,* 56**,** 2080-91.

AITMAN, T. J., DONG, R., VYSE, T. J., NORSWORTHY, P. J., JOHNSON, M. D., SMITH, J., MANGION, J., ROBERTON-LOWE, C., MARSHALL, A. J., PETRETTO, E., HODGES, M. D., BHANGAL, G., PATEL, S. G., SHEEHAN-ROONEY, K., DUDA, M., COOK, P. R., EVANS, D. J., DOMIN, J., FLINT, J., BOYLE, J. J., PUSEY, C. D. & COOK, H. T. 2006. Copy number polymorphism in Fcgr3 predisposes to glomerulonephritis in rats and humans. *Nature,* 439**,** 851-5.

AMULIC, B., CAZALET, C., HAYES, G. L., METZLER, K. D. & ZYCHLINSKY, A. 2012. Neutrophil function: from mechanisms to disease. *Annu Rev Immunol,* 30**,** 459-89.

ANDERSON, M. S. & BLUESTONE, J. A. 2005. The NOD mouse: a model of immune dysregulation. *Annu Rev Immunol,* 23**,** 447-85.

ATKINSON, M. A. & LEITER, E. H. 1999. The NOD mouse model of type 1 diabetes: as good as it gets? *Nat Med,* 5**,** 601-4.

AUFFRAY, C., FOGG, D., GARFA, M., ELAIN, G., JOIN-LAMBERT, O., KAYAL, S., SARNACKI, S., CUMANO, A., LAUVAU, G. & GEISSMANN, F. 2007. Monitoring of blood vessels and tissues by a population of monocytes with patrolling behavior. *Science,* 317**,** 666-70.

BAE, S., KIM, H., LEE, N., WON, C., KIM, H. R., HWANG, Y. I., SONG, Y. W., KANG, J. S. & LEE, W. J. 2012. alpha-Enolase expressed on the surfaces of monocytes and macrophages induces robust synovial inflammation in rheumatoid arthritis. *J Immunol,* 189**,** 365-72.

BANK, U., KUPPER, B., REINHOLD, D., HOFFMANN, T. & ANSORGE, S. 1999. Evidence for a crucial role of neutrophil-derived serine proteases in the inactivation of interleukin-6 at sites of inflammation. *FEBS Lett,* 461**,** 235-40.

BAUER, S., ABDGAWAD, M., GUNNARSSON, L., SEGELMARK, M., TAPPER, H. & HELLMARK, T. 2007. Proteinase 3 and CD177 are expressed on the plasma membrane of the same subset of neutrophils. *J Leukoc Biol,* 81**,** 458-64.

BAXTER, A. G. & COOKE, A. 1993. Complement lytic activity has no role in the pathogenesis of autoimmune diabetes in NOD mice. *Diabetes,* 42**,** 1574-8.

BELGE, K. U., DAYYANI, F., HORELT, A., SIEDLAR, M., FRANKENBERGER, M., FRANKENBERGER, B., ESPEVIK, T. & ZIEGLER-HEITBROCK, L. 2002. The proinflammatory CD14+CD16+DR++ monocytes are a major source of TNF. *J Immunol,* 168**,** 3536-42.

BELIAKOVA-BETHELL, N., MASSANELLA, M., WHITE, C., LADA, S., DU, P., VAIDA, F., BLANCO, J., SPINA, C. A. & WOELK, C. H. 2014. The effect of cell subset isolation method on gene expression in leukocytes. *Cytometry A,* 85**,** 94-104.

BELTRAN, B., MATHUR, A., DUCHEN, M. R., ERUSALIMSKY, J. D. & MONCADA, S. 2000. The effect of nitric oxide on cell respiration: A key to understanding its role in cell survival or death. *Proc Natl Acad Sci U S A,* 97**,** 14602-7.

BERTI, A., CAVALLI, G., CAMPOCHIARO, C., GUGLIELMI, B., BALDISSERA, E., CAPPIO, S., SABBADINI, M. G., DOGLIONI, C. & DAGNA, L. 2015. Interleukin-6 in ANCA-associated vasculitis: Rationale for successful treatment with tocilizumab. *Semin Arthritis Rheum,* 45**,** 48-54.

BETTENCOURT, I. A. & POWELL, J. D. 2017. Targeting Metabolism as a Novel Therapeutic Approach to Autoimmunity, Inflammation, and Transplantation. *J Immunol,* 198**,** 999-1005.

BEURA, L. K., HAMILTON, S. E., BI, K., SCHENKEL, J. M., ODUMADE, O. A., CASEY, K. A., THOMPSON, E. A., FRASER, K. A., ROSATO, P. C., FILALI-MOUHIM, A., SEKALY, R. P., JENKINS, M. K., VEZYS, V., HAINING, W. N., JAMESON, S. C. & MASOPUST, D. 2016. Normalizing the environment recapitulates adult human immune traits in laboratory mice. *Nature,* 532**,** 512-6.

BILLERBECK, E., BARRY, W. T., MU, K., DORNER, M., RICE, C. M. & PLOSS, A. 2011. Development of human CD4+FoxP3+ regulatory T cells in human stem cell factor-, granulocyte-macrophage colony-stimulating factor-, and interleukin-3-expressing NOD-SCID IL2Rgamma(null) humanized mice. *Blood,* 117**,** 3076-86.

BOOTH, A. D., ALMOND, M. K., BURNS, A., ELLIS, P., GASKIN, G., NEILD, G. H., PLAISANCE, M., PUSEY, C. D., JAYNE, D. R. & PAN-THAMES RENAL RESEARCH, G. 2003. Outcome of ANCA-associated renal vasculitis: a 5-year retrospective study. *Am J Kidney Dis,* 41**,** 776-84.

BORAO-CENGOTITA-BENGOA, M., CORRAL-GUDINO, L., DEL PINO-MONTES, J. & LERMA-MARQUEZ, J. L. 2010. Long-term follow-up of microscopic polyangiitis, 17-year experience at a single center. *Eur J Intern Med,* 21**,** 542-7.

BOYETTE, L. B., MACEDO, C., HADI, K., ELINOFF, B. D., WALTERS, J. T., RAMASWAMI, B., CHALASANI, G., TABOAS, J. M., LAKKIS, F. G. & METES, D. M. 2017. Phenotype, function, and differentiation potential of human monocyte subsets. *PLoS One,* 12**,** e0176460.

BRADLEY, J. R. 2008. TNF-mediated inflammatory disease. *J Pathol,* 214**,** 149-60.

BREHM, M. A., CUTHBERT, A., YANG, C., MILLER, D. M., DIIORIO, P., LANING, J., BURZENSKI, L., GOTT, B., FOREMAN, O., KAVIRAYANI, A., HERLIHY, M., ROSSINI, A. A., SHULTZ, L. D. & GREINER, D. L. 2010. Parameters for establishing humanized mouse models to study human immunity: analysis of human hematopoietic stem cell engraftment in three immunodeficient strains of mice bearing the IL2rgamma(null) mutation. *Clin Immunol,* 135**,** 84-98.

BREHM, M. A., RACKI, W. J., LEIF, J., BURZENSKI, L., HOSUR, V., WETMORE, A., GOTT, B., HERLIHY, M., IGNOTZ, R., DUNN, R., SHULTZ, L. D. & GREINER, D. L. 2012. Engraftment of human HSCs in nonirradiated newborn NOD-scid IL2rgamma null mice is enhanced by transgenic expression of membrane-bound human SCF. *Blood,* 119**,** 2778-88.

BROOKS, C. J., KING, W. J., RADFORD, D. J., ADU, D., MCGRATH, M. & SAVAGE, C. O. 1996. IL-1 beta production by human polymorphonuclear leucocytes stimulated by anti-neutrophil cytoplasmic autoantibodies: relevance to systemic vasculitis. *Clin Exp Immunol,* 106**,** 273-9.

BROUDY, V. C. 1997. Stem cell factor and hematopoiesis. *Blood,* 90**,** 1345-64.

BROUWER, E., HUITEMA, M. G., MULDER, A. H., HEERINGA, P., VAN GOOR, H., TERVAERT, J. W., WEENING, J. J. & KALLENBERG, C. G. 1994. Neutrophil activation in vitro and in vivo in Wegener's granulomatosis. *Kidney Int,* 45**,** 1120-31.

BRUNET DE LA GRANGE, P., IVANOVIC, Z., LEPRIVEY-LORGEOT, V. & PRALORAN, V. 2002. Angiotensin II that reduces the colony-forming ability of

hematopoietic progenitors in serum free medium has an inverse effect in serum-supplemented medium. *Stem Cells,* 20**,** 269-71.
BRUNINI, F., PAGE, T. H., GALLIENI, M. & PUSEY, C. D. 2016. The role of monocytes in ANCA-associated vasculitides. *Autoimmun Rev,* 15**,** 1046-1053.
BUCK, M. D., O'SULLIVAN, D. & PEARCE, E. L. 2015. T cell metabolism drives immunity. *J Exp Med,* 212**,** 1345-60.
BURKE, B., AHMAD, R., STAPLES, K. J., SNOWDEN, R., KADIOGLU, A., FRANKENBERGER, M., HUME, D. A. & ZIEGLER-HEITBROCK, L. 2008. Increased TNF expression in CD43++ murine blood monocytes. *Immunol Lett,* 118**,** 142-7.
CAMPANELLI, D., DETMERS, P. A., NATHAN, C. F. & GABAY, J. E. 1990. Azurocidin and a homologous serine protease from neutrophils. Differential antimicrobial and proteolytic properties. *J Clin Invest,* 85**,** 904-15.
CAO, X., SHORES, E. W., HU-LI, J., ANVER, M. R., KELSALL, B. L., RUSSELL, S. M., DRAGO, J., NOGUCHI, M., GRINBERG, A., BLOOM, E. T. & ET AL. 1995. Defective lymphoid development in mice lacking expression of the common cytokine receptor gamma chain. *Immunity,* 2**,** 223-38.
CARTIN-CEBA, R., PEIKERT, T. & SPECKS, U. 2010. Pathogenesis of ANCA-Associated Vasculitis. *Rheumatic diseases clinics of North America,* 36**,** 463-477.
CHARLES, L. A., FALK, R. J. & JENNETTE, J. C. 1992. Reactivity of antineutrophil cytoplasmic autoantibodies with mononuclear phagocytes. *J Leukoc Biol,* 51**,** 65-8.
CHEN, J., LIAO, M. Y., GAO, X. L., ZHONG, Q., TANG, T. T., YU, X., LIAO, Y. H. & CHENG, X. 2013. IL-17A induces pro-inflammatory cytokines production in macrophages via MAPKinases, NF-kappaB and AP-1. *Cell Physiol Biochem,* 32**,** 1265-74.
CHEN, M., XING, G. Q., YU, F., LIU, G. & ZHAO, M. H. 2009. Complement deposition in renal histopathology of patients with ANCA-associated pauci-immune glomerulonephritis. *Nephrol Dial Transplant,* 24**,** 1247-52.
CHEON, D. J. & ORSULIC, S. 2011. Mouse models of cancer. *Annu Rev Pathol,* 6**,** 95-119.
CHERUKURI, A., DYKSTRA, M. & PIERCE, S. K. 2001. Floating the raft hypothesis: lipid rafts play a role in immune cell activation. *Immunity,* 14**,** 657-60.
CHOUDHARY, S. K., REZK, N. L., INCE, W. L., CHEEMA, M., ZHANG, L., SU, L., SWANSTROM, R., KASHUBA, A. D. & MARGOLIS, D. M. 2009. Suppression of human immunodeficiency virus type 1 (HIV-1) viremia with reverse transcriptase and integrase inhibitors, CD4+ T-cell recovery, and viral rebound upon interruption of therapy in a new model for HIV treatment in the humanized Rag2-/-{gamma}c-/- mouse. *J Virol,* 83**,** 8254-8.
CHURG, J. & STRAUSS, L. 1951. Allergic granulomatosis, allergic angiitis, and periarteritis nodosa. *Am J Pathol,* 27**,** 277-301.
CIOFANI, M. & ZUNIGA-PFLUCKER, J. C. 2005. Notch promotes survival of pre-T cells at the beta-selection checkpoint by regulating cellular metabolism. *Nat Immunol,* 6**,** 881-8.
CLARKE, B. E., HAM, K. N., TANGE, J. D. & RYAN, G. B. 1983. Macrophages and glomerular crescent formation. Studies with rat nephrotoxic nephritis. *Pathology,* 15**,** 75-81.
CONSTANTINESCU, C. S., FAROOQI, N., O'BRIEN, K. & GRAN, B. 2011. Experimental autoimmune encephalomyelitis (EAE) as a model for multiple sclerosis (MS). *British Journal of Pharmacology,* 164**,** 1079-1106.

COUGHLAN, A. M., FREELEY, S. J. & ROBSON, M. G. 2012a. Animal models of anti-neutrophil cytoplasmic antibody-associated vasculitis. *Clin Exp Immunol,* 169**,** 229-37.

COUGHLAN, A. M., FREELEY, S. J. & ROBSON, M. G. 2012b. Humanised mice have functional human neutrophils. *J Immunol Methods,* 385**,** 96-104.

CRAIG, A., MAI, J., CAI, S. & JEYASEELAN, S. 2009. Neutrophil recruitment to the lungs during bacterial pneumonia. *Infect Immun,* 77**,** 568-75.

CROS, J., CAGNARD, N., WOOLLARD, K., PATEY, N., ZHANG, S. Y., SENECHAL, B., PUEL, A., BISWAS, S. K., MOSHOUS, D., PICARD, C., JAIS, J. P., D'CRUZ, D., CASANOVA, J. L., TROUILLET, C. & GEISSMANN, F. 2010. Human CD14dim monocytes patrol and sense nucleic acids and viruses via TLR7 and TLR8 receptors. *Immunity,* 33**,** 375-86.

CSERNOK, E., ERNST, M., SCHMITT, W., BAINTON, D. F. & GROSS, W. L. 1994. Activated neutrophils express proteinase 3 on their plasma membrane in vitro and in vivo. *Clin Exp Immunol,* 95**,** 244-50.

CSERNOK, E. & GROSS, W. L. 2013. Current understanding of the pathogenesis of granulomatosis with polyangiitis (Wegener's). *Expert Rev Clin Immunol,* 9**,** 641-8.

CSERNOK, E., SZYMKOWIAK, C. H., MISTRY, N., DAHA, M. R., GROSS, W. L. & KEKOW, J. 1996. Transforming growth factor-beta (TGF-beta) expression and interaction with proteinase 3 (PR3) in anti-neutrophil cytoplasmic antibody (ANCA)-associated vasculitis. *Clin Exp Immunol,* 105**,** 104-11.

CSERNOK, E., TRABANDT, A., MULLER, A., WANG, G. C., MOOSIG, F., PAULSEN, J., SCHNABEL, A. & GROSS, W. L. 1999. Cytokine profiles in Wegener's granulomatosis: predominance of type 1 (Th1) in the granulomatous inflammation. *Arthritis Rheum,* 42**,** 742-50.

DAVID, A., FRIDLICH, R. & AVIRAM, I. 2005. The presence of membrane Proteinase 3 in neutrophil lipid rafts and its colocalization with FcgammaRIIIb and cytochrome b558. *Exp Cell Res,* 308**,** 156-65.

DAVID, A., KACHER, Y., SPECKS, U. & AVIRAM, I. 2003. Interaction of proteinase 3 with CD11b/CD18 (beta2 integrin) on the cell membrane of human neutrophils. *J Leukoc Biol,* 74**,** 551-7.

DAVIES, D. J., MORAN, J. E., NIALL, J. F. & RYAN, G. B. 1982. Segmental necrotising glomerulonephritis with antineutrophil antibody: possible arbovirus aetiology? *Br Med J (Clin Res Ed),* 285**,** 606.

DE MENTHON, M., LAMBERT, M., GUIARD, E., TOGNARELLI, S., BIENVENU, B., KARRAS, A., GUILLEVIN, L. & CAILLAT-ZUCMAN, S. 2011. Excessive interleukin-15 transpresentation endows NKG2D+CD4+ T cells with innate-like capacity to lyse vascular endothelium in granulomatosis with polyangiitis (Wegener's). *Arthritis Rheum,* 63**,** 2116-26.

DESHMANE, S. L., KREMLEV, S., AMINI, S. & SAWAYA, B. E. 2009. Monocyte chemoattractant protein-1 (MCP-1): an overview. *J Interferon Cytokine Res,* 29**,** 313-26.

DEVADAS, S., ZARITSKAYA, L., RHEE, S. G., OBERLEY, L. & WILLIAMS, M. S. 2002. Discrete generation of superoxide and hydrogen peroxide by T cell receptor stimulation: selective regulation of mitogen-activated protein kinase activation and fas ligand expression. *J Exp Med,* 195**,** 59-70.

DIETL, K., RENNER, K., DETTMER, K., TIMISCHL, B., EBERHART, K., DORN, C., HELLERBRAND, C., KASTENBERGER, M., KUNZ-SCHUGHART, L. A., OEFNER, P. J., ANDREESEN, R., GOTTFRIED, E. & KREUTZ, M. P. 2010. Lactic acid and acidification inhibit TNF secretion and glycolysis of human monocytes. *J Immunol,* 184**,** 1200-9.

DINARELLO, C. A. 2009. Immunological and inflammatory functions of the interleukin-1 family. *Annu Rev Immunol,* 27**,** 519-50.

DINARELLO, C. A. 2011. Interleukin-1 in the pathogenesis and treatment of inflammatory diseases. *Blood,* 117**,** 3720-32.

DINARELLO, C. A., DONATH, M. Y. & MANDRUP-POULSEN, T. 2010. Role of IL-1beta in type 2 diabetes. *Curr Opin Endocrinol Diabetes Obes,* 17**,** 314-21.

DISTLER, J. H., JUNGEL, A., CARETTO, D., SCHULZE-HORSEL, U., KOWAL-BIELECKA, O., GAY, R. E., MICHEL, B. A., MULLER-LADNER, U., KALDEN, J. R., GAY, S. & DISTLER, O. 2006. Monocyte chemoattractant protein 1 released from glycosaminoglycans mediates its profibrotic effects in systemic sclerosis via the release of interleukin-4 from T cells. *Arthritis Rheum,* 54**,** 214-25.

DIXIT, N. & SIMON, S. I. 2012. Chemokines, selectins and intracellular calcium flux: temporal and spatial cues for leukocyte arrest. *Front Immunol,* 3**,** 188.

DRESCHER, B. & BAI, F. 2013. Neutrophil in viral infections, friend or foe? *Virus Res,* 171**,** 1-7.

EHRENGRUBER, M. U., GEISER, T. & DERANLEAU, D. A. 1994. Activation of human neutrophils by C3a and C5A. Comparison of the effects on shape changes, chemotaxis, secretion, and respiratory burst. *FEBS Lett,* 346**,** 181-4.

EVANS, H. G., GULLICK, N. J., KELLY, S., PITZALIS, C., LORD, G. M., KIRKHAM, B. W. & TAAMS, L. S. 2009. In vivo activated monocytes from the site of inflammation in humans specifically promote Th17 responses. *Proc Natl Acad Sci U S A,* 106**,** 6232-7.

EVANS, W. H. & KARNOVSKY, M. L. 1962. The biochemical basis of phagocytosis. IV. Some aspects of carbohydrate metabolism during phagocytosis. *Biochemistry,* 1**,** 159-66.

EVERTS, B., AMIEL, E., VAN DER WINDT, G. J., FREITAS, T. C., CHOTT, R., YARASHESKI, K. E., PEARCE, E. L. & PEARCE, E. J. 2012. Commitment to glycolysis sustains survival of NO-producing inflammatory dendritic cells. *Blood,* 120**,** 1422-31.

FALK, R. J. & JENNETTE, J. C. 1988. Anti-neutrophil cytoplasmic autoantibodies with specificity for myeloperoxidase in patients with systemic vasculitis and idiopathic necrotizing and crescentic glomerulonephritis. *N Engl J Med,* 318**,** 1651-7.

FALK, R. J., TERRELL, R. S., CHARLES, L. A. & JENNETTE, J. C. 1990. Anti-neutrophil cytoplasmic autoantibodies induce neutrophils to degranulate and produce oxygen radicals in vitro. *Proc Natl Acad Sci U S A,* 87**,** 4115-9.

FEI, F., LEE, K. M., MCCARRY, B. E. & BOWDISH, D. M. 2016. Age-associated metabolic dysregulation in bone marrow-derived macrophages stimulated with lipopolysaccharide. *Sci Rep,* 6**,** 22637.

FIELDING, C. A., MCLOUGHLIN, R. M., MCLEOD, L., COLMONT, C. S., NAJDOVSKA, M., GRAIL, D., ERNST, M., JONES, S. A., TOPLEY, N. & JENKINS, B. J. 2008. IL-6 regulates neutrophil trafficking during acute inflammation via STAT3. *J Immunol,* 181**,** 2189-95.

FLANAGAN, F. L., DEHDASHTI, F., SIEGEL, B. A., TRASK, D. D., SUNDARESAN, S. R., PATTERSON, G. A. & COOPER, J. D. 1997. Staging of esophageal cancer with 18F-fluorodeoxyglucose positron emission tomography. *AJR Am J Roentgenol,* 168**,** 417-24.

FLETCHER, J. M., LONERGAN, R., COSTELLOE, L., KINSELLA, K., MORAN, B., O'FARRELLY, C., TUBRIDY, N. & MILLS, K. H. 2009. CD39+Foxp3+ regulatory T Cells suppress pathogenic Th17 cells and are impaired in multiple sclerosis. *J Immunol,* 183**,** 7602-10.

FRANSSEN, C., GANS, R., KALLENBERG, C., HAGELUKEN, C. & HOORNTJE, S. 1998. Disease spectrum of patients with antineutrophil cytoplasmic autoantibodies of defined specificity: distinct differences between patients with anti-proteinase 3 and anti-myeloperoxidase autoantibodies. *J Intern Med,* 244**,** 209-16.

FREE, M. E., BUNCH, D. O., MCGREGOR, J. A., JONES, B. E., BERG, E. A., HOGAN, S. L., HU, Y., PRESTON, G. A., JENNETTE, J. C., FALK, R. J. & SU, M. A. 2013. Patients with antineutrophil cytoplasmic antibody-associated vasculitis have defective Treg cell function exacerbated by the presence of a suppression-resistant effector cell population. *Arthritis Rheum,* 65**,** 1922-33.

FREEMERMAN, A. J., JOHNSON, A. R., SACKS, G. N., MILNER, J. J., KIRK, E. L., TROESTER, M. A., MACINTYRE, A. N., GORAKSHA-HICKS, P., RATHMELL, J. C. & MAKOWSKI, L. 2014. Metabolic reprogramming of macrophages: glucose transporter 1 (GLUT1)-mediated glucose metabolism drives a proinflammatory phenotype. *J Biol Chem,* 289**,** 7884-96.

FRIDLENDER, Z. G. & ALBELDA, S. M. 2012. Tumor-associated neutrophils: friend or foe? *Carcinogenesis,* 33**,** 949-55.

GABAY, J. E., SCOTT, R. W., CAMPANELLI, D., GRIFFITH, J., WILDE, C., MARRA, M. N., SEEGER, M. & NATHAN, C. F. 1989. Antibiotic proteins of human polymorphonuclear leukocytes. *Proc Natl Acad Sci U S A,* 86**,** 5610-4.

GALVAN-PENA, S. & O'NEILL, L. A. 2014. Metabolic reprograming in macrophage polarization. *Front Immunol,* 5**,** 420.

GAN, P. Y., STEINMETZ, O. M., TAN, D. S., O'SULLIVAN, K. M., OOI, J. D., IWAKURA, Y., KITCHING, A. R. & HOLDSWORTH, S. R. 2010. Th17 cells promote autoimmune anti-myeloperoxidase glomerulonephritis. *J Am Soc Nephrol,* 21**,** 925-31.

GANICK, D. J., SARNWICK, R. D., SHAHIDI, N. T. & MANNING, D. D. 1980. Inability of intravenously injected monocellular suspensions of human bone marrow to establish in the nude mouse. *Int Arch Allergy Appl Immunol,* 62**,** 330-3.

GEISSMANN, F., JUNG, S. & LITTMAN, D. R. 2003. Blood monocytes consist of two principal subsets with distinct migratory properties. *Immunity,* 19**,** 71-82.

GELINAS, L., FALKENHAM, A., OXNER, A., SOPEL, M. & LEGARE, J. F. 2011. Highly purified human peripheral blood monocytes produce IL-6 but not TNFalpha in response to angiotensin II. *J Renin Angiotensin Aldosterone Syst,* 12**,** 295-303.

GESSLER, P., NEU, S., NEBE, T. & SPEER, C. P. 1999. Granulocyte colony-stimulating factor receptor expression on neutrophils of term and preterm neonates with and without signs of infection. *Eur J Pediatr,* 158**,** 497-500.

GLEESON, L. E., SHEEDY, F. J., PALSSON-MCDERMOTT, E. M., TRIGLIA, D., O'LEARY, S. M., O'SULLIVAN, M. P., O'NEILL, L. A. & KEANE, J. 2016. Cutting Edge: Mycobacterium tuberculosis Induces Aerobic Glycolysis in Human Alveolar Macrophages That Is Required for Control of Intracellular Bacillary Replication. *J Immunol,* 196**,** 2444-9.

GODMAN, G. C. & CHURG, J. 1954. Wegener's granulomatosis: pathology and review of the literature. *AMA Arch Pathol,* 58**,** 533-53.

GOLDSCHMEDING, R., TERVAERT, J. W., GANS, R. O., DOLMAN, K. M., VAN DEN ENDE, M. E., KUIZINGA, M. C., KALLENBERG, C. G. & VON DEM BORNE, A. E. 1990. Different immunological specificities and disease associations of c-ANCA and p-ANCA. *Neth J Med,* 36**,** 114-6.

HAGEN, E. C., DAHA, M. R., HERMANS, J., ANDRASSY, K., CSERNOK, E., GASKIN, G., LESAVRE, P., LUDEMANN, J., RASMUSSEN, N., SINICO, R. A., WIIK, A. & VAN DER WOUDE, F. J. 1998. Diagnostic value of standardized assays for anti-neutrophil cytoplasmic antibodies in idiopathic systemic

vasculitis. EC/BCR Project for ANCA Assay Standardization. *Kidney Int,* 53**,** 743-53.
HAJJAR, E., MIHAJLOVIC, M., WITKO-SARSAT, V., LAZARIDIS, T. & REUTER, N. 2008. Computational prediction of the binding site of proteinase 3 to the plasma membrane. *Proteins,* 71**,** 1655-69.
HALBWACHS-MECARELLI, L., BESSOU, G., LESAVRE, P., LOPEZ, S. & WITKO-SARSAT, V. 1995. Bimodal distribution of proteinase 3 (PR3) surface expression reflects a constitutive heterogeneity in the polymorphonuclear neutrophil pool. *FEBS Lett,* 374**,** 29-33.
HARA, T. & MIYAJIMA, A. 1992. Two distinct functional high affinity receptors for mouse interleukin-3 (IL-3). *EMBO J,* 11**,** 1875-84.
HARA, T. & MIYAJIMA, A. 1996. Function and signal transduction mediated by the interleukin 3 receptor system in hematopoiesis. *Stem Cells,* 14**,** 605-18.
HARADA, A., SEKIDO, N., AKAHOSHI, T., WADA, T., MUKAIDA, N. & MATSUSHIMA, K. 1994. Essential involvement of interleukin-8 (IL-8) in acute inflammation. *J Leukoc Biol,* 56**,** 559-64.
HARPER, L., COCKWELL, P., ADU, D. & SAVAGE, C. O. 2001a. Neutrophil priming and apoptosis in anti-neutrophil cytoplasmic autoantibody-associated vasculitis. *Kidney Int,* 59**,** 1729-38.
HARPER, L., RADFORD, D., PLANT, T., DRAYSON, M., ADU, D. & SAVAGE, C. O. 2001b. IgG from myeloperoxidase-antineutrophil cytoplasmic antibody-positive patients stimulates greater activation of primed neutrophils than IgG from proteinase 3-antineutrophil cytosplasmic antibody-positive patients. *Arthritis Rheum,* 44**,** 921-30.
HASCHEMI, A., KOSMA, P., GILLE, L., EVANS, C. R., BURANT, C. F., STARKL, P., KNAPP, B., HAAS, R., SCHMID, J. A., JANDL, C., AMIR, S., LUBEC, G., PARK, J., ESTERBAUER, H., BILBAN, M., BRIZUELA, L., POSPISILIK, J. A., OTTERBEIN, L. E. & WAGNER, O. 2012. The sedoheptulose kinase CARKL directs macrophage polarization through control of glucose metabolism. *Cell Metab,* 15**,** 813-26.
HATTAR, K., BICKENBACH, A., CSERNOK, E., ROSSEAU, S., GRANDEL, U., SEEGER, W., GRIMMINGER, F. & SIBELIUS, U. 2002. Wegener's granulomatosis: antiproteinase 3 antibodies induce monocyte cytokine and prostanoid release-role of autocrine cell activation. *J Leukoc Biol,* 71**,** 996-1004.
HERON, M., GRUTTERS, J. C., VAN VELZEN-BLAD, H., VELTKAMP, M., CLAESSEN, A. M. & VAN DEN BOSCH, J. M. 2008. Increased expression of CD16, CD69, and very late antigen-1 on blood monocytes in active sarcoidosis. *Chest,* 134**,** 1001-8.
HESS, C., SADALLAH, S. & SCHIFFERLI, J. A. 2000. Induction of neutrophil responsiveness to myeloperoxidase antibodies by their exposure to supernatant of degranulated autologous neutrophils. *Blood,* 96**,** 2822-7.
HEWINS, P. & SAVAGE, C. 2003. Anti-neutrophil cytoplasm antibody associated vasculitis. *The International Journal of Biochemistry & Cell Biology,* 35**,** 277-282.
HILHORST, M., VAN PAASSEN, P., TERVAERT, J. W. & LIMBURG RENAL, R. 2015. Proteinase 3-ANCA Vasculitis versus Myeloperoxidase-ANCA Vasculitis. *J Am Soc Nephrol,* 26**,** 2314-27.
HOFFMAN, G. S., KERR, G. S., LEAVITT, R. Y., HALLAHAN, C. W., LEBOVICS, R. S., TRAVIS, W. D., ROTTEM, M. & FAUCI, A. S. 1992. Wegener granulomatosis: an analysis of 158 patients. *Ann Intern Med,* 116**,** 488-98.

HOLLENBAUGH, J. A., MUNGER, J. & KIM, B. 2011. Metabolite profiles of human immunodeficiency virus infected CD4+ T cells and macrophages using LC-MS/MS analysis. *Virology,* 415**,** 153-9.

HORDYJEWSKA, A., POPIOLEK, L. & HORECKA, A. 2015. Characteristics of hematopoietic stem cells of umbilical cord blood. *Cytotechnology,* 67**,** 387-96.

HUNTER, C. A. & JONES, S. A. 2015. IL-6 as a keystone cytokine in health and disease. *Nat Immunol,* 16**,** 448-57.

HUUGEN, D., XIAO, H., VAN ESCH, A., FALK, R. J., PEUTZ-KOOTSTRA, C. J., BUURMAN, W. A., TERVAERT, J. W., JENNETTE, J. C. & HEERINGA, P. 2005. Aggravation of anti-myeloperoxidase antibody-induced glomerulonephritis by bacterial lipopolysaccharide: role of tumor necrosis factor-alpha. *Am J Pathol,* 167**,** 47-58.

HUYNH, A., DUPAGE, M., PRIYADHARSHINI, B., SAGE, P. T., QUIROS, J., BORGES, C. M., TOWNAMCHAI, N., GERRIETS, V. A., RATHMELL, J. C., SHARPE, A. H., BLUESTONE, J. A. & TURKA, L. A. 2015. Control of PI(3) kinase in Treg cells maintains homeostasis and lineage stability. *Nat Immunol,* 16**,** 188-96.

INGERSOLL, M. A., SPANBROEK, R., LOTTAZ, C., GAUTIER, E. L., FRANKENBERGER, M., HOFFMANN, R., LANG, R., HANIFFA, M., COLLIN, M., TACKE, F., HABENICHT, A. J., ZIEGLER-HEITBROCK, L. & RANDOLPH, G. J. 2010. Comparison of gene expression profiles between human and mouse monocyte subsets. *Blood,* 115**,** e10-9.

ISHIDA-OKAWARA, A., ITO-IHARA, T., MUSO, E., ONO, T., SAIGA, K., NEMOTO, K. & SUZUKI, K. 2004. Neutrophil contribution to the crescentic glomerulonephritis in SCG/Kj mice. *Nephrol Dial Transplant,* 19**,** 1708-15.

ITO, R., TAKAHASHI, T., KATANO, I. & ITO, M. 2012. Current advances in humanized mouse models. *Cellular and Molecular Immunology,* 9**,** 208-214.

JACOBS, L., NAWROT, T. S., DE GEUS, B., MEEUSEN, R., DEGRAEUWE, B., BERNARD, A., SUGHIS, M., NEMERY, B. & PANIS, L. I. 2010. Subclinical responses in healthy cyclists briefly exposed to traffic-related air pollution: an intervention study. *Environ Health,* 9**,** 64.

JANAS, M. L., VARANO, G., GUDMUNDSSON, K., NODA, M., NAGASAWA, T. & TURNER, M. 2010. Thymic development beyond beta-selection requires phosphatidylinositol 3-kinase activation by CXCR4. *J Exp Med,* 207**,** 247-61.

JARROT, P. A. & KAPLANSKI, G. 2014. Anti-TNF-alpha therapy and systemic vasculitis. *Mediators Inflamm,* 2014**,** 493593.

JAYNE, D. R., BRUCHFELD, A. N., HARPER, L., SCHAIER, M., VENNING, M. C., HAMILTON, P., BURST, V., GRUNDMANN, F., JADOUL, M., SZOMBATI, I., TESAR, V., SEGELMARK, M., POTARCA, A., SCHALL, T. J., BEKKER, P. & GROUP, C. S. 2017. Randomized Trial of C5a Receptor Inhibitor Avacopan in ANCA-Associated Vasculitis. *J Am Soc Nephrol*.

JENNETTE, J. C. & FALK, R. J. 2015. ANCAs are also antimonocyte cytoplasmic autoantibodies. *Clin J Am Soc Nephrol,* 10**,** 4-6.

JENNETTE, J. C., FALK, R. J., BACON, P. A., BASU, N., CID, M. C., FERRARIO, F., FLORES-SUAREZ, L. F., GROSS, W. L., GUILLEVIN, L., HAGEN, E. C., HOFFMAN, G. S., JAYNE, D. R., KALLENBERG, C. G., LAMPRECHT, P., LANGFORD, C. A., LUQMANI, R. A., MAHR, A. D., MATTESON, E. L., MERKEL, P. A., OZEN, S., PUSEY, C. D., RASMUSSEN, N., REES, A. J., SCOTT, D. G., SPECKS, U., STONE, J. H., TAKAHASHI, K. & WATTS, R. A. 2013. 2012 revised International Chapel Hill Consensus Conference Nomenclature of Vasculitides. *Arthritis Rheum,* 65**,** 1-11.

JENNETTE, J. C., FALK, R. J. & GASIM, A. H. 2011. Pathogenesis of ANCA Vasculitis. *Current opinion in nephrology and hypertension,* 20**,** 263-270.

JERKE, U., ROLLE, S., DITTMAR, G., BAYAT, B., SANTOSO, S., SPORBERT, A., LUFT, F. & KETTRITZ, R. 2011. Complement receptor Mac-1 is an adaptor for NB1 (CD177)-mediated PR3-ANCA neutrophil activation. *J Biol Chem,* 286**,** 7070-81.

JHA, A. K., HUANG, S. C., SERGUSHICHEV, A., LAMPROPOULOU, V., IVANOVA, Y., LOGINICHEVA, E., CHMIELEWSKI, K., STEWART, K. M., ASHALL, J., EVERTS, B., PEARCE, E. J., DRIGGERS, E. M. & ARTYOMOV, M. N. 2015. Network integration of parallel metabolic and transcriptional data reveals metabolic modules that regulate macrophage polarization. *Immunity,* 42**,** 419-30.

JIA, T., SERBINA, N. V., BRANDL, K., ZHONG, M. X., LEINER, I. M., CHARO, I. F. & PAMER, E. G. 2008. Additive roles for MCP-1 and MCP-3 in CCR2-mediated recruitment of inflammatory monocytes during Listeria monocytogenes infection. *J Immunol,* 180**,** 6846-53.

JILKA, R. L. 2016. The Road to Reproducibility in Animal Research. *J Bone Miner Res,* 31**,** 1317-9.

JOHNSON, V. J., YUCESOY, B. & LUSTER, M. I. 2005. Prevention of IL-1 signaling attenuates airway hyperresponsiveness and inflammation in a murine model of toluene diisocyanate-induced asthma. *J Allergy Clin Immunol,* 116**,** 851-8.

JONES, R. B. 2014. Rituximab in the treatment of anti-neutrophil cytoplasm antibody-associated vasculitis. *Nephron Clin Pract,* 128**,** 243-9.

KAIN, R., EXNER, M., BRANDES, R., ZIEBERMAYR, R., CUNNINGHAM, D., ALDERSON, C. A., DAVIDOVITS, A., RAAB, I., JAHN, R., ASHOUR, O., SPITZAUER, S., SUNDER-PLASSMANN, G., FUKUDA, M., KLEMM, P., REES, A. J. & KERJASCHKI, D. 2008. Molecular mimicry in pauci-immune focal necrotizing glomerulonephritis. *Nat Med,* 14**,** 1088-96.

KAIN, R., MATSUI, K., EXNER, M., BINDER, S., SCHAFFNER, G., SOMMER, E. M. & KERJASCHKI, D. 1995. A novel class of autoantigens of anti-neutrophil cytoplasmic antibodies in necrotizing and crescentic glomerulonephritis: the lysosomal membrane glycoprotein h-lamp-2 in neutrophil granulocytes and a related membrane protein in glomerular endothelial cells. *J Exp Med,* 181**,** 585-97.

KALLENBERG, C. G. & HEERINGA, P. 2013. Complement is crucial in the pathogenesis of ANCA-associated vasculitis. *Kidney Int,* 83**,** 16-8.

KAMINSKI, P., MALAKOWSKA, I., GAWRYCHOWSKI, K., SKOPINSKA-ROZEWSKA, E. & MARIANOWSKI, L. 1996. [Evaluation of selected parameters of lymphocyte activity in umbilical cord blood. III. Expression of receptors for SRCB susceptible and insusceptible to theophylline]. *Ginekol Pol,* 67**,** 60-4.

KAO, R. C., WEHNER, N. G., SKUBITZ, K. M., GRAY, B. H. & HOIDAL, J. R. 1988. Proteinase 3. A distinct human polymorphonuclear leukocyte proteinase that produces emphysema in hamsters. *J Clin Invest,* 82**,** 1963-73.

KAY, J. & CALABRESE, L. 2004. The role of interleukin-1 in the pathogenesis of rheumatoid arthritis. *Rheumatology (Oxford),* 43 Suppl 3**,** iii2-iii9.

KELLEY, J. L., ROZEK, M. M., SUENRAM, C. A. & SCHWARTZ, C. J. 1987. Activation of human blood monocytes by adherence to tissue culture plastic surfaces. *Exp Mol Pathol,* 46**,** 266-78.

KHOURY, P., GRAYSON, P. C. & KLION, A. D. 2014. Eosinophils in vasculitis: characteristics and roles in pathogenesis. *Nat Rev Rheumatol,* 10**,** 474-83.

KINKADE, J. M., JR., PEMBER, S. O., BARNES, K. C., SHAPIRA, R., SPITZNAGEL, J. K. & MARTIN, L. E. 1983. Differential distribution of distinct forms of myeloperoxidase in different azurophilic granule subpopulations from human neutrophils. *Biochem Biophys Res Commun,* 114**,** 296-303.

KLIMPEL, G. R. 1980. Soluble factor(s) from LPS-activated macrophages induce cytotoxic T cell differentiation from alloantigen-primed spleen cells. *J Immunol,* 125**,** 1243-9.

KLINGER, H. 1931. Grenzformen der periarteritis nodosa. *Z Pathol***,** 455-480.

KLINKE, A., NUSSBAUM, C., KUBALA, L., FRIEDRICHS, K., RUDOLPH, T. K., RUDOLPH, V., PAUST, H. J., SCHRODER, C., BENTEN, D., LAU, D., SZOCS, K., FURTMULLER, P. G., HEERINGA, P., SYDOW, K., DUCHSTEIN, H. J., EHMKE, H., SCHUMACHER, U., MEINERTZ, T., SPERANDIO, M. & BALDUS, S. 2011. Myeloperoxidase attracts neutrophils by physical forces. *Blood,* 117**,** 1350-8.

KOPF, H., DE LA ROSA, G. M., HOWARD, O. M. & CHEN, X. 2007. Rapamycin inhibits differentiation of Th17 cells and promotes generation of FoxP3+ T regulatory cells. *Int Immunopharmacol,* 7**,** 1819-24.

KRAMER, P. A., RAVI, S., CHACKO, B., JOHNSON, M. S. & DARLEY-USMAR, V. M. 2014. A review of the mitochondrial and glycolytic metabolism in human platelets and leukocytes: implications for their use as bioenergetic biomarkers. *Redox Biol,* 2**,** 206-10.

LAN, P., TONOMURA, N., SHIMIZU, A., WANG, S. & YANG, Y. G. 2006. Reconstitution of a functional human immune system in immunodeficient mice through combined human fetal thymus/liver and CD34+ cell transplantation. *Blood,* 108**,** 487-92.

LAU, D., MOLLNAU, H., EISERICH, J. P., FREEMAN, B. A., DAIBER, A., GEHLING, U. M., BRUMMER, J., RUDOLPH, V., MUNZEL, T., HEITZER, T., MEINERTZ, T. & BALDUS, S. 2005. Myeloperoxidase mediates neutrophil activation by association with CD11b/CD18 integrins. *Proc Natl Acad Sci U S A,* 102**,** 431-6.

LEE, B. H., GAUNA, A. E., PAULEY, K. M., PARK, Y. J. & CHA, S. 2012. Animal models in autoimmune diseases: lessons learned from mouse models for Sjogren's syndrome. *Clin Rev Allergy Immunol,* 42**,** 35-44.

LEPSE, N., ABDULAHAD, W. H., KALLENBERG, C. G. & HEERINGA, P. 2011. Immune regulatory mechanisms in ANCA-associated vasculitides. *Autoimmun Rev,* 11**,** 77-83.

LEPUS, C. M., GIBSON, T. F., GERBER, S. A., KAWIKOVA, I., SZCZEPANIK, M., HOSSAIN, J., ABLAMUNITS, V., KIRKILES-SMITH, N., HEROLD, K. C., DONIS, R. O., BOTHWELL, A. L., POBER, J. S. & HARDING, M. J. 2009. Comparison of human fetal liver, umbilical cord blood, and adult blood hematopoietic stem cell engraftment in NOD-scid/gammac-/-, Balb/c-Rag1-/-gammac-/-, and C.B-17-scid/bg immunodeficient mice. *Hum Immunol,* 70**,** 790-802.

LIANG, W. & FERRARA, N. 2016. The Complex Role of Neutrophils in Tumor Angiogenesis and Metastasis. *Cancer Immunol Res,* 4**,** 83-91.

LIASKOU, E., ZIMMERMANN, H. W., LI, K. K., OO, Y. H., SURESH, S., STAMATAKI, Z., QURESHI, O., LALOR, P. F., SHAW, J., SYN, W. K., CURBISHLEY, S. M. & ADAMS, D. H. 2013. Monocyte subsets in human liver disease show distinct phenotypic and functional characteristics. *Hepatology,* 57**,** 385-98.

LITTLE, M. A., AL-ANI, B., REN, S., AL-NUAIMI, H., LEITE, M., JR., ALPERS, C. E., SAVAGE, C. O. & DUFFIELD, J. S. 2012. Anti-proteinase 3 anti-neutrophil cytoplasm autoantibodies recapitulate systemic vasculitis in mice with a humanized immune system. *PLoS One,* 7**,** e28626.

LITTLE, M. A., SMYTH, C. L., YADAV, R., AMBROSE, L., COOK, H. T., NOURSHARGH, S. & PUSEY, C. D. 2005. Antineutrophil cytoplasm antibodies directed against myeloperoxidase augment leukocyte-microvascular interactions in vivo. *Blood,* 106**,** 2050-8.

LITTLE, M. A., SMYTH, L., SALAMA, A. D., MUKHERJEE, S., SMITH, J., HASKARD, D., NOURSHARGH, S., COOK, H. T. & PUSEY, C. D. 2009. Experimental autoimmune vasculitis: an animal model of anti-neutrophil cytoplasmic autoantibody-associated systemic vasculitis. *Am J Pathol,* 174**,** 1212-20.

LOPEZ-LAZARO, M. 2008. The warburg effect: why and how do cancer cells activate glycolysis in the presence of oxygen? *Anticancer Agents Med Chem,* 8**,** 305-12.

LOWE, D. M., REDFORD, P. S., WILKINSON, R. J., O'GARRA, A. & MARTINEAU, A. R. 2012. Neutrophils in tuberculosis: friend or foe? *Trends Immunol,* 33**,** 14-25.

LOWRY, P. A., SHULTZ, L. D., GREINER, D. L., HESSELTON, R. M., KITTLER, E. L., TIARKS, C. Y., RAO, S. S., REILLY, J., LEIF, J. H., RAMSHAW, H., STEWART, F. M. & QUESENBERRY, P. J. 1996. Improved engraftment of human cord blood stem cells in NOD/LtSz-scid/scid mice after irradiation or multiple-day injections into unirradiated recipients. *Biol Blood Marrow Transplant,* 2**,** 15-23.

LUBECK, M. D., STEPLEWSKI, Z., BAGLIA, F., KLEIN, M. H., DORRINGTON, K. J. & KOPROWSKI, H. 1985. The interaction of murine IgG subclass proteins with human monocyte Fc receptors. *J Immunol,* 135**,** 1299-304.

LUDEMANN, J., UTECHT, B. & GROSS, W. L. 1990. Anti-neutrophil cytoplasm antibodies in Wegener's granulomatosis recognize an elastinolytic enzyme. *J Exp Med,* 171**,** 357-62.

LUTZ, T. A. & WOODS, S. C. 2012. Overview of Animal Models of Obesity. *Current protocols in pharmacology / editorial board, S.J. Enna (editor-in-chief) ... [et al.],* CHAPTER**,** Unit5.61-Unit5.61.

LYONS, P. A., RAYNER, T. F., TRIVEDI, S., HOLLE, J. U., WATTS, R. A., JAYNE, D. R., BASLUND, B., BRENCHLEY, P., BRUCHFELD, A., CHAUDHRY, A. N., COHEN TERVAERT, J. W., DELOUKAS, P., FEIGHERY, C., GROSS, W. L., GUILLEVIN, L., GUNNARSSON, I., HARPER, L., HRUSKOVA, Z., LITTLE, M. A., MARTORANA, D., NEUMANN, T., OHLSSON, S., PADMANABHAN, S., PUSEY, C. D., SALAMA, A. D., SANDERS, J. S., SAVAGE, C. O., SEGELMARK, M., STEGEMAN, C. A., TESAR, V., VAGLIO, A., WIECZOREK, S., WILDE, B., ZWERINA, J., REES, A. J., CLAYTON, D. G. & SMITH, K. G. 2012. Genetically distinct subsets within ANCA-associated vasculitis. *N Engl J Med,* 367**,** 214-23.

MA, S. D., HEGDE, S., YOUNG, K. H., SULLIVAN, R., RAJESH, D., ZHOU, Y., JANKOWSKA-GAN, E., BURLINGHAM, W. J., SUN, X., GULLEY, M. L., TANG, W., GUMPERZ, J. E. & KENNEY, S. C. 2011. A new model of Epstein-Barr virus infection reveals an important role for early lytic viral protein expression in the development of lymphomas. *J Virol,* 85**,** 165-77.

MACIVER, N. J., MICHALEK, R. D. & RATHMELL, J. C. 2013. Metabolic regulation of T lymphocytes. *Annu Rev Immunol,* 31**,** 259-83.

MANZ, M. G. 2007. Human-hemato-lymphoid-system mice: opportunities and challenges. *Immunity,* 26**,** 537-41.

MARKIEWSKI, M. M. & LAMBRIS, J. D. 2007. The Role of Complement in Inflammatory Diseases From Behind the Scenes into the Spotlight. *The American Journal of Pathology,* 171**,** 715-727.

MARTIN, D. B. & VAGELOS, P. R. 1962. The mechanism of tricarboxylic acid cycle regulation of fatty acid synthesis. *J Biol Chem,* 237**,** 1787-92.

MEISER, J., KRAMER, L., SAPCARIU, S. C., BATTELLO, N., GHELFI, J., D'HEROUEL, A. F., SKUPIN, A. & HILLER, K. 2016. Pro-inflammatory Macrophages Sustain Pyruvate Oxidation through Pyruvate Dehydrogenase for the Synthesis of Itaconate and to Enable Cytokine Expression. *J Biol Chem,* 291**,** 3932-46.

METCALF, D. 2007. On hematopoietic stem cell fate. *Immunity,* 26**,** 669-73.

MICHALEK, R. D., GERRIETS, V. A., JACOBS, S. R., MACINTYRE, A. N., MACIVER, N. J., MASON, E. F., SULLIVAN, S. A., NICHOLS, A. G. & RATHMELL, J. C. 2011. Cutting edge: distinct glycolytic and lipid oxidative metabolic programs are essential for effector and regulatory CD4+ T cell subsets. *J Immunol,* 186**,** 3299-303.

MICHELUCCI, A., CORDES, T., GHELFI, J., PAILOT, A., REILING, N., GOLDMANN, O., BINZ, T., WEGNER, A., TALLAM, A., RAUSELL, A., BUTTINI, M., LINSTER, C. L., MEDINA, E., BALLING, R. & HILLER, K. 2013. Immune-responsive gene 1 protein links metabolism to immunity by catalyzing itaconic acid production. *Proc Natl Acad Sci U S A,* 110**,** 7820-5.

MILLS, EVANNA L., KELLY, B., LOGAN, A., COSTA, ANA S. H., VARMA, M., BRYANT, CLARE E., TOURLOMOUSIS, P., DÄBRITZ, J. HENRY M., GOTTLIEB, E., LATORRE, I., CORR, SINÉAD C., MCMANUS, G., RYAN, D., JACOBS, HOWARD T., SZIBOR, M., XAVIER, RAMNIK J., BRAUN, T., FREZZA, C., MURPHY, MICHAEL P. & O'NEILL, LUKE A. 2016. Succinate Dehydrogenase Supports Metabolic Repurposing of Mitochondria to Drive Inflammatory Macrophages. *Cell,* 167**,** 457-470.e13.

MONIUSZKO, M., BODZENTA-LUKASZYK, A., KOWAL, K., LENCZEWSKA, D. & DABROWSKA, M. 2009. Enhanced frequencies of CD14++CD16+, but not CD14+CD16+, peripheral blood monocytes in severe asthmatic patients. *Clin Immunol,* 130**,** 338-46.

MORGAN, M. D., DAY, C. J., PIPER, K. P., KHAN, N., HARPER, L., MOSS, P. A. & SAVAGE, C. O. 2010. Patients with Wegener's granulomatosis demonstrate a relative deficiency and functional impairment of T-regulatory cells. *Immunology,* 130**,** 64-73.

MUKHOPADHYAY, S., FARVER, C. F., VASZAR, L. T., DEMPSEY, O. J., POPPER, H. H., MANI, H., CAPELOZZI, V. L., FUKUOKA, J., KERR, K. M., ZEREN, E. H., IYER, V. K., TANAKA, T., NARDE, I., NOMIKOS, A., GUMURDULU, D., ARAVA, S., ZANDER, D. S. & TAZELAAR, H. D. 2012. Causes of pulmonary granulomas: a retrospective study of 500 cases from seven countries. *J Clin Pathol,* 65**,** 51-7.

MULDER, A. H., HEERINGA, P., BROUWER, E., LIMBURG, P. C. & KALLENBERG, C. G. 1994. Activation of granulocytes by anti-neutrophil cytoplasmic antibodies (ANCA): a Fc gamma RII-dependent process. *Clin Exp Immunol,* 98**,** 270-8.

MUNOZ, L., ALBILLOS, A., NIETO, M., REYES, E., LLEDO, L., MONSERRAT, J., SANZ, E., DE LA HERA, A. & ALVAREZ-MON, M. 2005. Mesenteric Th1 polarization and monocyte TNF-alpha production: first steps to systemic inflammation in rats with cirrhosis. *Hepatology,* 42**,** 411-9.

MUNRO, J. M., POBER, J. S. & COTRAN, R. S. 1989. Tumor necrosis factor and interferon-gamma induce distinct patterns of endothelial activation and associated leukocyte accumulation in skin of Papio anubis. *Am J Pathol,* 135**,** 121-33.

MURRAY, P. J., ALLEN, J. E., BISWAS, S. K., FISHER, E. A., GILROY, D. W., GOERDT, S., GORDON, S., HAMILTON, J. A., IVASHKIV, L. B., LAWRENCE, T., LOCATI, M., MANTOVANI, A., MARTINEZ, F. O., MEGE, J. L., MOSSER, D. M., NATOLI, G., SAEIJ, J. P., SCHULTZE, J. L., SHIREY, K. A., SICA, A.,

SUTTLES, J., UDALOVA, I., VAN GINDERACHTER, J. A., VOGEL, S. N. & WYNN, T. A. 2014. Macrophage activation and polarization: nomenclature and experimental guidelines. *Immunity,* 41**,** 14-20.

NAHRENDORF, M., SWIRSKI, F. K., AIKAWA, E., STANGENBERG, L., WURDINGER, T., FIGUEIREDO, J. L., LIBBY, P., WEISSLEDER, R. & PITTET, M. J. 2007. The healing myocardium sequentially mobilizes two monocyte subsets with divergent and complementary functions. *J Exp Med,* 204**,** 3037-47.

NEUMANN, I., BIRCK, R., NEWMAN, M., SCHNULLE, P., KRIZ, W., NEMOTO, K., YARD, B., WALDHERR, R. & VAN DER WOUDE, F. J. 2003. SCG/Kinjoh mice: a model of ANCA-associated crescentic glomerulonephritis with immune deposits. *Kidney Int,* 64**,** 140-8.

NINOMIYA, M., KIYOI, H., ITO, M., HIROSE, Y., ITO, M. & NAOE, T. 2004. Retinoic acid syndrome in NOD/scid mice induced by injecting an acute promyelocytic leukemia cell line. *Leukemia,* 18**,** 442-8.

NISHIYA, K., CHIKAZAWA, H., HASHIMOTO, K. & MIYAWAKI, S. 1999. Antineutrophil cytoplasmic antibody in patients with primary Sjogren's syndrome. *Clin Rheumatol,* 18**,** 268-71.

NOGUEIRA, E., HAMOUR, S., SAWANT, D., HENDERSON, S., MANSFIELD, N., CHAVELE, K. M., PUSEY, C. D. & SALAMA, A. D. 2010. Serum IL-17 and IL-23 levels and autoantigen-specific Th17 cells are elevated in patients with ANCA-associated vasculitis. *Nephrol Dial Transplant,* 25**,** 2209-17.

NORONHA, I. L., KRUGER, C., ANDRASSY, K., RITZ, E. & WALDHERR, R. 1993. In situ production of TNF-alpha, IL-1 beta and IL-2R in ANCA-positive glomerulonephritis. *Kidney Int,* 43**,** 682-92.

O'NEILL, L. A. & HARDIE, D. G. 2013. Metabolism of inflammation limited by AMPK and pseudo-starvation. *Nature,* 493**,** 346-55.

O'NEILL, L. A., KISHTON, R. J. & RATHMELL, J. 2016. A guide to immunometabolism for immunologists. *Nat Rev Immunol,* 16**,** 553-65.

O'SULLIVAN, D., VAN DER WINDT, G. J., HUANG, S. C., CURTIS, J. D., CHANG, C. H., BUCK, M. D., QIU, J., SMITH, A. M., LAM, W. Y., DIPLATO, L. M., HSU, F. F., BIRNBAUM, M. J., PEARCE, E. J. & PEARCE, E. L. 2014. Memory CD8(+) T cells use cell-intrinsic lipolysis to support the metabolic programming necessary for development. *Immunity,* 41**,** 75-88.

O'HARE, F. M., WATSON, R. W. G., O'NEILL, A., BLANCO, A., DONOGHUE, V. & MOLLOY, E. J. 2016. Persistent systemic monocyte and neutrophil activation in neonatal encephalopathy. *The Journal of Maternal-Fetal & Neonatal Medicine,* 29**,** 309-316.

OHLSSON, S. M., PETTERSSON, A., OHLSSON, S., SELGA, D., BENGTSSON, A. A., SEGELMARK, M. & HELLMARK, T. 2012. Phagocytosis of apoptotic cells by macrophages in anti-neutrophil cytoplasmic antibody-associated systemic vasculitis. *Clin Exp Immunol,* 170**,** 47-56.

OREN, R., FARNHAM, A. E., SAITO, K., MILOFSKY, E. & KARNOVSKY, M. L. 1963. Metabolic patterns in three types of phagocytizing cells. *J Cell Biol,* 17**,** 487-501.

OWEN, C. A., CAMPBELL, M. A., BOUKEDES, S. S., STOCKLEY, R. A. & CAMPBELL, E. J. 1994. A discrete subpopulation of human monocytes expresses a neutrophil-like proinflammatory (P) phenotype. *Am J Physiol,* 267**,** L775-85.

PADRINES, M., WOLF, M., WALZ, A. & BAGGIOLINI, M. 1994. Interleukin-8 processing by neutrophil elastase, cathepsin G and proteinase-3. *FEBS Lett,* 352**,** 231-5.

PALFRAMAN, R. T., JUNG, S., CHENG, G., WENINGER, W., LUO, Y., DORF, M., LITTMAN, D. R., ROLLINS, B. J., ZWEERINK, H., ROT, A. & VON ANDRIAN,

U. H. 2001. Inflammatory chemokine transport and presentation in HEV: a remote control mechanism for monocyte recruitment to lymph nodes in inflamed tissues. *J Exp Med,* 194**,** 1361-73.

PALMER, C. S., ANZINGER, J. J., ZHOU, J., GOUILLOU, M., LANDAY, A., JAWOROWSKI, A., MCCUNE, J. M. & CROWE, S. M. 2014. Glucose transporter 1-expressing proinflammatory monocytes are elevated in combination antiretroviral therapy-treated and untreated HIV+ subjects. *J Immunol,* 193**,** 5595-603.

PALMER, C. S., CHERRY, C. L., SADA-OVALLE, I., SINGH, A. & CROWE, S. M. 2016. Glucose Metabolism in T Cells and Monocytes: New Perspectives in HIV Pathogenesis. *EBioMedicine,* 6**,** 31-41.

PALMER, C. S. & CROWE, S. M. 2014. How does monocyte metabolism impact inflammation and aging during chronic HIV infection? *AIDS Res Hum Retroviruses,* 30**,** 335-6.

PALSSON-MCDERMOTT, E. M., CURTIS, A. M., GOEL, G., LAUTERBACH, M. A., SHEEDY, F. J., GLEESON, L. E., VAN DEN BOSCH, M. W., QUINN, S. R., DOMINGO-FERNANDEZ, R., JOHNSTON, D. G., JIANG, J. K., ISRAELSEN, W. J., KEANE, J., THOMAS, C., CLISH, C., VANDER HEIDEN, M., XAVIER, R. J. & O'NEILL, L. A. 2015. Pyruvate kinase M2 regulates Hif-1alpha activity and IL-1beta induction and is a critical determinant of the warburg effect in LPS-activated macrophages. *Cell Metab,* 21**,** 65-80.

PALSSON-MCDERMOTT, E. M. & O'NEILL, L. A. 2013. The Warburg effect then and now: from cancer to inflammatory diseases. *Bioessays,* 35**,** 965-73.

PARK, M. J., LEE, S. Y., MOON, S. J., SON, H. J., LEE, S. H., KIM, E. K., BYUN, J. K., SHIN, D. Y., PARK, S. H., YANG, C. W. & CHO, M. L. 2016. Metformin attenuates graft-versus-host disease via restricting mammalian target of rapamycin/signal transducer and activator of transcription 3 and promoting adenosine monophosphate-activated protein kinase-autophagy for the balance between T helper 17 and Tregs. *Transl Res,* 173**,** 115-130.

PEARCE, E. L. & PEARCE, E. J. 2013. Metabolic pathways in immune cell activation and quiescence. *Immunity,* 38**,** 633-43.

PEARSON, T., GREINER, D. L. & SHULTZ, L. D. 2008. Creation of "humanized" mice to study human immunity. *Curr Protoc Immunol,* Chapter 15**,** Unit 15 21.

PFEIFFER, T., SCHUSTER, S. & BONHOEFFER, S. 2001. Cooperation and competition in the evolution of ATP-producing pathways. *Science,* 292**,** 504-7.

PFISTER, H., OLLERT, M., FROHLICH, L. F., QUINTANILLA-MARTINEZ, L., COLBY, T. V., SPECKS, U. & JENNE, D. E. 2004. Antineutrophil cytoplasmic autoantibodies against the murine homolog of proteinase 3 (Wegener autoantigen) are pathogenic in vivo. *Blood,* 104**,** 1411-8.

PHILLIP, R. & LUQMANI, R. 2008. Mortality in systemic vasculitis: a systematic review. *Clin Exp Rheumatol,* 26**,** S94-104.

POPAT, R. J., HAKKI, S., THAKKER, A., COUGHLAN, A. M., WATSON, J., LITTLE, M. A., SPICKETT, C. M., LAVENDER, P., AFZALI, B., KEMPER, C. & ROBSON, M. G. 2017. Anti-myeloperoxidase antibodies attenuate the monocyte response to LPS and shape macrophage development. *JCI Insight,* 2**,** e87379.

PORGES, A. J., REDECHA, P. B., KIMBERLY, W. T., CSERNOK, E., GROSS, W. L. & KIMBERLY, R. P. 1994. Anti-neutrophil cytoplasmic antibodies engage and activate human neutrophils via Fc gamma RIIa. *J Immunol,* 153**,** 1271-80.

PRIMO, V. C., MARUSIC, S., FRANKLIN, C. C., GOLDMANN, W. H., ACHAVAL, C. G., SMITH, R. N., ARNAOUT, M. A. & NIKOLIC, B. 2010. Anti-PR3 immune

responses induce segmental and necrotizing glomerulonephritis. *Clin Exp Immunol,* 159**,** 327-37.

RALSTON, D. R., MARSH, C. B., LOWE, M. P. & WEWERS, M. D. 1997. Antineutrophil cytoplasmic antibodies induce monocyte IL-8 release. Role of surface proteinase-3, alpha1-antitrypsin, and Fcgamma receptors. *J Clin Invest,* 100**,** 1416-24.

RAMER, P. C., CHIJIOKE, O., MEIXLSPERGER, S., LEUNG, C. S. & MUNZ, C. 2011. Mice with human immune system components as in vivo models for infections with human pathogens. *Immunol Cell Biol,* 89**,** 408-16.

RAROK, A. A., STEGEMAN, C. A., LIMBURG, P. C. & KALLENBERG, C. G. 2002. Neutrophil membrane expression of proteinase 3 (PR3) is related to relapse in PR3-ANCA-associated vasculitis. *J Am Soc Nephrol,* 13**,** 2232-8.

REBER, L. L., GILLIS, C. M., STARKL, P., JONSSON, F., SIBILANO, R., MARICHAL, T., GAUDENZIO, N., BERARD, M., ROGALLA, S., CONTAG, C. H., BRUHNS, P. & GALLI, S. J. 2017. Neutrophil myeloperoxidase diminishes the toxic effects and mortality induced by lipopolysaccharide. *J Exp Med,* 214**,** 1249-1258.

RHEE, E. P., LALIBERTE, K. A. & NILES, J. L. 2010. Rituximab as maintenance therapy for anti-neutrophil cytoplasmic antibody-associated vasculitis. *Clin J Am Soc Nephrol,* 5**,** 1394-400.

RICH, P. R. 2003. The molecular machinery of Keilin's respiratory chain. *Biochem Soc Trans,* 31**,** 1095-105.

RIMBERT, M., HAMIDOU, M., BRAUDEAU, C., PUECHAL, X., TEIXEIRA, L., CAILLON, H., NEEL, A., AUDRAIN, M., GUILLEVIN, L. & JOSIEN, R. 2011. Decreased numbers of blood dendritic cells and defective function of regulatory T cells in antineutrophil cytoplasmic antibody-associated vasculitis. *PLoS One,* 6**,** e18734.

RODRIGUEZ-BORLADO, L., BARBER, D. F., HERNANDEZ, C., RODRIGUEZ-MARCOS, M. A., SANCHEZ, A., HIRSCH, E., WYMANN, M., MARTINEZ, A. C. & CARRERA, A. C. 2003. Phosphatidylinositol 3-kinase regulates the CD4/CD8 T cell differentiation ratio. *J Immunol,* 170**,** 4475-82.

RODRIGUEZ-PRADOS, J. C., TRAVES, P. G., CUENCA, J., RICO, D., ARAGONES, J., MARTIN-SANZ, P., CASCANTE, M. & BOSCA, L. 2010. Substrate fate in activated macrophages: a comparison between innate, classic, and alternative activation. *J Immunol,* 185**,** 605-14.

ROLLINS, B. J. 1997. Chemokines. *Blood,* 90**,** 909-28.

RONGVAUX, A., WILLINGER, T., MARTINEK, J., STROWIG, T., GEARTY, S. V., TEICHMANN, L. L., SAITO, Y., MARCHES, F., HALENE, S., PALUCKA, A. K., MANZ, M. G. & FLAVELL, R. A. 2014. Development and function of human innate immune cells in a humanized mouse model. *Nat Biotechnol,* 32**,** 364-72.

ROOT, R. K. & DALE, D. C. 1999. Granulocyte colony-stimulating factor and granulocyte-macrophage colony-stimulating factor: comparisons and potential for use in the treatment of infections in nonneutropenic patients. *J Infect Dis,* 179 Suppl 2**,** S342-52.

ROSSOL, M., KRAUS, S., PIERER, M., BAERWALD, C. & WAGNER, U. 2012. The CD14(bright) CD16+ monocyte subset is expanded in rheumatoid arthritis and promotes expansion of the Th17 cell population. *Arthritis Rheum,* 64**,** 671-7.

ROUSSELLE, A., KETTRITZ, R. & SCHREIBER, A. 2017. Monocytes Promote Crescent Formation in Anti-Myeloperoxidase Antibody-Induced Glomerulonephritis. *Am J Pathol,* 187**,** 1908-1915.

SALAMA, A. D. & LITTLE, M. A. 2012. Animal models of antineutrophil cytoplasm antibody-associated vasculitis. *Curr Opin Rheumatol,* 24**,** 1-7.

SANDERS, J. S., HUITMA, M. G., KALLENBERG, C. G. & STEGEMAN, C. A. 2006. Plasma levels of soluble interleukin 2 receptor, soluble CD30, interleukin 10 and B cell activator of the tumour necrosis factor family during follow-up in vasculitis associated with proteinase 3-antineutrophil cytoplasmic antibodies: associations with disease activity and relapse. *Ann Rheum Dis,* 65**,** 1484-9.

SANDERS, J. S., STASSEN, P. M., VAN ROSSUM, A. P., KALLENBERG, C. G. & STEGEMAN, C. A. 2004. Risk factors for relapse in anti-neutrophil cytoplasmic antibody (ANCA)-associated vasculitis: tools for treatment decisions? *Clin Exp Rheumatol,* 22**,** S94-101.

SATO, K. & KOYANAGI, Y. 2011. The mouse is out of the bag: insights and perspectives on HIV-1-infected humanized mouse models. *Exp Biol Med (Maywood),* 236**,** 977-85.

SATO, K., NIE, C., MISAWA, N., TANAKA, Y., ITO, M. & KOYANAGI, Y. 2010. Dynamics of memory and naive CD8+ T lymphocytes in humanized NOD/SCID/IL-2Rgammanull mice infected with CCR5-tropic HIV-1. *Vaccine,* 28 Suppl 2**,** B32-7.

SAVAGE, C. O., POTTINGER, B. E., GASKIN, G., PUSEY, C. D. & PEARSON, J. D. 1992. Autoantibodies developing to myeloperoxidase and proteinase 3 in systemic vasculitis stimulate neutrophil cytotoxicity toward cultured endothelial cells. *Am J Pathol,* 141**,** 335-42.

SCHLITT, A., HEINE, G. H., BLANKENBERG, S., ESPINOLA-KLEIN, C., DOPHEIDE, J. F., BICKEL, C., LACKNER, K. J., IZ, M., MEYER, J., DARIUS, H. & RUPPRECHT, H. J. 2004. CD14+CD16+ monocytes in coronary artery disease and their relationship to serum TNF-alpha levels. *Thromb Haemost,* 92**,** 419-24.

SCHON, M., BEHMENBURG, C., DENZER, D. & SCHON, M. P. 2001. Pathogenic function of IL-1 beta in psoriasiform skin lesions of flaky skin (fsn/fsn) mice. *Clin Exp Immunol,* 123**,** 505-10.

SCHREIBER, A., LUFT, F. C. & KETTRITZ, R. 2004. Membrane proteinase 3 expression and ANCA-induced neutrophil activation. *Kidney Int,* 65**,** 2172-83.

SCHREIBER, A., OTTO, B., JU, X., ZENKE, M., GOEBEL, U., LUFT, F. C. & KETTRITZ, R. 2005. Membrane proteinase 3 expression in patients with Wegener's granulomatosis and in human hematopoietic stem cell-derived neutrophils. *J Am Soc Nephrol,* 16**,** 2216-24.

SCHREIBER, A., PHAM, C. T., HU, Y., SCHNEIDER, W., LUFT, F. C. & KETTRITZ, R. 2012. Neutrophil serine proteases promote IL-1beta generation and injury in necrotizing crescentic glomerulonephritis. *J Am Soc Nephrol,* 23**,** 470-82.

SCHREIBER, A., XIAO, H., FALK, R. J. & JENNETTE, J. C. 2006. Bone marrow-derived cells are sufficient and necessary targets to mediate glomerulonephritis and vasculitis induced by anti-myeloperoxidase antibodies. *J Am Soc Nephrol,* 17**,** 3355-64.

SENA, L. A., LI, S., JAIRAMAN, A., PRAKRIYA, M., EZPONDA, T., HILDEMAN, D. A., WANG, C. R., SCHUMACKER, P. T., LICHT, J. D., PERLMAN, H., BRYCE, P. J. & CHANDEL, N. S. 2013. Mitochondria are required for antigen-specific T cell activation through reactive oxygen species signaling. *Immunity,* 38**,** 225-36.

SERBINA, N. V., JIA, T., HOHL, T. M. & PAMER, E. G. 2008. Monocyte-mediated defense against microbial pathogens. *Annu Rev Immunol,* 26**,** 421-52.

SHANAFELT, A. B., JOHNSON, K. E. & KASTELEIN, R. A. 1991. Identification of critical amino acid residues in human and mouse granulocyte-macrophage colony-stimulating factor and their involvement in species specificity. *J Biol Chem,* 266**,** 13804-10.

SHI, C. & PAMER, E. G. 2011. Monocyte recruitment during infection and inflammation. *Nat Rev Immunol,* 11**,** 762-74.

SHIOKAWA, M., TAKAHASHI, T., MURAKAMI, A., KITA, S., ITO, M., SUGAMURA, K. & ISHII, N. 2010. In vivo assay of human NK-dependent ADCC using NOD/SCID/gammac(null) (NOG) mice. *Biochem Biophys Res Commun,* 399**,** 733-7.

SHULTZ, L. D., BREHM, M. A., BAVARI, S. & GREINER, D. L. 2011. Humanized mice as a preclinical tool for infectious disease and biomedical research. *Ann N Y Acad Sci,* 1245**,** 50-4.

SHULTZ, L. D., ISHIKAWA, F. & GREINER, D. L. 2007. Humanized mice in translational biomedical research. *Nat Rev Immunol,* 7**,** 118-30.

SHULTZ, L. D., LYONS, B. L., BURZENSKI, L. M., GOTT, B., CHEN, X., CHALEFF, S., KOTB, M., GILLIES, S. D., KING, M., MANGADA, J., GREINER, D. L. & HANDGRETINGER, R. 2005. Human lymphoid and myeloid cell development in NOD/LtSz-scid IL2R gamma null mice engrafted with mobilized human hemopoietic stem cells. *J Immunol,* 174**,** 6477-89.

SHULTZ, L. D., SCHWEITZER, P. A., CHRISTIANSON, S. W., GOTT, B., SCHWEITZER, I. B., TENNENT, B., MCKENNA, S., MOBRAATEN, L., RAJAN, T. V., GREINER, D. L. & ET AL. 1995. Multiple defects in innate and adaptive immunologic function in NOD/LtSz-scid mice. *J Immunol,* 154**,** 180-91.

SILVESCU, C. I. & SACKSTEIN, R. 2014. G-CSF induces membrane expression of a myeloperoxidase glycovariant that operates as an E-selectin ligand on human myeloid cells. *Proc Natl Acad Sci U S A,* 111**,** 10696-701.

SKRZECZYNSKA-MONCZNIK, J., BZOWSKA, M., LOSEKE, S., GRAGE-GRIEBENOW, E., ZEMBALA, M. & PRYJMA, J. 2008. Peripheral blood CD14high CD16+ monocytes are main producers of IL-10. *Scand J Immunol,* 67**,** 152-9.

SMITH, J. A., STALLONS, L. J. & SCHNELLMANN, R. G. 2014. Renal cortical hexokinase and pentose phosphate pathway activation through the EGFR/Akt signaling pathway in endotoxin-induced acute kidney injury. *Am J Physiol Renal Physiol,* 307**,** F435-44.

SOUSSAN, M., ABISROR, N., ABAD, S., NUNES, H., TERRIER, B., POP, G., EDER, V., VALEYRE, D., SBERRO-SOUSSAN, R., GUILLEVIN, L., DHOTE, R., FAIN, O. & MEKINIAN, A. 2014. FDG-PET/CT in patients with ANCA-associated vasculitis: case-series and literature review. *Autoimmun Rev,* 13**,** 125-31.

SPECKS, U. & DEREMEE, R. A. 1990. Granulomatous vasculitis. Wegener's granulomatosis and Churg-Strauss syndrome. *Rheum Dis Clin North Am,* 16**,** 377-97.

STANSFIELD, B. K. & INGRAM, D. A. 2015. Clinical significance of monocyte heterogeneity. *Clin Transl Med,* 4**,** 5.

STEGEMAN, C. A., TERVAERT, J. W., SLUITER, W. J., MANSON, W. L., DE JONG, P. E. & KALLENBERG, C. G. 1994. Association of chronic nasal carriage of Staphylococcus aureus and higher relapse rates in Wegener granulomatosis. *Ann Intern Med,* 120**,** 12-7.

STEPPICH, B., DAYYANI, F., GRUBER, R., LORENZ, R., MACK, M. & ZIEGLER-HEITBROCK, H. W. 2000. Selective mobilization of CD14(+)CD16(+) monocytes by exercise. *Am J Physiol Cell Physiol,* 279**,** C578-86.

STEWART, R., HAMMOND, S. A., OBERST, M. & WILKINSON, R. W. 2014. The role of Fc gamma receptors in the activity of immunomodulatory antibodies for cancer. *Journal for ImmunoTherapy of Cancer,* 2**,** 29.

STODDART, C. A., MAIDJI, E., GALKINA, S. A., KOSIKOVA, G., RIVERA, J. M., MORENO, M. E., SLOAN, B., JOSHI, P. & LONG, B. R. 2011. Superior human leukocyte reconstitution and susceptibility to vaginal HIV transmission in humanized NOD-scid IL-2Rgamma(-/-) (NSG) BLT mice. *Virology,* 417**,** 154-60.

STOJKO, R. & WITEK, A. 2005. [Umbilical cord blood--a perfect source of stem cells?]. *Ginekol Pol,* 76**,** 491-7.

SULLIVAN, G. W., CARPER, H. T., SULLIVAN, J. A., MURATA, T. & MANDELL, G. L. 1989. Both recombinant interleukin-1 (beta) and purified human monocyte interleukin-1 prime human neutrophils for increased oxidative activity and promote neutrophil spreading. *J Leukoc Biol,* 45**,** 389-95.

SUN, Z., DENTON, P. W., ESTES, J. D., OTHIENO, F. A., WEI, B. L., WEGE, A. K., MELKUS, M. W., PADGETT-THOMAS, A., ZUPANCIC, M., HAASE, A. T. & GARCIA, J. V. 2007. Intrarectal transmission, systemic infection, and CD4+ T cell depletion in humanized mice infected with HIV-1. *J Exp Med,* 204**,** 705-14.

TABARKIEWICZ, J., POGODA, K., KARCZMARCZYK, A., POZAROWSKI, P. & GIANNOPOULOS, K. 2015. The Role of IL-17 and Th17 Lymphocytes in Autoimmune Diseases. *Archivum Immunologiae et Therapiae Experimentalis,* 63**,** 435-449.

TAKAGI, S., SAITO, Y., HIJIKATA, A., TANAKA, S., WATANABE, T., HASEGAWA, T., MOCHIZUKI, S., KUNISAWA, J., KIYONO, H., KOSEKI, H., OHARA, O., SAITO, T., TANIGUCHI, S., SHULTZ, L. D. & ISHIKAWA, F. 2012. Membrane-bound human SCF/KL promotes in vivo human hematopoietic engraftment and myeloid differentiation. *Blood,* 119**,** 2768-77.

TAL, T., SHARABANI, M. & AVIRAM, I. 1998. Cationic proteins of neutrophil azurophilic granules: protein-protein interaction and blockade of NADPH oxidase activation. *J Leukoc Biol,* 63**,** 305-11.

TALOR, M. V., STONE, J. H., STEBBING, J., BARIN, J., ROSE, N. R. & BUREK, C. L. 2007. Antibodies to selected minor target antigens in patients with anti-neutrophil cytoplasmic antibodies (ANCA). *Clin Exp Immunol,* 150**,** 42-8.

TAM, F. W., SANDERS, J. S., GEORGE, A., HAMMAD, T., MILLER, C., DOUGAN, T., COOK, H. T., KALLENBERG, C. G., GASKIN, G., LEVY, J. B. & PUSEY, C. D. 2004. Urinary monocyte chemoattractant protein-1 (MCP-1) is a marker of active renal vasculitis. *Nephrol Dial Transplant,* 19**,** 2761-8.

TANNAHILL, G. M., CURTIS, A. M., ADAMIK, J., PALSSON-MCDERMOTT, E. M., MCGETTRICK, A. F., GOEL, G., FREZZA, C., BERNARD, N. J., KELLY, B., FOLEY, N. H., ZHENG, L., GARDET, A., TONG, Z., JANY, S. S., CORR, S. C., HANEKLAUS, M., CAFFREY, B. E., PIERCE, K., WALMSLEY, S., BEASLEY, F. C., CUMMINS, E., NIZET, V., WHYTE, M., TAYLOR, C. T., LIN, H., MASTERS, S. L., GOTTLIEB, E., KELLY, V. P., CLISH, C., AURON, P. E., XAVIER, R. J. & O'NEILL, L. A. 2013. Succinate is an inflammatory signal that induces IL-1beta through HIF-1alpha. *Nature,* 496**,** 238-42.

TAO, J., DIAZ, R. K., TEIXEIRA, C. R. & HACKMANN, T. J. 2016. Transport of a Fluorescent Analogue of Glucose (2-NBDG) versus Radiolabeled Sugars by Rumen Bacteria and Escherichia coli. *Biochemistry,* 55**,** 2578-89.

TARZI, R. M., LIU, J., SCHNEITER, S., HILL, N. R., PAGE, T. H., COOK, H. T., PUSEY, C. D. & WOOLLARD, K. J. 2015. CD14 expression is increased on monocytes in patients with anti-neutrophil cytoplasm antibody (ANCA)-associated vasculitis and correlates with the expression of ANCA autoantigens. *Clin Exp Immunol,* 181**,** 65-75.

THIESEN, S., JANCIAUSKIENE, S., URONEN-HANSSON, H., AGACE, W., HOGERKORP, C. M., SPEE, P., HAKANSSON, K. & GRIP, O. 2014. CD14(hi)HLA-DR(dim) macrophages, with a resemblance to classical blood monocytes, dominate inflamed mucosa in Crohn's disease. *J Leukoc Biol,* 95**,** 531-41.

THOMAS, G., TACKE, R., HEDRICK, C. C. & HANNA, R. N. 2015. Nonclassical patrolling monocyte function in the vasculature. *Arterioscler Thromb Vasc Biol,* 35**,** 1306-16.

TODD, S. K., PEPPER, R. J., DRAIBE, J., TANNA, A., PUSEY, C. D., MAURI, C. & SALAMA, A. D. 2014. Regulatory B cells are numerically but not functionally deficient in anti-neutrophil cytoplasm antibody-associated vasculitis. *Rheumatology (Oxford),* 53**,** 1693-703.

TOSATO, G. & JONES, K. D. 1990. Interleukin-1 induces interleukin-6 production in peripheral blood monocytes. *Blood,* 75**,** 1305-10.

VAN DER GELD, Y. M., HELLMARK, T., SELGA, D., HEERINGA, P., HUITEMA, M. G., LIMBURG, P. C. & KALLENBERG, C. G. 2007. Rats and mice immunised with chimeric human/mouse proteinase 3 produce autoantibodies to mouse Pr3 and rat granulocytes. *Ann Rheum Dis,* 66**,** 1679-82.

VAN DER WOUDE, F. J. 1985. Anticytoplasmic antibodies in Wegener's granulomatosis. *Lancet,* 2**,** 48.

VAN DER WOUDE, F. J., RASMUSSEN, N., LOBATTO, S., WIIK, A., PERMIN, H., VAN ES, L. A., VAN DER GIESSEN, M., VAN DER HEM, G. K. & THE, T. H. 1985. Autoantibodies against neutrophils and monocytes: tool for diagnosis and marker of disease activity in Wegener's granulomatosis. *Lancet,* 1**,** 425-9.

VAN RIJN, R. S., SIMONETTI, E. R., HAGENBEEK, A., HOGENES, M. C., DE WEGER, R. A., CANNINGA-VAN DIJK, M. R., WEIJER, K., SPITS, H., STORM, G., VAN BLOOIS, L., RIJKERS, G., MARTENS, A. C. & EBELING, S. B. 2003. A new xenograft model for graft-versus-host disease by intravenous transfer of human peripheral blood mononuclear cells in RAG2-/- gammac-/- double-mutant mice. *Blood,* 102**,** 2522-31.

VATS, D., MUKUNDAN, L., ODEGAARD, J. I., ZHANG, L., SMITH, K. L., MOREL, C. R., GREAVES, D. R., MURRAY, P. J. & CHAWLA, A. 2006. Oxidative metabolism and PGC-1β attenuate macrophage-mediated inflammation. *Cell Metabolism,* 4**,** 13-24.

VILLANI, A. C., SATIJA, R., REYNOLDS, G., SARKIZOVA, S., SHEKHAR, K., FLETCHER, J., GRIESBECK, M., BUTLER, A., ZHENG, S., LAZO, S., JARDINE, L., DIXON, D., STEPHENSON, E., NILSSON, E., GRUNDBERG, I., MCDONALD, D., FILBY, A., LI, W., DE JAGER, P. L., ROZENBLATT-ROSEN, O., LANE, A. A., HANIFFA, M., REGEV, A. & HACOHEN, N. 2017. Single-cell RNA-seq reveals new types of human blood dendritic cells, monocytes, and progenitors. *Science,* 356.

VISIOLI, F., MARANGONI, F., MOI, D., RISE, P. & GALLI, C. 2000. In vitro differentiation of human monocytes to macrophages results in depletion of antioxidants and increase in n-3 fatty acids levels. *FEBS Lett,* 471**,** 75-7.

VON VIETINGHOFF, S., TUNNEMANN, G., EULENBERG, C., WELLNER, M., CRISTINA CARDOSO, M., LUFT, F. C. & KETTRITZ, R. 2007. NB1 mediates surface expression of the ANCA antigen proteinase 3 on human neutrophils. *Blood,* 109**,** 4487-93.

WAHL, D. R., PETERSEN, B., WARNER, R., RICHARDSON, B. C., GLICK, G. D. & OPIPARI, A. W. 2010. Characterization of the metabolic phenotype of chronically activated lymphocytes. *Lupus,* 19**,** 1492-501.

WAINWRIGHT, J. & DAVSON, J. 1950. The renal appearances in the microscopic form of periarteritis nodosa. *J Pathol Bacteriol,* 62**,** 189-96.

WALLACE, C. & KEAST, D. 1992. Glutamine and macrophage function. *Metabolism,* 41**,** 1016-20.

WANG, X., ZHANG, J., YUAN, Y., LI, T., ZHANG, L., DING, J., JIANG, S., LI, J., ZHU, L. & ZHANG, K. 2017. Cerebral metabolic change in Parkinson's disease patients with anxiety: A FDG-PET study. *Neurosci Lett*.

WARBURG, O. 1956. On the origin of cancer cells. *Science,* 123**,** 309-14.

WATTS, R. A., LANE, S. E., SCOTT, D. G., KOLDINGSNES, W., NOSSENT, H., GONZALEZ-GAY, M. A., GARCIA-PORRUA, C. & BENTHAM, G. A. 2001. Epidemiology of vasculitis in Europe. *Ann Rheum Dis,* 60**,** 1156-7.

WEGE, A. K., MELKUS, M. W., DENTON, P. W., ESTES, J. D. & GARCIA, J. V. 2008. Functional and phenotypic characterization of the humanized BLT mouse model. *Curr Top Microbiol Immunol,* 324**,** 149-65.

WEGENER, F. 1939. Über eine eigenartige rhinogene Granulomatose mit besonderer Beteilgung des Arteriensystems und der Nieren. *Beitr Path Anat***,** 36-38.

WEI, J., LONG, L., YANG, K., GUY, C., SHRESTHA, S., CHEN, Z., WU, C., VOGEL, P., NEALE, G., GREEN, D. R. & CHI, H. 2016. Autophagy enforces functional integrity of regulatory T cells by coupling environmental cues and metabolic homeostasis. *Nat Immunol,* 17**,** 277-85.

WEIDNER, S., CARL, M., RIESS, R. & RUPPRECHT, H. D. 2004. Histologic analysis of renal leukocyte infiltration in antineutrophil cytoplasmic antibody-associated vasculitis: importance of monocyte and neutrophil infiltration in tissue damage. *Arthritis Rheum,* 50**,** 3651-7.

WEIDNER, S., NEUPERT, W., GOPPELT-STRUEBE, M. & RUPPRECHT, H. D. 2001. Antineutrophil cytoplasmic antibodies induce human monocytes to produce oxygen radicals in vitro. *Arthritis Rheum,* 44**,** 1698-706.

WEINER, L. M., LI, W., HOLMES, M., CATALANO, R. B., DOVNARSKY, M., PADAVIC, K. & ALPAUGH, R. K. 1994. Phase I trial of recombinant macrophage colony-stimulating factor and recombinant gamma-interferon: toxicity, monocytosis, and clinical effects. *Cancer Res,* 54**,** 4084-90.

WEST, A. P., BRODSKY, I. E., RAHNER, C., WOO, D. K., ERDJUMENT-BROMAGE, H., TEMPST, P., WALSH, M. C., CHOI, Y., SHADEL, G. S. & GHOSH, S. 2011. TLR signalling augments macrophage bactericidal activity through mitochondrial ROS. *Nature,* 472**,** 476-80.

WHITE, R. E., RAMER, P. C., NARESH, K. N., MEIXLSPERGER, S., PINAUD, L., ROONEY, C., SAVOLDO, B., COUTINHO, R., BODOR, C., GRIBBEN, J., IBRAHIM, H. A., BOWER, M., NOURSE, J. P., GANDHI, M. K., MIDDELDORP, J., CADER, F. Z., MURRAY, P., MUNZ, C. & ALLDAY, M. J. 2012. EBNA3B-deficient EBV promotes B cell lymphomagenesis in humanized mice and is found in human tumors. *J Clin Invest,* 122**,** 1487-502.

WILDE, B., THEWISSEN, M., DAMOISEAUX, J., KNIPPENBERG, S., HILHORST, M., VAN PAASSEN, P., WITZKE, O. & COHEN TERVAERT, J. W. 2013. Regulatory B cells in ANCA-associated vasculitis. *Ann Rheum Dis,* 72**,** 1416-9.

WILDE, B., THEWISSEN, M., DAMOISEAUX, J., VAN PAASSEN, P., WITZKE, O. & TERVAERT, J. W. 2010. T cells in ANCA-associated vasculitis: what can we learn from lesional versus circulating T cells? *Arthritis Res Ther,* 12**,** 204.

WITKO-SARSAT, V., LESAVRE, P., LOPEZ, S., BESSOU, G., HIEBLOT, C., PRUM, B., NOEL, L. H., GUILLEVIN, L., RAVAUD, P., SERMET-GAUDELUS, I., TIMSIT, J., GRUNFELD, J. P. & HALBWACHS-MECARELLI, L. 1999. A large subset of neutrophils expressing membrane proteinase 3 is a risk factor for vasculitis and rheumatoid arthritis. *J Am Soc Nephrol,* 10**,** 1224-33.

WONG, K. L., TAI, J. J., WONG, W. C., HAN, H., SEM, X., YEAP, W. H., KOURILSKY, P. & WONG, S. C. 2011. Gene expression profiling reveals the defining features of the classical, intermediate, and nonclassical human monocyte subsets. *Blood,* 118**,** e16-31.

WOOLLARD, K. J. & GEISSMANN, F. 2010. Monocytes in atherosclerosis: subsets and functions. *Nature reviews. Cardiology,* 7**,** 77-86.

WRIGHT, H. L., CROSS, A. L., EDWARDS, S. W. & MOOTS, R. J. 2014. Effects of IL-6 and IL-6 blockade on neutrophil function in vitro and in vivo. *Rheumatology (Oxford),* 53**,** 1321-31.

XIAO, H., DAIRAGHI, D. J., POWERS, J. P., ERTL, L. S., BAUMGART, T., WANG, Y., SEITZ, L. C., PENFOLD, M. E., GAN, L., HU, P., LU, B., GERARD, N. P., GERARD, C., SCHALL, T. J., JAEN, J. C., FALK, R. J. & JENNETTE, J. C. 2014. C5a receptor (CD88) blockade protects against MPO-ANCA GN. *J Am Soc Nephrol,* 25**,** 225-31.

XIAO, H., HEERINGA, P., HU, P., LIU, Z., ZHAO, M., ARATANI, Y., MAEDA, N., FALK, R. J. & JENNETTE, J. C. 2002. Antineutrophil cytoplasmic autoantibodies specific for myeloperoxidase cause glomerulonephritis and vasculitis in mice. *Journal of Clinical Investigation,* 110**,** 955-963.

XIAO, H., HEERINGA, P., LIU, Z., HUUGEN, D., HU, P., MAEDA, N., FALK, R. J. & JENNETTE, J. C. 2005. The role of neutrophils in the induction of glomerulonephritis by anti-myeloperoxidase antibodies. *Am J Pathol,* 167**,** 39-45.

XIAO, H., SCHREIBER, A., HEERINGA, P., FALK, R. J. & JENNETTE, J. C. 2007. Alternative complement pathway in the pathogenesis of disease mediated by anti-neutrophil cytoplasmic autoantibodies. *Am J Pathol,* 170**,** 52-64.

XING, G. Q., CHEN, M., LIU, G., HEERINGA, P., ZHANG, J. J., ZHENG, X., E, J., KALLENBERG, C. G. & ZHAO, M. H. 2009. Complement activation is involved in renal damage in human antineutrophil cytoplasmic autoantibody associated pauci-immune vasculitis. *J Clin Immunol,* 29**,** 282-91.

YANG, J., ZHANG, L., YU, C., YANG, X. F. & WANG, H. 2014. Monocyte and macrophage differentiation: circulation inflammatory monocyte as biomarker for inflammatory diseases. *Biomark Res,* 2**,** 1.

YANG, J. J., TUTTLE, R. H., HOGAN, S. L., TAYLOR, J. G., PHILLIPS, B. D., FALK, R. J. & JENNETTE, J. C. 2000. Target antigens for anti-neutrophil cytoplasmic autoantibodies (ANCA) are on the surface of primed and apoptotic but not unstimulated neutrophils. *Clin Exp Immunol,* 121**,** 165-72.

YANG, Z., FUJII, H., MOHAN, S. V., GORONZY, J. J. & WEYAND, C. M. 2013. Phosphofructokinase deficiency impairs ATP generation, autophagy, and redox balance in rheumatoid arthritis T cells. *J Exp Med,* 210**,** 2119-34.

YASUKAWA, K., HIRANO, T., WATANABE, Y., MURATANI, K., MATSUDA, T., NAKAI, S. & KISHIMOTO, T. 1987. Structure and expression of human B cell stimulatory factor-2 (BSF-2/IL-6) gene. *EMBO J,* 6**,** 2939-45.

YATES, M., WATTS, R. A., BAJEMA, I. M., CID, M. C., CRESTANI, B., HAUSER, T., HELLMICH, B., HOLLE, J. U., LAUDIEN, M., LITTLE, M. A., LUQMANI, R. A., MAHR, A., MERKEL, P. A., MILLS, J., MOONEY, J., SEGELMARK, M., TESAR, V., WESTMAN, K., VAGLIO, A., YALCINDAG, N., JAYNE, D. R. & MUKHTYAR, C. 2016. EULAR/ERA-EDTA recommendations for the management of ANCA-associated vasculitis. *Ann Rheum Dis,* 75**,** 1583-94.

YOON, B. R., YOO, S. J., CHOI, Y., CHUNG, Y. H., KIM, J., YOO, I. S., KANG, S. W. & LEE, W. W. 2014. Functional phenotype of synovial monocytes modulating inflammatory T-cell responses in rheumatoid arthritis (RA). *PLoS One,* 9**,** e109775.

ZAWADA, A. M., ROGACEV, K. S., ROTTER, B., WINTER, P., MARELL, R. R., FLISER, D. & HEINE, G. H. 2011. SuperSAGE evidence for CD14++CD16+ monocytes as a third monocyte subset. *Blood,* 118**,** e50-61.

ZEILHOFER, H. U. & SCHORR, W. 2000. Role of interleukin-8 in neutrophil signaling. *Curr Opin Hematol,* 7**,** 178-82.

ZEMAN, K., FORNALCZYK-WACHOWSKA, E., POKOCA, L., KANTORSKI, J., KAWIAK, J., BANASIK, M., HOSER, G., KARPINSKI, J., MALINOWSKI, A., ROMANISZYN, L., KARDAS-SOBANTKA, D. & PANKOWSKA, E. 1996. The composition of main lymphocyte subsets and NK cells in peripheral blood of the polish population. *Cent Eur J Immunol,* 21**,** 107-113.

ZHAO, L., DAVID, M. Z., HYJEK, E., CHANG, A. & MEEHAN, S. M. 2015. M2 macrophage infiltrates in the early stages of ANCA-associated pauci-immune necrotizing GN. *Clin J Am Soc Nephrol,* 10**,** 54-62.

ZHENG, J. 2012. Energy metabolism of cancer: Glycolysis versus oxidative phosphorylation (Review). *Oncol Lett,* 4**,** 1151-1157.

ZIEGLER-HEITBROCK, H. W., STROBEL, M., FINGERLE, G., SCHLUNCK, T., PFORTE, A., BLUMENSTEIN, M. & HAAS, J. G. 1991. Small (CD14+/CD16+) monocytes and regular monocytes in human blood. *Pathobiology,* 59**,** 127-30.

ZIEGLER-HEITBROCK, L. 2014. Monocyte subsets in man and other species. *Cell Immunol,* 289**,** 135-9.

ZIEGLER-HEITBROCK, L. 2015. Blood Monocytes and Their Subsets: Established Features and Open Questions. *Front Immunol,* 6**,** 423.

ZIEGLER-HEITBROCK, L., ANCUTA, P., CROWE, S., DALOD, M., GRAU, V., HART, D. N., LEENEN, P. J., LIU, Y. J., MACPHERSON, G., RANDOLPH, G. J., SCHERBERICH, J., SCHMITZ, J., SHORTMAN, K., SOZZANI, S., STROBL, H., ZEMBALA, M., AUSTYN, J. M. & LUTZ, M. B. 2010. Nomenclature of monocytes and dendritic cells in blood. *Blood,* 116**,** e74-80.

ZIEGLER-HEITBROCK, L. & HOFER, T. P. 2013. Toward a refined definition of monocyte subsets. *Front Immunol,* 4**,** 23.

ZIEGLER, M., ALT, K., PATERSON, B. M., KANELLAKIS, P., BOBIK, A., DONNELLY, P. S., HAGEMEYER, C. E. & PETER, K. 2016. Highly Sensitive Detection of Minimal Cardiac Ischemia using Positron Emission Tomography Imaging of Activated Platelets. *Sci Rep,* 6**,** 38161.

ZOU, C., WANG, Y. & SHEN, Z. 2005. 2-NBDG as a fluorescent indicator for direct glucose uptake measurement. *J Biochem Biophys Methods,* 64**,** 207-15.